Development of strategies for isolation and functional testing of cell lines for neuronal regeneration

Joana Neves dos Reis

UCL

PhD in Biochemical Engineering

I, Joana Neves dos Reis confirm that the work presented in this thesis is my own. Where information has been derived from other sources, I confirm that this has been indicated in the thesis.

To Mum and Dad for the constant faith in me even when I lacked it myself

Acknowledgments

I'd like to thank my funding bodies EPSRC and BBSRC; my supervisors: Ivan for the opportunity to join this project and for the vigilant supervision throughout my PhD and James for the invaluable guidance and support. I'd also like to thank my colleagues in Biochemical Engineering department, namely the Regenerative Medicine Lab. Each one of you taught me a valuable lesson, which I will never forget. I'd also like to thank to James' students at the Biomaterials and Tissue Engineering department for all the help especially to Kulraj for getting the primary cells, the support on my final assays and long talks about life and its meaning.

Finally I'd like to thank Reema and Gulsim for keeping sane throughout this PhD and to my dear friend Heather with whom I could be insane with. I would do not know how I would have done it without you.

Abstract

In the Central Nervous System there is limited neuronal regeneration ability after injury. Olfactory Ensheathing Cells are olfactory system cells guiding neurons and supporting regeneration from the olfactory mucosa to the bulb. They also promote structural and functional recovery *in vivo* in animal models of CNS injury. Nevertheless, patient sample variability results in inconsistent results in autologous transplants. A universal cell therapy seems to be the envisaged solution. This project aimed to optimise the culture of OECs from rat olfactory mucosa (investigating the impact of timing of addition of NT-3 and AraC exposure for 24h) and develop *in vitro* assays for testing a human conditionally immortalised OEC line (PA5) for neuronal regeneration ability. Significantly higher proportion of Thy1.1-positive cells was seen when NT3 was added later (day 6 versus day 1; $p<0.018$). There was no significant difference in cell yield and proportion with exposure to AraC. Rat OECs were tested in co-culture with NG108 neuronal cell line. OECs generally performed similarly to the positive control F7/SC in all measurements. The same assay with PA5 cells yielded inconclusive results. Rat DRG neurons were cultured on PA5 cells and had longer neurites comparing to culture on PLL ($P=0.010$). Finally PA5 cells were preliminarily tested for neuronal alignment. DRG neurons co-cultured on PA5 showed a low angles-skewed distribution and a difference in the distribution of DRG angles when compared to culture on F7/SC suggesting a tendency for PA5 cells to self-align and guide neurons in *in vitro*.

Overall this work reveals a tendency of PA5 cell line to promote regeneration of CNS neurons. Nevertheless much more work need to be undertaken to further confirm these results either using different models *in vitro* or *in vivo* or accessing other neuronal regeneration abilities.

Impact Statement

My thesis looked at different strategies for isolation and functional testing olfactory ensheathing cells (OECs). This glial cell regenerates and guides neurons naturally in the olfactory system between the Peripheral Nervous System (PNS) and the Central Nervous System (CNS) and it has the potential to do the same in CNS injuries (Y. Li, Field, & Raisman, 1998; Ramón-Cueto & Nieto-Sampedro, 1994; Ramón-Cueto, Plant, Avila, & Bunge, 1998).

The effective isolation, characterization and functional analysis of these cells through *in vitro* and *in vivo* testing and later clinical trials will allow the use of these cells for neuronal regeneration in patients. My project focused on optimizing culture of OECs and the initial testing of a conditionally immortalized OEC line PA5 for neuronal regeneration. The results of my thesis will inform the next steps in the study of this OEC line, namely neuronal regeneration assessment using human neuronal models and other indicators for neuronal regeneration ability in the CNS or PNS. Should these results further confirm the PA5 cell line ability to promote neuronal regeneration the next steps would be tests in animal models such as rat and dog. Confirmation of positive impact of this cell line on animal models could lead to pre-clinical and clinical studies in human subjects. Allogeneic transplants of this cell line would eliminate the sample variability that is typical with autologous implants (Choi, Li, Law, Powell, & Raisman, 2008) since the cells would be originated from the same cell population and hopefully decrease the variability in results for human functional recovery

studies. Positive results can open the door for a human allogeneic cell therapy for neuronal injury.

Table of Contents

Nomenclature

Abreviation	Derivation	Abreviation	Derivation
anti-GD3	Antiganglioside antibody 3	MMP	matrix metalloproteinase
AraC	Cytosine β-D-arabinofuranoside	MRI	Magnetic Resonance Imaging
ARTN	artemin	NCAM	Neural Cell adhesion molecule
BDNF	brain-derived neurotrophic factor	NGF	nerve growth factor
bFGF	basic Fibroblast growth factor	NNT1	novel neurotrophin 1
BSF3	B cell stimulating factor 3	NRTN	neurturin
CAM	Cell Adhesion Molecule	NT-3 (4 , 5, 6 or 7)	Neutrophin-3 (4, 5, 6 or 7)
CLC	cardiotrophin-like cytokine	NTR	neurotrophic receptor
CNS	Central Nervous System	O-2A	type 2 astrocytes, oligodendrocytes, and their precursors
CT-1	cardiotrophin 1	O-2A	type 2 astrocytes, oligodendrocytes, and their precursors
CNTF	ciliary neurotrophic factor	OB	Olfactory Bulb
CPSG	chondroitin sulphate proteoglycan	OECs	Olfactory Ensheathing Cells
DMEM	Dulbecco's Modified Eagle Medium	OMC	Olfactory mucosa cells
DRG	Dorsal Root Ganglia	PBS	phosphate buffer solution
1E8	Cytokeratin 8	PNS	Peripheral Nervous System
ECM	Extracellular Matrix	PFA	Paraformaldehyde
FBS	fetal bovine serum	P/S	Penicilin/ Streptomicin
GAL C	galactocerebroside	PSA	polysialic acid
GAP	Growth Associated Protein	PSPN	persephin
GDNF	Glial cell line-Derived Neurotrophic Factor	Ran-2	Rogue neural antigen-2
GFAP	Glial fibrillary acidic protein	RET	receptor tyrosine kinase
GFP	Green Fluorescent protein	SC	Schwann cells
GFRα1	GDNF family receptor alpha-1	SCI	Spinal cord injury
HBSS	Hanks Balanced Salt Solution	SD	Sprague-Dawley
HNK-1	Human Natural Killer-1	α-SMA	α-smooth muscle actin
IL-6 (11 or 27)	interleukin-6 (11 or 27)	Src	Proto-oncogene tyrosine-protein kinase
JNK	c-Jun N-terminal kinases	Thy1	Thymocyte antigen 1
LIF	leukaemia inhibitory factor		
LP	Lamina Propria		
LPA	Lysophosphatidic acid		
MAI	Myelin Associated Inhibitors		
MEM	Minimal essential Eagle's medium		

Figures

for 24. However none of those differences were significant.(B) There was a higher yield of α-SMA and S100β-positive mucosa-derived cells cultured with addition of AraC for 24h. However none of those differences were significant. Data are means ± SD, n=4.

Figure 3.7 - Culture of rat mucosa-derived cell populations at atmospheric oxygen (O_2) concentration at day 6, 9 and 12. *Following cell isolation, cells were cultured at atmospheric O2 (21%), on laminin + 2% serum +NT-3 (50 ng/mL). Scale bars are 400µm.*

Figure 3.8- Co-culture of NG108-15 neuronal cell line with rat olfactory mucosa-derived cell populations for 3 days at Physiologic and Atmospheric Oxygen. *Following cell isolation, cells were cultured at atmospheric O_2 (21%), on laminin + 2% serum +NT-3 (50 ng/mL). At day 14, NG108-15 cells were cultured with OECs, F7 Schwann cell line or on PLL. After 5 days cells were fixed and stained for S100β, βIII-tubulin (a neuronal marker) and Hoechst (stains the nuclei). Scale bars are 200µm.*

Figure 3.9- Co-culture of NG108-15 neuronal cell line with rat olfactory mucosa-derived cell populations for 5 days at Physiologic and Atmospheric Oxygen. *Following cell isolation, cells were cultured at atmospheric O_2 (21%), on laminin + 2% serum +NT-3 (50 ng/mL). At day 14, NG108-15 cells were cultured with OECs, F7 Schwann cell line or on PLL. After 5 days cells were fixed and stained for S100β, βIII-tubulin (a neuronal marker) and Hoechst. Scale bars are 200µm.*

Figure 3.10- Number of NG108 neurons per mm² after co-culture for 3 days with OECs, F7/SC or on PLL at physiologic (2-8%) and atmospheric oxygen (21%). *Quantification of the fluorescent micrographs revealed a significantly higher number of neurons/mm² when co-cultured with F7/SC compared with culture on PLL (P<0.01, Two-way MANOVA with Tukey's post-test). Data are means ± SD, n=4.*

Figure 3.11- NG108 neurite extension number per neuron after co-culture for 3 days with OECs, F7/SC or on PLL at physiologic (2-8%) and atmospheric oxygen (21%). *Quantification of the fluorescent micrographs revealed a higher number of neurites/ neuron when co-cultured at physiologic O_2 (P=0.036, two-way MANOVA with Tukey's HSD post-test) Data are means ± SD, n=4.*

Figure 3.12- NG108 neurite length per neurite after co-culture for 3 days with OECs, F7/SC or on PLL. *Quantification of the fluorescent micrographs revealed significantly a higher extension length when co-cultured with F7/SC when compared with culture on PLL (P<0.025, Two-way MANOVA with Tukey's HSD post-test). Data are means ± SD, n=4.*

Figure 3.13- NG108 neuron number per mm² after co-culture for 5 days with OECs, F7/SC or on PLL at physiologic (2-8%) and atmospheric oxygen (21%). *Quantification of the fluorescent micrographs revealed a higher number of neurons when co-cultured with OECs. Data are means ± SEM, n=4.*

Figure 3.14- NG108 neurite extension number per neuron after co-culture for 5 days with OECs, F7/SC or on PLL at physiologic (2-8%) and atmospheric oxygen (21%). *Quantification of the fluorescent micrographs revealed a higher number of neurites when cultured with OECs when compared with culture on PLL (P<0.01, two-way ANOVA, Tukey's post-hoc test) at physiologic O2. Data are means ± SEM, n=4.*

Figure 3.15- NG108 neurite length after co-culture for 5 days with OECs, F7/SC or on PLL at physiologic (2-8%) and atmospheric oxygen (21%). *Quantification of the fluorescent micrographs revealed a significantly higher extension length with culture at physiologic oxygen (P<0.001, two-way ANOVA, Tukey's post-hoc test). It also showed a higher neurite length with co-culture with OECs when compared with culture on PLL or with F7/SC (P<0.01 and P<0.05, respectively, two-way ANOVA, Tukey's post-hoc test). Data are means ± SD, n=4.*

Figure 3.16 - Culture PA5 cells at atmospheric oxygen (O_2) concentration. Cells were cultured at atmospheric O_2 (21%), on PLL with 10% serum. Scale bars are 1000 (left) and 400µm (right).

Figure 3.17- **Co-culture of NG108 neurons with human PA5 cell line for 3 or 5 days at atmospheric or physiologic oxygen.** Following cell culture, cells were cultured at atmospheric O_2 (21%), on PLL +

10% serum. NG108 neurons were cultured with PA5 cells, F7 Schwann cell line or on PLL. After 3 or 5 days cells were fixed and stained for S100β, βIII-tubulin and Hoechst. Scale bars are 200µm.

Figure 3.18- NG108 neuron number per mm² after co-culture for 3 or 5 days with PA5 cells, F7/SC or on PLL. *Quantification of the fluorescent micrographs revealed a higher number of neurons when cultured for 5 days. Data are means ± SD, n=4.*

Figure 3.19- NG108 neurite extension number per neuron after co-culture for 3 or 5 days with OECs, F7/SC or on PLL at physiologic (2-8%) and atmospheric oxygen (21%). *Quantification of the fluorescent micrographs revealed a higher number of neurites/ neuron when co-cultured with PA5 when compared to NG108 on PLL (P<0.0001) or NG108 + F7/SC (P<0.00001, three-way MANOVA with Tukey's HSD post-test).* All second degree interactions had a significant effect on the number of neurites/ neuron (co-culture*duration: P<0.00001, co-culture*level of oxygen: P<0.000001 and duration*level of oxygen: P<0.0001). The third degree interaction co-culture*duration*level of oxygen also had a significant effect on both the number of neurites/ neuron (P<0.00001). *Data are means ± SD, n=4.*

Figure 3.20 - NG108 neurite length after co-culture for 3 or 5 days with PA5 cells, F7/SC or on PLL at physiologic (2-8%) and atmospheric oxygen (21%). *Quantification of the fluorescent micrographs revealed no significant differences in extension length per neuron between culture type and duration.* The co-culture*duration second degree effect had a significant effect on neurite length/ neurite (P=0.007). The third degree interaction co-culture*duration*level of oxygen also had a significant effect on neurite length/ neurite (P=0.015). *Data are means ± SD, n=4.*

Figure 3.21 - Co-culture of primary DRG neurons with human PA5 cell line for 3 or 5 days at atmospheric or physiologic oxygen. Following cell culture, cells were cultured at atmospheric O_2 (21%), on PLL + 10% serum. DRG neurons were isolated and cultured with PA5 cells, F7 Schwann cell line or on PLL. After 3 or 5 days cells were fixed and stained for S100β, βIII-tubulin and Hoechst. Scale bars are 200µm.

Figure 3.22- DRG neurons number of neurites per neuron after co-culture for 3 or 5 days with PA5 cells, F7/SC or on PLL at physiologic (2-8%) and atmospheric oxygen (21%). *Quantification of the fluorescent micrographs revealed no significant differences in neurite number per neuron between culture types, durations or oxygen levels. Data are means ± SD, n=4*

Figure 3.23- DRG neurons neurite length after co-culture for 3 or 5 days with PA5 cells, F7/SC or on PLL at physiologic (2-8%) and atmospheric oxygen (21%). *Quantification of the fluorescent micrographs revealed a significant difference in neurite length per neurite between co-culture at 3 and 5 days (P=0.010, Three-way MANOVA, Bonferroni adjustment) and DRG + PA5 and DRGs on PLL (P=0.010, Three-way MANOVA, Tukey's HSD post-test). Data are means ± SD, n=4.*

Figure 3.24 – Collagen gel contraction for different cell densities (0.2, 0.5, 1 and 2 million cells per mL) after 2, 4, 6, 8 and 24h*. Cells were cultured at atmospheric O_2 (21%), on PLL + 10% serum, typsinased, resuspended in media and added to the collagen gel mixture. Pictures were taken after 2, 4, 6, 8 and 24h and gel contraction determined using ImageJ.*

Figure 3.25 - PA5 cell line proportion contraction after 2h, 4h, 6h, 8h and 24h. *Cell density of 0.5 x 10^6 cell/mL had a significantly higher gel contraction when compared to the lowest cell density of 0.2 x 10^6 cells/mL but did not differ from higher cell densities of 1 and 2 x 10^6 cell/mL. Data are means ± SD, n=4.*

Figure 3.26 - *PA5 cell line alignment after 4h, 5h, 6h, 8h and 10h for 1 x 10^6cell/mL. Fluorescent micrographs revealed a higher alignment after 10h (40x magnification, confocal imaging).*

Figure 3.27 - Collagen gel with F7/SC or PA5 aligned cells co-cultured with NG108 neurons for 5 days. *Following cell culture, cells were cultured at atmospheric O2 (21%) + 10% serum. NG108 cells were cultured with PA5 cells or F7 Schwann cell line loaded collagen gels. After 5 days cells were fixed and*

1. Introduction

Literature Review

Olfactory Ensheathing Cells

Olfactory Ensheathing Cells (OECs) constitute a unique type of glial cells limited to the olfactory system. They were first identified by Golgi (Golgi, 1875) during his work on olfactory nerve fibres using his new method for staining cells which consisted of hardening of the tissue pieces in a solution of potassium bichromate or ammonia and its subsequent immersion in a solution of silver nitrate (Shepherd, Greer, Mazzarello, & Sassoè-Pognetto, 2011). He described that "…*under certain circumstances it is possible to observe the nerve bundles separated from each other and themselves divided by numerous wide and thin connective tissue cells [glia] with long prolongations, partly thread-like, partly flat, but rarely ramified, which are absolutely similar to those found in the white matter of the cerebrum and spinal cord*…" (Golgi, 1875; Shepherd et al., 2011). This thin connective tissue cells appear to be the special type of glia around olfactory nerve axons that are now called Olfactory Ensheathing Cells (Shepherd et al., 2011).

Later, Blanes (1898) in his work describing morphological aspects of the olfactory pathway, defined the neuroglia in the olfactory bulb as an "*insulating neuroglia is present in all of the areas of the bulb where conductive fibers are, and, where the risk of an uncontrolled diffusion of the olfactory impulse is greater. Neuroglia, therefore, has in this case, the task of channelling currents, isolating from one another all of the expansions that*

pertain to systems of independent conduction…" (Blanes, 1898; Levine & Marcillo, 2008). It was believed that these cells were Schwann cells of the olfactory system since they ensheath nerve fibres from the olfactory mucosa back to the bulb (Barber & Lindsay, 1982; De Lorenzo, 1957; Gasser, 1956).

It soon became apparent though, that this type of glial cell had very distinctive features. They are located both in the Peripheral Nervous System (PNS) and Central Nervous System (CNS), lamina propria in the olfactory mucosa (OM) and olfactory bulb (OB), respectively and they resemble several types of glia (Gudiño-Cabrera & Nieto-Sampedro, 2000; Ramón-Cueto & Avila, 1998). Their function of support and repair, their formation of the glia limitans of the OB and ensheathment of neurons resemble both astrocytes and Schwann cells (SC) functions (R. Doucette, 1991). OECs regenerating properties make them a promising candidate for a cell therapy for neural lesions (Raisman, 2001; Raisman & Li, 2007; Richter & Roskams, 2008).

One of the differences between the OB and other CNS regions is the type of glia. In addition to astrocytes, oligodendrocytes and microglia, the OB also has OECs (Ramón-Cueto & Avila, 1998). These cells are particularly interesting due to their ability to regenerate neurons in the CNS, contrarily to other regions in the adult body where the environment after injury is adverse to neuron regeneration.

Olfactory Ensheathing Cells are a type of glia from the olfactory nervous system of mammals that has the function of ensheathing neuronal

axons from the olfactory mucosa epithelium where they are formed to the olfactory bulb in the brain during development and normal turnover every 4-8 weeks throughout adult life (Ramón-Cueto & Avila, 1998).

The ability to regenerate neurons is thought to be due to the neurotrophic properties of OECs (Yang, He, & Hao, 2014) and their ability to mingle with astrocytes in the olfactory bulb. OECs also have a phagocytic function in the olfactory system (Nazareth et al., 2014), similar to microglia and also some characteristics and functions of glial cells from both nervous systems, Schwann cells (PNS) and astrocytes (CNS) (Z Su & He, 2010). Moreover they express a marker for astrocytes GFAP (Barber & Lindsay, 1982) *in vivo* (J. R. Doucette, 1984) and *in vitro* (Denis-Donini & Estenoz, 1988) and a marker for non-myelinating Schwann cells (SC), p75NTR (Pixley, 1992; Ramón-Cueto & Nieto-Sampedro, 1992). They also have morphologies resembling astrocytes and Schwann cells, large cytoplasm around the nucleus and spindle shape, respectively (Pixley, 1992).

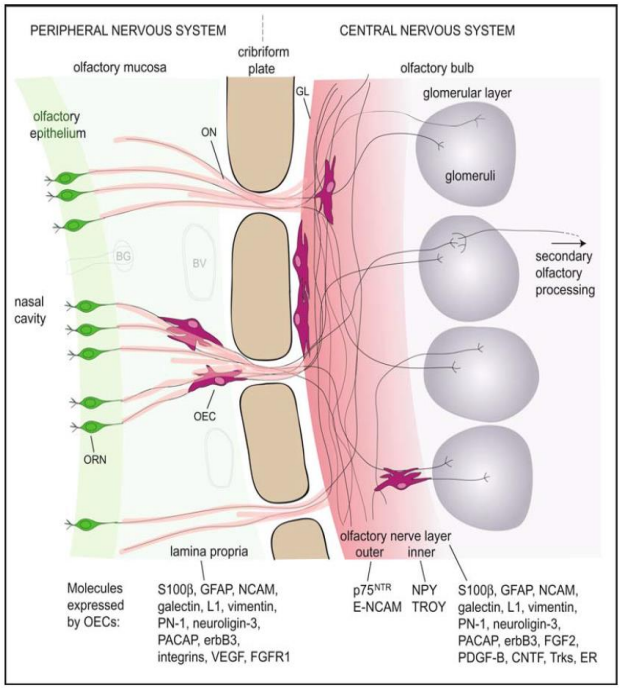

Figure 1.1- *A diagram representing the adult rat primary olfactory system: ensheathing of bundles in the olfactory mucosa and olfactory bulb (*Image reproduced with permission of the rights holder, *Springer Customer Service Centre GmbH: Springer Nature Journal of Neurocytology "Morphological and functional plasticity of olfactory ensheathing cells", Adele J. Vincent, Adrain K. West, & Meng inn Chuah, © Springer Science + Business Media, Inc. 2005)*

Developmental Origin of Olfactory Ensheathing Glia

At first it was thought that OECs would come from the olfactory placode like the rest of the olfactory system (Ramón-Cueto & Avila, 1998). During development of the olfactory nervous system a cluster of cells called migratory mass that includes OEC progenitors was observed leaving the base of the invaginating olfactory placode and migrating towards the telencephalic vesicles, often in contact with the developing olfactory nerve, and forming the olfactory bulb (Mendoza et al., 1982; Doucette, 1990). Conversely an avian fate-mapping study (Barraud et al., 2010) showed that the olfactory placodes do not form OECs: the Schwann cells on the olfactory nerve described in studies like quail-chick ANF fate-mapping experiments (Couly & Le Douarin, 1985) were in fact olfactory placode-derived neurons,

which migrate into the forebrain (Schwanzel-Fukuda & Pfaff, 1989; Wray, Grant, & Gainer, 1989) and can express GFAP *in vitro* (Laywell, Kukekov, & Steindler, 1999). OECs actually descend from the neural crest based on fluorescent tracking of neural crest cells in chick embryos and later characterization with p75NTR , S100β and GFAP (Katoh et al., 2011) and P_0 (Barraud et al., 2010) immunostaining also markers for non-myelinating Schwann cells, except for P_0 which stains immature non-myelinating Schwann cells from chicken lineage (Barber & Lindsay, 1982; Bhattacharyya, Frank, Ratner, & Brackenbury, 1991; K R Jessen, Morgan, Stewart, & Mirsky, 1990).

The neural crest forms a multipotent population of cells that arises from the border of the neural plate and migrates to differentiate and various types of cells in the embryo. The neural plate originates from the germ layer ectoderm and gives rise to sensory placodes and neural crest. The former structures have a very complex relationship in the olfactory system due to its common origin and because they give rise to different structures within it: the olfactory placode originates the olfactory sensory neurons and supporting cells of the olfactory epithelium and the cranial neural crest cells to the structural elements of the nose (Katoh et al., 2011).

OECs have several features that suggest that they have a neural crest origin like their resemblance to Schwann cell and the fact that they are peripheral glial cells and express p75NTR, a neural crest stem cell marker (Morrison, White, Zock, & Anderson, 1999; Stemple & Anderson, 1992). In

any case the origin of the olfactory placode and neural crest are intimately related (Katoh et al., 2011).

Isolation, culture and purification of Olfactory Ensheathing Cells

The demand for cost-effective, reproducible and safe cell therapies requires large numbers of cells. Several strategies have been reported to expand OECs. OECs derived from different developmental stages may exhibit different morphological, cytochemical and ultrastructural features (Ramón-Cueto & Avila, 1998). Culture conditions can also greatly influence OECs *in vitro*.

Most isolation protocols consist mainly in the dissecting the mucosa/ bulb from embryos/ neonates/ adult animals (usually rats) and placing in appropriate media (minimum essential Eagle's medium, MEM) or buffer (Phosphate Balance Solution, PBS or Hank's balanced salt solution, HBSS, Ca^{2+} and Mg^{2+} free) with or without antibiotics. Olfactory mucosa OECs are surrounded with primary olfactory neurons and fibroblasts, whereas olfactory bulb OECs are more associated with fibroblasts and astrocytes both *in vitro* and *in vivo* (Mayeur et al., 2013). Some studies report fibroblast contamination can be reduced by removing the meninges (membranes that envelop the brain and spinal cord of the central nervous system for protection) in the case of the bulb (M. Nadine Goodman et al., 1993). The olfactory epithelium containing the olfactory neurosensory cells and the supporting and basal cells can be dissected away from the mucosa (Jani & Raisman, 2004). Afterwards the tissue is washed with HBSS, sliced and incubated with a digesting solution of trypsin or dispase for 15-30 min at

37ºC, centrifuged, added to a solution of collagenase or DNAse, centrifuged again and plated onto coated flasks (laminin or poly-l-lysine) in appropriate medium (Dulbecco's modified Eagle's medium, DMEM) with usually 10% fetal bovine serum (FBS) and 1% Penicillin and Streptomycin (P/S) (M. Nadine Goodman et al., 1993; Pixley, 1992; Ramón-Cueto & Nieto-Sampedro, 1992).

The effect of different culture conditions and its implication on therapeutic treatment have been studied for OECs. Several methods have been explored to enrich OEC populations from the olfactory bulb and mucosa.

Addition of neurotrophins (NT-3, bFGF, NGF, etc…) has been shown to increase the proportion of OEC marker-positive cells (Bianco, Perry, Harkin, Mackay-Sim, & Féron, 2004). One of those growth factors, NT-3, is not produced by OECs (Boruch et al., 2001), but it is by neurons (Sieber-Blum, 1998) and has a reported effect on OEC proliferation comparable to FBS when added two days after initial plating in serum-containing medium (Bianco et al., 2004). Moreover, the addition of growth factors increases proliferation of glial cells (Alexander, Fitzgerald, & Barnett, 2002; Bianco et al., 2004; M. . I. Chuah & Teague, 1999).

OECs adhere slower than fibroblasts or other contaminating cells like endothelial cells that exist within the olfactory bulb and mucosa. Differential adhesion to tissue culture plastic is used as a strategy to remove mainly fibroblasts (Kawaja, Boyd, Smithson, Jahed, & Doucette, 2009). Some

studies also used cytotoxic elimination of fibroblasts (Richter, Westendorf, & Roskams, 2008) and sensitivity to trypsin (Pellitteri et al., 2014). Other simple method for purification is the addition of anti-mitogens like Cytosine β-D-arabinofuranoside (AraC), a cell killing agent constituted by a cytosine base and arabinose a sugar very similar to the deoxyribose constituent of DNA which allows it to incorporate the DNA and disrupt cell division removing the fast dividing, contaminating fibroblasts (Pellitteri et al., 2014; Vincent, Taylor, Choi-Lundberg, West, & Chuah, 2005).

More refined purification methods described previously were based on p75NTR and Thy1.1 expression by OECs (Franssen, De Bree, Essing, Ramón-Cueto, & Verhaagen, 2008; Guérout et al., 2010) like immunopanning (Ramón-Cueto & Nieto-Sampedro, 1994), mediated complement lysis and FACS (Jahed et al., 2007; Ramón-Cueto & Nieto-Sampedro, 1994; Richter, Fletcher, Liu, Tetzlaff, & Roskams, 2005; Rizek & Kawaja, 2006).

Nonetheless such methods do not exclude the possibility of contamination by Schwann Cells since they also express p75NTR (Dechant & Barde, 2002; K R Jessen et al., 1990; Kristjan R. Jessen & Mirsky, 2005; Z. Liu et al., 2015).

The variety of markers co-expressed by these cells and their contaminants makes it challenging to create a panel to identify them. Markers shared with fibroblasts and Schwann cells in particular complicates purification. Rat mucosal cells purified for p75NTR (98%) cultured for 4 days

had 74-85% of p75NTR–positive cells staining for fibronectin, a marker usually associated with fibroblasts (Kueh, Raisman, Li, Stevens, & Li, 2011).

The lack of alternatives to the use of bovine serum in cell culture creates yet another challenge to the sustainable, viable and accessible production of an autologous or allogeneic OEC cell therapy. Also as the central nervous system lacks oxygen (Erecińska & Silver, 2001), studying its effect on OECs is important to assure cell survival and potency at the site of injury.

In 2007 Zhao *et al.* tested the hypoxia and serum deprivation paradigm in rat OECs to evaluate ischemic damage. OECs went through a caspase-dependent apoptosis and a pan-caspase inhibitor specifically blocked the cell death. Pellitteri et al. 2014 studied mouse OEC culture at low oxygen, using neonatal rat olfactory bulb cells cultured in serum- and/or growth factors-supplemented media and created the low oxygen environment by upturning the glass coverslips where the cells were on. It was shown that low oxygen conditions lead to only 30% of cell viability after one week. OECs, SC and astrocytes were also cultured in serum-free conditions for one week. OECs displayed a flat morphology and the number of both OECs and astrocytes was much lower (about 80%) than that of cells grown in serum, whereas the number of SCs showed an increase. OEC viability was rescued by bFGF under serum-deprived conditions. The same was showed later where serum deprivation resulted in modified morphology, reduced cell survival and marker expression (Pellitteri, Cova, Zaccheo, Silani, & Bossolasco, 2016). Growth factor addition to the serum free medium

condition also had a positive effect on survival and restored basal marker expression.

A study using serum-free media to grow dog OECs showed an increase in the proportion and absolute p75NTR positive cell numbers when compared to a 10% serum media control (Ito et al., 2007). It can be argued however that the increased numbers included contaminant Schwann Cells and therefore do not correspond necessarily to an increase in OECs proportion or numbers. The authors also switched to standard media because preliminary data suggested cell multiplication was inhibited in serum-free conditions after two weeks. A combination of serum-free media for 14 days and standard media for 7 days was used to yield sufficient transplantation cell numbers in adult dogs (~5 x 10^6 cells).

Genetic profiling

To understand the biological mechanisms underlying OECs course of action in neuronal lesions and since OECs have such complex expression patterns, several studies were made to unveil the gene expression of OECs in comparison with other glial cells (Schwann cells and Astrocytes) (Franssen et al., 2008; Ruitenberg, Vukovic, Sarich, Busfield, & Plant, 2006; Vincent, Taylor, et al., 2005), between bulb and mucosa (Guérout et al., 2010; Kueh et al., 2011) and how it may affect its regenerative properties (Franssen et al., 2008; Pastrana et al., 2006).

Although similar, OECs, Astrocytes and Schwann cells differentially express many genes, namely the ones involved in wound healing, ECM

formation, and cellular adhesion (Franssen et al., 2008; Vincent, Taylor, et al., 2005). Moreover it is interesting to note other features of OECs that can be inferred from their transcripts (Vincent, Taylor, et al., 2005) and confirmed by posterior studies like an antimicrobial function (Chuah M.I., 2011; Leung et al., 2008; Panni et al., 2013) and a positive effect on immune response and inflammation (Ebel, Brandes, Radtke, Rohn, & Wewetzer, 2013; Harris, West, & Chuah, 2009; Zhida Su et al., 2013).

Comparing olfactory mucosa and bulb, it has been shown that mucosal cells express more extracellular matrix (ECM) regulating genes, in particular the matrix metalloproteinase (MMPs) important for migration process in interaction with ECM (Guérout et al., 2010). This seems to be in accordance with previous studies when MMP was suggested to be associated with neurite outgrowth promoting potential (Pastrana et al., 2006). Mucosal OECs also preferably express genes related to collagen and fibronectin. All evidence indicates that OECs from mucosal origin are more prone to regulate ECM suggesting an explanation to mucosal OECs migratory capacities described *in vivo*. OECs from bulbar origin overexpressed genes relating to inflammation, namely pro-inflammatory processes haematopoiesis and angiogenesis. Furthermore, bulbar OECs expressed CXCR4 gene a chemo-attractant for a number of cells namely stem cells for which is known to have a significant part in stem cell endogenous trafficking (Peled et al., 1999). All these factors taken together indicate that mucosal and bulbar OECs exhibit distinct gene expression patterns, which suggests that they may be involved in different physiological processes. Bulbar OECs

had genetic expression more related with in specific nervous system development processes and mucosal with the establishment of wound healing process and ECM regulation (Guérout et al., 2010).

There is also a study comparing two populations of p75NTR-positive bulbar OECs: a population with high expression of p75NTR and a population with low expression of p75NTR. The high expression population seems to express genes related with ECM and cell sorting while the low expression population expresses more genes related with axonal guidance and inflammation regulation (Honoré et al., 2012).

Immunocytochemistry

OECs also express several plasma membrane and cytoskeleton proteins, neurotrophic factors (Pellitteri, Spatuzza, Stanzani, & Zaccheo, 2010; Ramón-Cueto & Avila, 1998) and ECM molecules (Pellitteri et al., 2010; Yang et al., 2014). Universal markers for OECs (i.e. independent of the species of origin) are p75NTR, S100β and GFAP. Although inconsistently all these markers are expressed at some point in culture for most species. Nevertheless there is not a specific marker that OECs express consistently since the immunocytochemistry of OECs varies *in vivo* or *in vitro* (Ramón-Cueto & Avila, 1998), with animal species (Pellitteri et al., 2010), with cell source (olfactory bulb or mucosa) (Higginson & Barnett, 2011; Jani & Raisman, 2004; Kueh et al., 2011), donor age (embryonic, postnatal or adult), if it is a cell line (Pixley, 1992; Ramón-Cueto & Avila, 1998; Ramón-Cueto & Nieto-Sampedro, 1992), culture conditions (e.g. with or without serum and growth factors) (Pellitteri et al., 2010; Ramón-Cueto & Avila,

1998), time in culture (Jani & Raisman, 2004; Ramón-Cueto & Avila, 1998) and if there was an injury (Barber & Dahl, 1987; Rubén López-Vales, García-Alías, Forés, Navarro, & Verdú, 2004). Although it is known that OEC expression varies with animal species (same group of markers but expressed differently) there has not been a study at this point comparing the different expression profiles between the most studied species: rat, dog and human.

There is several studies performed in rat tissue sections that reveal the OECs' phenotype during development and in adulthood. It appears that OECs play an important role during neuron development and in post-natal stages as it expresses growth factors, hormones and membrane proteins, like platelet-derived growth factor, neuropeptide Y and S100β, respectively, related to cell growth and survival in various systems. It also expresses L-NGFR (Physiologic affinity nerve growth factor receptor or p75NTR neurotrophin receptor) a receptor of neutrophins, a type of neurotrophic factors, growth factors responsible for growth and survival of developing neurons and maintenance of matures ones (Hapner, Boeshore, Large, & Lefcort, 1998). Cell adhesion molecules (CAM) such as Laminin, L1 (or L1CAM) and NCAM are also expressed by OECs and are related to axonal growth (Ramón-Cueto & Avila, 1998).

OECs most abundant intermediate filament is vimentin (Ramón-Cueto & Avila, 1998), the major component of mesenchymal stem cells (Leader, Collins, Patel, & Henry, 1987), during development and in adulthood. Other component of OECs cytoskeleton is nestin, an

intermediate filament found in dividing cells in developing stages (Michalczyk & Ziman, 2005), in embryos and neonates. Other markers used to characterize OECs were GAP-43 a phophoprotein associated with growth expressed in immature neuron at all ages, anti-galactocerebroside (Gal C) which marks oligodendrocytes and Schwann cells, O4 which recognizes an antigen on the surface of cells of O-2A lineage (type 2 astrocytes, oligodendrocytes, and their precursors), HNK-1 (Human Natural Killer-1), which is known to label O-2A lineage cells and Schwann cells and 1E8, an early marker for Schwann cell linage and mature myelinating and non-myelinating Schwann cells in mature chickens (Bhattacharyya et al., 1991; Ramón-Cueto & Avila, 1998). Only O4 and 1E8 seem to be expressed by ensheathing glia (Ramón-Cueto & Avila, 1998). O4 expression was lost however when rat neonatal olfactory bulb cells were cultured showing that O4 is not a true expression since the labelling is due to axonal fragments presented by OECs when freshly dissected from the bulb. This is a result of OECs' strong phagocytosis of axonal debris (Wewetzer, Kern, Ebel, Radtke, & Brandes, 2005).

Cultured OECs from embryonic origin presented immunoreactivity against S100β, considered a glial-specific marker expressed mostly by astrocytes (Donato, 1986) and nestin. L-NGFR (or p75NTR) is expressed by part of this cells and GFAP by very few (Ramón-Cueto & Avila, 1998).

OECs from neonates vary greatly their expression with culture conditions and time in culture. Regardless the culture media, all 1-day-old OECs cell culture are positive for nestin, vimentin, N-CAM related to cell to

cell and cell to matrix adhesion during development, regulation of neuron interactions and neurite outgrowth (Rønn, Hartz, & Bock, 1998), S100β, Ran-2, a glial lineage marker recognized by non-myelinating Schwann cells and astrocytes (K R Jessen & Mirsky, 1984; Salzer, Lovejoy, Linder, & Rosen, 1998), A5E3, a non-myelin forming Schwann cell marker (K R Jessen & Mirsky, 1984), O4 and 7B11A6-C7 monoclonal antibody (M. N. Goodman, Silver, & Jacobberger, 1993), a marker for astrocytes and their precursors (Szigeti & Miller, 1993). Nevertheless, in cultures with media containing serum, a few cells express GFAP (14%), polysialic acid (PSA) (48%) and L-NGFR (or p75NTR) (2%). No cells stain for anti-GD3, A2B5, HNK-1, which are markers for O-2A progenitors and cells of the O-2A lineage (Card & Pfeiffer, 1990; Hardy & Reynolds, 1991; R. H. Miller, Ffrench-constant, & Raff, 1989; Raff & Miller, 1983), Gal-C (which marks oligodendrocytes and Schwann cells) (K. R. Jessen & Mirsky, 1991; Mirsky et al., 1980) or A4 (a marker of neural tube derivatives)(R. H. Miller, Williams, Cohen, & Raff, 1984). With serum removal, most cells express GFAP (94%) but continue to express markers described before (vimentin, nestin, S100β, N-CAM, Ran-2, A5E3, 7B11A6-C7, PSA, L-NGFR). Later with 7 days or 3 weeks in culture OECs maintain their immunocytochemical properties apart from O4, GFAP and p75NTR (or L-NGFR). In serum-free media all cells exhibit GFAP immunolabelling with two identifiable populations, and very few (5%) O4 positive cells. L-NGFR expression increases after 7 days in culture until all cells express it in long term cultures.

Both in serum containing and serum-free media there is two populations of rat OECs: Astrocyte-like and Schwann-cell like immunolabelled for S100β and p75NTR. In serum free media Schwann cell-like OECs also express PSA (Polysialic acid) and p75NTR (Franceschini & Barnett, 1996).

Cultured adult rat OECs also express GFAP and vimentin in their filaments, L1, Laminin and fibronectin adhesion molecules and p75NTR. They do not seem to express some of the markers for oligodendrocytes, microglial cells, astrocytes, Schwann cells or O-2-A lineage cells (Ramón-Cueto & Nieto-Sampedro, 1992; Ramón-Cueto, Pérez, & Nieto-Sampedro, 1993).

OEC cell lines made from neonatal and adult donors by retroviral infection and one by spontaneous immortalization have a similar immunoreactivity to long-term cultures: GFAP and vimentin in their filaments and p75NTR and S100β on their membranes, except from one adult OEC that did not express p75NTR. All adult OECs cell lines, but the retroviral infection derived one also expressed 7B11A6-C7. Similarly to mortal cell cultures spontaneous immortalized cells yield ECM molecules such as laminin and N-CAM (Kueh et al., 2011; Ramón-Cueto & Avila, 1998).

Morphology

The morphology of olfactory ensheathing cells *in vivo* varies between a flat, stellate astrocyte-like shape and a spindle-like shape typical of Schwann cells. The proportion of each type of cell varies *in vitro*, with culture

conditions (time, media composition, co-culture, etc...), developmental stage, anatomic origin (olfactory bulb or mucosa) (Ramón-Cueto & Avila, 1998) and animal species (Pellitteri et al., 2010). In terms of ultrastructure, OECs exhibit the same appearance *in vivo* and *in vitro* and have a less electron-dense cytoplasm when compared with Schwann Cells (R. Doucette, 1989).

In the developing olfactory system, neural crest cells can be found closely associated with the olfactory nerve at early stages of embryonic development of chickens expressing Sox10 which regulates the expression of the myelin-related gene P0 (Chan, Wong, Lui, Tam, & Sham, 2003). In later stages cells and processes expressing OEC markers P0 and $p75^{NTR}$ are associated with olfactory axons in the lamina propria and ensheathing bundles of axons in the olfactory nerve (Barraud et al., 2010). OECs also seem to have two different cytoplasmic electron densities, suggesting the existence of unique OEC subpopulations (Cuschieri & Bannister, 1975). Some of them became spindle shape and are considered mature cells whilst others remain round and are most likely OEC progenitors that later differentiate into mature cells (Valverde, Santacana, & Heredia, 1992). In the adult, these cells acquire a spindle shape and mingle with neuronal axons ensheathing them from the olfactory mucosa back to the olfactory bulb (Raisman, 1985; Valverde & Lopez-Mascaraque, 1991).

Cultures from the olfactory epithelium, lamina propria, olfactory nerves, and outer olfactory bulb layer of embryonic, neonatal or adult rats and mice exhibit varied OEC morphologies, including flat, bipolar and

tripolar (E. Au & Roskams, 2003; R. Doucette, 1993; Fracek, Guo, & Schafer, 1994; Pixley, 1992; Ramón-Cueto & Nieto-Sampedro, 1992; Rakesh J. Sonigra, Brighton, Jacoby, Hall, & Wigley, 1999; Van Den Pol & Santarelli, 2003; Vincent, West, & Chuah, 2003).

Cells from embryonic origin present a different morphology when cultured in serum containing media or serum-free media. The former media produces flat multipolar cells and the latter spindle bipolar or multipolar cells (R. Doucette, 1993). Cultures from olfactory epithelium from neonatal rodents exhibit various morphologies with and without serum supplement. In serum-containing media most cells are flat with a large cytoplasm (Barber & Lindsay, 1982), although there is some multipolar with long processes (M. I. Chuah & Au, 1991; Pixley, 1992, 1996). Serum-free media, however seems to increase the number of bipolar or multipolar cells (Pixley, 1992, 1996). Unlike the olfactory epithelium, cultures from the neonatal olfactory bulb in serum appear mostly flat and fibroblast-like (S.C. Barnett, Hutchins, & Noble, 1993; Franceschini & Barnett, 1996). Without serum the population of cells splits into two types: fibroblast-like and spindle shape.

OECs also change morphology in contact with neurons. However it is highly dependent on contact points with axons and independent on donor age or culture conditions (M. I. Chuah & Au, 1991; Devon & Doucette, 1992; Gong, Liu, Srodon, Foster, & Shipley, 1996; Ramón-Cueto et al., 1993). In co-culture with neurons OECs became spindle shape and are able to enfold them individually, contrarily to the situation *in vivo*. Moreover, when

ensheathing dorsal root ganglion neurons, myelinated *in vivo*, they are able to myelinate them as well (Devon & Doucette, 1992).

Several cell lines of OECs have been created by different research groups. With cell lines of the olfactory nerve from adult rat bulb created by retroviral infection each group had a different morphology: flat morphology with some spindle shape ones at physiologic density and aggregates of spindle shape ones at higher density (Franceschini & Barnett, 1996) and bipolar elongated morphology capable of multilayer growth. (M. N. Goodman et al., 1993). Another group spontaneously immortalized cells from the olfactory nerve of the bulb of adult rat and cells became cobblestone shape growing in sheets in a serum-containing media. Just like non-immortalized cells, cells from cell lines line up with axons in a spindle shape (R J Sonigra, Kandiah, & Wigley, 1996).

Heterogeneity and Plasticity of Olfactory Ensheathing Cells

Since they were discovered it is known that OECs are a unique heterogeneous population of cells (Higginson & Barnett, 2011) based on differentially expressed markers which vary with time and culture conditions and donor age (Barber & Lindsay, 1982; Pixley, 1992) and with particular features in common with several cells and a remarkable plasticity.

Although many studies have reported heterogeneity amongst OECs, comparison between studies is difficult as different research groups used different culture conditions, cell source and OEC characterization (Alexander et al., 2002; Barber & Lindsay, 1982; M. I. Chuah & Au, 1993; Pixley, 1992).

A review from 2005 (Vincent, West, & Chuah, 2005) points out however that the data so far suggests more of an intrinsic plasticity of OECs than heterogeneous interchangeable subpopulations. *In vivo* uniform structure in all the olfactory nerve layer (W. W. Au, Treloar, & Greer, 2002; R. Doucette, 1989; Valverde et al., 1992); modulation of OEC markers expression such as p75NTR by environmental stimuli like axonal contact (Ramón-Cueto et al., 1993; Vickland, Westrum, Kott, Patterson, & Bothwell, 1991; Wewetzer et al., 2005) and *in vitro* morphological flexibility (Van Den Pol & Santarelli, 2003; Vincent et al., 2003) and following transplantation into injured CNS tissue (Vincent, West, et al., 2005) support these observations.

Permissive environment

Growth factors have an essential role on mammalian cell development and maintenance. Secreted by producer cells, they induce functional responses in surrounding cells. These responses can include cell proliferation, migration or differentiation (*www.nlm.nih.gov/cgi/mesh/2011/MB_cgi?mode=&term=Growth+Factors*, accessed 28/05/2015). A class of growth factors called neurotrophic factors is responsible for the growth, regeneration and maintenance of neurons. Most of them belong to one of three families: Nerve Growth Factor or neurotrophins, glial cell-line derived neurotrophic factor family ligands and neuropoietic cytokines. Although activating different neural cells pathways there is some degree of overlay (J. G. Boyd & Gordon, 2003). The neurotrophin family includes nerve growth factor (NGF), brain-derived

neurotrophic factor (BDNF), neurotrophin 3 (NT-3), 4 (NT-4, also known as NT-5 and NT-4/5) and 6 (NT-6) and neurotrophin-7 (NT-7) that were only found in some teleost fish species (Bartkowska, Turlejski, & Djavadian, 2010). The Glial cell line-Derived Neurotrophic Factor family ligands consists of Glial cell line-Derived Neurotrophic Factor (GDNF), neurturin (NRTN), artemin (ARTN), and persephin (PSPN) (Airaksinen & Saarma, 2002). The interleukin-6 (IL-6), IL-11, IL-27, leukaemia inhibitory factor (LIF), ciliary neurotrophic factor (CNTF), cardiotrophin 1 (CT-1), neuropoietin and cardiotrophin-like cytokine (CLC; also known as novel neurotrophin 1 (NNT1) and B cell stimulating factor 3, BSF3) belong to the neuropoietic cytokine family (Bauer, Kerr, & Patterson, 2007).

Neurotrophic factors effect on neurons have been studied based on neuronal cell survival, phenotypic maintenance and neurite outgrowth both individually and in combination with other neurotrophic factors *in vitro* (Hartnick et al., 1996; D. M. Jones, Tucker, Rahimtula, & Mearow, 2003; Stoop & Poo, 1996) and *in vivo* (Averill et al., 2004; J. Boyd & Gordon, 2003; E. T. Cheng et al., 1998; Lewin, Utley, Cheng, Verity, & Terris, 1997; McCallister, Tang, Smith, & Trumble, 2001). A study from 2006 (Deister & Schmidt, 2006) used a combination of 50 ng/mL of NGF and 10 ng/mL of GDNF and CNTF on neonatal rat Dorsal Root Ganglion (DRG) which increased the neurite outgrowth in 752% when compared with untreated cells.

The observation of OEC production of several Neurotrophic factors and ECM molecules suggests the creation of an environment that either enhances or does not prevent neuron regeneration. There is several studies

reporting OECs' effect on axonal regeneration and remyelination (J. G. Boyd, Doucette, & Kawaja, 2005; Franklin, 2003) and trophic support after injury through neurotrophic factors also used as an autocrine and paracrine effect (Boruch et al., 2001; Chung et al., 2004; Lipson, Widenfalk, Lindqvist, Ebendal, & Olson, 2003; M. Teresa Moreno-Flores, Díaz-Nido, Wandosell, & Avila, 2002; Wewetzer, Grothe, & Claus, 2001; Woodhall, West, & Chuah, 2001). Nevertheless there is still plenty of controversy on what sub-populations comprise the OEC population and on how exactly they act to regenerate neurons as each study uses different methods to purify the cell population for the end application.

Besides the production of neurotrophic factors OECs are known to produce ECM and adhesion molecules involved in cell differentiation, cell growth and enzyme activity regulation (Y. Liu et al., 2010), affecting neurite outgrowth (M. I. Chuah & Au, 1994; Tisay & Key, 1999) and early neuronal development (Crandall et al., 2000). Nonetheless it has been suggested that the adhesion molecules that promote neurite outgrowth might not be the same as for astrocytes: L1 (also called L1CAM), N-cadherin and NCAM (M. I. Chuah, David, & Blaschuk, 1991; Tisay & Key, 1999).

Myelination

OECs share many features with Schwann cells and astrocytes including myelination.

Although OECs do not ensheath neurons in the olfactory system, because of its small diameter, they are able to do so *in vivo* if placed in

environments where axons have a bigger diameter (more than one micron) (Franklin, 2003). This feature was observed in an *in vitro* model of rat embryo Dorsal Root Ganglia (DRG) with dissociated embryo cells (Devon & Doucette, 1992, 1995) however cultured OECs failed to express myelin associated markers (S.C. Barnett et al., 1993; Devon & Doucette, 1995). Conversely, cultured postnatal and adult rat bulb OECs were shown to myelinate DRG neurons (Babiarz et al., 2011).

An OEC line (Franceschini & Barnett, 1996) was used to make sure the cells myelinating the neurons were not contaminant Schwann cells as clonality can be proved. The cell line was transplanted into demyelinated axons in rat spinal cord and myelinated them with P0-positive myelin sheaths (Franklin, Gilson, Franceschini, & Barnett, 1996). Nevertheless when transplanted into optical nerve fibres, also CNS, although enabling regeneration of severed retinal ganglion cell axons through the graft region none of the regenerating axons are ensheathed by the transplanted cells neither the regenerating axons became myelinated by either central or peripheral type myelin (Ying Li, Li, & Raisman, 2007). OECs were also shown to move into the focal demyelinated lesion and remyelinate local axons with a peripheral type of myelin (Lankford, Sasaki, Radtke, & Kocsis, 2008).

On the other hand when using OECs in contact with oligodendrocytes to myelinate CNS neurons *in vitro* neurite ensheathment, myelination or oligodendrocyte process extension was decreased when compared with culture on neurosphere-derived astrocytes monolayers (Sorensen, Moffat, Thomson, & Barnett, 2008). Comparatively OECs do not inhibit

oligodendrocyte myelination through a heat labile factor(s) like SC (Lamond & Barnett, 2013).

There are several studies showing OECs myelination potential on different kinds of neurons *in vitro* and *in vivo*. Olfactory ensheathing cells from E18 rat embryos (Devon & Doucette in 1992) and from juvenile and adult rats (Babiarz et al., 2011) can myelinate larger axons in dorsal root ganglion neurites *in vitro*. A study from 1996 (Franklin et al., 1996) provides the first evidence that rat olfactory bulb-ensheathing cells are able to produce peripheral-type myelin sheaths around axons of suitable size *in vivo* in a rat model for SCI with X-irradiation and ethidium bromide injection. A similar study in 2000 proved that human OECs were also capable of myelinating CNS axons *in vivo* in a rat model for SCI (S. C. C. Barnett et al., 2000). Transplanted OECs' myelinating properties are well stablished as well as their intrinsic myelinating potential and how this can be augmented by the presence of meningeal cells (Franklin, 2003). Nevertheless the mechanisms by which they promote myelination are not well defined with several studies defying the notion that OECs have a direct influence in the process. There is the claim that OECs instead stimulate axon regeneration and functional recovery indirectly by enhancing the entrinsic ability of host Schwann cells to invade the damaged spinal cord (J. G. Boyd et al., 2005).

Other study in a rat model of SCI with X-irradiation and ethidium bromide injection demonstrated that besides forming myelin, transplanted GFP-OECs creates a promoting environment for development and maturation of nodes of Ranvier and the restoration of impulse conduction

in central demyelinated axons (Sasaki et al., 2006). Yet depending on the assay OECs perform differently to Schwann cells when it comes to myelination. OECs transplanted into the optic nerve induced regeneration of the severed retinal ganglion cell axons in the graft region, but failed to myelinate them. In contrast a considerable number of the regenerating axons became myelinated by peripheral type myelin produced by transplanted Schwann cells (Ying Li et al., 2007).

Interestingly, there is *in vitro* data indicating that OECs allows neurite extension and oligodendrocyte proliferation, but lacks secreted factor(s) and possible cell-cell contact that is necessary for oligodendrocyte process extension and axonal myelination (Sorensen et al., 2008).

Phagocytic Activity of Olfactory Ensheathing Cells

It is known that macrophages (Graziadei & Graziadei, 1979) and supporting cells (Yuko Suzuki, Takeda, & Farbman, 1996) are part of the olfactory system phagocytising dead cell bodies (Y Suzuki, Schafer, & Farbman, 1995). It has been recently discovered that OECs do not only share features with Schwann cells and astrocytes but also with other type of glia: microglia. It has been described that part of OEC function of allowing neural regeneration is to phagocyte cell debris just like microglia does in the CNS (brain and spinal cord).

OECs clear the lamina propria and olfactory bulb from axonal debris (Chuah l., Tennent, & Jacobs, 1995; Zhida Su et al., 2013). A 2008 study showed that OECs extended significantly more pseudopodia when they were exposed to *Escherichia coli* than in the absence of bacteria (Leung et al., 2008). Later in 2013 Panni et al. observed the ability of mouse OECs and Schwann cells from the trigeminal nerve and dorsal root ganglia glia to phagocytose *Escherichia coli* and *Burkholderia thailandensis in vitro*. They found that all three sources of glia were equally able to phagocytose *E. coli* with 75-85% of glia having phagocytosed bacteria within 24h. They also show that human OECs phagocytosed *E. coli*. In contrast, the mouse OECs and Schwann cells had little capacity to phagocytose *B. thailandensis*.

In 2013 OECs were identified by Su et al. 2013 to exist in two different states, resting and reactive, in which resting OECs functioned as phagocytes for cleaning apoptotic olfactory receptor neurons' debris. Notably, engulfment of olfactory nerve debris by OECs was found in

olfactory mucosa under normal turnover and was significantly increased in the animal model of olfactory bulbectomy, while little phagocytosis by microglia/macrophages was observed. Also during early development OECs are the main phagocytic cells that remove axon debris during early development of the olfactory system (Nazareth et al., 2014). Other study in 2014 showed that OECs can engulf an amount of degenerated neuron debris and this phagocytosis can make a substantial contribution to neuron growth (B. R. He, Xie, Wu, Hao, & Yang, 2014). These results suggest a cellular and molecular mechanism by which ORNs debris are removed during olfactory nerve turnover and regeneration and OEC role in the repair of traumatic CNS injury and neurodegenerative diseases.

Migratory Features of Olfactory Ensheathing Cells

OECs' role in neuron regeneration is to improve neuron survival and promote axonal growth. Since olfactory neurons cross the frontier between PNS and CNS from the olfactory mucosa to the olfactory bulb the extension of their growth is accompanied by OECs that migrate along with the neuronal axons longitudinally and laterally in the injured CNS (Ramón-Cueto & Avila, 1998). Although it is well established that OEC migration enhances axonal extension after injury, little is known of its mechanisms and the extension to which they migrate is controversial.

Some studies identified several factors that influence OEC migration. Lysophosphatidic acid (LPA) was observed to stimulate proliferation and migration of OECs. It also induced actin cytoskeleton reorganization and focal adhesion assembly (H. Yan, Lu, & Rivkees, 2003).

OECs migration *in vitro* was demonstrated to be GDNF-induced depending on GFRα1 and RET receptor, and activation of JNK and SRC signalling cascades. GDNF was found to promote implanted OECs migration in a spinal cord hemisection injury model (Cao et al., 2006). Windus et al. 2007 reported that lamellipodial protrusions, cytoskeletal protein actin projections on the leading edge of the cell, were critical on OECs migration and were dependent of glial cell line-derived neurotrophic factor and inhibitors of the JNK and SRC kinases. BDNF was also shown to promote the migration of cultured OECs requiring TRPCs for BDNF-induced OEC migration (Y. Wang et al., 2016).

It has also been described that recombinant Nogo-66 enhanced the adhesion of OECs and inhibited their migration (Zhida Su et al., 2007). In fact rodent OECs express all the components of the Nogo receptor complex and that their migration is blocked by myelin. The same group was also able to relate the decrease of traction force of OEC with lower migratory capacity over myelin, which correlates with changes in the F-actin cytoskeleton and focal adhesion distribution. OEC traction force and migratory capacity is enhanced after cell incubation with the Nogo receptor inhibitor NEP1-40 which confirms Nogo's role in cell migration (Nocentini et al., 2011). In fact, Nogo is a known receptor of MAI (myelin associated inhibitors) (Fournier, Gould, Liu, & Strittmatter, 2002; X. L. He et al., 2003) abundant in the glial scar (Geoffroy & Zheng, 2014).

TNF-alpha was found to be released by reactive astrocytes in glial scar and attract OECs migration by interacting with TNFR1 expressed on

OECs via regulation of ERK signalling (Zhida Su et al., 2009). This effect on migration of OECs towards reactive astrocytes could suggest a guidance mechanism to the glial scar leading to OEC-mediated axon regrowth in the spinal cord lesion.

A 2008 study found that distinct OEC subpopulations displayed different migratory properties and attractive migratory responses to a gradient of LPA using time-lapse imaging of single cells and single migration assays, respectively (Huang et al., 2008).

Lamina Propria (LP) and Olfactory Bulb (OB) OECs exhibit intrinsic biological differences in proliferation and migration that, after transplantation into the lesioned CNS, result in differences in spinal cord neuropathology and anatomical and behavioural regeneration outcomes that also vary depend on the transplantation method. Lamina propria OECs showed an increased mitotic rate and migratory ability *in vitro* and *in vivo* in rat showing an ability to migrate within the spinal cord, reducing cavity formation and lesion dimensions, and differentially stimulate outgrowth of axonal subpopulations compared with OB OECs (Richter et al., 2005).

OECs migratory responses are also dependent of the type of spinal cord lesion. Although extensively described OECs migration seems to be restricted or non-existent in a number of models for spinal cord injury varying with the methods used (M. R. Andrews & Stelzner, 2007; Collazos-Castro, Muñetón-Gómez, & Nieto-Sampedro, 2005; Lee et al., 2004; P. Lu et al., 2006; Maria Teresa Moreno-Flores & Avila, 2006; Damien Daniel Pearse

et al., 2007; Ramer et al., 2004). The location of transplantation is one of them varying from the injury site (Collazos-Castro et al., 2005; Damien Daniel Pearse et al., 2007; Ramer et al., 2004; Richter et al., 2005), outer injury site (Damien Daniel Pearse et al., 2007; Reginensi et al., 2015; Richter et al., 2005) or both (M. R. Andrews & Stelzner, 2007; Maria Teresa Moreno-Flores & Avila, 2006).

There has been reports where OECs transplanted into uninjured spinal cord (C. Deng et al., 2006; Lee et al., 2004) and X-radiated SC (T Imaizumi, Lankford, Waxman, Greer, & Kocsis, 1998; Lankford et al., 2008) and brain (Lankford, Brown, Sasaki, & Kocsis, 2014) exhibited migration. SCs and OECs transplanted into the contused adult rat spinal cord were unsuccessful in migrating from the lesion but OEC delivery outside of the injury resulted in the migration of a small number of them into the SC-injected injury site. Also host axons were seen in association with or ensheathed by transplanted glia (Damien Daniel Pearse et al., 2007). Freshly isolated GFP-expressing adult rat olfactory bulb-derived OECs and SCs were transplanted into normal and X-irradiated spinal cords. Both glial cells showed little survival and migration in normal spinal cord at 3 weeks. However, OECs, unlike SCs, widely migrated in both grey and white matter of the X-irradiated spinal cord (T Imaizumi et al., 1998), and exhibited a phagocytic phenotype with OX-42 expression on their processes (Lankford et al., 2008).

Nonetheless OECs transplanted into a transected spinal cord and followed by magnetic resonance imaging (MRI) were unable to cross the

fissure in the spinal cord although travelling a short distance, half that in normal spinal cord (Lee et al., 2004). There is also reports of shorter distances (≤1mm) (C. Deng et al., 2006; Ramer et al., 2004; Reginensi et al., 2015; Richter et al., 2005).

In a hemisection model done on the opposite side of the body and some mm rostral to the transfer site, OECs migrated extensively although less than in an uninjured spinal cord (C. Deng et al., 2006). Other study reports migration from sites rostral and caudal to the injury site with lamina propria OECs performing better than olfactory bulb OECs (Richter et al., 2005). There seems to be little OECs migration along the dorso-ventral axis after injection in various locations 1mm caudal and rostral to the injury (Maria Teresa Moreno-Flores & Avila, 2006). Moreover limited migration was also described in a subsequent study (M. R. Andrews & Stelzner, 2007). Nonetheless in a SCI contusion model the rostral and caudal migration increased for OECs secreting NOGO receptor ectodomain to reduce MAI-associated inhibition (Reginensi et al., 2015). MAI is one of the components of the glial scar (Geoffroy & Zheng, 2014). Mostly OECs tend to migrate better in uninjured spinal cords. They are able to migrate to the lesion but fail to migrate out and cross the gap in some contexts when transplanted to the center of the injury site.

Previous results support the notion that the majority of the factors inhibiting axon elongation and regrowth after lesion might also influence OEC migration (Reginensi et al., 2015). Actually all the inhibitors of OEC migration are present in the glial scar after injury (NogoA, CSPGs, fibulin-3

and Slit2) (Cregg et al., 2014; Z. He & Koprivica, 2004; Lukovic et al., 2014; Nocentini et al., 2012; Reginensi et al., 2015; Vukovic et al., 2009).

Spinal Cord Injury

Spinal cord injury (SCI) is defined as any sort of damage to the spinal cord or its elements leading to the deficiency or loss, either temporary or permanent, of motor and/or sensory and/or autonomic function in the segments of the spinal cord due to damage of neural elements within the spinal cavity. Patients with spinal cord injury usually have permanent and often devastating neurologic deficits and disability. The classification of SCI is broad. It depends of the site of injury, of what it affects or if it is partial or complete injury. The more commonly used terms to classify any kind of impairment caused by spinal cord injury are paraplegia and tetraplegia. The term tetraplegia (preferred to 'quadriplegia') refers to deficiency or loss of motor and/or sensory function in the cervical (C1 to C7) segments of the spinal cord. Tetraplegia results in impairment of function in the arms as well as in the trunk, legs and pelvic organs. It does not include brachial plexus lesions or injury to peripheral nerves outside the neural canal. Paraplegia refers to impairment or loss of motor and/or sensory function in the thoracic, lumbar or sacral (but not cervical) segments of the spinal cord (Th1 to L5), secondary to damage of neural elements within the spinal cavity. With paraplegia, arm functioning is spared, but, depending on the level of injury, the trunk, legs and pelvic organs may not be spared. The term is not used in referring to lumbosacral plexus lesions or injury to peripheral nerves outside the neural canal (Ditunno, Young, Donovan, & Creasey, 1994). It is

classified usually using the ASIA (American Spinal Injury Association) Impairment scale from A to E, A being complete (no motor or sensory function is preserved in the sacral segments S4-S5) and E normal (motor or sensory function are normal) (Roberts, Leonard, & Cepela, 2017).

Spinal Cord Injuries (SCI) are a major health problem. Every year, between 250 000 and 500 000 people suffer a spinal cord injury worldwide with an estimate of 40 to 80 cases per million population global incidence. It affects predominantly 20 to 29 and over 70 year old males and females between 15 and 19 years old and over 60. There are also studies revelling two times more incidence in men than in women, sometimes even more. (http://www.who.int, 19/02/2015)

SCI patients also have 2 to 5 more mortality risk compared to the general population, especially in the first year after the injury. The mortality rate is closely related to access to proper and readily available medical care, being key factors the time between the injury and hospital admission and method of transfer to hospital. Infections due to untreated pressure ulcers are still the leading causes of death of SCI patients in developing countries. (http://www.who.int, 19/02/2015)

Besides physical, social and psychological consequences for the patients and their families, there is also tremendous healthcare costs. It is estimated in the US that the annual direct medical and living expenses costs associated with patients with chronic SCI (ie, > years after injury) varies on average from $71,172 for paraplegia patients to $191,436 for high tetraplegia patients

(Spinal Cord Injury Facts and Figures at a Glance, 2018, https://www.nscisc.uab.edu, accessed 13/04/2019).

Spinal Cord injury Biology

Spinal cord injury is a consequence of a compression damage, bleeding and/ or ischemia, which interferes with the bone component of the spine, the spinal cord and its elements (Ditunno et al., 1994) leading to permanent or temporary impaired or lost motor and/or sensory and/or anatomical function. There is several causes for this injury the most common being bone fracture (Ahuja, Martin, & Fehlings, 2016; Kirke Rogers & Todd, 2016; McDonald & Sadowsky, 2002). Traumatic SCI include features such as axon demyelination as a result of loss of glial substrate due to necrosis, apoptosis and autophagy (McDonald & Sadowsky, 2002; Plemel et al., 2014). SCI can generally be divided into 3 different clinical phases:

1. Acute: Destruction of the blood-brain barrier, modifications to the microvasculature of the grey matter and generation of petechial haemorrhages resulting in neuronal cell death and axonal damage (Gerzanich et al., 2009; Griffiths, Burns, & Crawford, 1978; Losey & Anthony, 2014; Losey, Young, Krimholtz, Bordet, & Anthony, 2014; Yu & Fehlings, 2011) Inflammatory cells have also been detected as early as 3 min after injury (Griffiths et al., 1978; Taoka et al., 1997; Yu & Fehlings, 2011). There is also a loss of ionic regulation that results in loss of nerve impulses and oedema formation. The free intracellular calcium rises which triggers proteases and phospholipases that are involved in the destruction of myelin (Balentine, 1988). Due to the release of glutamate and aspartate there is also

the an excessive excitation of viable neurons and disruption of redox homeostasis leading to the generation of free radicals (Tator & Fehlings, 1991)

2. Subacute: glial activation happens as a result of necrosis, haemorrhage and local ischemia and there is also neuronal and oligodendroglial apoptosis (Spitzbarth et al., 2011; Tator & Koyanagi, 1997; Yu & Fehlings, 2011)

3. Chronic: the degenerative process continues and spreads outside the initial lesion (Gomez, 2009; McDonald & Sadowsky, 2002; Tator & Koyanagi, 1997).

CNS neurons ability to regenerate is radically reduced in adulthood and contributes to their inability to regenerate properly after injury (Blesch & Tuszynski, 2009; Goldberg, Klassen, Hua, & Barres, 2002; Plunet, Kwon, & Tetzlaff, 2002; Seijffers & Benowitz, 2008) and to have poor functional recovery with the exception of a small hypothalamus pathway and olfactory system axons. Adult neurons are incapable of regrowth (Horner & Gage, 2000) due to the presence of an adverse environment that prevents or do not support neuronal regeneration (Cajal, 1991): neurons inherent low expression of genes implicated in axon regrowth/ regeneration (Bomze, Bulsara, Iskandar, Caroni, & Pate Skene, 2001; Hannila & Filbin, 2008), existence of inhibitory factors in the glial scar that develops after the injury (P Bovolenta, Fernaud-Espinosa, Mendez-Otero, & Nieto-Sampedro, 1997; P Bovolenta, Wandosell, & Nieto-Sampedro, 1992; Paola Bovolenta, Wandosell, & Nieto-Sampedro, 1993; Cregg et al., 2014; David & Lacroix,

2003; Sandvig, Berry, Barrett, Butt, & Logan, 2004; Silver & Miller, 2004; Yiu & He, 2006) mainly extracellular matrix (Busch & Silver, 2007; Filbin, 2003; Yiu & He, 2006) and absence of trophic factors for neuroprotection and regeneration (Blesch, Fischer, & Tuszynski, 2012; Hendriks, Ruitenberg, Blits, Boer, & Verhaagen, 2004; Hollis & Tuszynski, 2011; L. L. Jones, Oudega, Bunge, & Tuszynski, 2001; Sharma & Hari Shanker Sharma, 2007).

Moreover every time there is an injury to the CNS it responds with a phenomenon called gliosis. Gliosis consists in several changes involving several cells that act cooperatively at different time points like astrocytes, microglia and oligodendrocytes precursors. The first line of defence in the first hours of injury is the macrophages from blood circulation and the microglia from the underling tissue. In 3-5 days oligodendrocytes migrate to the injury site and if the damage has reach the meninges (membranes that protect the CNS organs) meningeal cells will migrate to cover the exposed CNS tissue. Finally the glial scar is constituted of astrocytes that migrate and proliferate filling the empty spaces and proteoglycans forming a physical barrier (P Bovolenta et al., 1997; Carri, Perris, Johansson, & Ebendal, 1988; Davies, Goucher, Doller, & Silver, 1999; Dou & Levine, 1994; Fawcett & Asher, 1999; Fidler et al., 1999; R J McKeon, Schreiber, Rudge, & Silver, 1991; Robert J. McKeon, Höke, & Silver, 1995; Muir, Engvall, Varon, & Manthorpe, 1989; Niederöst, Zimmermann, Schwab, & Bandtlow, 1999; Smith-Thomas et al., 1994). Actually in most spinal injuries it is more prominent the hypertrophy and increase in the production of cytoskeleton filaments such as GFAP and vimentin by reactive glial cells than its proliferation (Silver &

Miller, 2004). After SCI all reactive macrophages, oligodendrocyte precursor cells and reactive astrocytes change the ECM at the wound producing cytokines, myelin associated inhibitors (MAI) and chondroitin sulphate proteoglycan (CSPG) that strongly prevent axonal growth (L. L. Jones, Margolis, & Tuszynski, 2003; L. L. Jones, Yamaguchi, Stallcup, & Tuszynski, 2002; Snow, Lemmon, Carrino, Caplan, & Silver, 1990). The lesion site forms cystic or trabeculated cavities to which injured neurons incapable to attach (L. L. Jones, Sajed, & Tuszynski, 2003) compromising their growth and morphology. The glial scar serves as an immune response to isolate the site of injury from the rest of the CNS to prevent further damage (Silver & Miller, 2004).

In most cases SCI injury results in neuronal withdrawal with few axons sprouting for small distances. The latter tend to display degenerated and enlarged terminations where they are in contact with the adverse environment. They unsuccessfully produce growth cones resulting in failed regeneration (Knoferle et al., 2010). Therefore unlike the peripheral nervous system, the CNS fails to have an organized microtubules network in growth cones (Smith, Skene, Lichtman, Sanes, & Milner, 1997).

Interestingly, although belonging to the PNS, there is evidence that SC invade and migrate into the injured spinal cord in several animal models (Blakemore, 1975; Bresnahan, 1978; Gilmore & Duncan, 1968; Hirano, Zimmerman, & Levine, 1969; Raine, 1976; Reier, 1994; Takami et al., 2002) including long term human spinal cord injuries (Feigin & Ogata, 1971; Reier, 1994). While only myelinating 5% of remaining sensory axons it was found

that it could still conduct action potentials in adult cat 3-month-old thoracic contusion injury (Blight & Young, 1989).

Spinal Cord Injury effects on the rest of the body and mitigation treatments

A cut in the nerves of the spinal cord means that the communication between the central nervous system and the rest of the body is disconnected or impaired. Depending on the location of the lesion it can affect several body functions like breathing, circulation, muscle tone, autonomic nervous system (control of autonomic functions like heart beating, bladder and bowel function) and sexual function.

Lesions between C1 to C4 vertebras are able to stop breathing and intubation through the nose or throat is necessary even if just temporarily to push oxygen into the lungs and remove carbon dioxide. There can also be difficulties in coughing and freeing the lungs from secretions and special training might be necessary in swallowing and breathing. Also intubated patients have higher risk of pneumonia related to the use of assisted breathing and need to be watched and treated with antibiotics in case of symptom development.

Another problem related to spinal cord injury is bad circulation. Even days after the injury there can appear problems like blood pressure instability, abnormal heart rhythms (arrhythmias) and blood clots. Blood pressure needs to be closely monitored and anticoagulant drugs and compression tights must be used to increase blood flow in the lower legs and feet.

Derived from the nature of the disability itself as the lower limbs stop being used they became rigid (spasticity) and stunted. Also the lack of movement and continuous pressure on the skin leads to pressure sores, regions where the skin breaks. Physiotherapy is advised as treatment for spasticity. Changing position frequently and a good hygiene and nutrition helps prevent pressure sores.

Other consequences of spinal cord injury are neurogenic pain or intense burning caused by various factors. The treatment consists of medications, acupuncture, spinal or brain electrical stimulation and surgery. Also the constant use of the wheelchair leads to shoulder pain in paraplegic patients.

Since the nerves that control organs associated with bladder and bowel functions have their connections to the brain cut down there is no information arriving. Bladder control may be lost and a catheter might be needed for urine removal. Patients might retain bowel function but it might also happen that need to use diapers or adopt other methods to clear their intestines.

Depending on the extension of the trauma and recovery sexual function and fertility might be affected. Specialist can advise patients in the several existent options.

Several SCI patients suffer also from depression due to the dramatic life changes and the new circumstances they have to face living with a disability. Psychological support and several pharmaceuticals might help to

combat depression (http://www.ninds.nih.gov/disorders/sci/detail_sci.htm#268123233, accessed 27/04/2015).

Current research on CNS regeneration

Thus it is urgent to find a safe and effective therapy to cater for CNS axonal regeneration and functional recovery of existing and new neurons. It known that several species, including humans are able to produce neurons in adulthood with a turnover of 4-6 weeks (Ramón-Cueto & Avila, 1998). As CNS injuries and their limited functional recover are very complex the induction of neuronal regeneration making use of their inherent growth potential is a promising option. Due to the great complexity of CNS injuries and functional recovery processes, external interventions are needed, along with the improving injured neuron extrinsic environment, to stimulate some of the remaining intrinsic plasticity of neurons and, thus, to foster the healing of the otherwise non-regenerative CNS.

Recovery from SCI is closely related to its physiopathology, the physiological processes or mechanisms by which the injury develops and progresses (Tator, 1998). Several approaches have been used including providing of neurotrophic factors (L. L. Jones et al., 2001) and cell transplantation (Assinck, Duncan, Hilton, Plemel, & Tetzlaff, 2017; Bunge, 2008; L. L. Jones et al., 2001; M. T. Moreno-Flores & Avila, 2010; Maria Teresa Moreno-Flores & Avila, 2006).

Members of the neurotrophin family, including nerve growth factor (NGF), brain-derived neurotrophic factors (BDNF), and neurotrophin 3 (NT-

3), are capable of supporting survival of damaged CNS neurons both *in vitro* and *in vivo*. They also promote neurite outgrowth, necessary for reorganization of the injured CNS, and the expression of fundamental enzymes for neurotransmitter synthesis that may need to be upregulated to compensate for reduced innervation (Mocchetti & Wrathall, 2009). Neutrophic factors also promote axonal growth, though combined with Schwann cell grafts, further amplify axonal extension after injury (L. L. Jones et al., 2001). Adult *in vivo* models have demonstrated the capacity of exogenous neurotrophic factors (NTFs) to shield against neuronal damage caused by traumatic or chemical experimental lesions, particularly with regard to easily identifiable neurons such as cholinergic and dopaminergic ones. Other models have shown beneficial effects of NTF administration with regard to axonal regeneration inside CNS tissue (Varon, Conner, & Kuang, 1995). Despite the numerous reports of neurotrophins promoting nerve regeneration after injury, inhibitory effects of neurotrophin treatments on damaged nerve repair have also been reported. This issue is of important consideration when combinatorial approaches are used in treatment. A better understanding of the molecular mechanisms and therapeutic application for NT treatments is needed (Kelamangalath & Smith, 2013).

Several cell types were transplanted into various animal models of different degrees of SCI severity with encouraging outcomes. Schwann cells (H. Cheng, Cao, & Olson, 1996; Kanno, Pearse, Ozawa, Itoi, & Bunge, 2015), different types of stem cells (Assinck et al., 2017; Deshpande et al., 2006;

Erceg et al., 2010; P. Lu et al., 2012; Okano, 2002) including ependymal stem cells (Moreno-Manzano et al., 2009), bone marrow mesenchymal stem cells (Laroni, Novi, De Rosbo, & Uccelli, 2013; Novikova, Brohlin, Kingham, Novikov, & Wiberg, 2011; M. Zurita et al., 2008; Mercedes Zurita & Vaquero, 2006) and mesenchymal stem cells from the human mucosa lamina propria (Lindsay et al., 2017; Lindsay, Riddell, & Barnett, 2010; Lindsay & Barnett, 2017). Fibroblasts, including genetically modified, have also been transplanted into spinal cord injuries (Franzen, Martin, Daloze, Moonen, & Schoenen, 1999; R. J. Grill, Blesch, & Tuszynski, 1997; R. Grill, Murai, Blesch, Gage, & Tuszynski, 1997; Mark H. Tuszynski, Murai, Blesch, Grill, & Miller, 1997).

Glial cell transplantation aims to provide shield the neurons and/ or stimulate plasticity/ myelination of spared neurites and/ or to foster axon regeneration through the release of trophic factors. The goal of transplanting stem cells is to provide new glial cells for myelination or protection, or to replace the lost neurons and/ or to deliver synaptic relays (Erceg et al., 2010; P. Lu et al., 2012; M. T. Moreno-Flores & Avila, 2010; Maria Teresa Moreno-Flores & Avila, 2006; Moreno-Manzano et al., 2009; Okano, 2002; M. Zurita et al., 2008; Mercedes Zurita & Vaquero, 2006).

Schwann cells, a key constituent of the peripheral nervous system, myelinate and ensheath neuronal axons and have a critical role in PNS nerve repair following injury. They are able to digest myelin debris (Allt, 1975), proliferate greatly by cue of axonal membrane and myelin debris (Salzer & Bunge, 1980) and macrophages (Baichwal, Bigbee, & DeVries, 1988) and

express several growth factors (Acheson, Barker, Alderson, Miller, & Murphy, 1991; Heumann et al., 1987; Meyer, Matsuoka, Wetmore, Olson, & Thoenen, 1992; Neuberger & De Vries, 1993; Offenhäuser, Böhm-Matthaei, Tsoulfas, Parada, & Meyer, 1995; Springer, Mu, Bergmann, & Trojanowski, 1994) which allows them to create a permissive environment for PNS nerve regeneration.

Schwann cells have been previously transplanted into rat CNS in various studies showing neuroprotective effect (Damien D Pearse et al., 2004; Schaal et al., 2007; Takami et al., 2002), promotion of axonal regeneration (Oudega & Xu, 2006; Takami et al., 2002; M H Tuszynski et al., 1998; Xu, Chen, Guénard, Kleitman, & Bunge, 1997) and myelination (Blakemore & Crang, 1985; Franklin, Gilson, & Blakemore, 1997).

Nonetheless their healing effect is not enough to produce full locomotor function recovery (Fouad, 2005; Kanno et al., 2014). Without further action, supraspinal axons generally do not grow into the SC transplant, and axons that do fail to exit and grow into and beyond the spinal tissue (Chau et al., 2004; Golden et al., 2007; Takami et al., 2002). This limitation might be due to low survival rate once transplanted to the injury site (Barakat et al., 2005; Hill et al., 2007; Damien Daniel Pearse et al., 2007) specially 3 weeks after transplantation via necrotic and apoptotic cell death (Hill et al., 2007). The cause might be the adverse environment they are being transplanted into with low oxygen levels, reactive oxygen species, inflammatory cytokines and a cell-mediated immune response (Hill et al., 2007; Damien Daniel Pearse et al., 2007). Removal of trophic/ mitogenic

factors and detachment from cell culture substrate also affect Schwann cell survival *post* transplantation (Damien Daniel Pearse et al., 2007).

It is clear that that the delivery of SC needs to be combined with other strategies that improve SC survival and addresses the healing aspects that the SC transplant alone does not. Various matrices (Moradi et al., 2012; Patel et al., 2010; H. Wang, Liu, & Ma, 2012), growth factors and other molecules (Golden et al., 2007; Hill, Guller, Raffa, Hurtado, & Bunge, 2010; Kanno et al., 2014; Siriphorn, Chompoopong, & Floyd, 2010) have been used to improve SC survival post transplantation. Transplantation of modified SC to over-express or produce foreign molecules have also been used (Daniel Pearse et al., 2004; L.-X. Deng et al., 2013; L. X. Deng et al., 2011; Flora et al., 2013; Damien D Pearse et al., 2004; J. F. Zhang et al., 2011).

More recently a Phase I human trial has been done to evaluate the safety of autologous human SC transplantation into injury epicentre of six subjects with subacute (2 days to 2 weeks after injury, Rowland *et al.*, 2008) neurologically complete, trauma-induced spinal cord lesions. The study established that one year post-transplantation, there were no surgical, medical, or neurological complications showing that the timing or procedure for the cell transplantation was safe (Anderson et al., 2017).

OECs seem like a good candidate to investigate for use in a spinal cord therapy because of their ability to promote and support neuron regeneration (S. C. S. C. Barnett & Chang, 2004; Susan C Barnett & Riddell, 2007; Franssen, de Bree, & Verhaagen, 2007; Higginson & Barnett, 2011; Ying Li et al., 2007; M. T. Moreno-Flores & Avila, 2010; M. Teresa Moreno-

Flores et al., 2002; Raisman, 2001; Richter & Roskams, 2008; Yang et al., 2014).

OECs were also shown in rat models *in vivo* and *in vitro* to reduce the inflammation at the lesion site, cavitation and size of the glial scar, promote angiogenesis and axon regrowth/ plasticity or remyelination occasionally followed by functional recovery (M. R. Andrews & Stelzner, 2007; García-Alías, López-Vales, Forés, Navarro, & Verdú, 2004; Lakatos, Barnett, & Franklin, 2003; Lakatos, Franklin, & Barnett, 2000; Rubén López-Vales et al., 2004; O'Toole, West, Chuah, et al., 2007; Plant, Christensen, Oudega, & Bunge, 2003; Ramer et al., 2004; Ruitenberg et al., 2003, 2005; Takami et al., 2002).

Another advantage of OECs is their ability to interact with astrocytes *in vitro* and *in vivo* (M. R. Andrews & Stelzner, 2007; Franssen, Roet, de Bree, & Verhaagen, 2009; Lakatos et al., 2000; Ying Li, Li, & Raisman, 2005; Maria Teresa Moreno-Flores & Avila, 2006; Ramer et al., 2004; Santos-Silva et al., 2007). Unlike SC, OECs produce heparan sulphate proteoglycans (HSPGs) with lower sulphate than SC which prevents them from forming boundaries with astrocytes (Higginson et al., 2012). Nonetheless SC can be engineered to secrete low sulphate HSPGs and mingle with astrocytes without forming boundaries (O'Neill et al., 2017).

The interface between the OECs and astrocytes involves a modification of the glial scar with the OEC membranes forming a bridge to fill the gap, production of extracellular matrix proteases and entry into the scar tissue of the spinal cord which is associated with corticalspinal tract

regeneration (Pastrana et al., 2006). Furthermore it was shown that OECs can decrease astrocyte reactivity and CSPGs expression (García-Alías et al., 2004; Lakatos et al., 2003; O'Toole, West, & Chuah, 2007).

Neurite outgrowth

Spinal cord damage is in most cases a transection of neurons. Therefore it makes sense that one of the first experiments to be made when it comes to testing the effect of OECs on neural regeneration is its influence on neurite outgrowth both *in vitro* and *in vivo*. Several kinds of neurons were used: retinal ganglion, olfactory receptors and cortical.

In 1993 Goodman *et al.* co-cultured chicken retinal ganglion cell neurons with neonatal and adult rat olfactory bulb astrocyte and ensheathing cell lines transduced with SV40 large T antigen. Olfactory bulb ensheathing cells both neonatal and adult have shown to provide higher neurite outgrowth than astrocytes. OB astrocytes and ensheathing cells were selected after immortalization by cellular and colony morphology, expanded, and tested further. Clones that exhibited a distinct bipolar, elongated cellular morphology and were capable of multilayer growth were selected as ensheathing cell lines and clones that were consistently stellate and formed strict monolayers were selected as OB astrocyte cell lines. Ensheathing cell lines were positive for GFAP and S100β, glial cell markers (Barber & Dahl, 1987; Donato, 1986), 217C, a marker for non-myelinating Schwann cells (K R Jessen et al., 1990), 7B11A6C7, a marker for astrocytes and their precursors not detectable in Schwann cells (Szigeti & Miller, 1993) and vimentin, the most abundant intermediate filament in OECs (Ramón-

Cueto & Avila, 1998). All astrocytes cell lines were 217C negative, GFAP, S100β and vimentin positive. Only the neonatal ones were 7B11A6C7 positive (M. Nadine Goodman et al., 1993).

In another study from 1999, Kafitz *et al.* co-cultured embryonic olfactory and cortical neurons on hippocampal and ensheathing glial cells and laminin. Olfactory Ensheathing cells were obtained from the rat olfactory bulb and plated onto Poly-L-Lysine-coated coverslips. Their characterization shown that most of them stained for p75NTR, a marker of non-myelinating Schwann cells, and GFAP. Olfactory neurons with ensheathing cells as a substrate had the longest primary neurites. Cortical neurons however had identical neurite extension grown on ensheathing cells and hippocampal cells.

Later in 2006, Leaver *et al.* showed that co-culture of retinal ganglion cells with OECs in collagen significantly increased the number of neurites.

In these last two studies the neurons were grown on a heterogeneous population of olfactory bulb cells that expressed p75NTR so one cannot rule out the possibility of non-myelinating Schwann cell contamination since they also express p75NTR (K R Jessen et al., 1990).

Pellitteri *et al*. in 2009 used rat olfactory bulb nerve layer cells positive for S100β, a glial cell marker, on co-cultures with hippocampal neurons to test neurite extension. They also tested the effect of several growth factors and conditioned media on neurite outgrowth. Their results shown that

olfactory bulb nerve layer cells increase the number of neurons and neurite outgrowth. (Pellitteri, Spatuzza, Russo, Zaccheo, & Stanzani, 2009)

A 2015 study (Khankan, Wanner, & Phelps, 2015a) revealed that p75NTR-positive rat olfactory bub cells not only increase neurite outgrowth in a scar-like environment in 60% as neurons aligned with them are three times longer in inhibitory meningeal fibroblast environment and twice as long in a reactive astrocyte zone when compared with neurons with no ensheathing cells.

Concerning *in vivo* work, Ramón-Cueto *et al.* in 1994 transplanted p75NTR positive rat olfactory bulb cells into a rat rhizotomized spinal cord segment. Three weeks after transplantation it was possible to see several dorsal root axons regenerating into the spinal cord using a flurescent carbocyanine (Ramón-Cueto & Nieto-Sampedro, 1994). Later in 1998 Ramón-Cueto *et al.* injected p75NTR positive-olfactory bulb cells onto four sites in the stumps of transected adult rat spinal cord bridged with Schwann cell packed matrigel channel grafts. Supraspinal axons identified by GAP-43 and neurofilament staining crossed the gap through connective tissue bridges formed on the exterior of the channels, avoiding the channel interior (Ramón-Cueto et al., 1998).

Neurite alignment

Alignment of glial cells have been suggested to have an important role in axonal guidance. Astrocyte alignment during development revealed to be crucial in the appropriate outgrowth of corticospinal tract fibers

(Joosten & Gribnau, 1989) and in 3D collagen gels (East, de Oliveira, Golding, & Phillips, 2010). Aligned Schwann cells have also been shown to direct axonal growth without other directing cues (Georgiou et al., 2013; Hompson & Uettner, 2006). A spontaneously aligned OEC population injection also displayed directional growth of host axons through local structural barriers on site (Pérez-Bouza, Wigley, Nacimiento, Noth, & Brook, 1998). Moreover biomatrix aligned OECs and ONF (olfactory nerve fibroblasts) showed to direct cortical neuron outgrowth and enhance the length of the longest neurite (R. Deumens et al., 2004). Lastly OECs neurite alignment also improved neurite outgrowth in scar-like cultures (Khankan et al., 2015a).

Cells can be aligned by culturing them on biodegradable matrices such as poly(D,L)-lactide. Although many studies reported good cell viability using biologically degradable scaffolds there are few suggesting cell orientation (Bamber et al., 2001; Oudega et al., 1997; Rabchevsky & Streit, 1997; Woerly, Plant, & Harvey, 1996; Xu, Guénard, Kleitman, & Bunge, 1995). Glial cell loaded-biomimetic scaffolds have been used to direct alignment of neurons *in vitro* (East et al., 2010; Georgiou et al., 2013; Georgiou, Golding, Loughlin, Kingham, & Phillips, 2015; Martens et al., 2014) but few using OECs.

Functional recovery

Transplantation of OECs into the nerve system has become a possible therapy for CNS or PNS damage as well as other neural diseases in animal models. Evidently it is important to attain functional recovery in transplanted animals to consider an OEC therapy viable for SCI. Functional

recovery after OEC transplantation can be measured in several ways. OECs can be from autologous origin, meaning the donor and recipient are the same individual, or from a cell line, which is an establish cell population with well-defined characteristics.

Transplantation of OECs into animal models have been shown to produce axonal regrowth and repairing. Neurites in contact with OEC grafts were detected using fluorescence and immunocytochemistry of markers like GAP-43, calcitonin gene-related peptide, neurofilament, serotonin and noradrenalin (M. I. Chuah et al., 2004; García-Alías et al., 2004; Ibrahim, Kirkwood, Raisman, & Li, 2009; Toshio Imaizumi, Lankford, & Kocsis, 2000; Y. Li et al., 1998; Y Li, Field, & Raisman, 1997; Rubèn López-Vales, Forés, Navarro, & Verdú, 2007; Rubèn López-Vales, Forés, Verdú, & Navarro, 2006; J. Lu et al., 2002; J. Lu, Féron, Ho, Mackay-Sim, & Waite, 2001; M Teresa Moreno-Flores et al., 2006; Plant et al., 2003; Ramón-Cueto, Cordero, Santos-Benito, & Avila, 2000; Ramón-Cueto & Nieto-Sampedro, 1994; Ramón-Cueto et al., 1998; Richter et al., 2005). Axonal regrowth into and through a lesion can also be measured with electrophysiological studies (García-Alías et al., 2004; Ibrahim et al., 2009; Toshio Imaizumi, Lankford, Burton, Fodor, & Kocsis, 2000; Toshio Imaizumi, Lankford, & Kocsis, 2000; B. C. Li, Li, Chen, Chang, & Duan, 2011; Y Li, Sauve, Li, Lund, & Raisman, 2003; Rubèn López-Vales et al., 2007, 2006; J. Lu et al., 2001; Toft, Scott, Barnett, & Riddell, 2007).

The animal studies using OECs indicated functional recovery using some behavioural motor and sensory measurements and in some studies

backed the respective anatomical results further confirming the axon repair by OECs even after chronic SCI (DeLucia et al., 2003; García-Alías et al., 2004; Ibrahim et al., 2009; B. C. Li et al., 2011; Y Li et al., 2003; Rubèn López-Vales et al., 2007, 2006; J. Lu & Ashwell, 2002; J. Lu et al., 2001; M Teresa Moreno-Flores et al., 2006; Plant et al., 2003; Ramón-Cueto et al., 2000; Ruitenberg et al., 2003). Nonetheless it was not proven the same using mucosal OECs (Yamamoto, Raisman, Li, & Li, 2009) and recovery was poorer when comparing with bulb derived cells (Ruitenberg et al., 2005). Moreover it is still unknown the mechanism by which OECs improve function. Instead of facilitating neuronal reconnections in disconnected nerve fibres they might be promoting regeneration through secondary routes such as protection of remaining fibres or creation of other pathways such as collateral sprouting or reconnection through long propriospinal interneurons (Bareyre et al., 2004; Ronald Deumens et al., 2006; Toft et al., 2007; Yamamoto et al., 2009).

The vast majority of animal studies using OECs were made in rat models. The lesions vary from dorsal cord crush, transection or section and contusion usually at the thoracic level at the subacute and acute phase of the injury. The recovery has been modest to none on mostly locomotion scales like grid climbing or walking (Gómez et al., 2018). In 2012 a group in Cambridge did an autologous transplant of olfactory mucosal OECs in dog. They measured the effects of intraspinal transplantation of cells (containing a mean of ~50% OECs) into severe chronic thoracolumbar (equivalent to ASIA grade 'A' human patients at ~12 months after injury) spinal cord-injured companion dogs mimicking many of the potential challenges involved in

biomedical research translation. Olfactory mucosal cell transplanted dogs had significantly better fore-hind coordination than dogs receiving cell transport medium alone although there were no significant differences in outcome between treatment groups in measures of long tract functionality. This suggests that intraspinal olfactory mucosal cell transplantation improves communication across the injured region of the spinal cord, even in chronically injured individuals (Granger, Blamires, Franklin, & Jeffery, 2012).

There is several clinical trials in human using autologous transplants which have established safety of OEC transplant but little to no recovery (Chhabra et al., 2009; Féron et al., 2005; Lima et al., 2006, 2010; Mackay-Sim et al., 2008; Tabakow et al., 2013, 2014; Zheng, Liu, Chen, & Wei, 2013). Not surprisingly most studies used autologous mucosal olfactory ensheathing cells, a less invasive and more accessible source of cells when compared to bulb origin. In the latest study olfactory bulb OECs were transplanted into a stab wound in an adult male spinal cord on an autologous sural nerve (PNS). The patient's improvements included transition from ASIA A to ASIA C, trunk stability, partial recovery of the voluntary movements of the lower extremities and an increase of the muscle mass in the left thigh, as well as partial recovery of superficial and deep sensation. Imaging also confirmed that the implants had connected the left side of the spinal cord, where the most nerve grafts were implanted and neurophysiological examinations confirmed the regeneration of the corticospinal tracts (Tabakow et al., 2014). Nevertheless in the same study it was concluded after 1 year that

isolating, culturing and transplanting autologous olfactory ensheathing cells was safe and feasible but it would require a larger numbers of patients to obtain significance of the neurological improvement and the extent to which the cell transplants contributed to it (Tabakow et al., 2013).

Tissue repair engineering using biomimetic protein scaffolds

The human body has limited regeneration capacity. Since the beginning of time when an injury occurs that is more than superficial or of a certain extend we need aid in its regeneration.

The three-dimensional (3D) organisation of various tissues in the body gives them vital functional properties. Cell and ECM 3D alignment is common in several biological tissues particularly those of the musculoskeletal system and some parts of the nervous system and is essential for their role in the body. Therefore failing to mimic that 3D environment of the native tissue with its different properties in different directions (anisotropy) limits clinical repair and reconstruction leading to scarring and reduced recovery of mechanical properties (R. A. Brown, Wiseman, Chuo, Cheema, & Nazhat, 2005; Tomasek, Gabbiani, Hinz, Chaponnier, & Brown, 2002). The manufacturing of aligned cellular structures *in vitro* is consequently usually the purpose of regenerative medicine researchers trying to mimic complex tissues. Several methods have been investigated including gradients of chemical and mechanical properties, electrical and magnetic fields, mechanical loading of cellular constructs, and numerous anisotropic biomaterial scaffolds (Lim & Donahue, 2007; Park et al., 2007).

In an attempt to mimic the cellular environment anisotropic scaffolds have been used to provide ECM-like alignment to the cells and consequently their mechanical properties (Lim & Donahue, 2007; Park et al., 2007; Phillips & Brown, 2011). Concentration and consequently density of matrix gels influences cell growth, the diffusion of factors and cell migration (Burke, Naughton, & Cassai, 1985; Klingman & Armstrong, 1986; Labrador, Butí, & Navarro, 1995).

Anisotropic biomaterial scaffolds are usually used to engineer tissue to align cells through limiting or regulating their adherence and dispersion on structured constructs (Bettinger, Langer, & Borenstein, 2009; Bozkurt et al., 2009; Gerberich & Bhatia, 2013; Kalbermatten et al., 2008; Lietz, Dreesmann, Hoss, Oberhoffner, & Schlosshauer, 2006).

Tethered Collagen gels have been used combining cellular self-alignment with stabilization following the removal of interstitial fluid. This technique as described in Georgiou et al., 2013 generated a new process for the fabrication of aligned cellular biomaterials for peripheral nerve repair. The aligned cells became uniformly dispersed within a stable aligned matrix made from native type I collagen. Efficiently organized in the aligned structure cells and matrix deploy integrin-mediated interactions and cytoskeletal contraction. In response to the resulting tension that develops longitudinally in the tethered rectangular gels through cell contraction and consequent strain to their local 3D matrix environment, cells and collagen fibrils become aligned (Phillips & Brown, 2011). Clearly this method can be

used to produce other highly organized tissues such as muscle or CNS neuronal constructs where anisotropy is necessary.

Remaining Challenges

Spinal cord injury starts with the damage of the blood-brain barrier which results in vascular changes and haemorrhages and leads to neuronal death and axonal damage. The damage to neuronal cells occurs in numerous aspects such as ionic deregulation causing the loss of nerve impulses, myelin destruction due to increase in intracellular calcium which activates proteases and phospholipases and excessive excitation of viable neurons caused by glutamate and aspartate release (Balentine, 1988; Gerzanich et al., 2009; Griffiths et al., 1978; Losey & Anthony, 2014; Losey et al., 2014; Tator & Fehlings, 1991; Yu & Fehlings, 2011). Glial cell activation (oligodendrocyte precursor cells and astrocytes) happens afterwards as a result of necrosis, haemorrhage and local ischemia and neuronal and oligodendrocyte death takes place. The lesion spreads beyond the initial starting point and degeneration continues. After SCI the damage to function is due to the disconnection in the spinal tract and there is several aspects that unable function recovery such as: the innate neuronal limitation in axon regrowth/ regeneration gene expression (Bomze et al., 2001; Hannila & Filbin, 2008); adverse environment in the glial scar (Cregg et al., 2014; Silver & Miller, 2004; Yiu & He, 2006) and absence of trophic factors for neuronal protection and regeneration (L. L. Jones et al., 2001; Sharma & Hari Shanker Sharma, 2007).

Over time all reactive macrophages, oligodendrocyte precursor cells and reactive astrocytes change the ECM at the wound producing cytokines, myelin associated inhibitors (MAI) and chondroitin sulphate proteoglycan (CSPG) that constitutes the hostile milieu of the glial scar which is also a physical barrier that strongly prevents axonal growth (L. L. Jones, Margolis, et al., 2003; L. L. Jones et al., 2002; Snow et al., 1990). The main challenge for regeneration of neurons in the spinal cord is to overcome their reduced ability for spontaneous axonal regeneration and adverse environment, get them across the glial scar, exit the scarred region and reconnect with their initial targets (Jenny A K Ekberg & St John, 2014; Novikova, Lobov, Wiberg, & Novikov, 2011).

Nonetheless several studies in recent years have shown rat OECs' neuronal regeneration ability in acute (García-Alías et al., 2004; Leng, He, Li, Wang, & Cao, 2013; Y. Li et al., 1998; Y Li et al., 1997; Rubèn López-Vales et al., 2006; Rubén López-Vales et al., 2004; J. Lu et al., 2001; Ramón-Cueto et al., 2000, 1998) and delayed/ chronic injuries in rat (Rubèn López-Vales et al., 2007, 2006; J. Lu et al., 2002; Plant et al., 2003). Cell based therapies have shown to be a promising solution to many current clinical demands. However there is still several challenges for clinical and commercial proposes such as establishing a reproducible and viable production of cell therapies such as profound understanding of the cell product critical attributes for safety and efficacy to be able to produce it with standard and optimized protocols (Heathman et al., 2015).

The first and main challenge in creating an OEC cell line is to characterize an OECs cell population on a primary culture. There still seem to be quite a controversy in how are OECs defined *in vitro*. Most studies on OECs rely on p75NTR expression and other glial marker such as S100β and GFAP to characterize them. Nevertheless, as said before, those are also markers for Schwann cells, also likely to exist in samples, especially from the olfactory mucosa. Besides, it has been shown that OECs do not express consistently some of those markers, such as GFAP and p75NTR (Jani & Raisman, 2004). Following OECs characterization and closely related to it, other challenge is cell purification.

Also probably related to characterization and purification issues there a higher variability in OEC number in human samples (Choi et al., 2008) which explains the variable results in autologous transplants.

One of the aspects holding back further developments is the production of growth media without animal derived components like serum. Since most components of serum are still undefined serum-free media is expensive, difficult to produce and results in lower quality and yield cell products (Froud, 1999; Gstraunthaler, 2003; Jochems, Van der Valk, Stafleu, & Baumans, 2002). Nevertheless it is known that some components of serum are Growth Factors (GF) and Extracellular Matrix (ECM) molecules. Furthermore it has been reported that some growth factors can be engineered to hold a high affinity binding domain that more effectively binds them to the ECM increasing its bioactivity Synthetic biology can provide the engineered factors that will more easily integrate the cell-secreted ECM and

optimize the bioprocess conditions by improving cell response (Mathur, Xiang, & Smolke, 2017; Phillips & Brown, 2011).

Project Aims

In an attempt to address the challenge of the variability of clinical samples my project aimed to develop strategies for isolation, culture and functional testing of Olfactory Ensheathing Cells (OECs) including a human OEC line. The conditionally immortalized human mucosa OEC cell line PA5 was produced within the research group at UCL Biochemical Engineering as a potential off-the-shelf product for therapeutic use in spinal cord injuries within the recommended 14 day time window post-injury. This work was carried out using a technology called c-mycERTAM employed to achieve conditional growth control (Littlewood, Hancock, Danielian, Parker, & Evan, 1995). Conditional immortalisation technologies aim to overcome this via controllable or inducible genes that, when transduced into cells and under permissive conditions, promote cell proliferation in an immortal state. Under non-permissive conditions, cells lose their immortality and return to a "normal" phenotype. Such an approach has been successfully applied to generate neural stem cell lines from human fetal cortical neuroepithelial cells following retroviral transduction with c-MycERTAM gene (Pollock et al., 2006). These cells can be conditionally immortalized in culture and silenced upon transplantation into the patient. This conditionally immortalized human OEC cell line has the potential for neuronal regeneration and can be a prospective allogeneic therapy for SCI treatment.

The central aim of this project was to test a human cell line for neuronal regeneration. To be able to test the hypothesis that the PA5 conditionally immortalized cell line promoted neuronal growth the isolation protocol and

the assays to test neuronal growth had to be established and tested for robustness. Therefore the firstly in section 3.1 it was investigated the effects of different culture parameters on proportion and yield of the characteristic OEC and fibroblast markers in order to establish a protocol that optimised the yield and purity of rat OECs. The culture parameters investigated were timing of addition of the neutrophic factor NT-3 and addition of the anti-mitogen Cytosine β-D-arabinofuranoside (AraC). By the end it was established a protocol to optimize the isolation and culture of OECs that could be used to isolate human OECs.

In section 3.2, it was established the assays to test the ability of OECS to promote neurite outgrowth when compared with a positive control of F7 Schwann cells in 2D co-culture using NG108 neurons. Firstly isolated rat OECs were used in the assay and once the assays were optimised the PA5 human cell line was tested. PA5 cells were also tested for their ability to stimulate neurite outgrowth using primary rat DRG neurons. All 2D co-cultures were tested at different oxygen levels (atmospheric and physiologic) and for different culture durations (3 and 5 days).

Finally it was performed the necessary contraction studies to optimise the cell density and contraction duration to obtain maximal cell alignment in collagen tethered gels for 3D co-culture studies on section 3.3. A 3D model of collagen tethered gel was used to access cell alignment. The effect of PA5 aligned cell loaded tethered gels on DRG neuronal alignment in comparison with F7/SC loaded gels positive control was preliminarily studied.

2. Materials & Methods

2.1 Cell isolation

Rat nasal olfactory mucosa was collected from adult (200-250 g) female, specific pathogen-free Sprague-Dawley (SD) rats obtained from the University College London Biological Services Unit. One experimental repeat was equal to 3 rats (6 mucosas). All experiments were carried out according to the Animals (Scientific Procedures) Act 1986 (ASPA).

Animals were culled by CO_2 asphyxiation and their necks broken severing the connection between the spinal cord and brain. The nasal turbinates were revealed by removal of the lower jaw and surrounding musculature, the lateral and medial cheekbones, and the incisors. The salivary glands, nasal turbinates, and cartilage on both sides of the nasal septum were removed to reveal the olfactory mucosa. It was readily identified by the yellowish colour and its posterior position on the nasal septum. Care was taken to avoid the anterior edge of the olfactory mucosa, which could be contaminated with respiratory epithelium.

The dissected mucosa was immediately placed in Dulbecco's Modified Eagle Medium/Ham's F12 with GlutaMax™ (DMEM/F12 + GlutaMax™-I; *Gibco® Life Technologies™*) with 1% Penicillin/ Streptomycin (P/S; *Sigma*).

The excised tissue was washed with Hanks Balanced Salt Solution (HBSS, calcium- and magnesium-free; *Gibco® Life Technologies™*), cut in small pieces (about 1 µm in lenth) using a scalpel and incubated for 45 min

at 37°C, 5 CO_2 in 1ml of Dispase II (2.4 U/ml; *Sigma*) in DMEM/F12 + GlutaMax™-I.

Figure 2.1*- Six rat olfactory mucosas in HBSS (equivalent to 1 experimental repeat).*

Following this, the tissue was centrifuged at 400g for 5 min (*eppendorf* Centrifuge 5810R) and was transferred into a 1 ml solution of 0.05% (w/v) Collagenase type I (*Sigma*) in serum-free media (DMEM/F12 + GlutaMax™-I; *Gibco® Life Technologies™*) and incubated for 15 min at 37°C/5% CO_2 and triturated every 5 min. The cell suspension was then centrifuged at 400g for 5 min and the cell pellet was resuspended in the appropriate culture medium (DMEM/F12 + GlutaMax™-I; *Gibco® Life Technologies™* with 2% of fetal bovine serum (FBS) *; Sigma* and 1% Penicillin/ Streptomycin, P/S; *Sigma*) and plated on tissue culture plastic for 24 hours for adherence of the fast-adhering contaminant cells like fibroblasts at 37ºC in a humidified incubator with 5% CO_2/95% air (unless stated otherwise). Following the 24 hour differential adhesion step, the supernatant was plated

on to laminin-coated flasks (20 mg/mL in HBSS, 4h at 37 °C in the incubator), cultured for up to day 14 before being passaged and used in experiments.

2.2 Culture of Rat Olfactory Mucosal Cells

2.2.1 Effect of timing of NT-3 addition

For this experiment, after the 24 hour differential adhesion step the supernatant was plated into flasks coated with laminin (20 mg/ mL in HBSS, coating for 4h at 37 °C; Millipore) and cultured for 14 days at 37ºC in a humidified incubator in 21% O_2.

At day 6 (5 days after plating onto laminin) the media was changed. From this point on media was changed every 3 days. After 12 days of culture in laminin-coated T25 flasks, the cells reached ~80% confluence and so were passaged using trypsin-EDTA (*Sigma*) and transferred onto laminin-coated glass coverslips (*BDH*, 13 µm diameter) and left to adhere for 48h at 37ºC in a humidified incubator with 5% CO_2/95% air. At day 14, cells were washed with HBSS before fixing at 4% PFA overnight at 4 °C. Two experimental test groups were investigated: 1. NT-3 addition (50µg/mL, *Cell Signaling Technology, New England Biolabs*) at day 1 (after the 24 hours differential adhesion step); and 2. NT-3 addition at day 6 (on the first media change, 5 days after plating).

2.2.2 Effect of Cytosine β-D-arabinofuranoside (AraC)

For this experiment, the two test groups investigated were: 1. no exposure to AraC and 2. exposure to AraC (10 µM) for 24 h (day 6). The exposure to AraC was done by changing the media on days 6 and 7 to all

conditions and adding AraC-supplemented media to the 24h condition only on day 6. From day 7 media was change every 3 days until day 14. The cells were trypsinised with Trypsin-EDTA (*Sigma*) and transferred onto laminin-coated glass coverslips (*BDH*, 13 µm diameter) and left to adhere for 24h at 37ºC in a humidified incubator with 5% CO_2/95% air. At day 14, cells were washed with HBSS before fixing at 4% PFA overnight at 4 °C.

2.2.3 Cell Imaging

Fluorescence microscopy (*EVOS FL*, *Life Technologies*) was used in the assessment of the number positive cells for each marker. Three random fields of view were analysed per experimental repeat per condition and per combination of markers. Images were captured using a 20x or 10x objective. Image analysis was conducted using ImageJ software. Cells were considered clearly positive when you can see a clear outline of the cell shape and a threshold for fluorescence intensity was set to keep consistency.

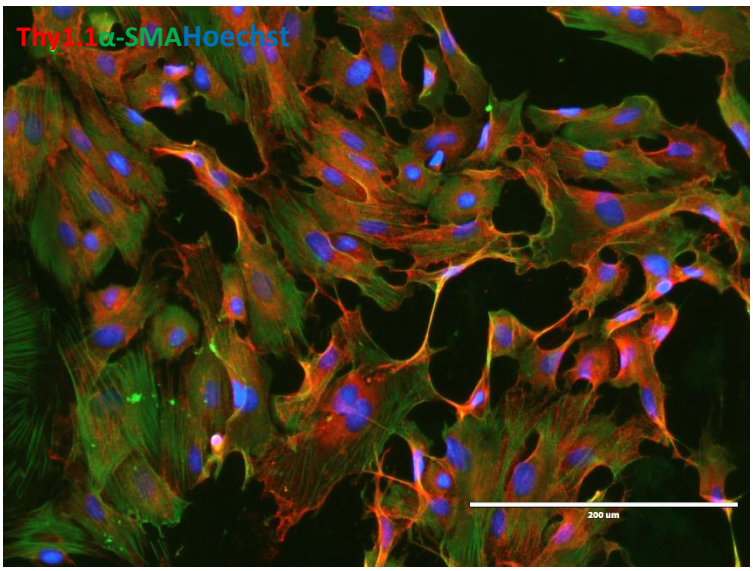

Figure 2.2- *Example of a fluorescent micrograph of a field of view (20x, scale bar 200µm).*

2.3 2D co-culture

2.3.1 Co-culture of rat olfactory mucosal cells (OEC) with neurons NG108

After 12 days of culture in laminin-coated T25 flasks OECs and F7/SC were trypsinised using trypsin-EDTA, counted and 10 000 cells of either were transferred onto PLL-coated glass coverslips (BDH, 13 mm diameter) and left to adhere for 48h at 37°C, 5% CO2. At day 14, 1000 (equivalent to ~5 cells per mm^2) NG108 neurons (mouse neuroblastoma x rat glioma hybrid cell line, Sigma Aldrich) were transferred onto the OEC or F7/SC (rat nerve sheath Schwann cell line, Sigma Aldrich) and co-cultured at atmospheric oxygen (21%) or physiologic oxygen (2-8%) for 3 or 5 days at 37ºC in a humidified incubator. The incubator was maintained at physiologic oxygen using nitrogen to drive oxygen levels down from ambient air oxygen to the target levels. The physiologic oxygen level were maintained at a set level of 2% which fluctuated between 2% and 8% throughout the experiment.

F7/SC were derived from neonatal Wistar rat Schwann cells after culture for several months with intermittent exposure to the mitogen, cholera toxin and occasional passaging to avoid premature transformation. After cloning one of these cultures by limiting dilution, the line SCL4.1/F7 was established growing without mitogen (https://www.sigmaaldrich.com/catalog/product/sigma/cb_93031204?lang=en&region=GB). NG108 were formed by Sendai virus-induced fusion of the mouse neuroblastoma clone N18TG-2 and the rat glioma clone C6 BV-1 (https://www.sigmaaldrich.com/catalog/product/sigma/cb_88112302?lang=en&region=GB&gclid=CjwKCAjwkcblBRB_EiwAFmfyy9ZIVSrOBElcPdd1N5TWqJGwoINbe

1jq2nXRW9ZlSmh07LufblZchRoCRAQQAvD_BwE). Both cell lines were cultured on DMEM/F12 + GlutaMax™-I; *Gibco® Life Technologies™* with 10% of fetal bovine serum.

The media (DMEM/F12 + GlutaMax™-I; *Gibco® Life Technologies™* with 2% of fetal bovine serum) was changed after 3 days for the 5 day co-culture. After 3 or 5 days cells were washed with HBSS before fixing at 4% PFA overnight at 4 °C. Due to the limited number of olfactory mucosal cells available per experimental repeat (mucosa from three rats pooled together, two per rat) it was chosen to test the effect of oxygen level and type of co-culture first on a three day co-culture period and on a second experiment over a five day co-culture period.

2.3.2 Co-culture of human PA5 cell line with neurons NG108

PA5 cells were cultured in Dulbecco's Modified Eagle Medium/Ham's F12 with GlutaMax™ (DMEM/F12 + GlutaMax™-I; *Gibco® Life Technologies™*) with 10% FBS and 1% Penicillin/ Streptomycin (P/S; *Sigma*) on PLL (0.1mg/mL, Sigma) in the incubator at 37 °C, 5% CO_2 and 21% O_2. Confluent flasks were passaged using Tryple E™ (*gibco by Life Technologies*). PA5 cells and F7/SC were detached, counted and 10 000 cells of either were transferred onto PLL-coated wells in a 24 well plate and left to adhere overnight at 37°C, 5% CO_2, 21% O_2. 1000 (equivalent to ~5 cells per mm^2) NG108 neurons were transferred onto the PA5 cells or F7/SC and co-cultured at atmospheric oxygen (21%) or physiologic oxygen (2-8%) for 3 or 5 days. The media was changed after 3 days for the 5 day co-culture. After 3 or 5 days cells were washed with HBSS before fixing with 4% PFA for 20 minutes at room temperature.

2.3.3 Co-culture of human PA5 cell line with DRG neurons

The PA5 conditionally immortalized cell line was obtained by mucosal biopsy, following informed consent under approval from the ethics committee. To enrich neuroprotective cell types such as OECs, late-adherent primary human olfactory mucosal cells were retrieved by first removing rapidly adherent cells (i.e. fibroblasts) with a 24-hour differential adhesion step. Cells remaining in the supernatant were then re-plated and expanded for 12 days to be transduced by retroviral infection. Stably transduced cells were selected with geneticin (G418), and incorporation of the c-MycERTAM transgene was further validated at DNA and protein level. This type of technology consists of a fusion gene encoding a chimeric protein composed of the transcription factor c-Myc and the hormone-binding domain of a mutant murine estrogen receptor (G525R). The gene product of this fusion no longer binds to 17b-estradiol or estrogen-like molecules present in cell culture media, but is responsive to activation by the presence of the synthetic drug 4-hydroxytamoxifen (4-OHT). The presence of 4-OHT promotes proliferation of PA5 cells.

Karyotype analysis and growth kinetics characterisation was performed. PA5 cells at passage 14 displayed a normal diploid male karyotype (46, XY) with no visible chromosomic aberrations, i.e. absence of polyploidy, pseudodiploidy, and hypodiploidy. Growth kinetics was also good with doubling times for PA5 cells increased from 0.43 days to 4.05 days between days 6 and 60. Biomarker expression of PA5 cells were assessed by immunocytochemistry to confirm the presence of characteristic glial

(p75NTR, S100 calcium-binding protein B (S100b), glial fibrillary acidic protein (GFAP), and oligodendrocyte marker O4), neuronal (b-III-tubulin and nestin), and fibroblast-associated (Thy1 and fibronectin) markers reported in primary human olfactory mucosal cells.

PA5 cells were cultured in Dulbecco's Modified Eagle Medium/Ham's F12 with GlutaMaxTM (DMEM/F12 + GlutaMaxTM-I; Gibco® Life Technologies™) with 10% FBS and 1% Penicillin/ Streptomycin (P/S; Sigma) and 100 nM 4-OHT (Sigma) on PLL (0.1mg/mL, Sigma) coated flasks in the incubator at 37 °C, 5% CO2 and 21% O2. Confluent flasks were passaged using trypsin-EDTA (Sigma). PA5 cells and F7/SC were trypsinazed, counted and 10 000 cells of either were transferred onto PLL-coated 24 well plates and left to adhere overnight at 37°C, 5% CO2, 21% O2.

DRG neurons were isolated from Sprague-Dawley rats as a source of primary neurons. To obtain the DRGs, the spinal cord was excised from rats that had been culled by CO_2 asphyxiation. The spinal column was divided in half in the sagittal plane to expose the spinal cord, and the cord tissue removed to expose the DRG and roots in the intervertebral foramen. Using the Olympus SZ40 dissecting microscope with Volpi, Intralux® 6000 optical fibre light source, the DRGs were removed and placed in a petri dish universal tube containing DMEM supplemented with P/S. Approximately twenty DRGS were collected from the thoracic and lumbar regions per animal. Using the forceps the ventral root was pulled and the neurons exposed. The DRG neurons were transferred to tube and incubated with 2.5 mL of type IV collagenase (0.125% (w/v) Sigma; prepared in serum-free

media supplemented with P/S) at 37ºC for 90 minutes. The collagenase-treated explants were mechanically dissociated by trituration with a 1 mL Gilson pipette. Collagenase was removed by two 20 mL spin washes in DMEM-complete media at 400g for 5 minutes. The pellet was resuspended in 10 mL Dulbecco's Modified Eagle Medium/Ham's F12 with GlutaMax™ (DMEM/F12 + GlutaMax™-I; *Gibco® Life Technologies™*) with 10% FBS and 1% Penicillin/ Streptomycin (P/S; *Sigma*), plated on PLL-coated flasks and incubated at 37 ºC, 5% CO_2 for up to 24h before use.

DRG neurons were trypsinazed and transferred onto the PA5 cells or F7/SC or PLL-coated flasks and co-cultured at atmospheric oxygen (21%) or physiologic oxygen (2-8%) for 3 or 5 days. The media was changed after 3 days for the 5 day co-culture. After 3 or 5 days cells were washed with HBSS before fixing with 4% PFA for 20 minutes at room temperature.

2.3.5 Immunocytochemistry

Following cell fixation with 4% PFA for 20 minutes at room temperature, the cells were washed with phosphate buffered saline (PBS) solution (Sigma) (3 x). Following this, cells were incubated in 0.25% Triton X® (*Sigma*) for 20 minutes at room temperature. Afterwards they were washed in PBS 3 times and incubated in 5% goat serum (*DAKO*) in PBS for 30 minutes at room temperature. The primary antibodies rabbit anti-p75NTR (*Millipore™*), rabbit anti-S100β (*DAKO)*, mouse anti-Thy1 (*Millipore™*), rabbit anti-α-smooth muscle actin (α-SMA) (*abcam®*), mouse anti-Neurofilament H & M (NF) (*BioLegend*) and mouse monoclonal anti-βII-tubulin (βII-tub) (*Sigma*) were added at 1:200, for 90 minutes at room temperature after washing 3 times with PBS. Finally the secondary antibodies (*invitrogen Goat Anti-mouse IgG (H+L) Dylight™ 594 conjugate and invitrogen Goat Anti-rabbit IgG (H+L) Dylight™ 488 conjugate*) and Hoechst (*Sigma*) were added at 1:200 and 1:1000 dilutions in PBS, respectively, for 45 minutes at room temperature and then washed 3 times using PBS. The coverslips were mounted onto glass slides with a drop of *FluorSave™* (*Calbiochem*), and then left to dry overnight before imaging. For co-culture with PA5 cells wells were left in PBS for imaging.

For tethered gels following cell fixation with 4% PFA overnight at 4 degrees celsius, the gels were washed with phosphate buffered saline (PBS) solution (Sigma) (3 x). Following this, gels were incubated in 0.25% Triton X® (*Sigma*) for 30 minutes at room temperature. Afterwards they were washed (3x) with PBS and then incubated in 5% goat serum (*DAKO*) in PBS for 45

minutes at room temperature. The primary antibodies rabbit anti-S100β (*DAKO)* and mouse monoclonal anti-βII-tubulin (βII-tub) (*Sigma*) were added at 1:200 for 3 hours at room temperature after washing 3 times with PBS. Finally the secondary antibodies (*invitrogen Goat Anti-mouse IgG (H+L) Dylight™ 594 conjugate and invitrogen Goat Anti-rabbit IgG (H+L) Dylight™ 488 conjugate*) and Hoechst (*Sigma*) were added at 1:200 and 1:1000 dilutions in PBS, respectively, for 90 minutes at room temperature and then washed (3x) using PBS.

2.3.6 2D co-culture imaging

Fluorescence microscopy (*EVOS FL*, *Life Technologies*) was used in the assessment of the number of neurons, neurites and neurite length in each co-culture. Three or five random fields of view were analysed per experimental repeat and per condition. Images were captured using a 20x objective. Image analysis was conducted using ImageJ software. All βIII-tubulin-positive neurites were traced within each field using a semi-automated image analysis plugin called Neuron J for neurite count and length determination.

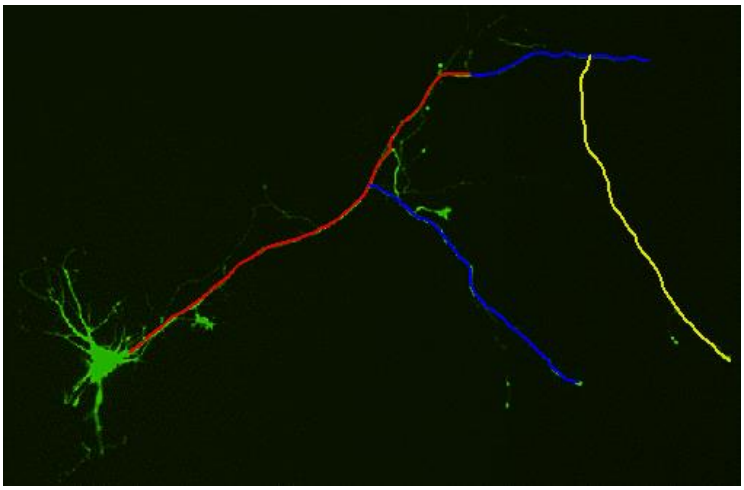

Figure 2.3*- Example of neurite tracing using ImageJ NeuronJ plugin (https://imagescience.org/meijering/software/neuronj/, accessed on 24/10/2018).*

2.4 3D co-culture

2.4.1 Production of collagen gels

All gels were prepared using 80% v/v type I rat tail collagen (2mg/mL in 0.6% acetic acid; First Link, UK) mixed with 10% v/v Minimal essential medium, MEM, (Sigma). PA5 cells were detached and counted. The collagen mixture was neutralized dropwise with concentrated (1 M) and diluted (0.1 M) sodium hydroxide (NaOH) before addition of 10% v/v cell suspension with the appropriate cell number to achieve the required final cell density. For the contraction studies 75µL of gel was added to each well of 96 well-plates. For align gels, 1 mL of the mixture was added to a PEEK (Polyether ether ketone) mould (manufactured by the Biochemical Engineering workshop) integrated with a tethering mesh (Darice®, #10 mesh plastic canvas rectangle- 10-1/2 x 13-1/2) at opposite ends and covered on one side with parafilm as described previously (Georgiou et al., 2013; Phillips & Brown, 2011). The gels were allowed to set up for up to 10 min at 37ºC in the incubator. Cellular gels from well plates were detached (termed free floating gels) using a needle and tethered gels were detached using an nº 11 scalpel (carbon Steel surgical blade, Swan Morton). All gels were immersed in culture medium (DMEM/F12 + Glutamax + 10% FBS (*Sigma*) + 1% P/S,

Sigma) and incubated at 37ºC in a humidified incubator with 5% CO_2/95% air up to 24h hours.

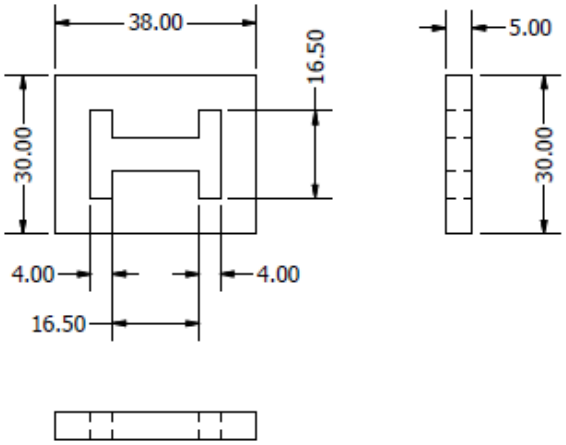

***Figure 2.4**- Mould dimensions in mm.*

For aligned gels a stabilization step after the contraction period was necessary. The media was taken from the petri dish and the gel was put upside down on an empty 60mm diameter Petri dish and the parafilm carefully removed. The tethered gel was separated from the tethering mesh with a number 4 blade (carbon Steel surgical blade, *Swan Morton*) and the align gel removed from the mould gently with a spatula. A RAFT™ absorber for 24-well plates (LONZA) was put on top of the gel for 15 minutes during which time the fluid was absorbed.

2.4.2 Contraction assays

For the contraction assays pictures of at least three wells were taken at each time point for each cell density. The average contraction of each cell density at each time point is the value of an experimental repeat.

2.4.3 Co-culture of aligned PA5 cells with NG108-15 cells

After stabilization with RAFT absorbers 20 000 NG108-15 cells were added to the gel and left to set up to 1h. Media was added and the petri dish was incubated in a humidified incubator with 5% CO_2/95% air.

2.4.4 Co-culture of PA5 cells with rat DRG neurons

After stabilization a volume of up to 50 µL of DRG neuron suspension was added at the centre of the gel and left to set up to 1h. Media was added and the petri dish was incubated in a humidified incubator with 5% CO_2/95% air for 3 or 5 days.

2.4.5 3D culture imaging

Confocal microscopy (Olympus Japan, BIORAD Radiance 2100 laser scanning system) was used in the assessment of glial cell alignment and neurite alignment in the EngNT-neuron co-cultures. 8 equivalent fields of view were analysed per gel using a standardised sampling protocol. Images were captured using a 40 water immersion lens and z-stacks of the whole gel were captured with a step size of 1 µm. Image analysis was conducted using Volocity™ software (Perkin Elmer, Waltham, MA) running automated 3D image analysis protocols to measure the angle of glial cells and neurites with the axis of the gel in each field. All S100β-positive glial cells and βIII-tubulin-positive neurites were traced within the confocal projection of each field. Angles of neurite with less than 10 µm were not measured.

2.5 Data analysis

In the section 3.1 in which the experiments accessed factors influencing proportion (the ratio between the number of positive cells and the total number of cells) and yield (ratio between the total number of cells and the total area they were in) of rat OEC cells these were manually counted on each image.

Marker expression varies with time in culture and has a correlation between different markers within the cells (Jani & Raisman, 2004; Ramón-Cueto & Avila, 1998). Therefore there are several measurable responses that are related so a MANOVA (Multivariate Analysis of Variance) was considered the best approach. It is used to evaluate several aspects of some interconnected subject (Tabachnick, Fidell, & Osterlind, 2001) analysing the effect of two or more independent variables on one or more dependent variables.

On the section 3.2 of the results the experiments investigated the effect of two (type of culture and oxygen level) or three (type of culture, oxygen level and duration) independent variables on three responses: NG108 neuron number per millimetre squared, number of neurites per neuron and neurite length per neurite. It was decided to use the ratio between the number of neurites and number of neurons and the neurite length and the number of neurites in each experimental repeat and condition to account for the increase of neurites due to the existence of more neurons and the increase in neurite length due to increase in number of neurites. As what was being measured was neuronal function, there is

several measurable aspects that are related. The number of neurons per squared unit will have an effect on space for neurite outgrowth and its extend and vice-versa so a MANOVA (Multivariate Analysis of Variance) was considered the best approach.

The assumptions of MANOVA are: that within each sample the observations are sampled randomly and independently of each other; the dependent variables are continuous; the independent variables consist of two or more categorical groups; there is no multivariate outliers; there is multivariate normality which cannot be directly tested with SPSS but by testing that each group sample has a normal distribution it gives the best guess; there is a linear relationship between each group of dependent variables; there is no multicollinearity and there is homogeneity of variance-covariance matrices (French et al., 2011).

The assumptions of MANOVA were tested. For rat OECs culture and co-culture with NG108 neurons all observations came from independent experimental repeats (four different sets of six rat mucosas) and random fields of view containing cells were captured. The dependent variables (yield and proportion of p75NTR, Thy1.1, S100β and α-SMA and number of neurons per unit of area, number of neurites per neuron and neurite length per neurite) are obviously continuous as they account for the number of positive cells per unit of area or per cell present in the well or for the number or length of structure and have an infinite number of possible values. The independent variables consist of two or more categories. The factor NT-3 addition timing was tested at two levels: NT-3 addition at day 1 and addition

at day 6 and addition of AraC was tested at two levels no added AraC and expose to AraC for 24h. For co-culture of rat OECs on NG108 neurons the factor type of co-culture was tested at three levels: NG108 neurons grown on PLL (negative control), NG108 neurons grown on F7/SC (positive control) and NG108 neurons grown on rat OECs. The factor oxygen tension was tested at two levels: atmospheric (21 %) and physiologic (2-8%).

In all PA5 co-cultures with NG108 experiments all experimental repeats were independent (experiments done on different days with cells from different thawed vials for PA5 cells) and all observations (pictures of fields of view containing cells in a well) within each sample for a set of conditions were collected randomly. The dependent variables are obviously continuous as they account for the number of neurons, neurites and neurite length and have an infinite number of possible values. The independent variables consist of two or more categories. The factor type of co-culture was tested at three levels: NG108 neurons grown on PLL (negative control), NG108 neurons grown on F7/SC (positive control) and NG108 neurons grown on conditionally immortalized human PA5 cells. The factor oxygen tension was tested at two levels: atmospheric (21 %) and physiologic (2-8%) and the duration of the co-culture was tested at two levels: three and five days.

To test for multivariate outliers, box plots were made for each data set to detect univariate outliers. Although having no univariate outliers does not guarantee not having multivariate outliers it is a good indication. To test for multivariate normality each sample was tested for each group for

normality using the Shapiro Wilk test (definition in Appendix). The linear relationship between each group of dependent variables was tested with scatter plots of each combination of variables. The existence of multicollinearity was tested through a regression statistics with all variables. And finally the homogeneity of variance-covariance matrices was tested with the Levene's test for equality of variances (definition in Appendix).

A Box M's test was also performed on each data set to evaluate the homogeneity of the variance of the error (definition in Appendix).

A multivariate analysis was performed on all experiments where the influence of the model is evaluated on the overall response. The sample size is small and unequal in most cases and there might be some violations of assumptions (linearity between pairs of dependent variables) so Pillai's trace will be considered for all MANOVAs (Tabachnick et al., 2001). The tests between subjects' effects evaluated the impact of each variable and the model on each response. With the pairwise comparisons and the multiple comparisons, in case of more than one level of a factor (like the case of the type of co-culture), it was determined where the significant difference was.

The collagen gel contraction experiments investigated the effect of two independent variables (time of contraction and cell density) on one response, floating gel contraction. Therefore the data was analysed with a two-way ANOVA (Analysis of Variance).

The assumptions of ANOVA are: the independent variables consist of two or more categories; observations and experimental repeats are random and independent; the dependent variables are continuous; there is

normality within each group for all combinations of factors and variance is equal across all groups (A. P. Field, 2009). The independent variables consist of two or more categories: the factor cell density has four levels (0.2, 0.5, 1 and 2 million cells per mL) and the factor time was tested at five levels (2, 4, 6, 8 and 24 hours of contraction). All experimental repeats were independent (experiments done on different days with cells from different thawed vials of PA5 cells) and observations (technical repeats) within each sample for a set of conditions were collected. The dependent variable is obviously continuous as it accounts for the contraction proportion. To test for normality each sample was tested for normality using the Shapiro Wilk test (definition in Appendix). The homogeneity of variance-covariance matrices was tested with the Levene's test for equality of variances (definition in Appendix).

For rat DRG alignment experiments rat primary DRG neurons were co-cultured on PA5 cells loaded collagen gels for 3 and 5 days. The experiments investigated the effect of aligned PA5 cells with the longitudinal axis of a collagen gel construct on the alignment of primary rat DRG neurons with that same axis when compared to the effect of aligned F7/SC positive control. It was also tested the assumption that either glial cells, PA5 and F7/SC, align primary rat DRG neurons before comparing the alignment of the DRG neurons with the gel longitudinal axis when grown on either cell loaded gels.

As what was being measured was neuronal axons or glial cell alignment with the axis of the gel the data obtained was a group of angle

values for each neuron/glial cell analysed in each condition. From the data a distribution was obtained by grouping the angles by value in ranges of 10 degrees.

A Kolmogorov-Smirnov (K-S) Test was performed between angle distributions of either PA5 cells or F7/SC in collagen gels and the DRG neurons grown on them and between DRG neurons angle distributions co-cultured on F7/SC and on PA5 cells. This test statistic quantifies a distance between the empirical distribution functions of two samples (Stephens, 1974).

Only one experimental repeat was performed per experiment which limits the conclusions one can draw from the K-S test statistics. The K-S is valid to use from a strictly statistical point of view because two distributions of values are being compared. The null hypothesis is that they come from the same distribution. From a biological variability point of view more experimental repeats are needed to confirm the effect studied. The size of the sample can be determined by determining the KS statistic which in itself is an effect size measure (quantifies the difference between distributions). That value can be used to determine the effect size. That value is 0.4 (using equation in Knuth & E., 1973) when comparing the distributions of DRG neurons angles on F7/SC and on PA5 which account for an effect size between medium and large. One could infer the sample size using a table like Cohen's table but with values for K-S for goodness of fit and contingency instead of Chi-square for goodness of fit and contingency. If the values are

similar to Chi-square test a sample size between 26 and 87 would be needed (Jacob Cohen, 1992a).

3. Results & Discussion

3.1 Effect of different culture conditions on yield and proportion OEC markers-positive cells

3.1.1 Effect of NT-3 addition timing

NT-3 has a reported effect on OEC proliferation comparable to FBS when added two days after initial plating in serum-containing medium (Bianco et al., 2004). Previously NT-3 had been added at day 6 of culture. It was hypothesised that addition of NT-3 at a different day would have an effect on the yield and proportion of OEC and fibroblast markers. Therefore the effect of the timing of addition of NT-3 on rat olfactory mucosa-derived cells was investigated by comparing two conditions: addition of NT-3 at day 1 or at day 6. Cells were isolated as described, including a differential adhesion step and then cultured on laminin in 2% serum and supplemented with NT-3 (50ng/ mL) (Georgiou et al., 2018). This time cells were re-plated on an equivalent surface area of laminin-coated coverslips to avoid trypsination. For the first test group NT-3 was added from day 1 and for the second test group the NT-3 was added from day 6, after 5 days of cell re-plating, the standard condition. Cells were fixed at day 14 and immunofluorescence labelling was performed to detect: p75NTR, S100β, fibroblast and possible OEC marker, α-SMA and olfactory fibroblast/ ensheathing marker, Thy1.1 and Hoechst.

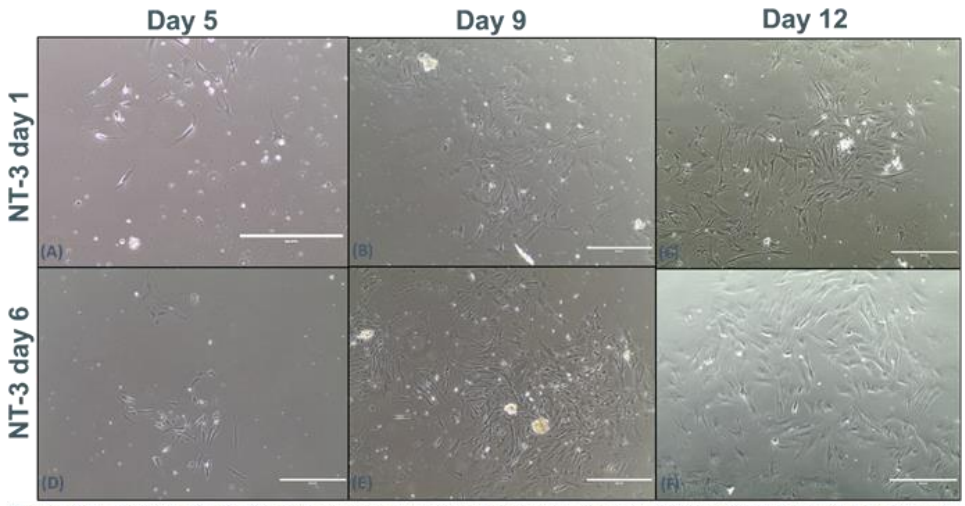

Figure 3.1 – Culture of rat olfactory mucosa-derived cell populations with addition of NT-3 at day 1 and day 6. *Following cell isolation, cells were cultured either with addition of NT-3 (50 ng/mL) at day 1 (A, B and C) or at day 6 (D, E and F) on laminin with 2% serum. Scale bars are 200µm. Bright field micrograph of the cell populations derived from rat olfactory mucosa at day 5, 8 and 14 with addition of NT-3 at day 1 (top row) and at day 6 (bottom row) suggest no difference in cell numbers and morphology between the two test groups. Scale bars are 400µm.*

Bright field and fluorescent micrographs do not show any difference in cell numbers between the two test groups (Figure 3.1). There was a higher proportion of Thy1.1 positive cells at NT-3 addition at day 6, compared to NT-3 addition at day 1. Furthermore both conditions seem to have few cells positive for the putative OEC marker p75NTR (Figure 3.2).

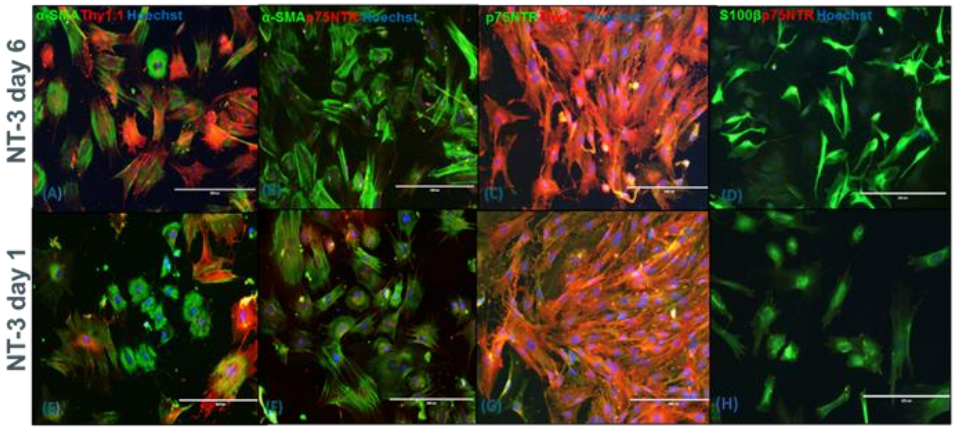

Figure 3.2- Characterization of rat olfactory mucosa-derived cell populations cultured with addition of NT-3 at day 1 (A, B, C and D) or day 6 (E, F, G and H). *Following cell isolation, cells were cultured at ambient O2 (21%), on laminin with 2% serum + NT-3 (50 ng/mL (added at day 1 or 6 for the two test groups, respectively). At day 14, cells were fixed and stained for p75NTR (a putative OEC marker), S100ß (peripheral nerve glial marker), Thy1.1 (olfactory fibroblast marker), α-smooth muscle actin (α-SMA). Scale bars are 200µm.*

The number per unit of area and proportion of positive cells for each of the markers was determined for the two studied conditions, addition of NT-3 at day 1 and addition at day 6 (Figure 3.3).

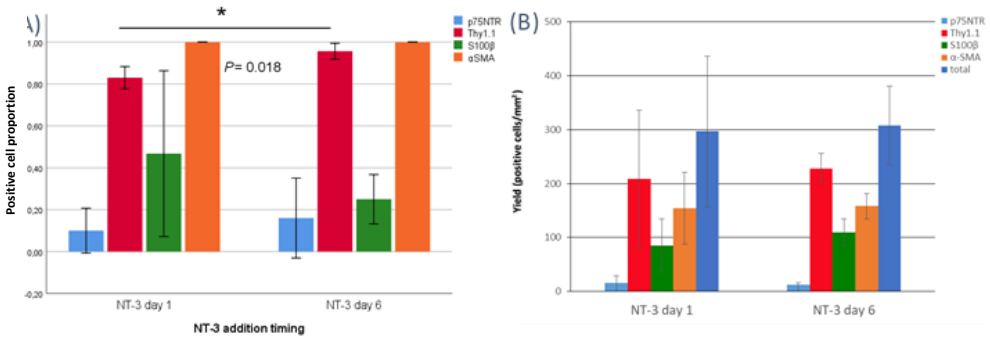

Figure 3.3- Cell purity (A) and yield (B) of OECs derived from rat olfactory mucosa at day 14 following NT-3 addition from day 1 or day 6. *(A) Quantification of the fluorescent micrographs revealed that cells were mostly positive for Thy1.1 and α-SMA and there is a significantly higher proportion of cells positive for Thy1.1 with later addition of NT-3 (day 6) (*P=0.018, one-way MANOVA). (B)There was a higher yield of Thy1.1- and α-SMA-positive mucosa-derived cells cultured in with earlier addition of NT-3 (day 1). However none of those differences were significant. Data are means ± SD, n=4.*

The multivariate test statistic Pillai's trace (see definition in Appendix) show that overall there is a significant effect of the addition timing of NT-3 on the markers proportion (P=0.050) but not yield (P=0.238). The tests of between-subjects effects show that the model which in this case is just the independent variable addition timing of NT-3 explains the variance in yield for all markers measured (p75NTR: P=0.050, Thy1.1: 0.006, S100β: 0.005 and α-SMA: P= 0.002) and only explains the variance for Thy1.1 proportion (P<0.0001). Looking at the pairwise comparisons there was a significant difference between addition of NT-3 on day 1 or day 6 for Thy1.1 proportion (day 1: 83% ± 11%, day 6: 94% ± 5%, P=0.018, one-way MANOVA with Bonferroni correction). Although it explained the variance on the tests between subjects' effects the variation of time of addition of NT-3 does not have a significant effect on individual variations on each marker yield response as shown on the pairwise comparisons.

In summary, the proportion and yield of the putative OEC marker, p75NTR, was lower although not significantly and the Thy1.1 proportion was higher with addition of NT-3 at day 6 (P=0.018, pairwise comparison, Bonferroni correction). Also the morphology of the cells seems to have changed from a bipolar form (Figure 3.2 A, B, C and D) to a more irregular and circular cell shape (Figure 3.2 E, F, G, H).

NT-3 is a neurotrophic factor in the NGF (Nerve Growth Factor) family of neutrophins. It has activity on some neurons of the peripheral nervous system, it supports survival, growth and differentiation of neurons (Maisonpierre et al., 1990). It was shown that NT-3 addition at the concentration of 50 ng/mL promoted enrichment and proliferation of human mucosal OECs and performed equally to 10% serum media (Bianco et al., 2004). Previous studies using rat mucosal isolation protocols also showed that addition of NT-3 increased p75NTR positive cells when added after 6 days of culture (Georgiou et al., 2018) when compared to no addition. To optimise the protocol these studies aimed to determine the effect of the timing of addition of the neurotrophic factor NT-3 on rat mucosal OECs. The hypothesis was that addition from day 1 would increase putative OEC marker-positive cells' proportion and yield.

There was not a significant difference in positive cells proportion or yield for neither of the OEC putative markers (S100β and p75NTR) suggesting that adding the neurotrophic factor NT-3 at different times of co-culture does not influence neither the proportion and yield of rat mucosal OECs.

Furthermore, there was a high proportion in Thy1.1 and α-SMA positive cells for both conditions when compared to the other markers. The proportion of Thy1.1 was significantly higher for addition of NT-3 at day 6. The data also indicates that there is a higher yield of α-SMA and Thy1.1 positive cells when compared to S100β and p75NTR positive cells for both conditions. Thy1 and α-SMA are known to be fibroblast markers as well as OECs (Jahed et al., 2007; Kemshead, Ritter, Cotmore, & Greaves, 1982; Nakamura et al., 2006). Even though the protocol for isolation comprises a differential adhesion step to selectively remove rapidly adherent contaminating cells (fibroblasts, possibly, which are known to proliferate faster), there is still the possibility of contaminating cells being present. It appears that differential addition of NT-3 had no influence on the proportion of fibroblastic cells either.

This study has the limitation of biological variability where the number of OECs in the rat mucosa tend to be low and therefore as shown in the statistical data analysis more experimental repeats would be needed to detect the apparently small effect of NT-3 addition on proportion and yield of these markers.

In conclusion, even though the proportion of Thy1.1-positive cells was significantly higher, there was only a difference of 10% between conditions. Moreover, it is not possible to draw any conclusions from a difference in just one marker as it does not define a cell phenotype completely. Overall, there were no significant differences in yield and proportion on cell phenotype at day 14 in culture, whether NT-3 was added at day 1 or from day 6.

Nevertheless the sample size is very small and more experimental repeats would be needed to effectively conclude the effect of NT-3 timing addition on the yield and proportion of OEC markers positive cells.

3.1.2 Effect of addition of Cytosine β-D-arabinofuranoside (AraC)

The addition of the anti-mitogen Cytosine β-D-arabinofuranoside (AraC), a cell killing agent constituted by a cytosine base and arabinose a sugar very similar to the deoxyribose constituent of DNA which allows it to incorporate the DNA and disrupt cell division removing the fast dividing, contaminating fibroblasts (Pellitteri et al., 2014; Vincent, Taylor, et al., 2005). It was hypothesised that addition of AraC would increase yield and proportion of OEC marker positive cells by removing fast proliferating fibroblasts and at the cost of a few OECs. Thus the effect of addition of AraC was investigated on the culture of rat olfactory mucosa-derived cells. The effect of exposure to AraC for 24 hrs was compared to no exposure. Cells were isolated as described (Georgiou et al., 2018), including a differential adhesion step and then cultured on laminin in 2% serum, supplemented with NT-3 (50 ng/ml) at day 6. The cells were exposed to AraC for 24h (at day 7). The time point for addition of AraC was chosen based on methods used in previous studies (Pellitteri et al., 2014; Vincent, West, et al., 2005) and because as the cells take about 5 days to adhere they would have to be centrifuged and resuspended in new media every time AraC was added or removed. Also the yield of the target cells is very low even after expansion, so the addition of AraC at the beginning might lower it even more.

The culture media was changed for all conditions every time for consistency. Cells were fixed at day 14 and immunolabelled to detect: p75NTR, S100β, α-SMA, Thy1.1 and Hoechst.

Bright field and fluorescent micrographs (Figures 3.4 and 3.5, respectively) do not show an obvious difference between cultures with no addition of AraC compared with the cultures where AraC was added for 24h at days 6, 7 and 10. The cell number appear to be low on both conditions of no AraC and exposure to AraC for 24h. This might be due to the low expression of the markers used (it can still be seen the Hoechst staining) and to the high variability of rat primary cell preparations.

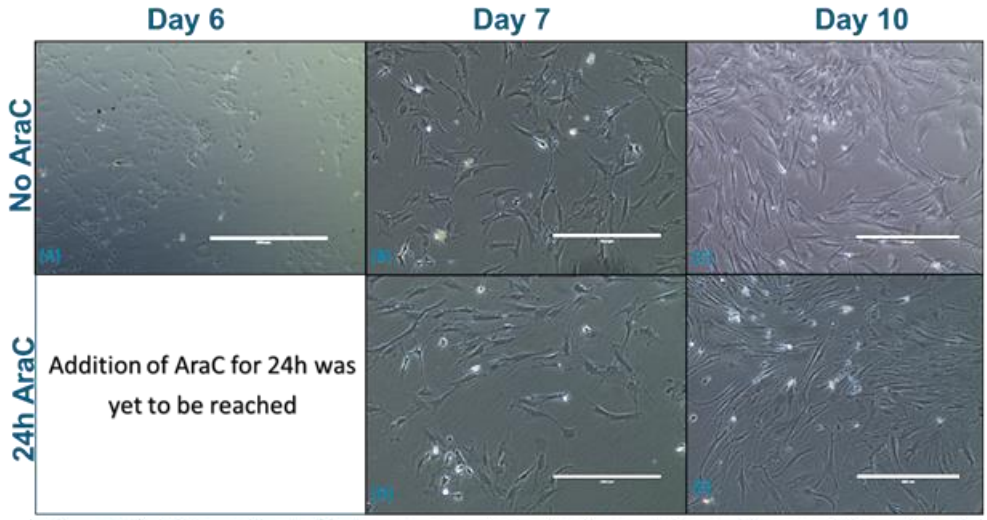

Figure 3.4 - Culture of rat olfactory mucosa-derived cell populations with no addition of AraC (A, B and C) or addition for 24h (D and E). Following cell isolation, cells were cultured with no addition of AraC, addition for 24h on laminin with 2% serum + NT-3 (50 ng/mL) on day 6. Scale bars are 400µm. Bright field micrograph images of a cell population derived from rat olfactory mucosa at day 6, 7 and 10 with no addition of AraC (top row) and addition for 24h (bottom row) show no evident difference between the two conditions. Scale bars are 400µm.

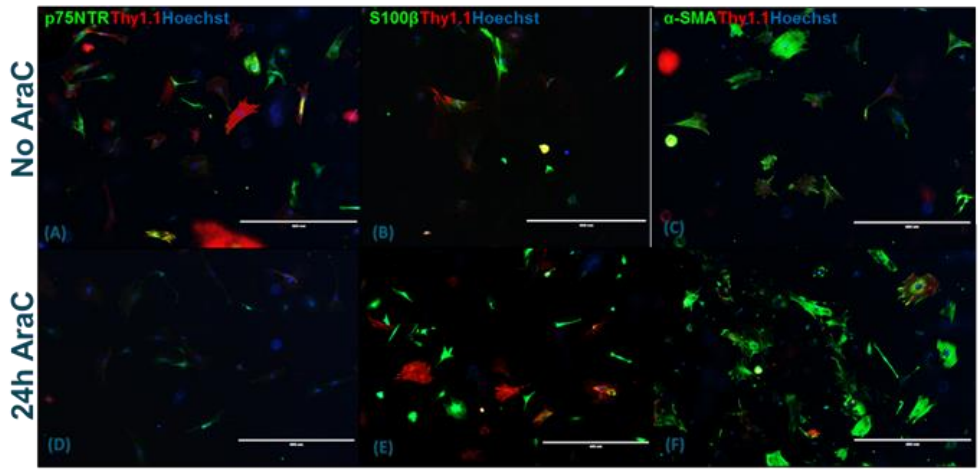

Figure 3.5- Characterization of rat olfactory mucosa-derived cell populations cultured with no addition of AraC (A, B and C), addition of AraC for 24h (D, E and F). *Following cell isolation, cells were cultured at atmospheric O_2 (21%), on laminin with 2% serum + NT-3 (50 ng/mL) starting at day 6. Also at day 6 AraC was added for 24h (test group 1). At day 14, cells were fixed and stained for p75NTR, S100β, Thy1.1 and α-SMA. Scale bars are 400µm.*

The number per unit of area and proportion of positive cells for each of the markers was determined for the two studied conditions, no addition of AraC and addition for 24h (Figure 3.6).

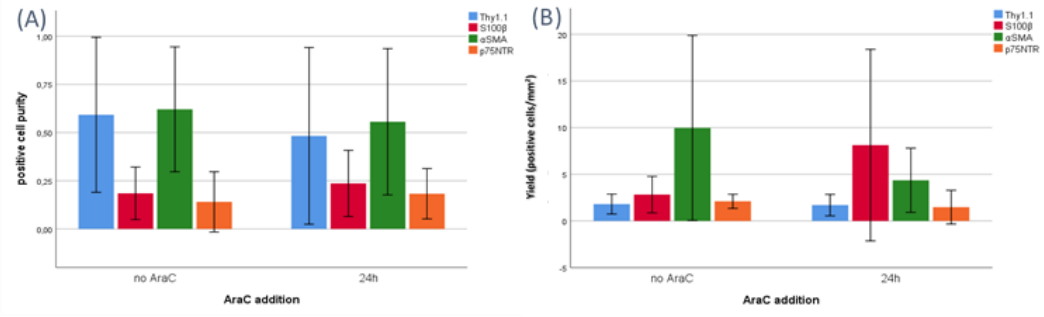

Figure 3.6- Cell yield and purity of OECs derived from rat olfactory mucosa after 14 days in culture following no addition of AraC, addition for 24h. *(A) Quantification of the fluorescent micrographs revealed that cells were mostly positive for α-SMA and there is higher proportion of cells positive Thy1.1 with no addition of AraC and a higher proportion of S100β-positive cells with addition of AraC for 24. However none of those differences were significant.(B) There was a higher yield of α-SMA and S100β-positive mucosa-derived cells cultured with addition of AraC for 24h. However none of those differences were significant. Data are means ± SD, n=4.*

The multivariate tests show that overall there is no significant effect of the addition of AraC for 24h on the markers yield or proportion. The tests of between-subjects effects show that the addition of AraC explains the yield variance for both p75NTR (P=0.032) and Thy1.1 (P=0.022) and all markers' proportion variance except p75NTR (Thy1.1: P=0.050, S100β: P=0.039 and α-SMA: P=0.017).

Interestingly looking at the individual responses from the pairwise comparisons neither total yield nor proportion for any given marker were significantly affected by the addition of AraC for 24h.

AraC is an anti-mitogen that interferes with DNA synthesis and kills dividing cells. It is commonly used in OEC purification usually after a differential adhesion step (Pellitteri et al., 2014; Vincent, West, et al., 2005). It is also used successfully in Schwann cell purification (Brockes, Fields, & Raff, 1979; Brockes & Raff, 1979; Weinstein & Wu, 2001). Nonetheless, there

is no reported studies investigating the effect of AraC on OEC proportion and yield thus reporting if the use of AraC as a purification step is worth at the cost of dividing glia. Therefore this study investigated the effect of exposure to AraC for 24h on proportion and yield of OECs putative markers positive cells. The hypothesis was that exposure to AraC for 24h would increase proportion and maintain or insignificantly decrease the yield.

The experiments exposing rat mucosal OECs to AraC for 24h showed no significant difference on the proportion and yield of the studied markers from culture on AraC-free media.

This study shows that OECs are sensitive to AraC exposure however this results should be interpreted with caution as the proportion of cells positive for fibroblast markers (Thy1.1 and α-SMA) was different and the total number of cells overall was lower when comparing with similar conditions in previous experiments which means that the experimental repeats used were already intrinsically different. Moreover there is a large variance within the samples which illustrates that biological responses can be different from different experimental repeats. This suggests the need for more experimental repeats to detect the effect of AraC exposure on yield and proportion.

The timing and the duration of AraC addition can be optimized. Nevertheless if we assume that the olfactory mucosa-derived cells need some time to adhere when isolated (note that in the protocol used that time is 5 days) the addition of AraC before that might be too harsh on the cell

population, therefore in this study the time chosen for addition of AraC was day 6. It cannot be concluded from these experiments which is the best duration for AraC addition as it was not possible to observe significant differences in cell proportion and yield between no addition of AraC and addition for 24h. Preliminary studies were conducted with exposure of rat mucosal OECs for 48h but there was little cell survival, so perhaps an exposure duration between 24h and 48h would be optimal.

3.2 *In vitro* 2D functional assays for characteristics relating to neuronal regeneration

3.2.1 Co-culture of rat Olfactory Mucosal Cells with NG108 neurons

To test the hypothesis that rat OECs would have an effect on neuronal growth in conditions similar to *in vivo* environment co-culture of rat OECs was done with NG108 neurons at physiologic oxygen. The oxygen level in the central nervous system ranges from 0.55% to 8% (Erecińska & Silver, 2001), considerably lower than the atmospheric conditions commonly used in cell culture and cell manufacturing environments. Therefore the effect of rat olfactory mucosa-derived cells co-culture with NG108 neuronal cell line with comparison with NG108 cell culture on poly-L-lysine (PLL) negative control or on F7 Schwann cells (F7/SC) positive control and at physiologic (2-8%) and ambient (21%) oxygen levels was investigated. Cells were isolated as described, including a differential adhesion step and then cultured on laminin in 2% serum at atmospheric O_2 and supplemented with NT3 (50ng/ml) at day 6. 1000 NG108 neurons were added to each well (~5 cells per mm^2). Cells were co-cultured from day 14 for 3 or 5 days and at physiologic and atmospheric oxygen and stained to detect: S100β glial cell marker and βIII-tubulin neural cell marker. The number of neurons, neurite number and total length was determined for the two conditions tested (atmospheric (21%) and physiologic (2-8%) oxygen concentration) in each experiment: after 3 days of co-culture and after 5 days of co-culture.

The following figure shows bright field micrograph images of a cell population derived from rat olfactory mucosa at day 6, 9 and 12 (Figure 3.7).

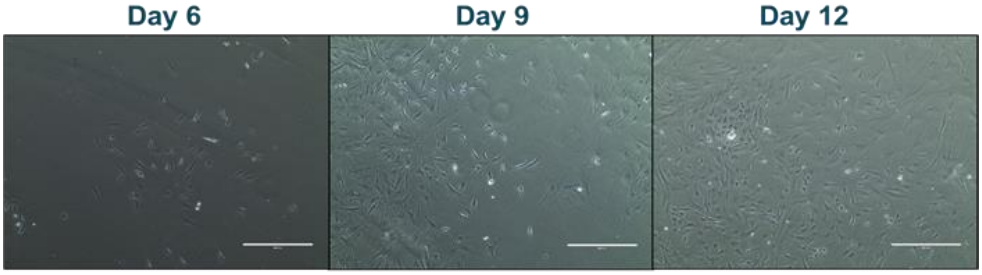

Figure 3.7 - Culture of rat mucosa-derived cell populations at atmospheric oxygen (O_2) concentration at day 6, 9 and 12. *Following cell isolation, cells were cultured at atmospheric O2 (21%), on laminin + 2% serum +NT-3 (50 ng/mL). Scale bars are 400µm.*

Fluorescent micrographs (Figure 3.8) for the three day co-culture show a higher number of neurons (white arrow) and neurites (pink arrow) when co-cultured with F7/SC or OEC at physiologic O_2. It is also evident a higher total neurite length with co-culture of NG108 with F7/SC at both atmospheric and physiologic O_2.

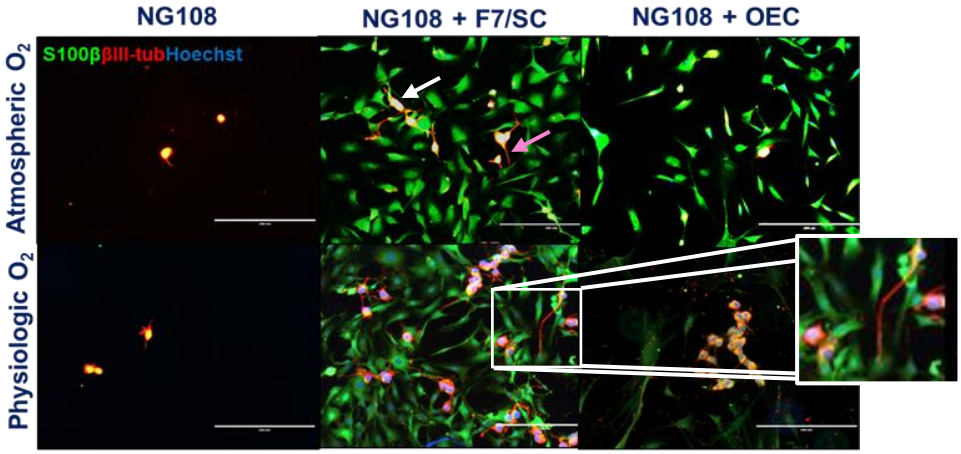

Figure 3.8- Co-culture of NG108-15 neuronal cell line with rat olfactory mucosa-derived cell populations for 3 days at Physiologic and Atmospheric Oxygen. *Following cell isolation, cells were cultured at atmospheric O_2 (21%), on laminin + 2% serum +NT-3 (50 ng/mL). At day 14, NG108-15 cells were cultured with OECs, F7 Schwann cell line or on PLL. After 5 days cells were fixed and stained for S100ß, ßIII-tubulin (a neuronal marker) and Hoechst (stains the nuclei). Scale bars are 200µm.*

For five day co-culture fluorescent micrographs (Figure 3.9) show a higher number of neurons (white arrow) and neurites (pink arrow) when cultured at physiologic O_2. It is also evident a higher total neurite length with co-culture of NG108 with F7/SC and OECs. The nucleus is shown yellow on

the NG108 on PLL culture due to the overlay of the blue of Hoechst staining and the red of β–tubulin staining.

The number of cells, neurites and their length in the NG108 cell population was determined for the two studied conditions, physiologic and atmospheric oxygen for all co-culture in both experiments: co-culture for three (Figure 3.10, 3.11 and 3.12) and five days (Figure 3.13, 3.14 and 3.15).

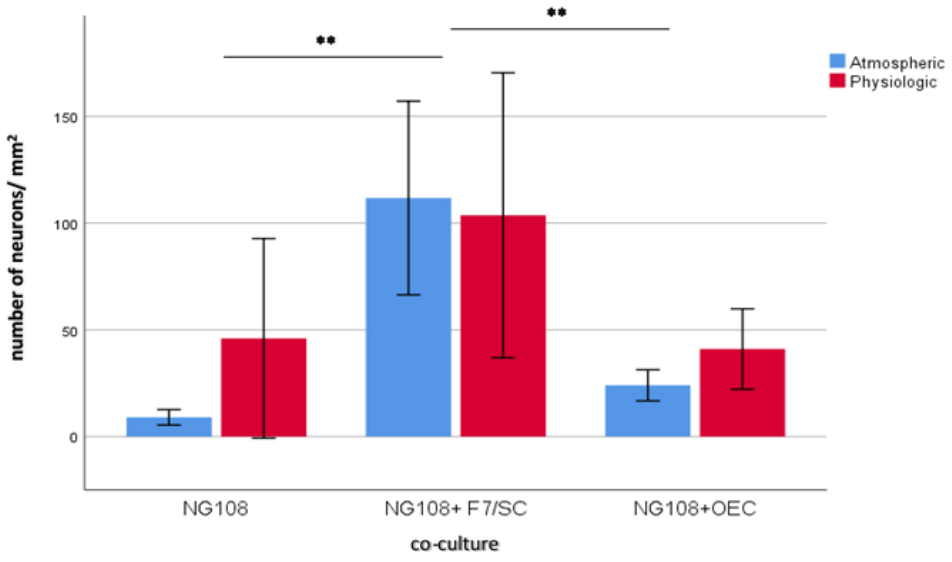

Figure 3.10- Number of NG108 neurons per mm² after co-culture for 3 days with OECs, F7/SC or on PLL at physiologic (2-8%) and atmospheric oxygen (21%). *Quantification of the fluorescent micrographs revealed a significantly higher number of neurons/mm² when co-cultured with F7/SC compared with culture on PLL (P<0.01, Two-way MANOVA with Tukey's post-test). Data are means ± SD, n=4.*

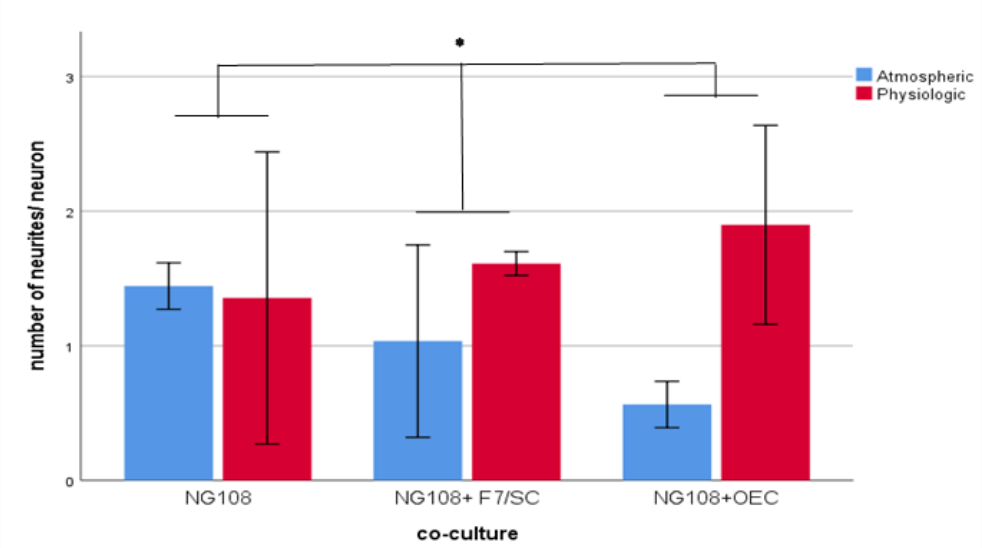

Figure 3.11- NG108 neurite extension number per neuron after co-culture for 3 days with OECs, F7/SC or on PLL at physiologic (2-8%) and atmospheric oxygen (21%). *Quantification of the fluorescent micrographs revealed a higher number of neurites/ neuron when co-cultured at physiologic O_2 (P=0.036, two-way MANOVA with Tukey's HSD post-test) Data are means ± SD, n=4.*

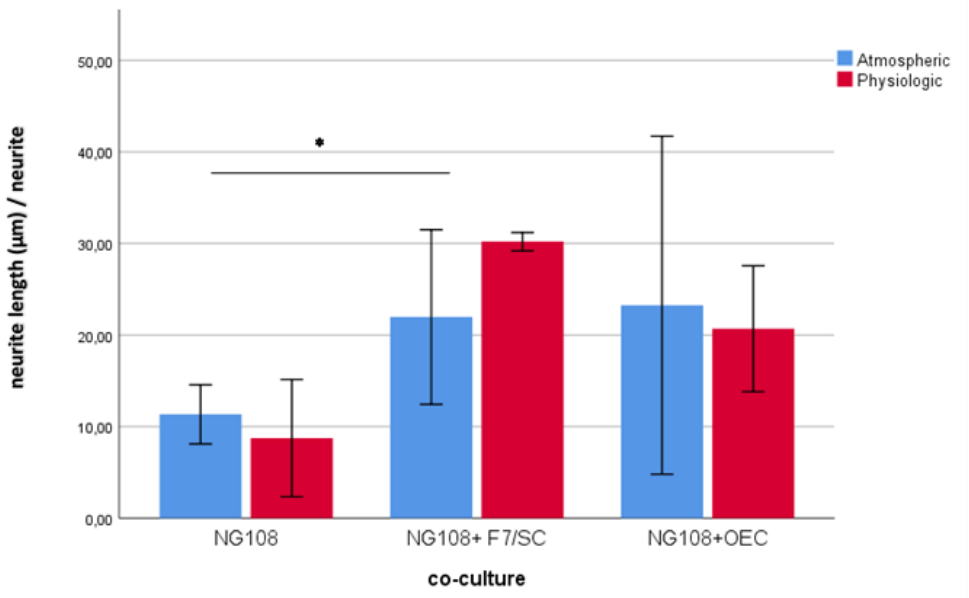

Figure 3.12- NG108 neurite length per neurite after co-culture for 3 days with OECs, F7/SC or on PLL. *Quantification of the fluorescent micrographs revealed significantly a higher extension length when co-cultured with F7/SC when compared with culture on PLL (P<0.025, Two-way MANOVA with Tukey's HSD post-test). Data are means ± SD, n=4.*

The multivariate test statistics Pillai's trace for the three day co-culture experiment showed that the factor type of co-culture has a P value lower than the level of alpha of 0.05 (P=0.009) indicating a significant effect on the overall response. Neither the factor level of oxygen nor the interaction between the culture type nor oxygen level had a significant effect on the overall response.

Now that a significant effect of the type of culture was determined it can be seen specifically in which responses it has a significant effect. According to the tests of between subjects effects the model as a whole explains the variance of the three responses (neurons/ mm^2: P< 0.001; neurites/ neuron: P< 0.001, neurite length/ neurite: P< 0.001). The type of culture explains the variance of the number of neurons/ mm^2 (P=0.0014) and on neurite length/ neurite (P=0.023) and the oxygen level explains the variance of the number of neurites per neuron (P=0.036).

For the three day co-culture of NG108 neurons with F7/SC had a significantly higher number of neurons/ mm^2 (physiologic oxygen: 104 ± 67 neurons/ mm^2, atmospheric oxygen: 111 ± 45 neurons/mm^2) compared with culture on PLL (physiologic oxygen: 46 ± 47 neurons/ mm^2, atmospheric oxygen: 9 ± 4 neurons/mm^2, $P< 0.01$, Two-way MANOVA with Tukey's HSD post-test) or co-culture with rat OECs (physiologic oxygen: 41 ± 19 neurons/ mm^2, atmospheric oxygen: 24 ± 7 neurons/mm^2, $P< 0.01$, two-way MANOVA with Tukey's HSD post-test) regardless of oxygen tension.

The level of oxygen has a significant effect on the number of neurites per neuron. Overall the number of neurites/ neuron for cultures at physiologic oxygen (NG108: 1 ± 1 neurites/ neuron, NG108 + F7/SC: 2 ± 0 neurites/ neuron, NG108 ± OECs: 2 ± 1 neurites/ neuron) was significantly higher when compared with cultures at atmospheric oxygen (NG108: 1 ± 0 neurites/ neuron, NG108 + F7/SC: 1 ± 1 neurites/ neuron NG108 ± OECs: 1 ± 0 neurites/ neuron, $P=0.047$, two-way MANOVA pairwise comparison Bonferroni correction). Nonetheless there was no significant difference between the different co-cultures.

There was also a significant difference for neurite length/ neurite between NG108 on PLL (physiologic: 9 ± 6 µm/neurite, atmospheric: 11 ± 3 µm/neurite) and NG108 on F7/SC (physiologic: 30 ± 1 µm/neurite, atmospheric: 22 ± 10 µm/neurite, $P<0.025$, Two-way MANOVA with Tukey's HSD post-test) for an alpha level of 0.025, irrespectively of oxygen level.

The multivariate test statistics Pillai's trace for the five day co-culture showed that both the factors type of culture and oxygen level have a P value

lower than the level of alpha of 0.05 (P=0.021 and P=0.029, respectively) showing a significant effect on the overall response. The interaction between the culture type and oxygen level had no significant effect on the overall response (P=0.607).

According to the tests of between subjects effects the model as a whole explains the variance of the three responses individually (neurons/ mm^2: P=0.006, neurites/ neuron: P<0.001, neurite length/ neurite: P<0.001), the type of culture and the level of oxygen explain the variance of the neurite length per neurite (P=0.005 and P=0.052, respectively). Although the P value for the oxygen level is above the alpha level of 0.05 looking closer with the pairwise comparisons it can be seen that it is significant (P=0.048, Two-way MANOVA with Bonferroni adjustment).

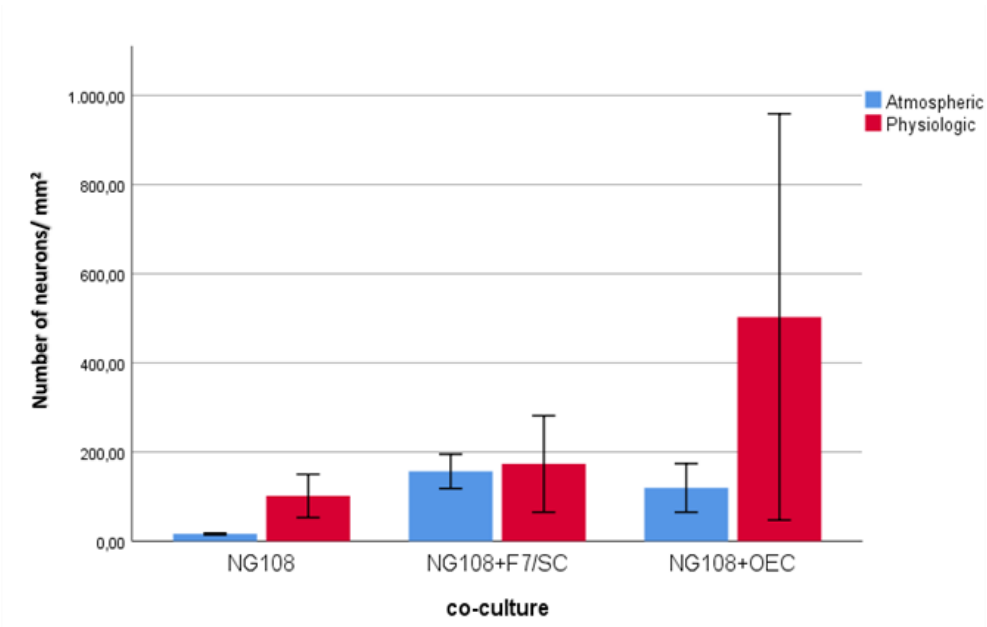

Figure 3.13- NG108 neuron number per mm² after co-culture for 5 days with OECs, F7/SC or on PLL at physiologic (2-8%) and atmospheric oxygen (21%). *Quantification of the fluorescent micrographs revealed a higher number of neurons when co-cultured with OECs. Data are means ± SEM, n=4.*

Five day co-culture showed a higher number of neurons per mm^2 with co-culture with F7/SC (physiologic: 173 ± 108 neurons/ mm^2; atmospheric: 157 ± 38 neurons/ mm^2) when compared with culture on PLL

(physiologic: 102 ± 49 neurons/ mm^2; atmospheric: 16 ± 2 neurons/ mm^2, P=0.005, two-way MANOVA, Tukey's HSD post-hoc test), regardless of oxygen tension.

The number of neurites per neuron has no significant differences between types of culture or oxygen levels (Figure 3.14).

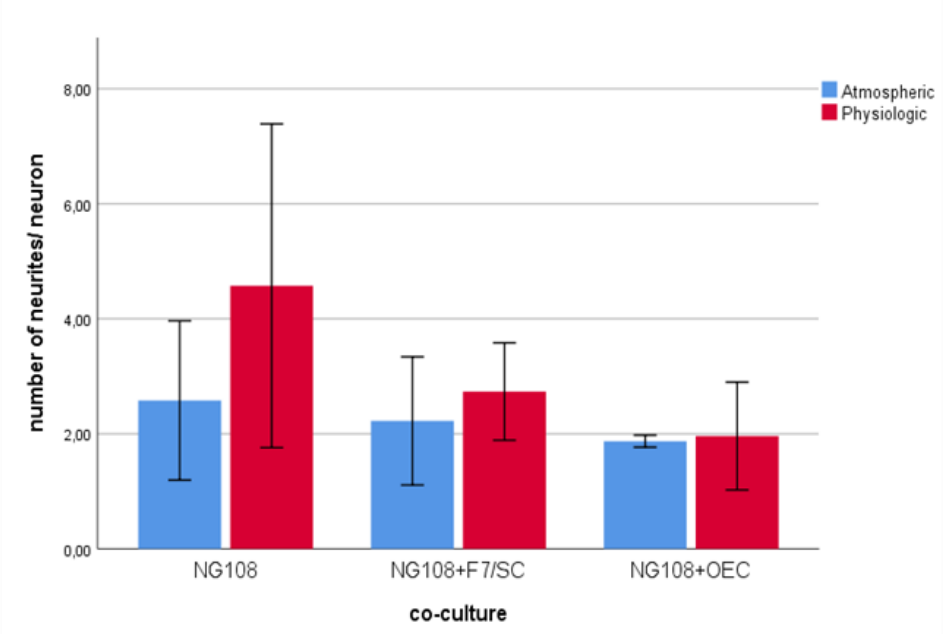

Figure 3.14- NG108 neurite extension number per neuron after co-culture for 5 days with OECs, F7/SC or on PLL at physiologic (2-8%) and atmospheric oxygen (21%). *Quantification of the fluorescent micrographs revealed a higher number of neurites when cultured with OECs when compared with culture on PLL (P<0.01, two-way ANOVA, Tukey's post-hoc test) at physiologic O2. Data are means ± SEM, n=4.*

There was a significant difference between the neurite length/ neurite (figure 9.14) for NG108 cells on PLL (physiologic: 9 ± 4 µm/neurite, atmospheric: 6 ± 0 µm/neurite) and NG108 on F7/SC (physiologic: 21 ± 8 µm/neurite, atmospheric: 15 ± 2 µm/neurite, P=0.005, two-way MANOVA, Tukey's HSD post-hoc test) for an alpha level of 0.05.

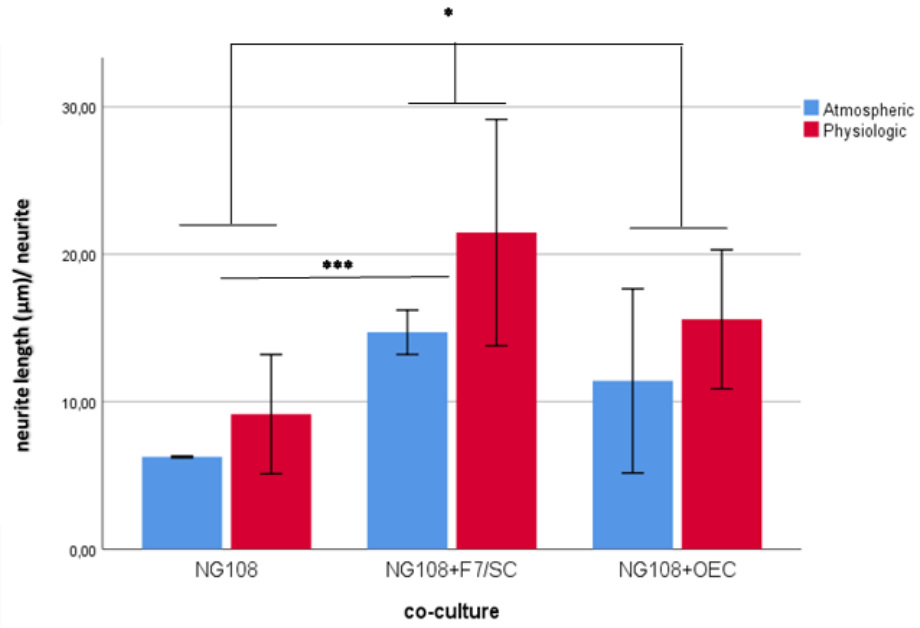

Figure 3.15- NG108 neurite length after co-culture for 5 days with OECs, F7/SC or on PLL at physiologic (2-8%) and atmospheric oxygen (21%). *Quantification of the fluorescent micrographs revealed a significantly higher extension length with culture at physiologic oxygen (P<0.001, two-way ANOVA, Tukey's post-hoc test). It also showed a higher neurite length with co-culture with OECs when compared with culture on PLL or with F7/SC (P<0.01 and P<0.05, respectively, two-way ANOVA, Tukey's post-hoc test). Data are means ± SD, n=4*

Although several *in vitro* neuronal outgrowth studies have been done with rat OECs most of them used cells from the olfactory bulb. In fact, extensive work has been undertaken using OEC rat olfactory bulb isolation protocols that served as ground work for a lot of assays (R. Doucette, 1989; Franceschini & Barnett, 1996; Pixley, 1992; Raff & Miller, 1983; Raisman, 1985; Ramón-Cueto & Avila, 1998; Valverde et al., 1992; Q. Yan & Johnson, 1988). Moreover bulb cells are potentially easier to purify with fewer subpopulations of cells than the olfactory mucosa. On the other hand the olfactory mucosa is a more accessible source of OECs and with robust isolation protocols, high quantities of OECs can be obtained (S.C. Barnett & Roskams, 2008; Richter et al., 2008).

The few studies performed with rat olfactory mucosa either just focussed on cell proportion according to OECs markers such as p75NTR or GFAP (E. Au & Roskams, 2003); or the OEC's ability to induce neurogenesis

in adult olfactory epithelium (Féron et al., 1999). Other *in vivo* studies using primary OECs also used mainly primary neurons as a model for neuronal regeneration. Therefore these studies aimed to determine the effect of rat mucosal OECs on NG108 neurons.

Several cell models to study neurite outgrowth have been used. These includes primary neuron culture such as cortical neurons, cerebellar granule neurons and cell lines such as PC12 cells, and neuroblastoma cells such as NG108 as SH-SY5Y (Lozano, Schmidt, & Roach, 1995; Simpson et al., 2001). The use of a neuronal cell line instead of primary cells aimed to establish reproducible neuronal regeneration assays by using a well-known cell line. This line, NG108, is a somatic cell hybrid formed by Sendai virus-induced fusion of the mouse neuroblastoma clone N18TG-2 and the rat glioma clone C6BV-1 (http://www.sigmaaldrich.com/catalog/product/sigma/88112302?lang=en&region=GB, 18/07/2017). These cells are similar to sympathetic ganglion neurons in terms of physiology as the parent neuroblastoma cells originate from this tissue. They also have been used extensively as a neuronal model in many applications including various neuronal regeneration assays (Kraus, Boyle, Leibig, Stark, & Penna, 2015; Pateman et al., 2015; Sowa et al., 2017; Sun & Downes, 2007; Tse et al., 2016). Amongst other advantages this cell line presents a consistent behaviour from cell to cell for the same conditions and it also has no satellite glia contamination, which often happens with primary neuronal cell cultures (Docherty & Brown, 1991).

Even so, it was not known how long it would take for OECs to have an effect on NG108 neurons or if that effect would be the same in physiologically relevant oxygen levels. It is known that the oxygen level in the central nervous system ranges from 0.55% to 8% (Erecińska & Silver, 2001), considerably lower than the atmospheric conditions commonly used in cell culture and cell manufacturing environments. There have been several neurite outgrowth co-culture studies using rat OECs, mostly from the bulb with durations ranging from 24h up to one week (Chung et al., 2004; M. Nadine Goodman et al., 1993; Hayat, Thomas, Afshar, Sonigra, & Wigley, 2003; Kafitz & Greer, 1999; Khankan, Wanner, & Phelps, 2015b; Leaver, Harvey, & Plant, 2006; Pellitteri et al., 2009; Ramón-Cueto & Valverde, 1995; Roloff, Ziege, Baumgärtner, Wewetzer, & Bicker, 2013; Sethi, Sethi, Redmond, & Lavik, 2014; Rakesh J. Sonigra et al., 1999; Tisay & Key, 1999). Interestingly there is few studies accessing OEC performance in neuronal regeneration under conditions closer to the spinal cord *in vitro* and/or accessing the influence of time in neuronal regeneration. Therefore the effect of rat OECs on NG108 neurons was investigated for 3 and 5 days at physiological (2-8%) or atmospheric oxygen (21%). The hypothesis were: 1) OEC would perform better or similarly to F7/SC and better than NG108 on PLL 2) Oxygen level would influence neuronal development 3) Culture duration would influence neuronal development.

In both co-cultures of 3 and 5 days duration the type of co-culture had an influence in the overall response, however only after 5 days of co-culture did oxygen level have an impact on the overall response. This

suggests that the oxygen level might have a time dependent influence on the neural responses analysed. In fact, NG108 cells are able to undergo differentiation with changes in the culture environment (Seeds, Gilman, Amano, & Nirenberg L, 1970), therefore when they are in a proliferative state they are a neuronal progenitor-like type of cell. Neuronal progenitors have been shown to have increased proliferation under physiologic oxygen conditions (Cui et al., 2011; Felling, 2006; P. Zhang et al., 2006) which explains the general increase in number of neurons per mm^2 for physiologic conditions.

These assays showed that co-culture with rat OECs after 5 days when compared to co-culture after 3 days have a much higher number of NG108 neurons per mm^2 but the same or lower number of neurites per neuron and neurite length per neurite suggesting time does not have an effect on neither the number nor length of each neurite. Interestingly physiologic oxygen conditions resulted in a general increase in the neuronal development responses measured in both co-culture durations. Although not significantly different after 5 days the rat OEC co-culture at physiologic oxygen has the highest number of neurons per mm^2 which is consistent with reports of OEC neuronal protection and survival (Pellitteri, Russo, Stanzani, & Zaccheo, 2015).

Oxygen level increases the number of neurites per neuron after 3 days of co-culture and neurite length per neurite after 5 days, regardless of co-culture type. Although a direct comparison to this study is not possible as the neurite length is represented per neuron and not per neurite, it was

observed that neurite length per neuron is higher for physiologic conditions in similar cell lines like PC12 cells (Genetos, Cheung, Decaris, & Leach, 2010). This cell line is derived from pheochromocytoma of the rat adrenal medulla and constituted by a mixture of neuroblastic cells and eosinophilic cells (Greene & Tischler, 1976). The best oxygen level was 4% with an average of 4000 µm per 100 random cells counted.

On both co-culture studies with different durations there were no significant differences between co-cultures for the number of extensions per neuron. The number of neurons per mm^2 and neurite length per neurite however are influenced by the co-culture type after 3 days. After 5 days the neurite length per neurite was also influenced by the type of co-culture.

Co-culture with F7/SC positive control performed better in both studies compared to the NG108 co-culture negative control. After three days of co-culture the number of neurons per mm^2 was higher compared to both NG108 on PLL (the negative control) and co-culture with rat OECs, the test condition. The neurite length per neurite was also higher in co-cultures with F7/SC when compared to the negative control. After five days of co-culture, neurite length in the F7/SC cultures perform better compared to the negative control, NG108.

A limitation of this study is the fact that F7/SC grow faster. Even though the same number of cells was seeded on each well after two days it was observed that there were more F7/SC than OECs which could influence their effect on neuronal growth, neurite extension length and cell number.

This leads to a different ratio of glial cells to neurons for the cells grown on rat OECs test group and cells grown on the positive control F7/SC.

This study suggests that rat mucosal OECs perform similarly to F7/SC in number of neurites per neuron and neurite length per neuron on NG108 neuronal cell line. As reported previously (Leaver et al., 2006; Roloff et al., 2013) OECs can enhance *in vitro* growth of neuronal fibres however these studies used rat olfactory and dog olfactory bulb, respectively. Nevertheless the sample size is small and as shown later on it is unlikely to detect all effects from all factors in this study. Therefore more experimental repeats would be needed for more conclusive results.

3.2.2 Co-culture of PA5 cell line with NG108 neurons

The effect of PA5 cell line co-culture with NG108 neuronal cell line with comparison with NG108 cell culture on poly-L-lysine (PLL) negative control or on F7 Schwann cells (F7/SC) positive control was investigated. Cells were cultured as described, on PLL in 10% serum at atmospheric O_2. Cells were co-cultured for 3 or 5 days and at atmospheric or physiologic oxygen and stained to detect: S100β glial cell marker and βIII-tubulin neural cell marker. The number of neurons, neurite number and total length was determined for all co-cultures.

The following figure shows bright field micrograph images of PA5 cell line before co-culture (Figure 3.16).

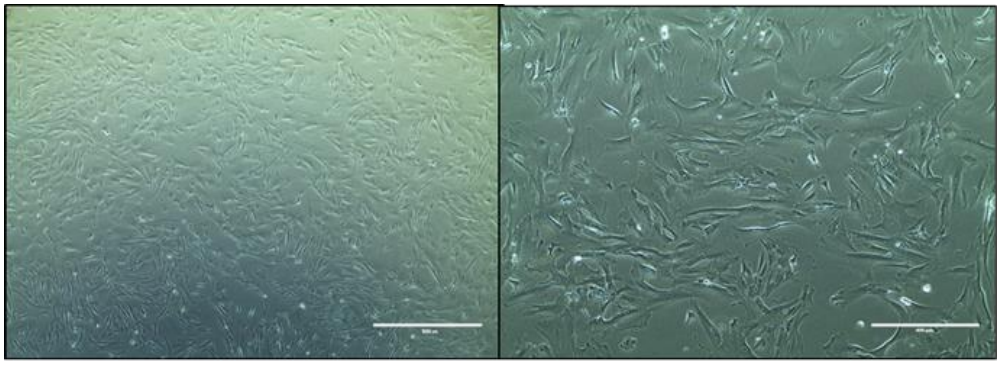

Figure 3.16 - Culture PA5 cells at atmospheric oxygen (O_2) concentration. Cells were cultured at atmospheric O_2 (21%), on PLL with 10% serum. Scale bars are 1000 (left) and 400μm (right).

Fluorescent micrographs (Figure 3.17) show a higher number of neurons and neurites when co-cultured with F7/SC or OEC for the five day co-culture. It was also evident that greater neurite length was seen with co-cultures of NG108 with F7/SC and PA5 cells, compared to negative controls. S100β expression is inconsistent for F7/SC and non-existent for PA5 cells which might be related to the antibody used or intrinsic S100β expression variation of these cells. It was therefore difficult to characterise them in culture although they are visible through Hoechst staining and not expressing βIII-tubulin.

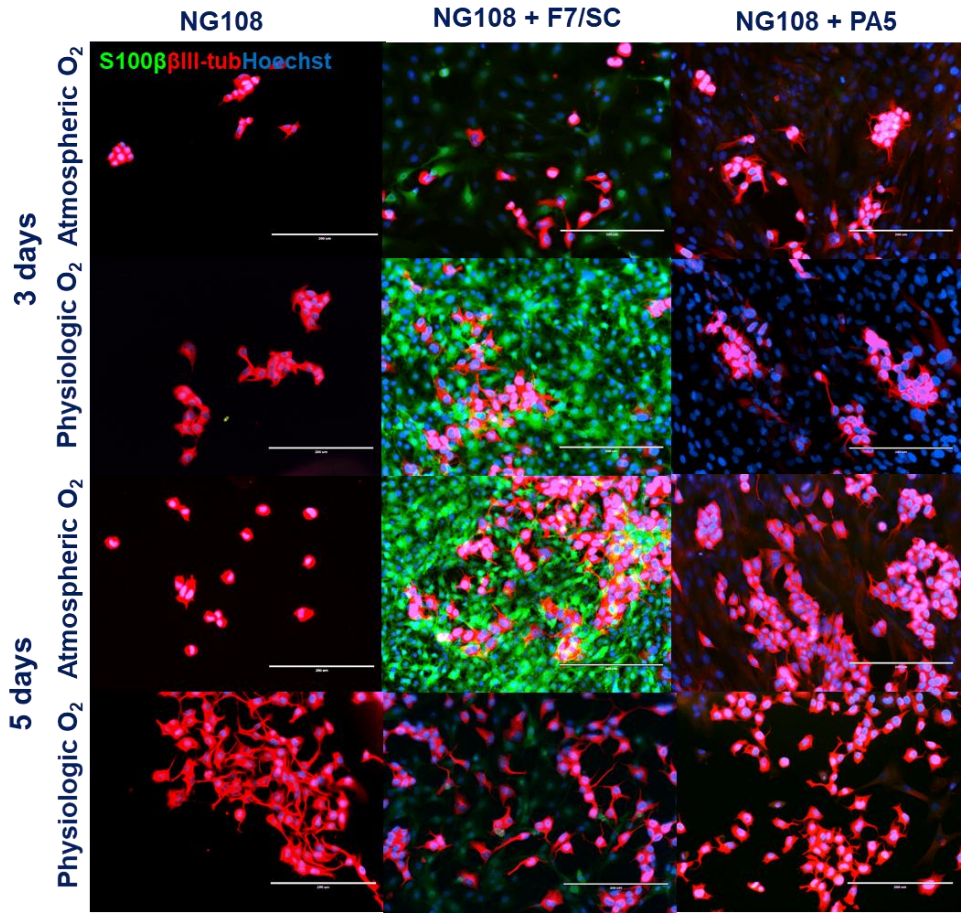

***Figure 3.17*- Co-culture of NG108 neurons with human PA5 cell line for 3 or 5 days at atmospheric or physiologic oxygen.** Following cell culture, cells were cultured at atmospheric O_2 (21%), on PLL + 10% serum. NG108 neurons were cultured with PA5 cells, F7 Schwann cell line or on PLL. After 3 or 5 days cells were fixed and stained for S100β, βIII-tubulin and Hoechst. Scale bars are 200µm.

The number of cells, neurites and their length in the NG108 cell population was determined for all co-cultures (Figure 3.18, 3.19 and 3.20).

According the multivariate test statistics Pillai's trace all factors studied had a significant effect on the overall results (co-culture: P<0.0001; culture duration: P<0.00001) and so did the second degree interactions (co-culture*culture duration: P=0.001, co-culture*level of oxygen: P=0.001 and culture duration*level of oxygen: P=0.001) and third degree interactions (co-culture*culture duration*oxygen: P=0.0005, oxygen level: P=0.018, three-way MANOVA).

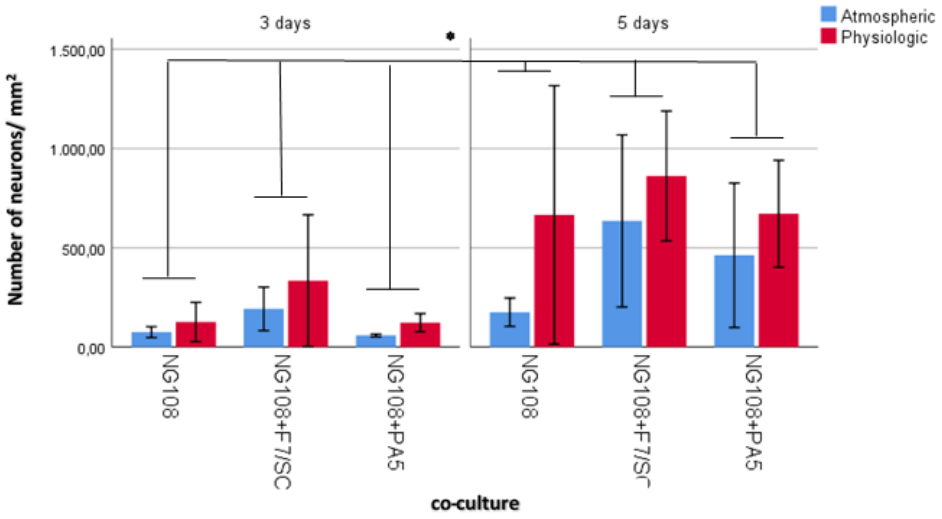

Figure 3.18- NG108 neuron number per mm² after co-culture for 3 or 5 days with PA5 cells, F7/SC or on PLL. *Quantification of the fluorescent micrographs revealed a higher number of neurons when cultured for 5 days. Data are means ± SD, n=4.*

On the tests between subjects' effects it can be seen that the model explains the variance of all three responses individually (number of neurons/ mm^2, number of neurites per neuron and neurite length per neurite). Nevertheless, the factor co-culture only explains the variance of the number of neurites per neuron (P<0.00001) and the level of oxygen the variance of the number of neurons/ mm^2 (P=0.043) and number of neurites per neurons (P=0.002). The factor duration of co-culture explains the variation of all

responses (number of neurons/ mm^2: P<0.0001, number of neurites/ neuron: P=0.003 and neurite length per neurite: P=0.027). None of the second degree interactions explains the variance of the number of neurons/mm^2 but they all had a significant effect on the number of neurites/ neuron (co-culture*duration: P<0.00001, co-culture*level of oxygen: P<0.000001 and duration*level of oxygen: P<0.0001). The co-culture*duration second degree effect also explains the variance of neurite length/ neurite (P=0.007). The third degree interaction co-culture*duration*level of oxygen explains the variance of both the number of neurites/ neuron (P<0.00001) and neurite length/ neurite (P=0.015).

The pairwise comparisons show a significant difference for all

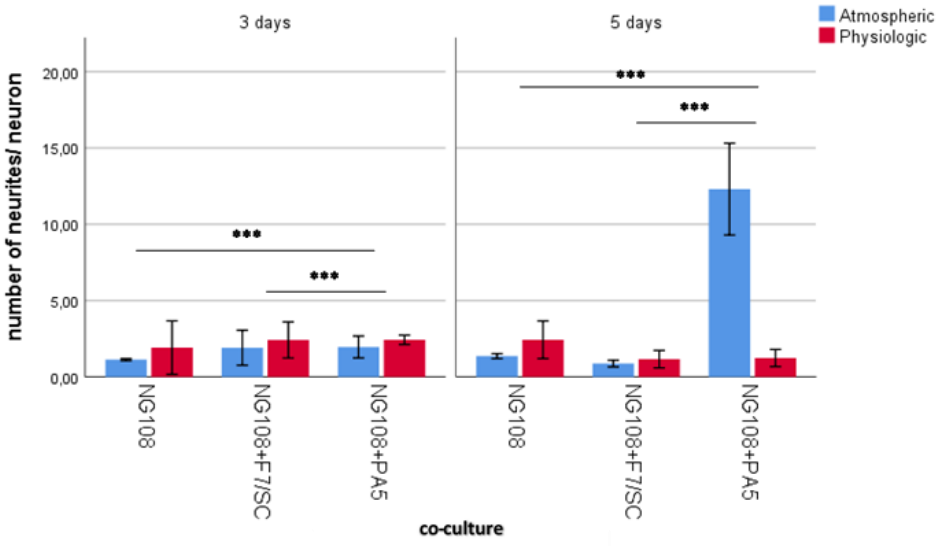

Figure 3.19- NG108 neurite extension number per neuron after co-culture for 3 or 5 days with OECs, F7/SC or on PLL at physiologic (2-8%) and atmospheric oxygen (21%). *Quantification of the fluorescent micrographs revealed a higher number of neurites/ neuron when co-cultured with PA5 when compared to NG108 on PLL (P<0.0001) or NG108 + F7/SC (P<0.00001, three-way MANOVA with Tukey's HSD post-test).* All second degree interactions had a significant effect on the number of neurites/ neuron (co-culture*duration: P<0.00001, co-culture*level of oxygen: P<0.000001 and duration*level of oxygen: P<0.0001). The third degree interaction co-culture*duration*level of oxygen also had a significant effect on both the number of neurites/ neuron (P<0.00001). *Data are means ± SD, n=4.*

responses between 3 and 5 days co-culture (number of neurons/ mm^2: P<0.001; number of neurite per neuron: P=0.003; neurite length: P=0.027, three-way MANOVA pairwise comparison Bonferroni adjustment). The level of oxygen has a significant effect on the number of neurons per mm^2 and

number of neurites per neuron (number of neurons/ mm^2: P=0.043; number of neurite per neuron: P=0.002, three-way MANOVA pairwise comparison with Bonferroni adjustment).

The multiple comparisons showed that there is a significant difference for the number of neurites/ neuron (figure 3.19) between NG108 + PA5 cells (3 days, atmospheric 2 ± 1 neurites/ neuron, physiologic: 2 ± 1 neurites/ neuron; 5 days, atmospheric: 16 ± 4 neurites/ neuron, physiologic: 1 ± 0 neurites/ neuron) and NG108 on PLL (3 days, atmospheric 1 ± 0 neurites/ neuron, physiologic: 2 ± 1 neurites/ neuron; 5 days, atmospheric: 1 ± 0 neurites/ neuron, physiologic: 2 ± 1 neurites/ neuron, P<0.0001, Three-way MANOVA Tukey's HSD post-test) or NG108 + F7/SC (3 days, atmospheric 2 ± 1 neurites/ neuron, physiologic: 2 ± 1 neurites/ neuron; 5 days, atmospheric: 1 ± 0 neurites/ neuron, physiologic: 1 ± 1 neurites/ neuron, P<0.00001, Three-way MANOVA Tukey's HSD post-hoc test).

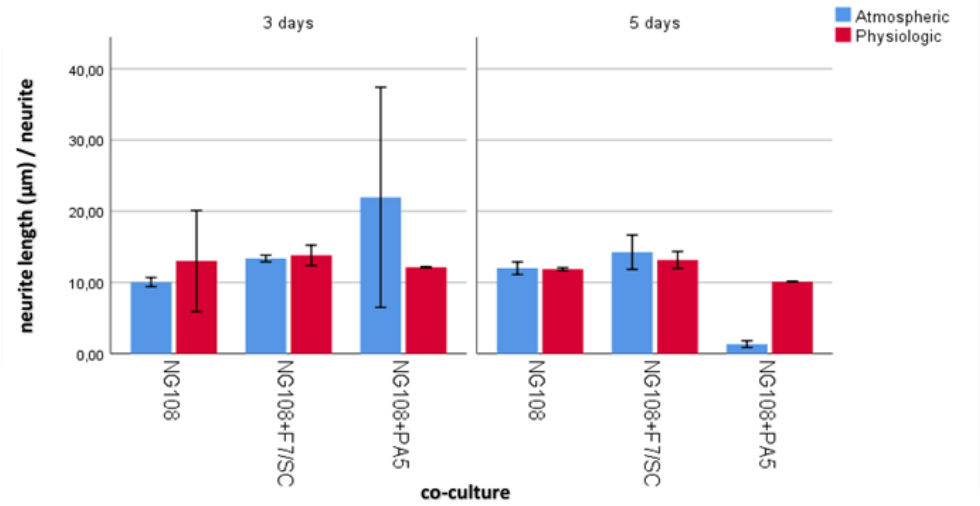

Figure 3.20 - NG108 neurite length after co-culture for 3 or 5 days with PA5 cells, F7/SC or on PLL at physiologic (2-8%) and atmospheric oxygen (21%). *Quantification of the fluorescent micrographs revealed no significant differences in extension length per neuron between culture type and duration.* The co-culture*duration second degree effect had a significant effect on neurite length/ neurite (P=0.007). The third degree interaction co-culture*duration*level of oxygen also had a significant effect on neurite length/ neurite (P=0.015). *Data are means ± SD, n=4.*

The multiple comparisons showed no significant difference between co-cultures for neuron number per mm^2 or neurite length per neuron.

Earlier studies assessing OEC neuronal outgrowth capacity used mostly rat bulb cells as a source of OECs. Although OEC neuronal regeneration ability can be evaluated in a first instance with rat cells it is useful to confirm that capacity and its extend using human cells for translational purposes. Though there is no *in vitro* neuronal regeneration assays using human mucosa OECs, there is evidence of remyelination after transplant into rat SCI (S. C. C. Barnett et al., 2000) and several pilot and phase I clinical trials with autologous human mucosal OECs transplants in which safety was established and functional recovery had varied results but none with significant functional improvement (Chhabra et al., 2009; Féron et al., 2005; Lima et al., 2006, 2010; Mackay-Sim et al., 2008).

In these studies we aimed to determine the effect of the human mucosa OEC conditionally immortalized cell line PA5 on NG108 neurons. These cells were genetically modified with a conditional immortalizing transgene, c-mycER(TAM) generating a fusion protein that in the presence of 4-hydroxy-tamoxifen (4-OHT) stimulates cell proliferation. The c-mycER^{TAM} gene can be silenced upon transplantation into the patient with no addition of 4-OHT (Littlewood et al., 1995). To confirm the OEC neuronal regeneration performance on NG108 neurons with a human cell line the effect of PA5 cells on NG108 neurons was investigated for 3 or 5 days at physiological (2-8%) or atmospheric oxygen (21%). Previous results suggested that after 5 days NG108 neurons cultured on rat OECs increased their cell number and that physiologic oxygen inflates cell number for all co-culture durations studied. So at this point there was an idea of the timescale

for OECs to have an effect on NG108 neurons although the particular effect of PA5 human OECs was unknown.

As mentioned at the beginning immunofluorescence labelling of PA5 did not reveal conclusive S100β labelling across all conditions and F7/SC in different conditions gave either bright staining or low intensity staining. Consequently results for these co-cultures need to be interpreted with caution.

Although the multivariate analysis show that all the factors have an impact on the overall response, the tests between subjects' effects and the pairwise comparisons show something different. There is a statistically significant impact of the co-culture duration on all responses, however considering the trend in the graphs this study seems to show that duration of the culture has little impact on number of neurites or neurite length as seen in the co-culture with rat OECs. It seems to have been highly influenced by the extreme values for number of neurites per neuron and neurite length per neurite for the condition NG108 co-culture with PA5 for 5 days at atmospheric oxygen. This might be explained by the fact that the tests between subjects' effects and the pairwise comparisons take into account the overall variance of a response for all combinations of factors in which extreme values like the one for the number of neurites per neuron or neurite length per neurite for co-culture of NG108 on PA5 at atmospheric oxygen after 5 days weights more on the influence a certain factor might have. The number of neurons per mm^2 however was significantly and clearly higher

after co-culture for 5 days, which was expected: the longer the culture the higher the number of neurons present until confluency potentially.

It was established that physiologic oxygen has an effect on number of neurons per mm^2 and neurites per neuron. Interestingly, although the statistical tests also showed a significant effect of the oxygen level on the number of neurites per neuron, looking at the graphs suggested that the oxygen level seemed to have little influence on the number of neurites per neuron. This might be explained by the extreme values of the number of neurites per neuron for NG108 co-culture with PA5 for 5 days at atmospheric oxygen. Contrarily to the previous studies of rat OECs co-culture with NG108 cells where physiologic oxygen has the tendency to perform similarly or better all measurements of neuronal development that was not replicated in this study which in general had about the same values except for number of neurons per mm^2. As explained before this might be due to NG108 cells being able to undergo differentiation with changes in the culture environment (Seeds et al., 1970) and therefore when they are in a proliferative state they are a neuronal progenitor-like type of cell. Therefore, cell complexity makes it difficult to draw clear conclusions.

The co-culture with F7/SC or PA5 cells or on PLL had no influence on the number of neurons per mm^2 or on neurite length. To be completely strict, the test between subjects' effects probably detected a significant difference in neurites per neuron because of the extreme value of the co-culture of NG108 on PA5 cells at atmospheric oxygen after 5 days. This condition seems to have several very short neurites which can also be seen

in figure 3.17. This might have led to a significant difference in neurites per neuron between NG108 culture on PA5 cells and culture on PLL or F7/SC, between atmospheric and physiologic oxygen, both durations, all second degree and the third degree interactions. The peak of neurites per neuron for co-culture of NG108 neurons with PA5 after 5 days at atmospheric oxygen might also be related to the fact that this condition had a lower number of neurons per mm^2 than the equivalent condition on F7/SC so a slight increase in number of neurites might have been magnified by a lower value in the denominator.

OEC lines derived from rat bulb have been used before to assess neuronal regeneration through both neurite outgrowth (M. Nadine Goodman et al., 1993) and functional recovery (DeLucia et al., 2003; M Teresa Moreno-Flores et al., 2006). Olfactory bulb derived OECs cell lines performed better in neurite outgrowth when compared to olfactory bulb astrocyte cell lines (M. Nadine Goodman et al., 1993). There has been also studies on human olfactory bulb conditionally immortalized cell lines: their effect on the axonal outgrowth of rat ganglion neurons and the feasibility of their implantation into the injured spinal cord of immunosuppressed rats. These cell lines retained both antigenic markers typical of ensheathing glial and their regenerative capacity *in vitro* comparing to primary culture human OECs (García-Escudero et al., 2011).

The present studies have not yielded conclusive results regarding functional capacity of this human conditionally immortalized OEC line. It is suspected at this point that the NG108 cell line, although presenting a

consistent behaviour from cell to cell in the same conditions, might not represent the kind of neuron it is intended to regenerate to its full extend. Furthermore the sample size is small and unlikely to detect all effects from all factors studied. Consequently more experimental repeats are needed to conclusively access the effect of PA5 cell line on NG108 neurons.

Another limitation of this study is that occasionally both F7/SC and PA5 cells might have proliferated to the point of start detaching. This might have led to unhealthy cells on the co-culture with the NG108 neurons which might have influenced the neuronal regeneration measurement results.

Finally, there is concerns regarding S100β antibody robustness. It was difficult to characterise the F7/SC and PA5 cells in co-culture. As it will be mentioned on the next chapter the antibody stains S100β-expressing cells so the problem might be on the inconsistent expression by PA5 cells and F7/SC. This urges the research for a more reliable marker or antibody.

3.2.3 Co-culture with primary rat DRG neurons

In the next set of experiments, NG108 cells were replaced with rat primary dorsal root ganglia (DRG) neurons and the effect of PA5 cell lines in co-culture were studied, in comparison with DRG neurons cultured on poly-L-lysine (PLL) negative control or on F7 Schwann cells (F7/SC) positive control. Cells were cultured as described, on PLL in 10% serum at atmospheric O_2. Cells were co-cultured for 3 or 5 days and at atmospheric or physiologic oxygen and stained to detect: S100β glial cell marker and βIII-tubulin neural cell marker. The number of neurites, neurite number and total neurite length was determined for all co-cultures. Given the variability of the primary cell culture of DRG neurons the number of neurites will be represented per neuron and the neurite length will be represented per neurite.

Fluorescent micrographs (Figure 3.21) for the five day co-culture show a higher number of neurons and neurites when co-cultured with F7/SC or OEC. It is also evident a higher neurite length with co-culture of NG108 with F7/SC and PA5 cells.

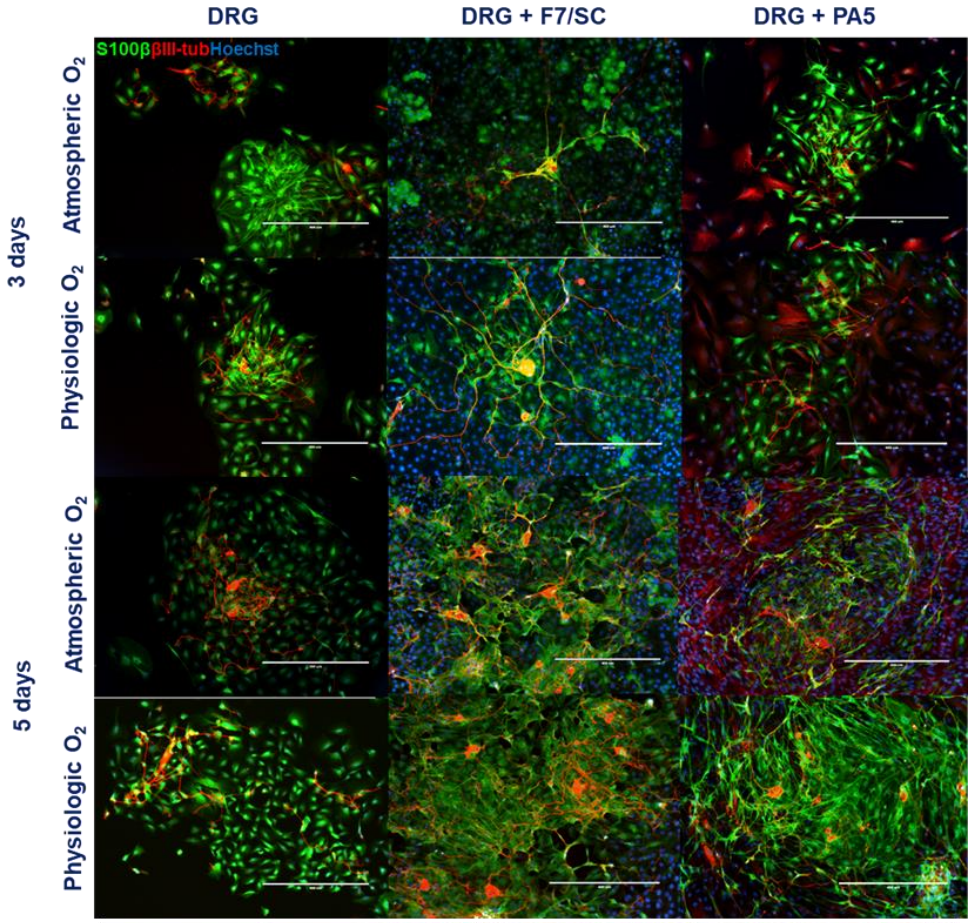

Figure 3.21 - Co-culture of primary DRG neurons with human PA5 cell line for 3 or 5 days at atmospheric or physiologic oxygen. Following cell culture, cells were cultured at atmospheric O_2 (21%), on PLL + 10% serum. DRG neurons were isolated and cultured with PA5 cells, F7 Schwann cell line or on PLL. After 3 or 5 days cells were fixed and stained for S100β, βIII-tubulin and Hoechst. Scale bars are 200µm.

The number of neurites per neuron and their length per neurite in the DRG neuron cell population was determined for all co-cultures (Figure 3.22, 3.23 and 3.24).

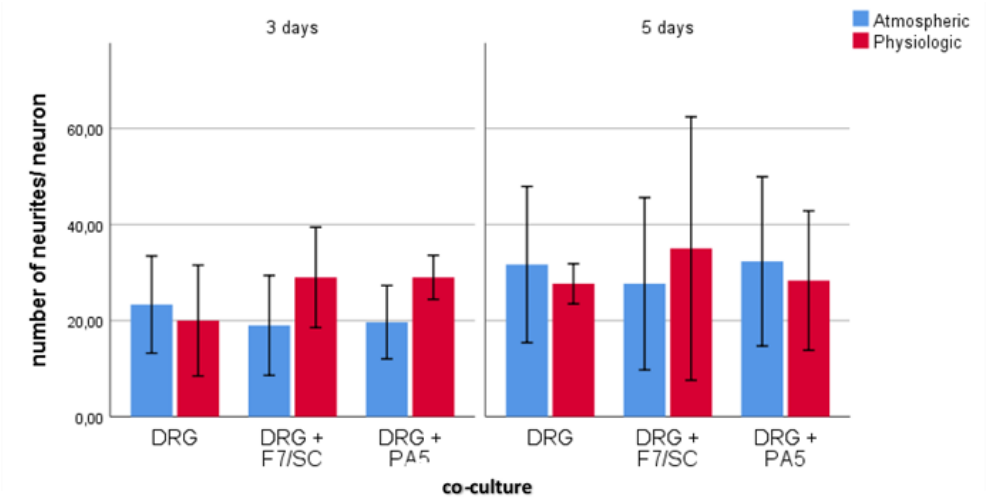

Figure 3.22- DRG neurons number of neurites per neuron after co-culture for 3 or 5 days with PA5 cells, F7/SC or on PLL at physiologic (2-8%) and atmospheric oxygen (21%). *Quantification of the fluorescent micrographs revealed no significant differences in neurite number per neuron between culture types, durations or oxygen levels. Data are means ± SD, n=4*

From the factors studied both co-culture type and culture duration had a significant effect on the overall results (co-culture: P=0.016; culture duration: P=0.001, three-way MANOVA). None of the second degree (co-culture*culture duration, co-culture*level of oxygen and culture duration*level of oxygen) or third degree interactions (co-culture*culture duration*oxygen) had a significant effect on the overall response.

On the tests between subjects' effects it can be seen the model explains the variance of both responses (number of neurites per neuron and neurite length per neurite) however the factors co-culture and duration only had a significant effect on the neurite length per neurite (P=0.010 and P=0.011, respectively, three-way MANOVA) and the level of oxygen had no significant effect on neither.

The pairwise comparisons between 3 and 5 days of co-culture show a significant increase in neurite length after 5 days of co-culture when compared to 3 days (P=0.011, three-way MANOVA with Bonferroni

adjustment). The pairwise comparisons between levels of oxygen show no significant difference on either responses.

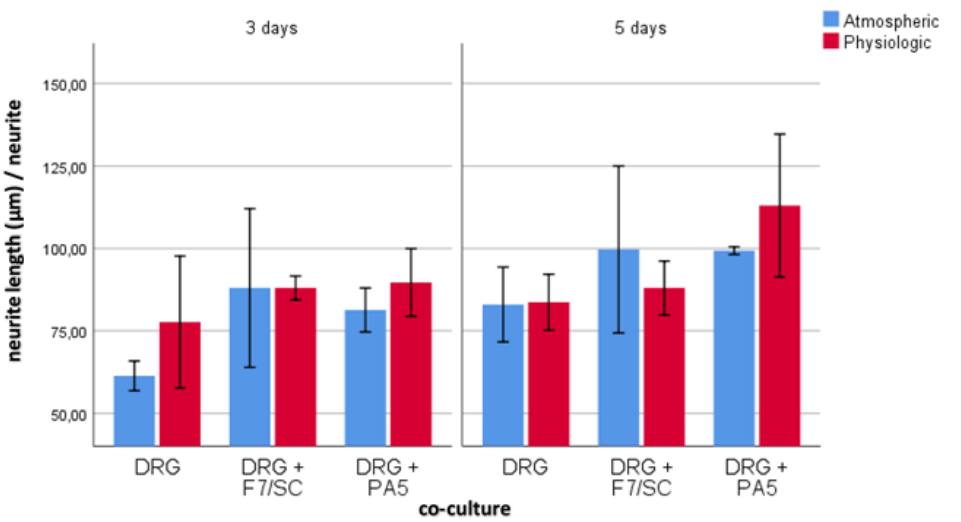

Figure 3.23- DRG neurons neurite length after co-culture for 3 or 5 days with PA5 cells, F7/SC or on PLL at physiologic (2-8%) and atmospheric oxygen (21%). *Quantification of the fluorescent micrographs revealed a significant difference in neurite length per neurite between co-culture at 3 and 5 days (P=0.010, Three-way MANOVA, Bonferroni adjustment) and DRG + PA5 and DRGs on PLL (P=0.010, Three-way MANOVA, Tukey's HSD post-test). Data are means ± SD, n=4.*

Furthermore the multiple comparisons show that for the neurite length/ neurite DRGs + PA5 cells (3 days, atmospheric 81 ± 4 µm/ neurite, physiologic: 90 ± 6 µm/ neurite; 5 days, atmospheric: 99 ± 1 µm/ neurite, physiologic: 113 ± 13 µm/ neurite) perform significantly better when compared to DRGs on PLL (3 days, atmospheric 62 ± 3 µm/ neurite, physiologic: 78 ± 11 µm/ neurite; 5 days, atmospheric: 83 ± 7 µm/ neurite, physiologic: 84 ± 5 µm/ neurite, P=0.010, Three-way MANOVA, Tukey's HSD post-hoc test).

DRG neurons come from the dorsal root, one of the roots connected to the spinal cord and to the dorsal root ganglia, an agglomerate of neurons (Purves & Williams, 2001). The axon terminals of dorsal root ganglion neurons have a variety of receptors that are triggered by movement,

temperature, chemical substances and toxic stimuli (Cho, Shin, Shin, Lee, & Oh, 2002).

Despite being a primary culture of neurons and therefore having a variable number of neurons per experimental repeat and being an heterogeneous mixture of different neuron phenotypes (Fudge & Mearow, 2013) this neuron source has been used in several neuronal regeneration studies (Babiarz et al., 2011; Devon & Doucette, 1992, 1995; Georgiou et al., 2013). They are easily accessible and close to the CNS environment. The advantage of using DRG neurons on this study is the fact that the human OEC PA5 cell line will be tested on mature CNS neurons, physiologically closer to the regenerating neurons in the spinal cord. The disadvantage is the satellite glia contamination which stains for S100β which is also a marker expressed by PA5 cells.

DRG neurons have also been used as proof of concept for several OECs regenerating effects. It was demonstrated by Devon and Doucette in 1992 that OECs myelinate DRG neurites and later Ramón-Cueto and Nieto-Sampedro in 1994 observed many regenerating dorsal root axons returning the spinal cord after three weeks of transplantation in to a rhizotomized rat spinal cord injury. Preferential growth of DRG neurons on canine olfactory mucosal cells when compared to Schwann cells or olfactory bulb OECs has also been noted (Ziege, Wewetzer, Schöne, & Baumgärtner, 2013).

In order to test these cells in an environment mimicking as close as possible the injury site in the spine (oxygen level in the central nervous

system ranges from 0.55% to 8%, Erecińska and Silver, 2001), these studies aimed to determine the effect of the human OEC conditionally immortalized cell line PA5 on rat primary dorsal root ganglia (DRG) neurons after 3 or 5 days at atmospheric or physiologic oxygen.

Although the multivariate analysis shows an effect of co-culture type and duration on the overall response, the tests between subjects' effects show that only the neurite length per neurite was influenced by the co-culture duration and type.

Contrarily to co-culture with NG108 neurons, co-culture with DRG neurons had a neurite length significantly higher with co-culture after 5 days. This might be explained by the fact that there was a lot more NG108 neurons in culture than there was DRGs which might have had an inhibition effect on neurite sprouting. Moreover DRGs co-culture with PA5 had significantly longer neurites than culture on PLL and no significant difference from co-culture with the positive control F7/SC regardless of oxygen level or culture duration. This positive shift in results comparing to the previous assays with NG108 neurons confirms the OECs' ability for neuronal outgrowth and is consistent with previous results in which OEC lines successfully promoted neurite outgrowth *in vivo* (García-Escudero et al., 2011; M. Nadine Goodman et al., 1993), albeit using different neuronal models (chick and rat retinal ganglion neurons, respectively) and measurements of neurite outgrowth (mean total neurite length and a parameter proportional to the average length of regenerated axons).

Nevertheless it is important to have in mind that this study used a small sample which means that it is unlikely it detected all effects for all factors studied. Hence more experimental repeats are needed to fully access the effect of PA5 cells on rat primary DRG neurons.

Another limitation of this study is similar to the previous one where the F7/SC and PA5 cells might have started detaching affecting the neuronal regeneration measurements' results. Moreover in this case there is several S100β-positive cells which are probably contaminant satellite glia from the rat DRG preparations which expresses S100β, demonstrating further the unreliability of using S100β to characterize PA5 cells.

3.3 In vitro 3D functional assays

The two dimensional study does not account for the guidance OECs could potentially provide to neurons *in vivo* (Chehrehasa et al., 2010; Lankford et al., 2008; Ramer et al., 2004; Ramón-Cueto et al., 1998; Toft, Tome, Barnett, & Riddell, 2013) which has been followed on several occasions by increase in neurite growth (R. Deumens et al., 2004) and directional growth of host axons through local structural barriers on site (Pérez-Bouza et al., 1998). OEC potential to align and guide neurons is therefore an important measure of neuronal regeneration potential. Therefore, the next step in this functional analysis was establishment and testing of a three dimensional model to study the effect of the PA5 cell line on neuronal alignment.

3.3.1 Contraction studies

The tension provided by tethered collagen gels containing cells will produce alignment. Tethered gels are a convenient approach in generating anisotropic tissues, but requires optimization of cell density, matrix concentration and time for each specific cell type. According to O'Rourke *et al.*, 2015 an assay can be used to determine the optimal cell density and time for maximal cell self-alignment by measuring the contraction of free floating gels in well plates. Therefore, in this next study, optimal cell density and time of contraction for maximal gel contraction were investigated for the PA5 cell line. The collagen concentration was not investigated because it had already been optimised for the positive control cell line F7 Schwann cells for maximal alignment (Georgiou et al., 2013).

Cells were cultured as described previously at atmospheric O_2 (21%), on PLL with 10% serum, trypsinased, re-suspended in media and added to the collagen gel mixture. Gel contraction was determined for 0.2, 0.5, 1 and 2 million cells per mL after 2, 4, 6, 8 and 24 hours of contraction. The images were analysed using Image J to measure the well and gel total area and determine the proportion of contraction.

The following figure (3.24) shows in general a higher contraction for higher cell densities and time of contraction.

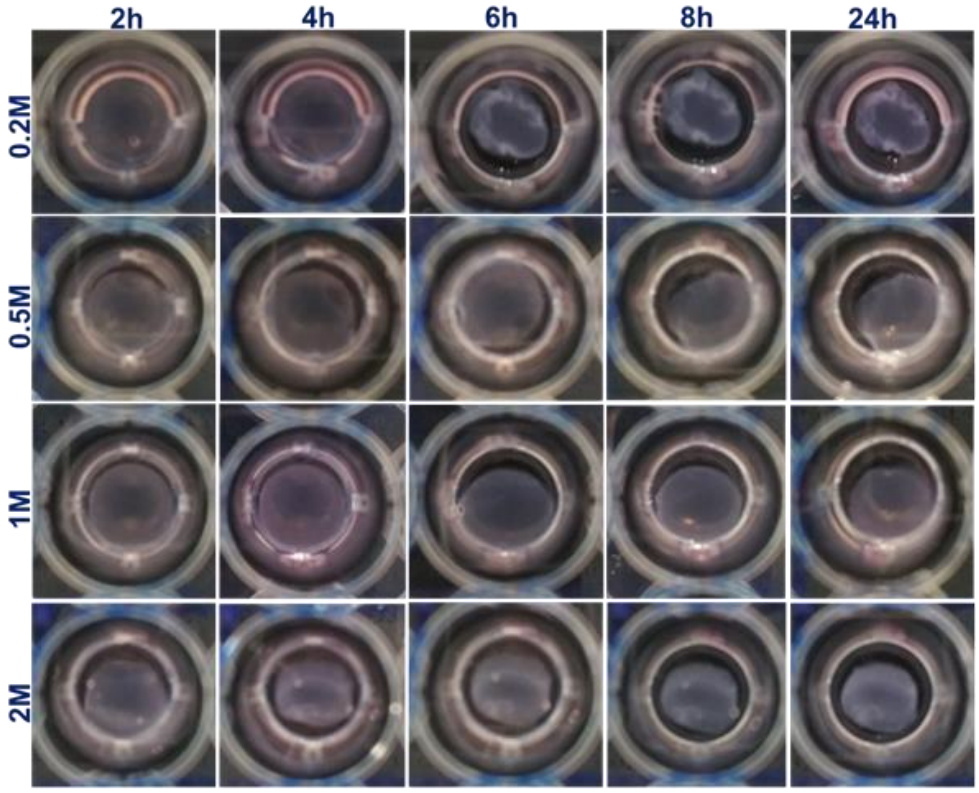

Figure 3.24 – Collagen gel contraction for different PA5 cell densities (0.2, 0.5, 1 and 2 million cells per mL) after 2, 4, 6, 8 and 24h. *PA5 cells were cultured at atmospheric O_2 (21%), on PLL + 10% serum, typsinased, resuspended in media and added to the collagen gel mixture. Pictures were taken after 2, 4, 6, 8 and 24h and gel contraction determined using ImageJ.*

The proportion of contraction was determined for all the conditions tested. The data shows that the maximal contraction happened after 24h with 0.5 x 10^6cells /mL cell density.

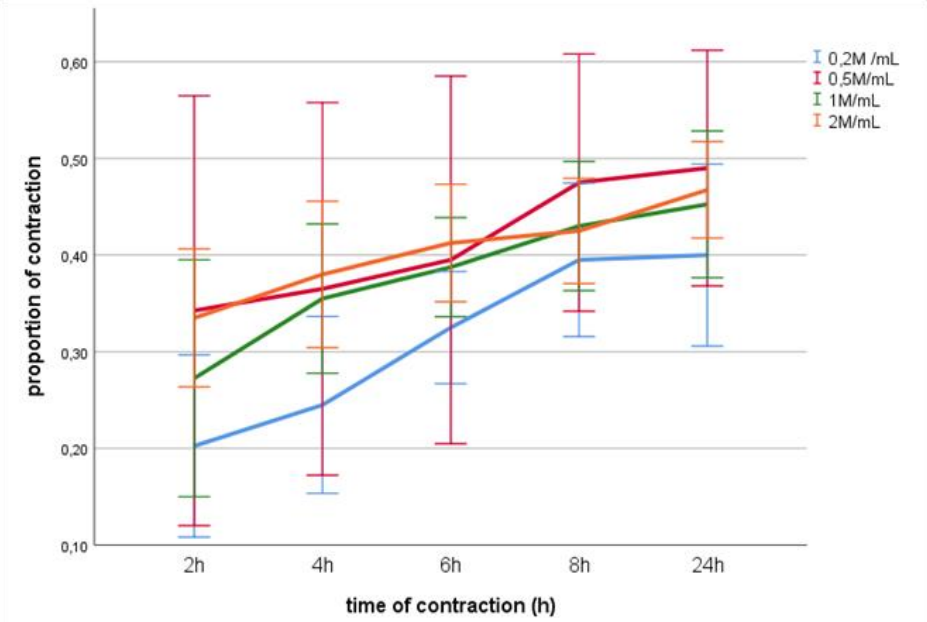

Figure 3.25 - PA5 cell line proportion contraction after 2h, 4h, 6h, 8h and 24h. *Cell density of 0.5 x 10^6 cell/mL had a significantly higher gel contraction when compared to the lowest cell density of 0.2 x 10^6 cells/mL but did not differ from higher cell densities of 1 and 2 x 10^6 cell/mL. Data are means ± SD, n=4.*

The tests of between subjects' effects (definition in Appendix) shows that the model with the two factors time of contraction and cell density explain well the variation in the dependent variable, proportion of contraction with a very low P value (P<<0.001). It also shows that both cell density and time of contraction have a significant effect on gel contraction (P=0.026 and P=0.0004), however the interaction between these two factors does not have a significant effect on the gel contraction. This result suggests that the rate at which the contraction develops is not affected by the cell density within the gel. Interestingly the development of contraction differs for the different cell densities suggesting there are more factors at play within the gels when the cell density is changed.

The Tukey HSD post-hoc test for multiple comparisons revealed that the cell density of 0.5 x 10^6 cell/mL had a significantly higher gel contraction

when compared to the lowest cell density of 0.2 x 10^6 cells/mL ($P<0.05$) but did not differ from higher cell densities of 1 and 2 x 10^6 cell/mL. It was also revealed that the gel contraction does not differ considerably until after 8h when it seems to stabilise around 45% contraction.

Cell density (cells/ mL)	0,2	0,5	1	2
0,2	-	*	NS	NS
0,5	-	-	NS	NS
1	-	-	-	NS
2	-	-	-	-

Table 3.1- Multiple comparisons for cell density (Tukey HSD post-hoc test).

Time of contraction (h)	2	4	6	8	24
2	-	NS	NS	**	***
4	-	-	NS	NS	*
6	-	-	-	NS	NS
8	-	-	-	-	NS
24	-	-	-	-	-

Table 3.2- Multiple comparisons for contraction time (Tukey HSD post-hoc test).

These results suggest a cell density of 0.5 x 10^6 cells/mL after 8 or 24h are the optimum conditions for maximal alignment.

As the goal of this sub-chapter is to test the human OEC conditionally immortalized cell line on a 3D environment it is important to get the right cellular and extracellular matrix organization.

Gel contraction modulation related to cell alignment is essential to build engineered tissues that use tension in tethered gels to induce cellular self-alignment. With this validated assay (O'Rourke et al., 2015) it was possible to determine the optimal contraction time and cell density conditions to obtain the maximal alignment of PA5 cells to mimic the aligned guiding fibers *in vivo* in the olfactory system (J. A. K. Ekberg, Amaya, Mackay-Sim, & St John, 2012; P. Field, Li, & Raisman, 2003; Zhu et al., 2010) for

neuronal regeneration. There must be enough tension developed through cell–ECM interaction and cytoskeletal activity to have cell self-orientation to achieve cell and matrix anisotropy within a 3D collagen environment. Therefore parameters related to both cell and ECM type need to be optimized such as cell density, collagen concentration and incubation time.

For this assay it was decided to study the evolution of gel contraction with time and cell density. The collagen concentration was optimized for the positive control cell line F7/SC in previous studies (Georgiou et al., 2013) and the same concentration was used to build the PA5 loaded gels. It can be seen in figure 3.25 that gel contraction increases over time but not with cell density or at least not linearly. Moreover, as it will be seen in the next sub-chapter, contraction is related to alignment just until certain extend. Although there seems to be a stabilization of contraction after 8h for the 96 well plate assay in the tethered gel context the cell alignment is not maximal. Furthermore even after 24h the PA5 cell contraction never reaches the plateau range of 75%-80% seen for other cell types (Nirmalanandhan, Levy, Huth, & Butler, 2006; O'Rourke et al., 2015; Redden & Doolin, 2003). Ironically, while not telling the whole story about PA5 alignment on collagen gels, this assay further proves that each cell type has its own set of optimized alignment parameters' values and this concentration of collagen does not seem to be one of them since the maximal contraction range was not achieved possibly because the optimal concentration of collagen was not studied. For feasibility purposes the concentration of collagen used was 2mg/mL, optimized for the F7/SC positive control (Georgiou et al., 2013).

The PA5 cell concentration and time of contraction used was 0.5 million cells per mL and 24h, respectively as these were the parameters values with highest contraction in the 96-well plate assay.

It is also worth mentioning that, as shown in sample size estimation later on, the sample size was small and therefore possibly did not detect all effects studied and therefore more experimental repeats are needed for a complete contraction profile assessment.

3.3.2 PA5 cell alignment

To confirm cell alignment the cell density of 1 million cells/mL was tested on tethered gels to confirm alignment over time. This was done before the previous experiment, the contraction study, was complete. The optimal cell density was not yet known. The contraction profile looked very similar for 1 and 2 million cells per mL, with both performing better than the rest of the cell densities so it was chosen the cell density of 1 million per mL (less cells required) to visualise alignment over time.

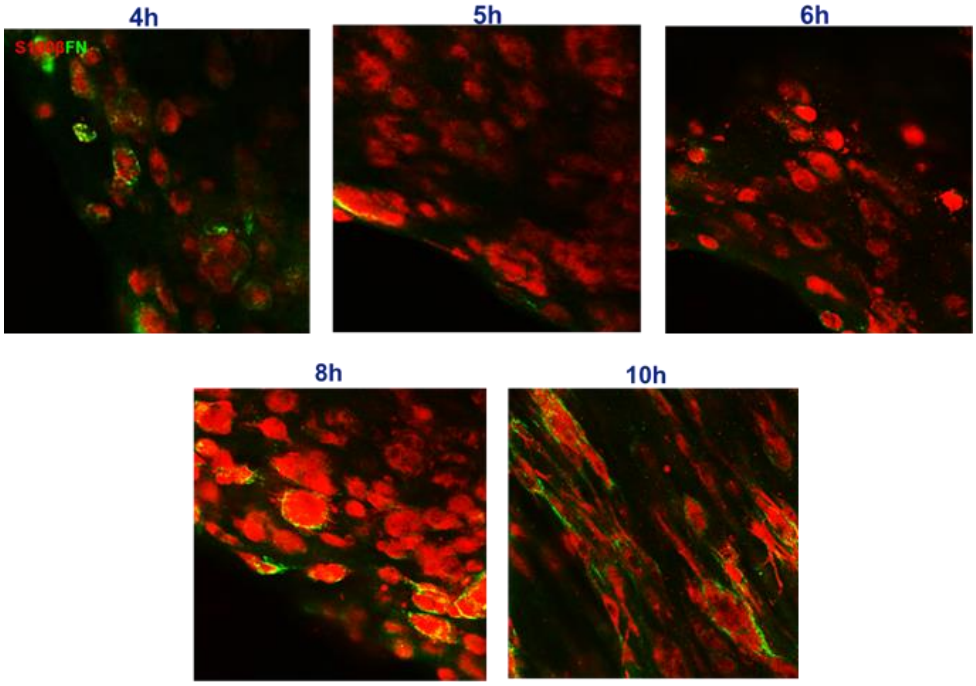

Figure 3.26 - PA5 cell line alignment after 4h, 5h, 6h, 8h and 10h for 1 x 10^6cell/mL. Fluorescent micrographs revealed a higher alignment after 10h (40x magnification, confocal imaging)

Contraction did not necessarily translate into alignment for the PA5 cell line. Although the maximal contraction happens after 8h it is only after 10h that alignment can be visualized since it takes time for cells to align after generating tension. Contraction for 24h was the condition used for the 3D assays in the next sub-chapter for practicality purposes (24h is also the best contraction time for the positive control F7/SC) and to make sure all PA5 cells were aligned.

3.3.3 Co-culture of aligned PA5 cells with NG108 neurons

The effect of PA5 cell line aligned cells on alignment of NG108 neuronal cell line with comparison with NG108 cell culture on aligned F7 Schwann cells (F7/SC) positive control was investigated. Cells were cultured as described, on PLL in 10% serum at atmospheric O_2 before production of the collagen gels. For the experiment cells were co-cultured for 3 or 5 days and at atmospheric O_2 and stained to detect: S100β glial cell marker and βIII-tubulin neuronal cell marker.

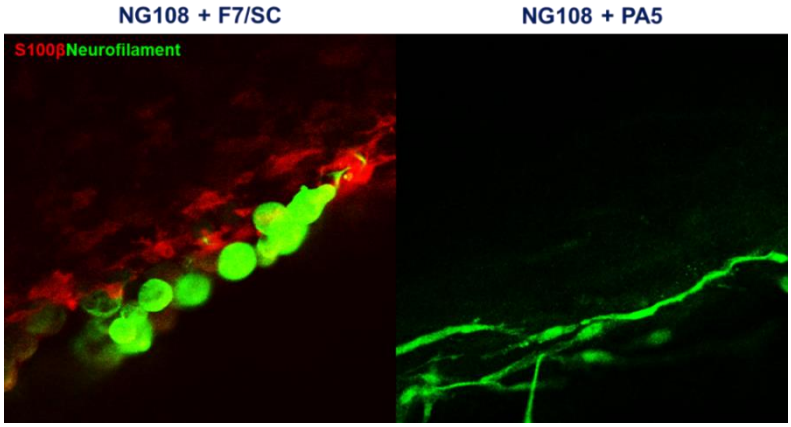

Figure 3.27 - Collagen gel with F7/SC or PA5 aligned cells co-cultured with NG108 neurons for 5 days (1st experimental repeat). *Following cell culture, cells were cultured at atmospheric O_2 (21%) + 10% serum. NG108 cells were cultured with PA5 cells or F7 Schwann cell line loaded collagen gels. After 5 days cells were fixed and stained for S100β and Neurofilament. Fluorescent micrographs did not reveal neuronal alignment (40x magnification, confocal imaging).*

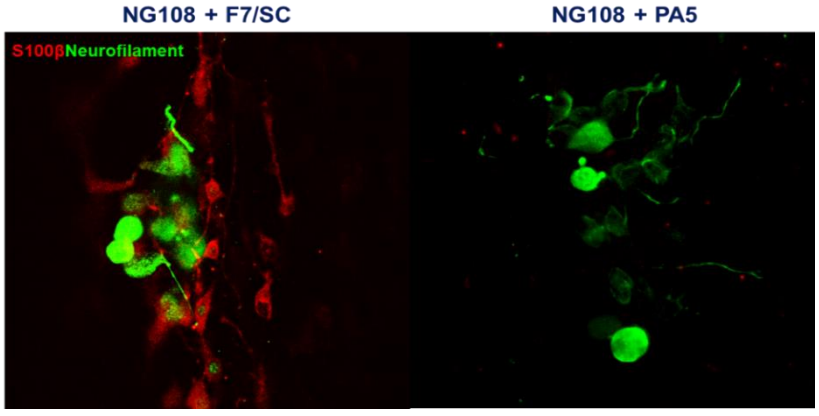

Figure 3.28 - Collagen gel with F7/SC or PA5 aligned cells co-cultured with NG108 neurons for 5 days (2nd experimental repeat). *Following cell culture, cells were cultured at atmospheric O_2 (21%) + 10% serum. NG108 cells were cultured with PA5 cells or F7 Schwann cell line loaded collagen gels. After 5 days cells were fixed and stained for S100β and Neurofilament. Fluorescent micrographs did not reveal neuronal alignment (40x magnification, confocal imaging).*

Preliminary experiments with co-culture of NG108 neurons on F7/SC and PA5 cells loaded tethered gels revealed the alignment was inconsistent between experimental repeats, resulting in an unreliable assay. Therefore the use of NG108 neurons for this assay was discarded.

3.3.4 Co-culture of PA5 cells with rat DRG neurons

The effect of PA5 cell line aligned cells on alignment of rat dorsal root ganglia (DRG) neurons with the longitudinal axis of the gel in comparison with alignment on align F7 Schwann cells (F7/SC) positive control was investigated. Cells were co-cultured for 3 and 5 days and stained to detect: S100β glial cell marker and βIII-tubulin neural cell marker.

Fluorescent micrographs for the three day co-culture (Figure 3.29) show similar alignment of neurites when co-cultured with F7/SC or PA5 cells whilst for five day co-culture (Figure 3.30) some DRG neurons seem to be tracking along with PA5 cells.

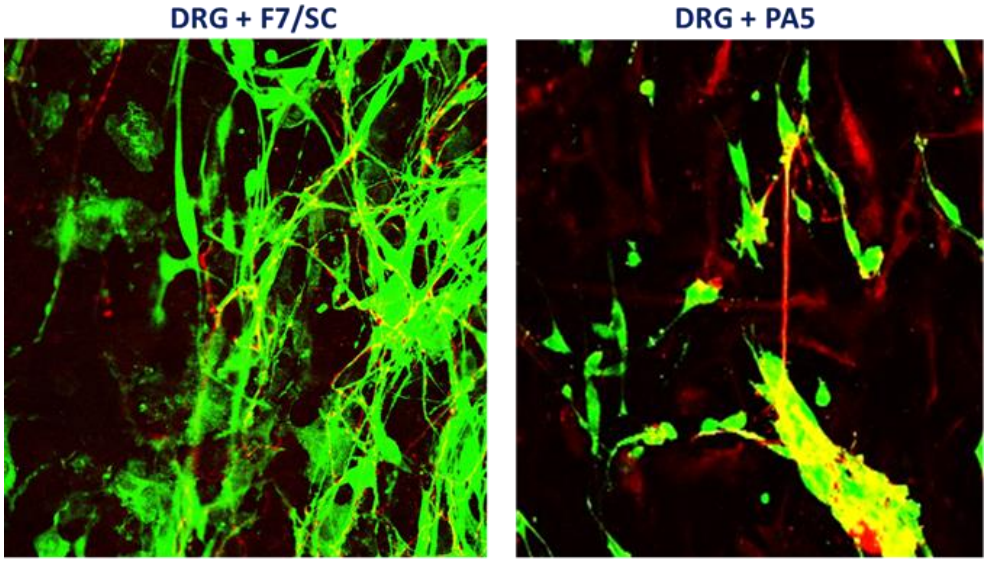

Figure 3.29 *- Collagen gel with F7/SC or PA5 aligned cells co-cultured with primary DRG neurons for 3 days. DRG neurons were cultured with PA5 cells or F7 Schwann cell line loaded collagen gels. After 3 days cells were fixed and stained for S100ß and Neurofilament. Fluorescent micrographs revealed some neuronal alignment (40x magnification, confocal imaging).*

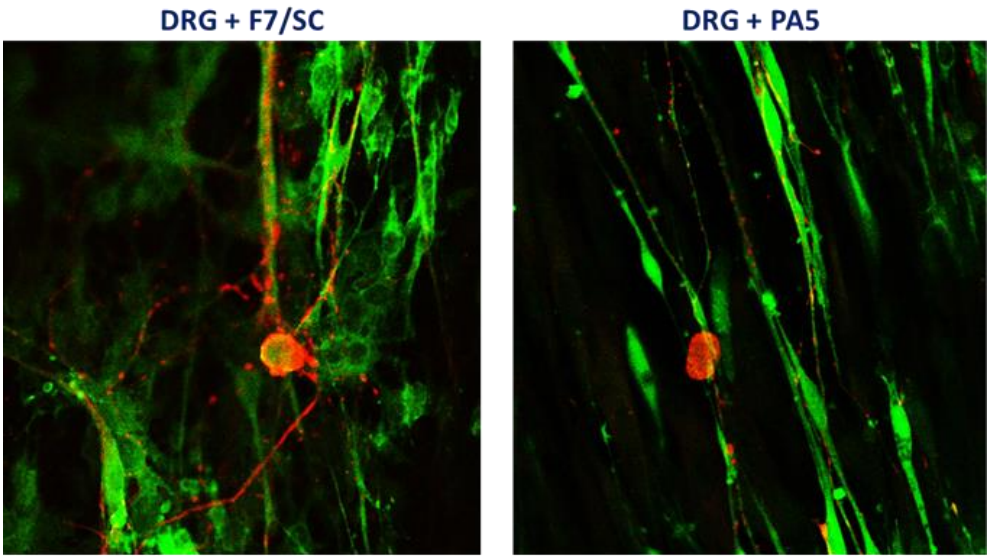

Figure 3.30 - **Collagen gel with F7/SC or PA5 aligned cells co-cultured with primary DRG neurons for 5 days. DRG neurons were cultured with PA5 cells or F7 Schwann cell line loaded collagen gels.** After 3 days cells were fixed and stained for S100β and Neurofilament. Fluorescent micrographs revealed neuronal alignment especially for co-culture with PA5 cell line (40x magnification, confocal imaging).

The angles between the DRG neurons neurites and the longitudinal axis of the glial cell loaded gel were determined. The number primary DRG neurons per an angle range of 10 degrees was determined for both experiments, co-culture for 3 (Figure 3.31) and 5 days (Figure 3.32). A Kolmogorov-Smirnov Test was performed for both experiments, 3 and 5 days co-culture, between the DRG neurons angle distribution for the co-culture on F7/SC and for the co-culture on PA5 cells.

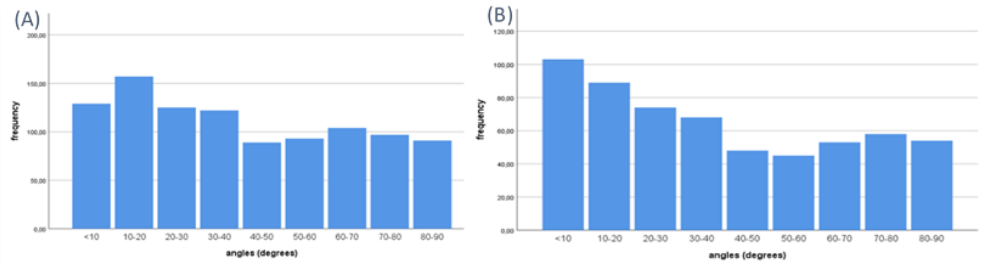

Figure 3.31 - DRG neurons angle distribution when cultured on F7/SC (A) or on PA5 cell line (B) after 3 days of co-culture. *Quantification of neuronal alignment revealed an increasing number the lower the neurite angle for co-culture with PA5 cell line. It can also be seen that the DRG neurons cultured on PA5 have an angle distribution skewed towards smaller angles when compared to DRG neurons cultured on F7/SC line. Data are values of n=1.*

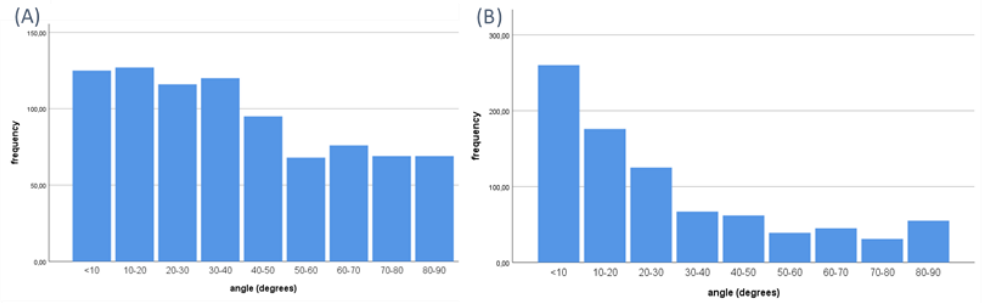

Figure 3.32 - DRG neurons angle distribution when cultured on F7/SC (A) or PA5 cell line (B) after 5 days of co-culture. *Quantification of neuronal alignment revealed significant difference between the DRG neuron angle distribution for co-culture with F7/SC and PA5 (Kolmogorov-Smirnov Test, P<0.001). It can also be seen that the DRG neurons cultured on PA5 have an angle distribution skewed towards smaller angles when compared to DRG neurons cultured on F7/SC line. Data are values of n=1.*

In the only experimental repeat for co-culture for 3 days the test revealed no significant difference between the DRG neuron angle distribution with co-culture on F7/SC and co-culture on PA5 (Kolmogorov-Smirnov Test, P=0.155). Given the number of experimental repeats it cannot be concluded that there is no influence in the neuronal angle after co-culture for 3 days and therefore no alignment. There is not a sufficient number of biological experimental repeats to give enough statistical power to detect this effect.

In the experimental repeat for co-culture for 5 days the test revealed significant difference between the DRG neurons angle distribution with co-culture on F7/SC and co-culture on PA5 (Kolmogorov-Smirnov Test, P<0.001), meaning there is possibly an influence in the neuronal angle after co-culture for 5 days. For DRG neurons cultured on PA5 cells there is also a clear skewedness towards smaller angles.

Although inconclusive due to the reduced number of biological experimental repeats this study demonstrated a clear trend of the DRG neurons cultured on PA5 cells to align with the longitudinal axis of the gel as can be seen in figure 3.32B by the higher number of neurons with low angles.

To explore the assumption that the glial cells align the DRG neurons and therefore any difference seen between co-cultures is due to the influence of the glial cells in the gel, it was also investigated the DRG neurons alignment with PA5 and F7/SC after 3 and 5 days. The angles between either PA5 or F7/SC aligned cells and the longitudinal axis of the loaded gel were determined for each experimental repeat of each co-culture experiment. The number glial cells per an angle range of 10 degrees was determined for both experiments, co-culture for 3 (Figure 3.33) and 5 days (Figure 3.34). A Kolmogorov-Smirnov Test was performed for both experimental repeats of both experiments, 3 and 5 days co-culture, between the DRG neurons angle distribution grown on each of the glial cells, F7/SC and PA5 (figures 3.31 and 3.32) and their respective cell angle distributions (figures 3.33 and 3.34).

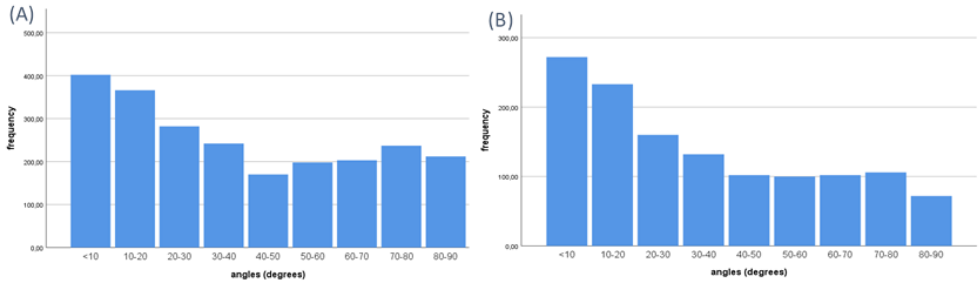

Figure 3.33- F7/SC (A) and PA5 (B) aligned cells angle distribution after 3 days of co-culture. *Quantification glial cell alignment revealed a significant difference between the DRG neuron angle distribution and glial cell angle distribution for co-culture with either F7/SC or PA5 (Kolmogorov-Smirnov Test, P=0.016 and P=0.014, respectively). It can also be seen that PA5 have an angle distribution skewed towards smaller angles when compared to the F7/SC line. Data are values of n=1.*

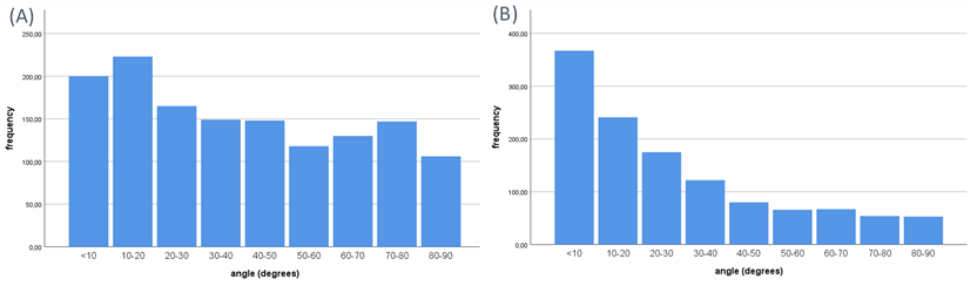

Figure 9.34- F7/SC (A) and PA5 (B) aligned cells angle distribution after 5 days of co-culture. *Quantification glial cell alignment revealed no significant difference between the DRG neuron angle distribution and glial cell angle distribution for co-culture with either F7/SC or PA5 (Kolmogorov-Smirnov Test, P=0.262 and P=0.887, respectively). It can also be seen that PA5 have an angle distribution skewed towards smaller angles when compared to the F7/SC line. Data are values of n=1.*

Although the Kolmogorov-Smirnov test between DRG neurite distribution of angles and both distribution of angles for PA5 or F7/SC had a significant difference after 3 days (P=0.016 and P=0.014, respectively) and no significant difference after 5 days (P=0.262 and P=0.887, respectively) this study is also inconclusive as to whether F7/SC or PA5 have the same alignment as the DRG neurons grown on them, due to the limited number of biological experimental repeats. In fact Georgiou *et al.*, 2013 demonstrated that F7/SC align DRG neurons on an engineering neural tissue after 3 days of co-culture so possibly with more experimental repeats the same conclusion would be reached. There is nonetheless a much clearer trend in PA5 cells alignment towards lower angles with the longitudinal axis of the gel when compared with the positive control cell line F7/SC.

OECs have an inherent ability to align and have a spindle shape form *in vivo* which allows them to guide olfactory neurons from the mucosa back to

the brain in the normal turnover of olfactory neurons (J. R. Doucette, 1984; R. Doucette, 1990, 1991; Raisman, 1985) and after injury (J. R. Doucette, 1984; J. R. Doucette, Kiernan, & Flumerfelt, 1983; R. Doucette, 1995; Harding et al., 1977). DRG neurons have been used extensively to determine several OECs regenerating effects (Devon & Doucette, 1992; Ramón-Cueto & Nieto-Sampedro, 1994; Ziege et al., 2013). Although not from human origin they provide a good model for neuronal regeneration especially because they are located at the interface between CNS and PNS similarly to OECs (Purves & Williams, 2001). Using these neurons for this final assay seems like the obvious choice to further complete this human OEC line neuronal regeneration ability evaluation using this model. They represent and resemble more closely the sensory neuron population which can be injured in SCI affecting the dorsal columns (Purves & Williams, 2001). Moreover they are mature cells contrarily to most of previous studies mentioned above and physiologically closer to the regenerating neurons in the spinal cord. As mentioned for the 2D co-culture with rat DRG neurons the disadvantage is the satellite glia contamination which stains for S100β which is also a marker expressed by PA5 cells. Nonetheless if neurofilament-positive cell (DRG neurons) align with S100β-positive cells the source of alignment can only be from the loaded PA5 cells aligned by tension within the tethered gel. Consequently the effect of the human OEC line PA5 on DRG neuronal alignment in collagen tethered gels was investigated after 3 and 5 days.

Preliminary results show a significant difference between the distributions of angles of the DRG neurites with the longitudinal axis of the

gel for neurons cultured on PA5 and F7/SC loaded gels for co-culture for 5 days. The distribution of angles for the co-culture of DRG on the PA5 loaded gels is visibly skewed towards smaller angles in both durations of the co-culture. The results obtained replicate what was already seen *in vitro* using different matrices such as poly(D,L)-lactide (R. Deumens et al., 2004). OECs and Schwann cells promoted neuronal alignment of neonatal cerebral cortical neurons after 2 days. It has also been observed *in vitro* that neurites aligned with OECs were almost three times longer when they grew on inhibitory meningeal fibroblast areas and twice as elongated on reactive astrocyte zones compared to neurites not aligned with OECs (Khankan et al., 2015b). Moreover *in vivo* studies using aligned mucosal olfactory stem cells in hyaluronic acid based-nerve guidance conduits showed regeneration across a 10mm sciatic nerve gap in Sprague Dawley rat and improved clinical and electrophysiological outcomes compared to cell free controls (Roche et al., 2017). This indicates a potential for mucosal OECs to also align neurons *in vivo* as they have the same origin as olfactory stem cells. Conclusively preliminary alignment data for this OEC human cell line suggests potential for neuronal alignment *in vitro* and subsequently possible alignment *in vivo*.

In these experiments the glial cells appeared to exhibit different alignment following co-culture for 3 days and 5 days. The distribution of glial cell angles might be expected to be the same for the 3 and 5 day co-culture because the cellular self-alignment protocol prior to co-culture was the same. The difference might be due to the fact that there is only one experimental repeat per experiment which reveals variability between glial

cells angle alignment distribution between experiments. This might also explain why there cannot be seen any DRG neuronal alignment with glial cells after 3 days of co-culture, especially for F7/SC as seen before (Georgiou et al., 2013). It is possible that more experimental repeats would confirm a neuronal alignment earlier than 5 days of co-culture. Nonetheless, regardless of the angle distribution of the glial cells in the co-culture for 3 or 5 days it is visible the PA5 tendency to align along the axis of the gel.

3.4 Conclusions

The aim of this project was to develop strategies for isolation, culture and functional testing of Olfactory Ensheathing Cells. Building on previous work (Georgiou et al., 2018) it was firstly investigated the influence of different culture and purification factors on proportion and yield of OEC markers-positive cells. Then with the optimized protocol the functionality features number of neurons, neurites and neurite length were assessed in a 2D co-culture with NG108 neurons. Those same assays were used on a conditionally immortalized human OEC cell line, PA5, whose cells were isolated using the same optimized protocol used for rat OECs. They were also used to test PA5 cells effect on rat primary DRG neurons. Finally a last functional aspect was tested for PA5 cells, neuronal alignment, on a 3D assay using a tethered collagen gel using primary rat DRG neurons.

Initially it was investigated the influence of the timing of addition of the neutrophic factor NT-3. The rationale behind this hypothesis testing was the previous observations that NT-3 addition at the concentration of 50 ng/mL promoted enrichment and proliferation of human mucosal OECs and was similar to 10% serum media (Bianco et al., 2004). Previous studies showed increase in p75NTR positive cells proportion with addition at day 6 (Georgiou et al., 2018) of culture so it was hypothesised if the an earlier addition of this neurotrophic factor would also have an influence in the cell yield and proportion in OEC putative markers. Although the proportion of Thy1.1-positive cells was significantly higher, it is not possible to deduct anything from a difference in just one marker as a panel of markers is needed to

define cell phenotype. It can be said that there was no significant differences in yield and proportion on cell phenotype at day 14 in culture, whether NT-3 was added at day 1 or from day 6. Potentially NT-3 only enhances rat mucosal p75NTR positive cells at a later stage when cells have been in culture for 6 days.

It was also investigated the influence of AraC exposure for 24h on the proportion and yield of OEC markers-positive cells. AraC is a known chemical used to deplete cell cultures of fast growing contaminating cells specially Schwann cells (Brockes et al., 1979; Brockes & Raff, 1979; Weinstein & Wu, 2001). This study showed no significant difference on the proportion and yield of the studied markers between culture on AraC-free media and exposure to AraC for 24h. The proportion of cells positive for fibroblast markers (Thy1.1 and α-SMA) was different when comparing with the same conditions in previous experiments and there is a fair variance within the samples which illustrates that biological responses can be different from different experimental repeats and therefore yield different results. Therefore these results should be carefully interpreted.

The second chapter studied the effect of both rat primary OECs and the conditionally immortalized cell line PA5 on some neuronal functional aspects in a 2D co-culture with NG108 neurons and rat primary DRG neurons with different co-culture durations and oxygen levels. These assays used F7/SC line as a positive control and culture of NG108/rat DRG neurons on PLL as a negative control. The results from the co-culture with rat OECs indicated that OECs perform similarly to F7/SC in number of neurons/mm^2

and neurite length per neuron on NG108 neuronal cell line. The studies on PA5 cell line effect on NG108 functional aspects studied have not yielded conclusive results. It is suspected that the NG108 cell line, although presenting a consistent behaviour from cell to cell in the same conditions, it might not have represented the kind of neuron it is intended to regenerate as well as it was anticipated. Therefore to confirm OECs ability to positively affect neurite number and length a co-culture assay was performed using primary rat DRG neurons. This study revealed a neurite length significantly higher with co-culture after 5 days contrasting with the results from co-culture with NG108 neurons which had no significant difference between co-culture durations. DRGs co-culture with PA5 also had significantly longer neurites when compared to culture on PLL and no significant difference from co-culture with the positive control F7/SC regardless of oxygen level or culture duration. This positive shift in results comparing to the previous assays with NG108 neurons not only confirms the OECs' ability for neuronal outgrowth, it is an encouraging a step towards a reproducible assay for neuronal regeneration using more physiologically and phenotypically closer cells to CNS cells and conditions this cell line is probably going to encounter when transplanted in to a lesion site.

Finally to test OECs' ability to guide and align neurons 3D assays were performed using tethered collagen gels. The optimal cell density and contraction time for maximal OEC alignment was determined through contraction studies at the beginning of the chapter. It was concluded that contraction/alignment is maximal with a cell density of 0.5 million cell per

mL after 24h hours of contraction. Preliminary studies using NG108 neurons cultured on F7/SC and PA5 cells loaded tethered gels revealed the alignment was variable between experimental repeats, resulting in an unreliable assay. Preliminary studies with rat primary DRG neurons revealed consistent neuronal alignment with PA5 align cells on the tethered collagen gel significantly different from alignment on F7/SC loaded gels after 5 days. The distribution of angles for the co-culture of DRG on the PA5 loaded gels is visibly skewed towards smaller angles in both durations of the co-culture.

In conclusion, the work in this project proved that an allogeneic cell product such as the conditionally immortalized cell line PA5 has the potential to promote neuronal regeneration *in vivo* and perform similarly to Schwann cells, the most studied cell type for spinal cord injury, either in neurite outgrowth or alignment. Moreover OECs have the advantage of mingling with astrocytes (Lakatos et al., 2003) which even if performing similarly to Schwann in other aspects of neuronal regeneration gives them a competitive advantage for transplantation into spinal cord injuries or other damage in the CNS.

3.5 Future work

This project aimed to optimise the isolation and culture of OECs and functionally test them for neuronal regeneration. The neuronal regeneration indicators that were possible to assess were cell number (for one neuronal model), neurite number, neurite length and alignment. Although they are just a few indicators of neuronal regeneration on non-human models of neuronal regeneration they give a good representation of the potential of the conditionally immortalised human cell line PA5.

Building on the 2D co-culture work from the second chapter it would be interesting to access different timings of addition of NG108 neurons to the culture of rat OEC and see if high proliferating cells would have an impact on neuronal development when comparing to slow proliferating cells. Also future work would involve finding alternatives to the S100β antibody used as the one used is not as robust as expected.

Furthermore the next step would be to finish the 3D study on PA5 cells neuronal alignment ability to confirm guidance promotion by these cells. Firstly by optimising the collagen concentration on the tethered gels for PA5 cells' maximal alignment and complete the contraction profile with more experimental repeats. Later by performing more experimental repeats of the 3D co-culture on the collagen tethered gels. According to the calculations made in the data analysis, using the effect size determined with the only experimental repeats done for each experiments in the 3D assays, a sample size of at least 26 would probably be need to detect a statistically

significant difference between the distributions of angles of the DRG neurons grown on PA5 cells and on F7/SC. Possibly alternative 3D assays such as miniaturized versions of the tethered gels used would be more sensible to use to achieve the necessary sample size.

The potential for neuronal regeneration for this cell line does not need to be restricted to the CNS. Depending on the final use envisaged, the follow-up assays to be performed on these cells will reflect the neuronal regeneration critical indicators for the target disease/ injury to be treated. As future work the same 2D assays would have to be done with a human neuronal cell line like human NT-2 teratocarcinoma cell line which resembles the human CNS phenotype more closely (Paquet-Durand & Bicker, 2007; Podrygajlo et al., 2009; Tegenge, Roloff, & Bicker, 2011). This cell line originates from a pluripotent human embryonal carcinoma, a tumour from the germ layer (P. W. Andrews et al., 1984). Differentiated neurons from NT-2 precursor cells display the morphology, markers and action potentials of neurons and have a clonally-derived identical cell population (Paquet-Durand & Bicker, 2007). On the other hand these cells are a human neuronal progenitors which could present challenges similar to the ones encountered when working with NG108 neurons such as an impact of hypoxia. It has been shown that hypoxia promotes proliferation of neuronal progenitors (Cui et al., 2011; Felling, 2006; Xie et al., 2014) and can influence key cell fate decision, specifically neuron or glia differentiation (L. Cheng et al., 2014; Xie et al., 2014).

PA5 cells could also potentially myelinate NT-2 derived differentiated neurons as shown *in vivo* with undifferentiated transplanted cells (Miyazono, Nowell, Finan, Lee, & Trojanowski, 1996). OEC ability to myelinate neuronal axons is controversial specially DRG neurons with articles showing opposite results (Devon & Doucette, 1992; Plant et al., 2002) by using OECs from rats at different ages (embryonic and adult, respectively). Nonetheless testing their ability to myelinate axons is another appropriate test for neuronal regeneration for this human cell line. A simple immunocytochemistry procedure using makers for CNS myelin such as Myelin Basic Protein (MBP) (Saxe, Takahashi., Hood, & Simon, 1985) and Myelin proteolipid protein (PLP) (Popot, Dinh, & Dautigny, 1991) or for PNS myelin P0 (or MPZ, myelin protein zero) (Shy, 2006) could give an indication of OEC potential for neuronal myelination.

Depending on the final use of these cells an assessment of astrocyte reactivity might be necessary for spinal cord or brain damage treatment. As mentioned before an injury in the CNS is always followed by a glial scar constituted by astrocytes that migrate and proliferate filling the empty spaces in the wound and proteoglycans forming a physical barrier (R J McKeon et al., 1991; Yiu & He, 2006). It makes sense therefore to assess these cells interaction with reactive astrocytes in a 3D environment (Phillips, 2014) and confirm OEC ability to mingle in astrocytic environments and reduce astrocyte response and chondroitin sulfate proteoglycans (CSPG) expression (Lakatos et al., 2003, 2000).

It is uncertain how many *in vitro* tests would be needed to have the degree of validation necessary for animal testing but other important feature of OECs *in vivo* and that could potentially be tested *in vitro* is their phagocytic ability of bacteria and cell debris (B. R. He et al., 2014; Leung et al., 2008; Panni et al., 2013).

4. Appendix

4.1 Statistical analysis

4.1.1 Effect of different culture conditions on yield and proportion of putative OEC markers positive cells

An exploratory analysis of descriptive statistics on SPSS was done for each group (combination of factors): NT-3 addition at day 1 and NT-3 addition at day 6 for all proportion and yield of each marker and no Arac exposure and AraC exposure for 24h.

To rule out multivariate outliers the data was represented in a boxplot to detect univariate outliers (figures 4.1 to 4.4). All boxplots in the statistical analysis section are shown without outliers. It can be seen that for Thy.1.1 yield with NT-3 addition at day 6 values are unevenly spread (figure 4.1). Looking at the values an outlier was identified and removed from the data set. For the AraC exposure experiment it can be seen that all

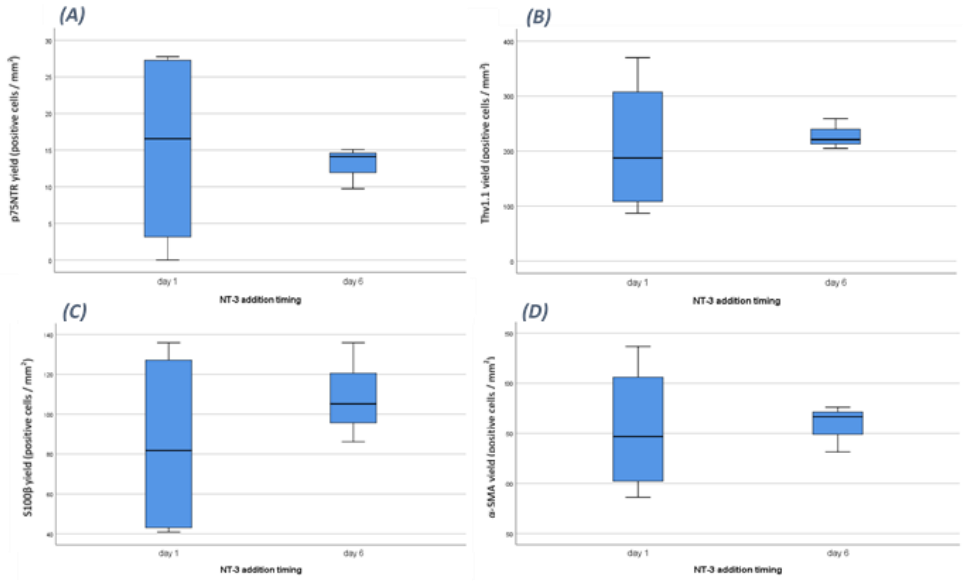

Figure 4.1- Boxplots for the yield in p75NTR (A), Thy1.1 (B), S100ß (C) and α-SMA (D) positive cells for the NT-3 addition timing experiment.

date sets are fairly evenly spread (figure 4.3 and 4.4).

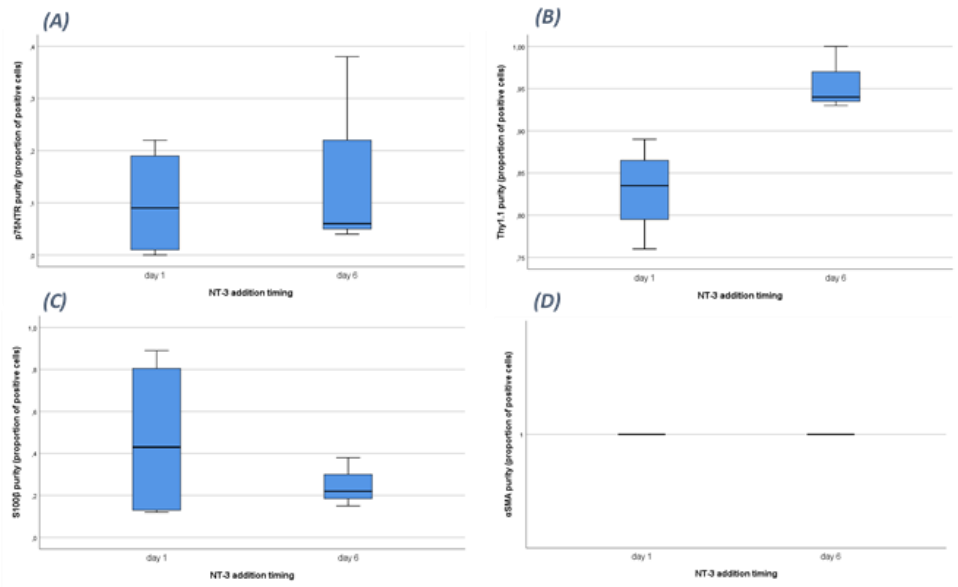

Figure 4.2- Boxplots for the proportion in p75NTR (A), Thy1.1 (B), S100β (C) and α-SMA (D) positive cells for the NT-3 addition timing experiment.

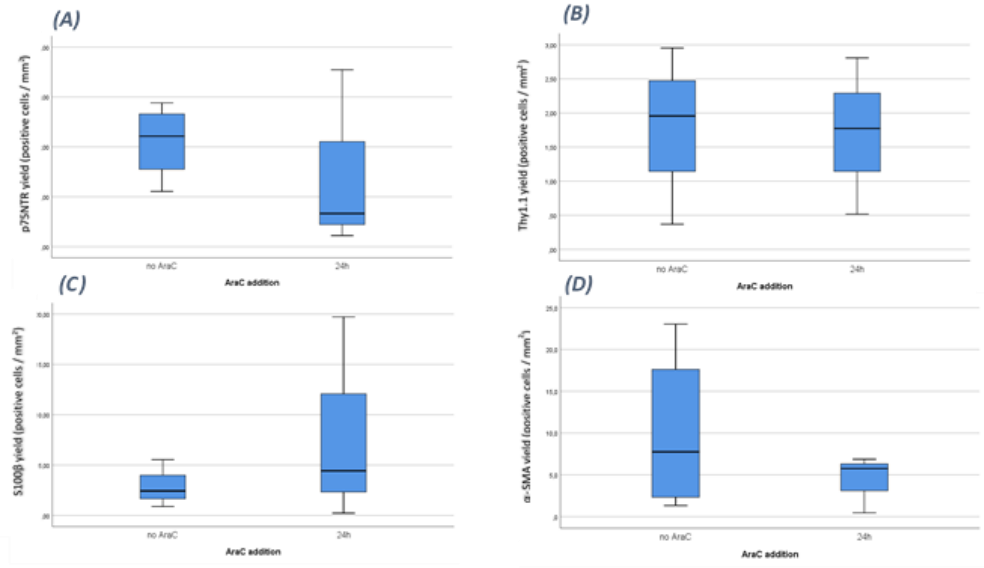

Figure 4.3- Boxplots for the yield in p75NTR (A), Thy1.1 (B), S100β (C) and α-SMA (D) positive cells for the AraC exposure experiment.

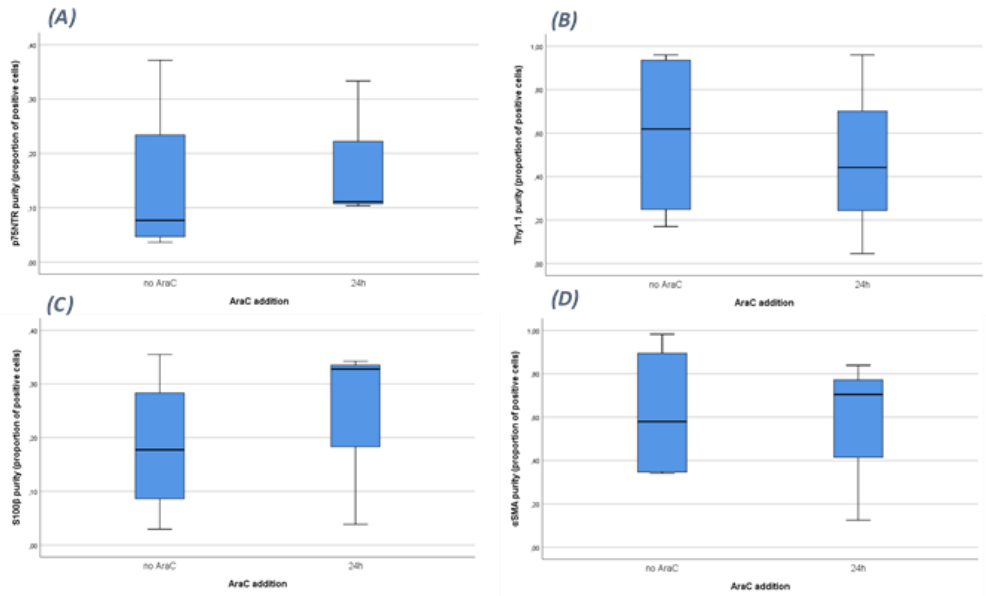

Figure 4.4- Boxplots for the proportion in p75NTR (A), Thy1.1 (B), S100β (C) and α-SMA (D) positive cells for the AraC exposure experiment.

A Shapiro-Wilk to test for normality (Shapiro & Wilk, 1965) was performed. All the data sets for each group had non-significant P values for alpha of 0.05 and were therefore normally distributed (tables 4.1 and 4.2). In the NT-3 experiment α-SMA does not have a p-value because all experimental repeats have the same value of 1 and therefore no distribution of values.

		Shapiro-Wilk		
	NT-3 addition timing	Statistic	df	Sig.
yield p75NTR	day 1	,840	4	,195
	day 6	,881	3	,328
yield Thy1.1	day 1	,944	4	,679
	day 6	,948	3	,559
yield S100β	day 1	,830	4	,168
	day 6	,982	3	,742
yield αSMA	day 1	,969	4	,833
	day 6	,901	3	,389
purity p75NTR	day 1	,885	4	,361
	day 6	,794	3	,100
purity Thy1.1	day 1	,963	4	,798
	day 6	,855	3	,253
purity S100β	day 1	,832	4	,174
	day 6	,951	3	,576
purity αSMA	day 1	.	4	.
	day 6	.	3	.

Table 4.1 - Shapiro-Wilk test for normality for all responses in the NT-3 addition timing experiment. The test was not computed for α-SMA because all experimental repeats have the same value.

		Shapiro-Wilk		
	AraC addition	Statistic	df	Sig.
Thy1.1 purity	24h	,994	3	,853
	no AraC	,845	4	,209
S100β purity	24h	,786	3	,080
	no AraC	,995	4	,982
αSMA purity	24h	,885	3	,340
	no AraC	,845	4	,212
p75NTR purity	24h	,775	3	,056
	no AraC	,768	4	,056
Thy1.1 yield (positive cells/ mm2)	24h	,997	3	,893
	no AraC	,933	4	,610
S100β yield (positive cells/ mm2)	24h	,903	3	,395
	no AraC	,895	4	,406
αSMA yield (positive cells/ mm2)	24h	,875	3	,309
	no AraC	,912	4	,496
p75NTR yield (positive cells/ mm2)	24h	,848	3	,235
	no AraC	,971	4	,850

Table 4.2 - Shapiro-Wilk test for normality for all responses for the AraC exposure experiment.

It was verified if there was a linear relationship between each pair of dependent variables by plotting each pair on a scatter plot (figures 4.5 to

4.8). There is not a linear relationship between some dependent variables so the power of the statistical test will be reduced for those variables.

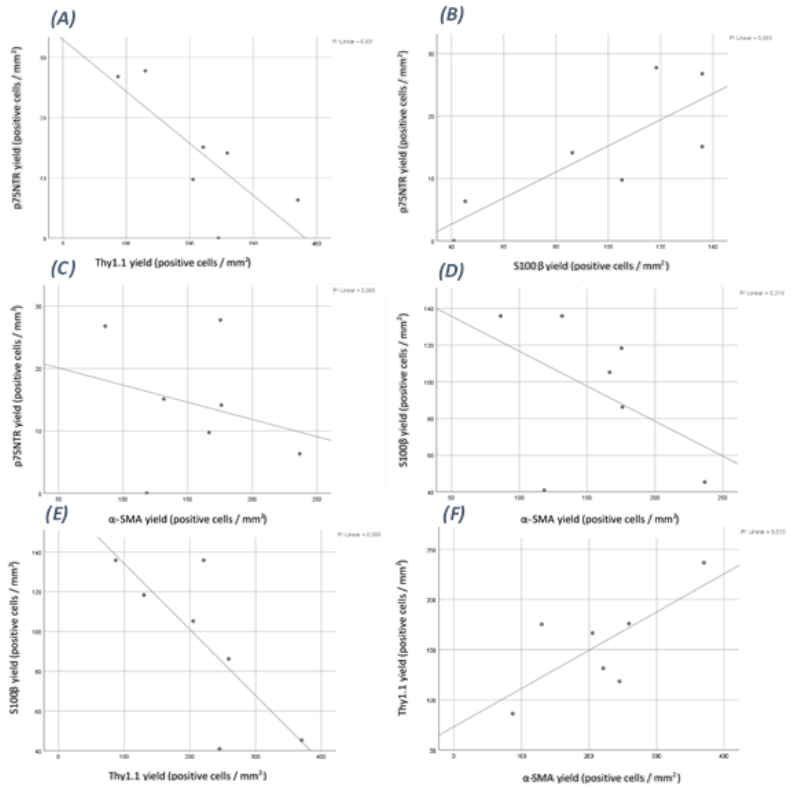

Figure 4.5 - Scatter plot with fit line for yield in p75NTR, Thy1.1, S100ß and α-SMA positive cells responses pairs for the NT-3 addition timing experiment.

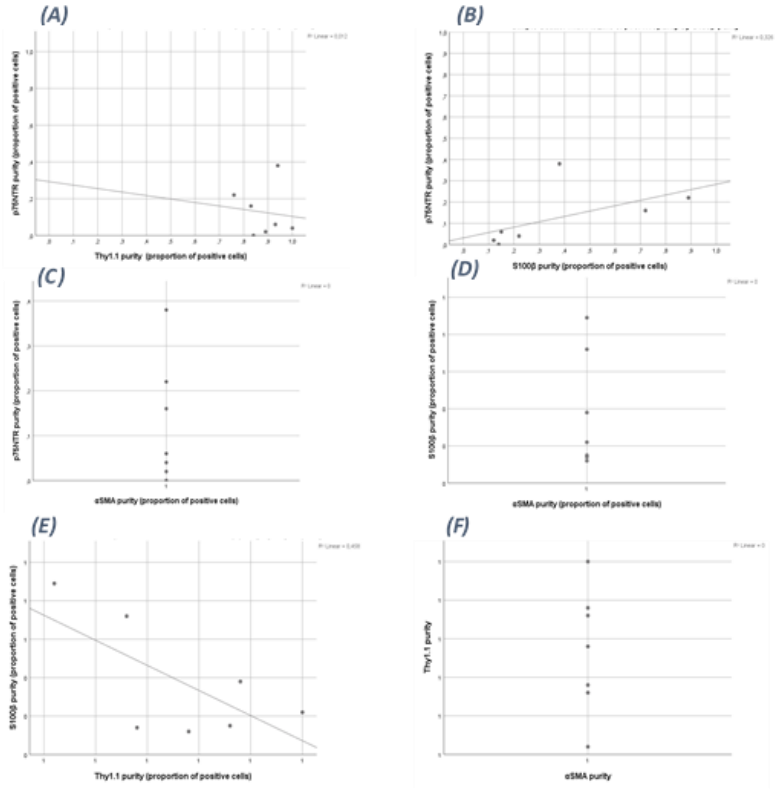

Figure 4.6- Scatter plot with fit line for proportion of p75NTR, Thy1.1, S100β and α-SMA positive cells responses pairs for the NT-3 addition timing experiment.

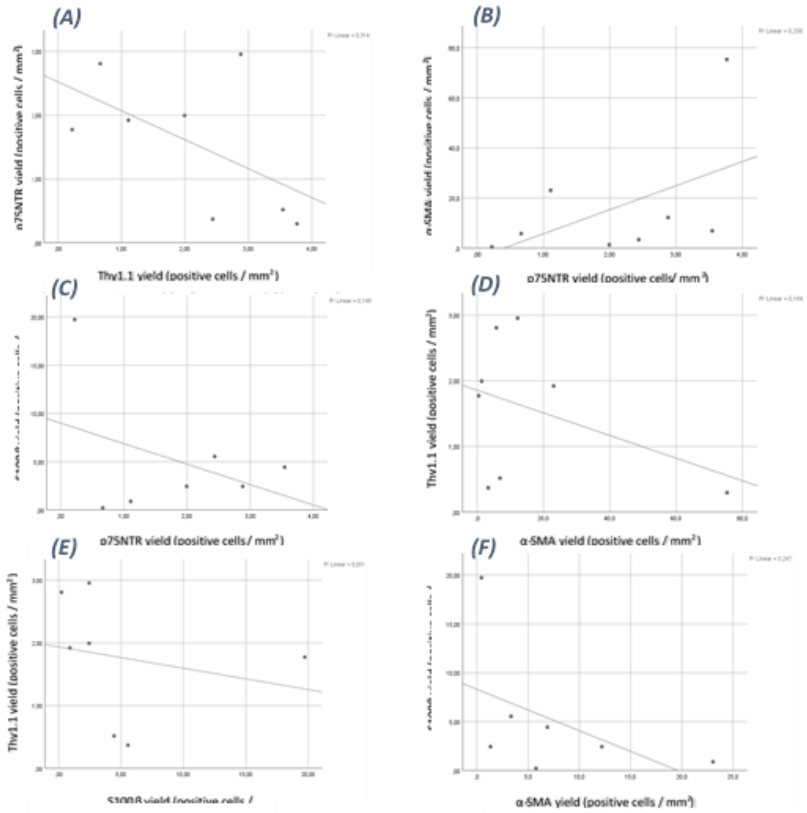

Figure 4.7 - Scatter plot with fit line for yield in p75NTR, Thy1.1, S100β and α-SMA positive cells responses pairs for AraC exposure experiment.

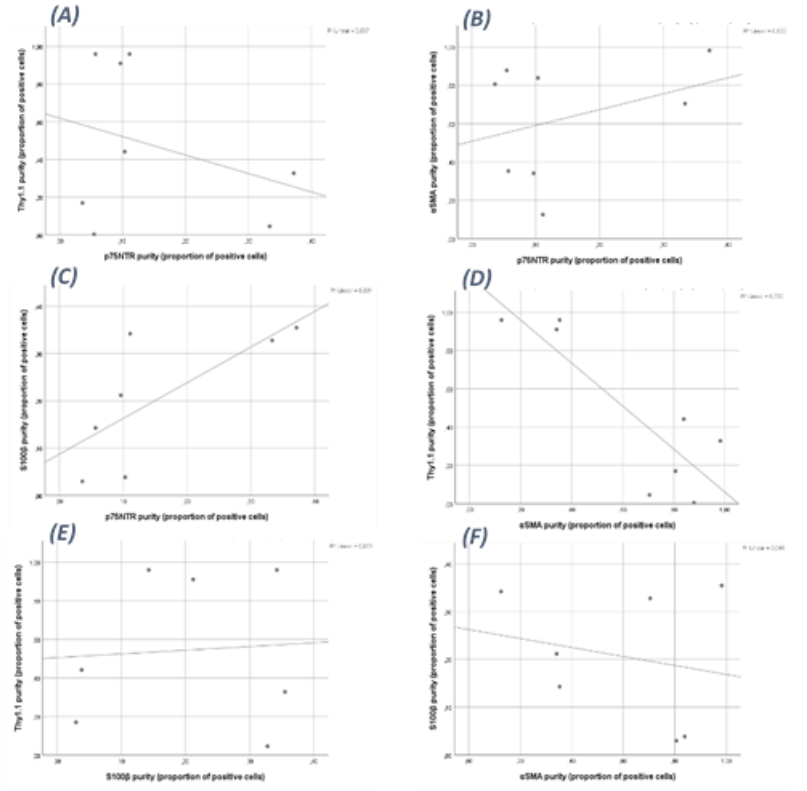

Figure 4.8 - Scatter plot with fit line for purity of p75NTR, Thy1.1, S100β and α-SMA positive cells responses pairs for AraC exposure experiment.

Lastly it was verified if the dependent variables were collinear by doing a regressions between all dependent variables for the whole data set (tables 4.3, 4.4, 4.5 and 4.6). The Variance Inflation factor (VIF) gives the proportion between the variance in a model with multiple terms and the variance of a model with one term (James, Witten, Hastie, & Tibshirani, 2013). A rule of thumb is that if VIF>10 (please see explanation in Definitions section) then multicollinearity is high (Kutner, Nachtsheim, & Neter, 2004). In this case all VIFs are well below 10 for all combinations of dependent variables which suggests that there is no multicollinearity.

(A)

Model		Collinearity Statistics	
		Tolerance	VIF
1	(Constant)		
	Thy1.1 yield (positive cells/ mm2)	,246	4,059
	S100β yield (positive cells/ mm2)	,397	2,520
	αSMA yield (positive cells/ mm2)	,468	2,137

a. Dependent Variable: p75NTR yield (positive cells/ mm2)

(B)

Model		Collinearity Statistics	
		Tolerance	VIF
1	(Constant)		
	S100β yield (positive cells/ mm2)	,268	3,731
	αSMA yield (positive cells/ mm2)	,739	1,353
	p75NTR yield (positive cells/ mm2)	,320	3,129

a. Dependent Variable: Thy1.1 yield (positive cells/ mm2)

(C)

Model		Collinearity Statistics	
		Tolerance	VIF
1	(Constant)		
	αSMA yield (positive cells/ mm2)	,222	4,511
	p75NTR yield (positive cells/ mm2)	,115	8,665
	Thy1.1 yield (positive cells/ mm2)	,269	3,717

a. Dependent Variable: S100β yield (positive cells/ mm2)

(D)

Model		Collinearity Statistics	
		Tolerance	VIF
1	(Constant)		
	p75NTR yield (positive cells/ mm2)	,291	3,440
	Thy1.1 yield (positive cells/ mm2)	,282	3,541
	S100β yield (positive cells/ mm2)	,344	2,907

a. Dependent Variable: αSMA yield (positive cells/ mm2)

Tables 4.3 - Regression statistics for yield in p75NTR (A), Thy1.1 (B), S100ß (C) and α-SMA (D) positive cells for the NT-3 addition timing experiment.

(A)

Model		Collinearity Statistics	
		Tolerance	VIF
1	(Constant)		
	Thy1.1 yield (positive cells/ mm2)	,246	4,059
	S100β yield (positive cells/ mm2)	,397	2,520
	αSMA yield (positive cells/ mm2)	,468	2,137

a. Dependent Variable: p75NTR yield (positive cells/ mm2)

(B)

Model		Collinearity Statistics	
		Tolerance	VIF
1	(Constant)		
	S100β yield (positive cells/ mm2)	,268	3,731
	αSMA yield (positive cells/ mm2)	,739	1,353
	p75NTR yield (positive cells/ mm2)	,320	3,129

a. Dependent Variable: Thy1.1 yield (positive cells/ mm2)

(C)

Model		Collinearity Statistics	
		Tolerance	VIF
1	(Constant)		
	αSMA yield (positive cells/ mm2)	,222	4,511
	p75NTR yield (positive cells/ mm2)	,115	8,665
	Thy1.1 yield (positive cells/ mm2)	,269	3,717

a. Dependent Variable: S100β yield (positive cells/ mm2)

(D)

Model		Collinearity Statistics	
		Tolerance	VIF
1	(Constant)		
	p75NTR yield (positive cells/ mm2)	,291	3,440
	Thy1.1 yield (positive cells/ mm2)	,282	3,541
	S100β yield (positive cells/ mm2)	,344	2,907

a. Dependent Variable: αSMA yield (positive cells/ mm2)

Tables 4.3 - Regression statistics for yield in p75NTR (A), Thy1.1 (B), S100ß (C) and α-SMA (D) positive cells for the NT-3 addition timing experiment.

(A)

Model		Collinearity Statistics	
		Tolerance	VIF
1	(Constant)		
	Thy1.1 purity	,542	1,847
	S100β purity	,542	1,847

a. Dependent Variable: p75NTR purity

(B)

Model		Collinearity Statistics	
		Tolerance	VIF
1	(Constant)		
	S100β purity	,674	1,483
	p75NTR purity	,674	1,483

a. Dependent Variable: Thy1.1 purity

(C)

Model		Collinearity Statistics	
		Tolerance	VIF
1	(Constant)		
	p75NTR purity	,988	1,012
	Thy1.1 purity	,988	1,012

a. Dependent Variable: S100β purity

Table 4.4 -Regression statistics for purity of p75NTR (A), Thy1.1 (B) and S100β (C) purity for the NT-3 addition timing. The α-SMA purity is constant therefore it was not analysed.

(A)

Model		Collinearity Statistics	
		Tolerance	VIF
1	(Constant)		
	S100β purity	,055	18,203
	αSMA purity	,090	11,126
	p75NTR purity	,044	22,629

a. Dependent Variable: Thy1.1 purity

(B)

Model		Collinearity Statistics	
		Tolerance	VIF
1	(Constant)		
	αSMA purity	,291	3,435
	p75NTR purity	,722	1,385
	Thy1.1 purity	,276	3,620

a. Dependent Variable: S100β purity

(C)

Model		Collinearity Statistics	
		Tolerance	VIF
1	(Constant)		
	p75NTR purity	,142	7,053
	Thy1.1 purity	,301	3,326
	S100β purity	,194	5,163

a. Dependent Variable: αSMA purity

(D)

Model		Collinearity Statistics	
		Tolerance	VIF
1	(Constant)		
	Thy1.1 purity	,281	3,559
	S100β purity	,913	1,095
	αSMA purity	,269	3,711

a. Dependent Variable: p75NTR purity

Tables 4.5 - Regression statistics for yield in Thy1.1 (A), S100β (B), α-SMA (C) and p75NTR (D) positive cells for the AraC exposure experiment.

(A)

Model		Collinearity Statistics	
		Tolerance	VIF
1	(Constant)		
	S100β purity	,055	18,203
	αSMA purity	,090	11,126
	p75NTR purity	,044	22,629

a. Dependent Variable: Thy1.1 purity

(B)

Model		Collinearity Statistics	
		Tolerance	VIF
1	(Constant)		
	αSMA purity	,291	3,435
	p75NTR purity	,722	1,385
	Thy1.1 purity	,276	3,620

a. Dependent Variable: S100β purity

(C)

Model		Collinearity Statistics	
		Tolerance	VIF
1	(Constant)		
	p75NTR purity	,142	7,053
	Thy1.1 purity	,301	3,326
	S100β purity	,194	5,163

a. Dependent Variable: αSMA purity

(D)

Model		Collinearity Statistics	
		Tolerance	VIF
1	(Constant)		
	Thy1.1 purity	,281	3,559
	S100β purity	,913	1,095
	αSMA purity	,269	3,711

a. Dependent Variable: p75NTR purity

Tables 4.6 - Regression statistics for proportion in Thy1.1 (A), S100β (B), α-SMA (C) and p75NTR (D) positive cells for the AraC exposure experiment.

A one way MANOVA was performed on both the proportion and yield responses for all markers for both experiments: effect of timing of addition of NT-3 and addition of AraC. The Box's M test (see definitions) for equality of covariance matrices across all the groups (Tabachnick et al., 2001) is not computed because there are fewer than two nonsingular cell covariance matrices due to unequal sample sizes.

For the effect of NT-3 addition timing experiment the assumption of equal variance was not met (table 4.7) for yield in p75NTR positive cells response according to the Levene's test (description in definition section). A more conservative alpha value of 0.025 was used in the statistical tests as recommended (Tabachnick et al., 2001). All absolute deviations in the α-SMA proportion data are constant within each cell so the Levene F statistics could be computed. For yield and proportion in the AraC addition experiment the Levene's test for equality of variances (tables in 4.8) have significance higher than the alpha level of 0.05 for all responses therefore the assumption of equal variance is met (Tabachnick et al., 2001).

		Levene Statistic	df1	df2	Sig.
p75NTR yield (positive cells/ mm2)	Based on Mean	36,849	1	5	,002
	Based on Median	23,604	1	5	,005
	Based on Median and with adjusted df	23,604	1	4,702	,005
	Based on trimmed mean	36,410	1	5	,002
Thy1.1 yield (positive cells/ mm2)	Based on Mean	5,938	1	5	,059
	Based on Median	5,108	1	5	,073
	Based on Median and with adjusted df	5,108	1	3,409	,098
	Based on trimmed mean	5,933	1	5	,059
S100β yield (positive cells/ mm2)	Based on Mean	10,789	1	5	,022
	Based on Median	8,089	1	5	,036
	Based on Median and with adjusted df	8,089	1	3,643	,052
	Based on trimmed mean	10,661	1	5	,022
αSMA yield (positive cells/ mm2)	Based on Mean	3,907	1	5	,105
	Based on Median	3,590	1	5	,117
	Based on Median and with adjusted df	3,590	1	4,293	,126
	Based on trimmed mean	3,913	1	5	,105

Table 4.7- Levene's test for yield in p75NTR, Thy1.1, S100β and α-SMA positive cells for NT-3 addition timing. All absolute deviations in the α-SMA proportion data are constant within each cell so the Levene F statistics could not be computed.

(A)

		Levene Statistic	df1	df2	Sig.
Thy1.1 purity	Based on Mean	,041	1	5	,848
	Based on Median	,078	1	5	,792
	Based on Median and with adjusted df	,078	1	2,458	,802
	Based on trimmed mean	,043	1	5	,844
S100β purity	Based on Mean	,408	1	5	,551
	Based on Median	,001	1	5	,977
	Based on Median and with adjusted df	,001	1	3,251	,978
	Based on trimmed mean	,347	1	5	,582
αSMA purity	Based on Mean	,029	1	5	,871
	Based on Median	,053	1	5	,827
	Based on Median and with adjusted df	,053	1	2,489	,836
	Based on trimmed mean	,017	1	5	,901
p75NTR purity	Based on Mean	,083	1	5	,785
	Based on Median	,029	1	5	,871
	Based on Median and with adjusted df	,029	1	4,981	,872
	Based on trimmed mean	,051	1	5	,830

(B)

		Levene Statistic	df1	df2	Sig.
Thy1.1 yield	Based on Mean	,018	1	5	,897
	Based on Median	,031	1	5	,866
	Based on Median and with adjusted df	,031	1	4,924	,866
	Based on trimmed mean	,022	1	5	,888
S100β yield	Based on Mean	9,854	1	5	,026
	Based on Median	1,858	1	5	,231
	Based on Median and with adjusted df	1,858	1	2,214	,295
	Based on trimmed mean	8,829	1	5	,031
αSMA yield	Based on Mean	3,390	1	5	,125
	Based on Median	2,695	1	5	,162
	Based on Median and with adjusted df	2,695	1	4,055	,175
	Based on trimmed mean	3,390	1	5	,125
p75NTR yield	Based on Mean	4,478	1	5	,088
	Based on Median	,491	1	5	,515
	Based on Median and with adjusted df	,491	1	2,454	,544
	Based on trimmed mean	3,923	1	5	,104

Table 4.8- Levene's test for the yield (A) and purity (B) of p75NTR, Thy1.1, S100ß and α-SMA positive cells for AraC exposure experiment.

According to the multivariate analysis (see definitions section) the factor NT-3 addition timing has a P value for Pillai's Trace test lower than 0.05 which means it has a significant effect on the overall yield in positive cells for the analyzed markers. It also has a very high effect size since it is the only studied variable. For the proportion in the analyzed markers the P value was also lower than 0.05 which also suggested a significant effect on the overall response. For the AraC exposure experiment both P values for yield and proportion are higher than the alpha value of 0.05 therefore there is no significant effect of the variable on the overall response.

(A)

Effect		Value	F	Hypothesis df	Error df	Sig.	Partial Eta Squared	Noncent. Parameter	Observed Power[d]
NT-3 addition timing	Pillai's Trace	1,937	23,135	8,000	6,000	,001	,969	185,083	1,000
	Wilks' Lambda	,001	20,097[b]	8,000	4,000	,006	,976	160,777	,989
	Hotelling's Trace	104,569	13,071	8,000	2,000	,073	,981	104,569	,512
	Roy's Largest Root	86,083	64,562[c]	4,000	3,000	,003	,989	258,248	1,000

(B)

Effect		Value	F	Hypothesis df	Error df	Sig.	Partial Eta Squared	Noncent. Parameter	Observed Power[d]
NT-3 addition timing	Pillai's Trace	1,457	3,574	6,000	8,000	,050	,728	21,445	,677
	Wilks' Lambda	,000	44,247[b]	6,000	6,000	,000	,978	265,483	1,000
	Hotelling's Trace	1110,493	370,164	6,000	4,000	,000	,998	2220,986	1,000
	Roy's Largest Root	1109,650	1479,533[c]	3,000	4,000	,000	,999	4438,598	1,000

Table 4.9- Multivariate tests for the yield (A) and propotion (B) of p75NTR, Thy1.1, S100ß and α-SMA positive cells for NT-3 addition timing experiment.

(A)

Effect		Value	F	Hypothesis df	Error df	Sig.	Partial Eta Squared	Noncent. Parameter	Observed Power[d]
AraC addition	Pillai's Trace	1,196	1,115	8,000	6,000	,460	,598	8,921	,211
	Wilks' Lambda	,030	2,401[b]	8,000	4,000	,207	,828	19,209	,307
	Hotelling's Trace	25,075	3,134	8,000	2,000	,264	,926	25,075	,190
	Roy's Largest Root	24,769	18,577[c]	4,000	3,000	,019	,961	74,306	,890

(B)

Effect		Value	F	Hypothesis df	Error df	Sig.	Partial Eta Squared	Noncent. Parameter	Observed Power[d]
AraC addition	Pillai's Trace	1,078	,877	8,000	6,000	,580	,539	7,019	,172
	Wilks' Lambda	,008	4,960[b]	8,000	4,000	,070	,908	39,682	,568
	Hotelling's Trace	107,924	13,490	8,000	2,000	,071	,982	107,924	,522
	Roy's Largest Root	107,828	80,871[c]	4,000	3,000	,002	,991	323,484	1,000

Table 4.10- Multivariate tests for the yield (A) and proportion (B) of p75NTR, Thy1.1, S100ß and α-SMA positive cells for AraC exposure experiment.

After the significant effect of all factors was determined it can be seen specifically in which responses it has a significant effect with the tests between subjects effects. There seems to be an influence of the factor NT-3 addition timing on all responses but the p75NTR proportion (α-SMA proportion is constant therefore no P value was determined, tables in 4.11). AraC addition had an influence on Thy1.1 and p75NTR yield and all proportions of markers positive cells (tables in 4.12).

(A)

Source	Dependent Variable	Type I Sum of Squares	df	Mean Square	F	Sig.	Partial Eta Squared	Noncent. Parameter	Observed Power[e]
Model	p75NTR yield	1432,330[a]	2	716,165	5,795	,050	,699	11,590	,596
	Thy1.1 yield	176427,863[b]	2	88213,931	9,079	,022	,784	18,159	,789
	S100β yield	64667,558[c]	2	32333,779	19,072	,005	,884	38,145	,979
	αSMA yield	169944,282[d]	2	84972,141	29,793	,002	,923	59,586	,999
NT-3 addition timing	p75NTR yield	1432,330	2	716,165	5,795	,050	,699	11,590	,596
	Thy1.1 yield	176427,863	2	88213,931	9,079	,022	,784	18,159	,789
	S100β yield	64667,558	2	32333,779	19,072	,005	,884	38,145	,979
	αSMA yield	169944,282	2	84972,141	29,793	,002	,923	59,586	,999

(B)

Source	Dependent Variable	Type I Sum of Squares	df	Mean Square	F	Sig.	Partial Eta Squared	Noncent. Parameter	Observed Power[e]
Model	p75NTR purity	,117[a]	2	,058	2,724	,158	,521	5,448	,321
	Thy1.1 purity	5,501[b]	2	2,751	1199,397	,000	,998	2398,794	1,000
	S100β purity	1,062[c]	2	,531	5,329	,058	,681	10,658	,560
	αSMA purity	7,000[d]	2	3,500	.	.	1,000	.	.
NT-3 addition timing	p75NTR purity	,117	2	,058	2,724	,158	,521	5,448	,321
	Thy1.1 purity	5,501	2	2,751	1199,397	,000	,998	2398,794	1,000
	S100β purity	1,062	2	,531	5,329	,058	,681	10,658	,560
	αSMA purity	7,000	2	3,500	.	.	1,000	.	.

Table 4.11- Tests of Between-subjects effects for the yield (A) and proportion (B) of p75NTR, Thy1.1, S100ß and α-SMA positive cells for NT-3 addition timing experiment.

(A)

Source	Dependent Variable	Type I Sum of Squares	df	Mean Square	F	Sig.	Partial Eta Squared	Noncent. Parameter	Observed Power[e]
Model	Thy1.1 yield	21,758[a]	2	10,879	8,974	,022	,782	17,948	,784
	S100β yield	229,980[b]	2	114,990	2,590	,169	,509	5,179	,308
	αSMA yield	454,714[c]	2	227,357	3,571	,109	,588	7,142	,405
	p75NTR yield	24,273[d]	2	12,137	7,371	,032	,747	14,742	,701
AraC	Thy1.1 yield	21,758	2	10,879	8,974	,022	,782	17,948	,784
	S100β yield	229,980	2	114,990	2,590	,169	,509	5,179	,308
	αSMA yield	454,714	2	227,357	3,571	,109	,588	7,142	,405
	p75NTR yield	24,273	2	12,137	7,371	,032	,747	14,742	,701

(B)

Source	Dependent Variable	Type II Sum of Squares	df	Mean Square	F	Sig.	Partial Eta Squared	Noncent. Parameter	Observed Power[e]
Model	Thy1.1 purity	2,101[a]	2	1,050	5,802	,050	,699	11,604	,596
	S100β purity	,304[b]	2	,152	6,652	,039	,727	13,304	,656
	αSMA purity	2,468[c]	2	1,234	10,236	,017	,804	20,472	,835
	p75NTR purity	,179[d]	2	,089	4,169	,086	,625	8,337	,461
AraC	Thy1.1 purity	2,101	2	1,050	5,802	,050	,699	11,604	,596
	S100β purity	,304	2	,152	6,652	,039	,727	13,304	,656
	αSMA purity	2,468	2	1,234	10,236	,017	,804	20,472	,835
	p75NTR purity	,179	2	,089	4,169	,086	,625	8,337	,461

Table 4.12- Tests of Between-subjects effects for the yield (A) and purity (B) of p75NTR, Thy1.1, S100ß and α-SMA positive cells for AraC exposure experiment.

Finally to determine significant differences between conditions in any of the yield and proportion responses pairwise comparisons with Bonferroni adjustment were made (tables 4.13 and 4.14). There seems to be

a significant difference between proportion of p75NTR positive cells for addition of NT-3 at day 1 and day 6 for alpha level of 0.05 (P=0.018). It appears that there is not a significant difference between no AraC exposure and exposure for 24h.

(A)

Dependent Variable	(I) NT-3 addition timing	(J) NT-3 addition timing	Mean Difference (I-J)	Std. Error	Sig.[a]	95% Confidence Interval for Difference[a] Lower Bound	Upper Bound
p75NTR yield	day 1	day 6	2,232	8,490	,803	-19,593	24,057
	day 6	day 1	-2,232	8,490	,803	-24,057	19,593
Thy1.1 yield	day 1	day 6	176,249	75,283	,066	-17,272	369,770
	day 6	day 1	-176,249	75,283	,066	-369,770	17,272
S100β yield	day 1	day 6	-23,984	31,447	,480	-104,822	56,854
	day 6	day 1	23,984	31,447	,480	-56,854	104,822
αSMA yield	day 1	day 6	-3,896	40,789	,928	-108,746	100,955
	day 6	day 1	3,896	40,789	,928	-100,955	108,746

(B)

Dependent Variable	(I) NT-3 addition timing	(J) NT-3 addition timing	Mean Difference (I-J)	Std. Error	Sig.[b]	95% Confidence Interval for Difference[b] Lower Bound	Upper Bound
p75NTR purity	day 1	day 6	-,060	,112	,615	-,347	,227
	day 6	day 1	,060	,112	,615	-,227	,347
Thy1.1 purity	day 1	day 6	-,127*	,037	,018	-,221	-,033
	day 6	day 1	,127*	,037	,018	,033	,221
S100β purity	day 1	day 6	,217	,241	,408	-,402	,837
	day 6	day 1	-,217	,241	,408	-,837	,402
αSMA purity	day 1	day 6	,000	,000	.	,000	,000
	day 6	day 1	,000	,000	.	,000	,000

Table 4.13- Pairwise comparisons for the yield (A) and purity (B) of p75NTR, Thy1.1, S100β and α-SMA positive cells for NT-3 addition timing experiment

(A)

Dependent Variable	(I) AraC addition	(J) AraC addition	Mean Difference (I-J)	Std. Error	Sig.[a]	95% Confidence Interval for Difference[a] Lower Bound	Upper Bound
Thy1.1 yield	no AraC	24h	,111	,841	,900	-2,051	2,273
	24h	no AraC	-,111	,841	,900	-2,273	2,051
S100β yield	no AraC	24h	-5,300	5,089	,345	-18,382	7,783
	24h	no AraC	5,300	5,089	,345	-7,783	18,382
αSMA yield	no AraC	24h	5,614	6,094	,399	-10,052	21,279
	24h	no AraC	-5,614	6,094	,399	-21,279	10,052
p75NTR yield	no AraC	24h	,628	,980	,550	-1,891	3,147
	24h	no AraC	-,628	,980	,550	-3,147	1,891

(B)

Dependent Variable	(I) AraC addition	(J) AraC addition	Mean Difference (I-J)	Std. Error	Sig.[a]	95% Confidence Interval for Difference[a] Lower Bound	Upper Bound
Thy1.1 purity	no AraC	24h	,110	,325	,750	-,726	,945
	24h	no AraC	-,110	,325	,750	-,945	,726
S100β purity	no AraC	24h	-,051	,115	,675	-,348	,245
	24h	no AraC	,051	,115	,675	-,245	,348
αSMA purity	no AraC	24h	,064	,265	,818	-,617	,746
	24h	no AraC	-,064	,265	,818	-,746	,617
p75NTR purity	no AraC	24h	-,042	,112	,720	-,330	,245
	24h	no AraC	,042	,112	,720	-,245	,330

Table 4.14- Pairwise comparisons for the yield (A) and purity (B) of p75NTR, Thy1.1, S100β and α-SMA positive cells for AraC exposure experiment.

4.1.2 *In vitro* 2D functional assays for characteristics relating to neuronal regeneration

An exploratory analysis of descriptive statistics on SPSS was done for each group (combination of factors) on each experiment.

To rule out multivariate outliers the data was represented in a boxplot to detect univariate outliers (figures 4.9-4.20). It can be seen that for the rat OECs 3 day co-culture at atmospheric level of oxygen the NG108 culture on PLL values are unevenly spread for the number of neurons per mm^2 and the number of neurites per neuron (figure 4.9A). For the second set of data (3 day co-culture at physiologic oxygen (figure 4.10) it can be seen that for physiologic level of oxygen that the NG108 culture on F7/SC values are unevenly spread among the four quartiles for the number of neurites per neuron and neurite length per neurite. For the rat OECs 5 day co-culture experiment all values in all data sets were evenly distributed (figures 4.11 and 4.12). For 3 day co-culture at atmospheric oxygen data set the NG108 culture on PA5 cells values are unevenly spread for the number of neurons per mm^2, NG108 on PLL for neurites per neuron and neurite length per neurite (figure 4.13 A, B and C). For the 3 day co-culture at physiologic oxygen (figure 4.14) it can be seen that the NG108 culture on PA5 cells values are unevenly spread for neurite length per neurite (figure 4.14C). It can be seen that the NG108 culture on PA5 cells values are unevenly spread for neurite length per neurite for the 5 days co-culture at atmospheric oxygen (figure 4.15C). For the 5 days co-culture at physiologic oxygen it can be seen that the NG108 culture on PA5 cells values are unevenly spread for neurite

length per neurite (figure 4.16C). For co-culture of PA5 cells with DRG neurons it can be seen that for 3 days co-culture at atmospheric oxygen the DRG culture on PLL and on PA5 cells values are unevenly spread for the number of neurite per neuron (figure 4.17A). It can also be seen that the DRG culture on PLL and on PA5 cells values for co-culture for 5 days at atmospheric oxygen are unevenly spread for the number of neurite per neuron (figure 4.19A). Lastly the 5 days co-culture at physiologic oxygen has values for DRG culture on PLL and on PA5 cells unevenly spread for the neurite length/ neurite (figure 4.20B). Looking at the values outliers were identified and removed from the data sets.

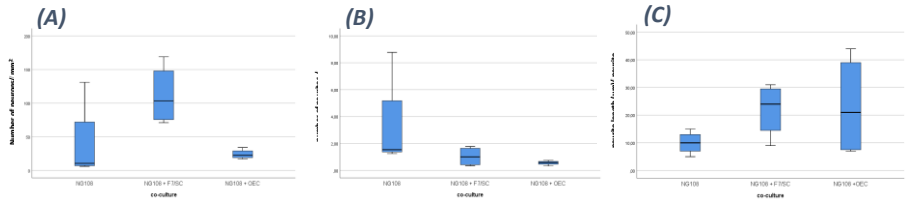

Figure 4.9- Boxplots for the number of neurons/mm² (A), number of neurites per neuron (B) and neurite length per neurite (C) for NG108 on PLL, NG108 + F7/SC and NG108+OEC for the 3 days co-culture at atmospheric oxygen data set.

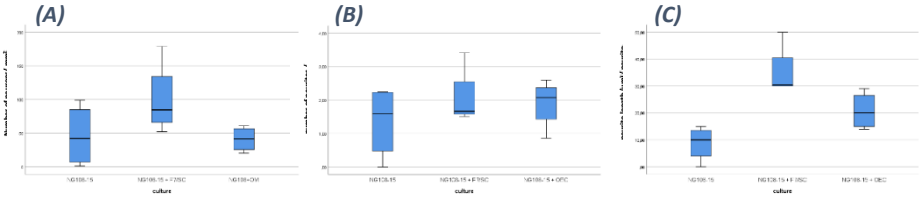

Figure 4.10- Boxplots for the number of neurons/mm² (A), number of neurites per neuron (B) and neurite length per neurite (C) for NG108 on PLL, NG108 + F7/SC and NG108+OEC for the 3 days co-culture at physiologic oxygen data set.

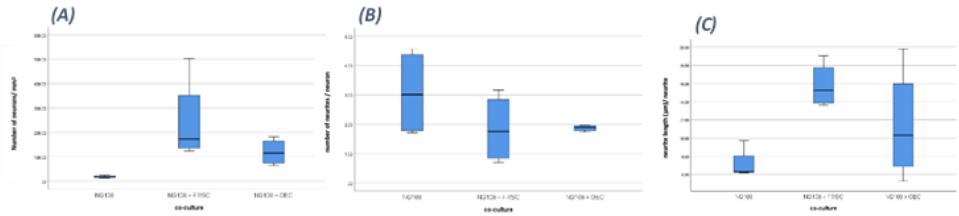

Figure 4.11- Boxplots for the number of neurons/mm² (A), number of neurites per neuron (B) and neurite length per neurite (C) for NG108 on PLL, NG108 + F7/SC and NG108+OEC for 5 days co-culture at atmospheric oxygen data set.

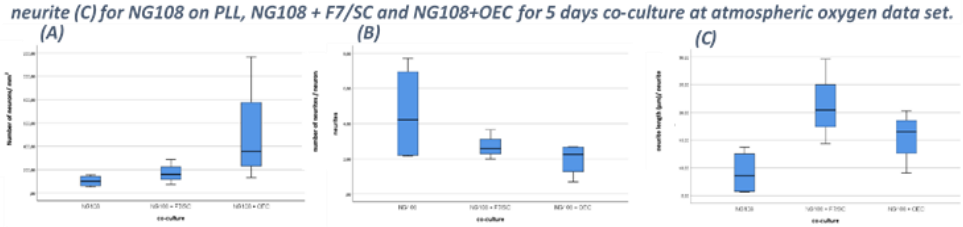

Figure 4.12- Boxplots for the number of neurons/mm² (A), number of neurites per neuron (B) and neurite length per neurite (C) for NG108 on PLL, NG108 + F7/SC and NG108+OEC for the 5 days co-culture at physiologic oxygen data set.

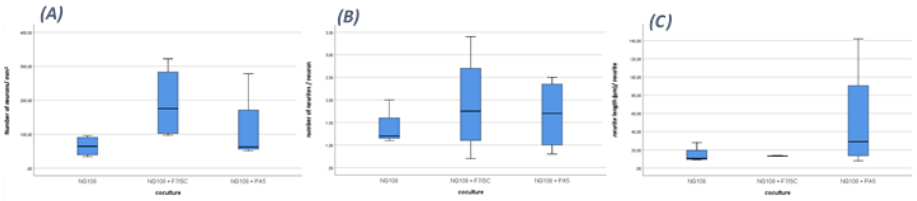

Figure 4.13- Boxplots for the number of neurons/mm² (A), number of neurites per neuron (B) and neurite length per neurite (C) for NG108 on PLL, NG108 +F7/SC and NG108 + PA5 for the 3 days co-culture at atmospheric oxygen data set.

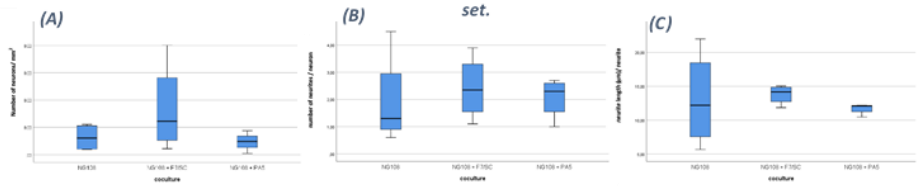

Figure 4.14- Boxplots for the number of neurons/mm² (A), number of neurites per neuron (B) and neurite length per neurite (C) for NG108 on PLL, NG108 +F7/SC and NG108 + PA5 for the 3 days co-culture at physiologic oxygen data set.

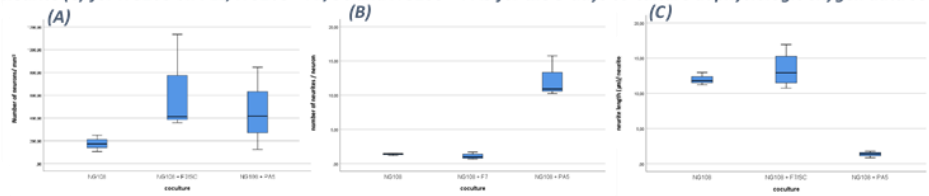

Figure 4.15- Boxplots for the number of neurons/mm² (A), number of neurites per neuron (B) and neurite length per neurite (C) for NG108 on PLL, NG108 + F7/SC and NG108 + PA5 for the 5 days co-culture at atmospheric oxygen data set.

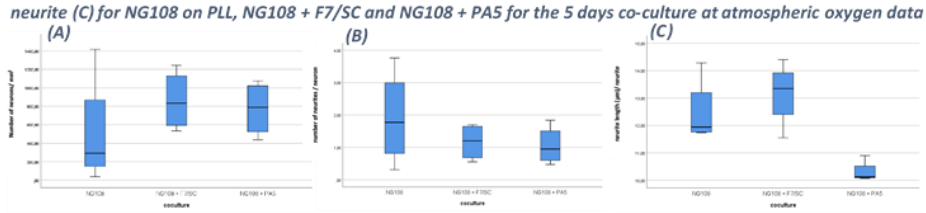

Figure 4.16- Boxplots for the number of neurons/mm² (A), number of neurites per neuron (B) and neurite length per neurite (C) for NG108 on PLL, NG108 + F7/SC and NG108 + PA5 for the 5 days co-culture at physiologic oxygen data set.

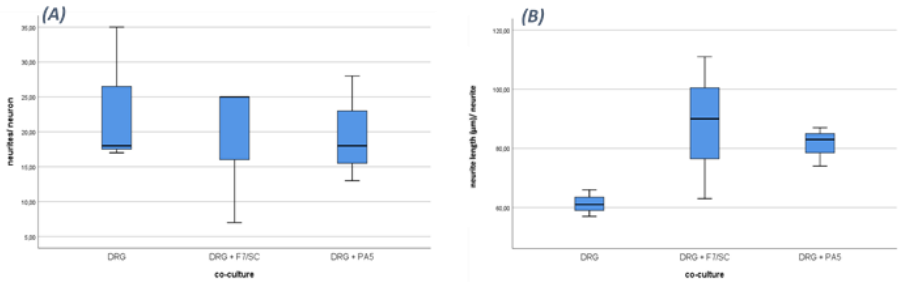

Figure 4.17- Boxplots for the number of neurites per neuron (A) and neurite length per neurite (B) for DRG on PLL, DRG + F7/SC and DRG + PA5 for the 3 days co-culture at atmospheric oxygen data set.

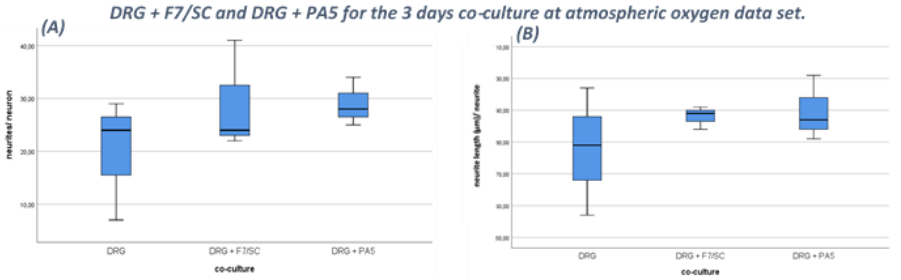

Figure 4.18- Boxplots for the number of neurites per neuron (A) and neurite length per neurite (B) for DRG on PLL, DRG + F7/SC and DRG + PA5 for the 3 days co-culture at physiologic oxygen data set.

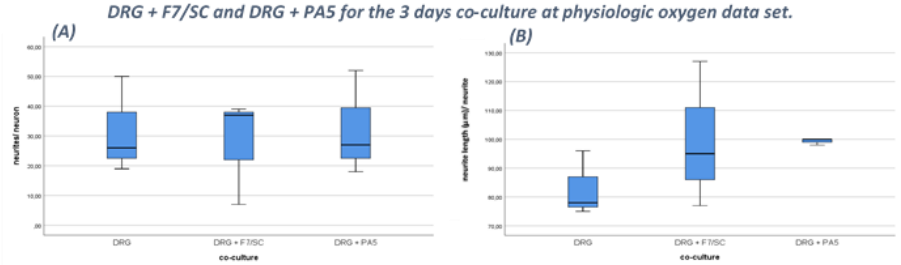

Figure 4.19- Boxplots for the number of neurites per neuron (A) and neurite length per neurite (B) for DRG on PLL, DRG + F7/SC and DRG + PA5 for the 5 days co-culture at atmospheric oxygen data set.

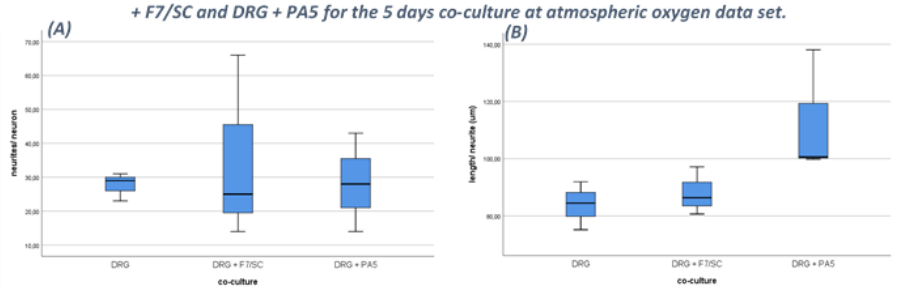

Figure 4.20- Boxplots for the number of neurites per neuron (A) and neurite length per neurite (B) for DRG on PLL, DRG + F7/SC and DRG + PA5 for the 5 days co-culture at physiologic oxygen data set.

A Shapiro-Wilk to test for normality (Shapiro & Wilk, 1965) was performed (tables 4.15-4.17). The data sets for each group in both co-culture with rat OECs and PA5 cells had non-significant P values for alpha of 0.05 and were therefore normally distributed.

(A)	co-culture	Shapiro-Wilk Statistic	df	Sig.
neurons	NG108	,942	3	,537
	NG108 + F7/SC	,915	4	,507
	NG108 + OEC	,939	4	,650
neurites	NG108	,920	3	,453
	NG108 + F7/SC	,862	4	,268
	NG108 + OEC	,929	4	,590
length	NG108	,962	3	,625
	NG108 + F7/SC	,933	4	,613
	NG108 + OEC	,837	4	,187

(B)	co-culture	Shapiro-Wilk Statistic	df	Sig.
neurons	NG108	,905	4	,459
	NG108 + F7/SC	,906	3	,404
	NG108 + OEC	,944	4	,682
neurites	NG108	,868	4	,288
	NG108 + F7/SC	,880	3	,323
	NG108 + OEC	,905	4	,457
length	NG108	,942	4	,667
	NG108 + F7/SC	,821	3	,167
	NG108 + OEC	,935	4	,627

Table 4.15- Shapiro-Wilk test for normality for all responses: number of neurons/ mm², neurite number/ neuron and neurite length/ neurite for 3 day co-culture at atmospheric (A) and physiologic oxygen (B) data set.

(A)	co-culture	Shapiro-Wilk Statistic	df	Sig.
neurons	NG108	,923	3	,463
	NG108 + F7/SC	,953	3	,581
	NG108 + OEC	,935	4	,626
neurites	NG108	,791	3	,094
	NG108 + F7/SC	,948	3	,562
	NG108 + OEC	,895	4	,405
length	NG108	,954	3	,585
	NG108 + F7/SC	,863	3	,277
	NG108 + OEC	,958	4	,765

(B)	co-culture	Shapiro-Wilk Statistic	df	Sig.
neurons	NG108	,920	4	,537
	NG108 + F7/SC	,987	3	,780
	NG108 + OEC	,834	4	,178
neurites	NG108	,842	4	,202
	NG108 + F7/SC	,973	3	,688
	NG108 + OEC	,860	4	,260
length	NG108	,858	4	,254
	NG108 + F7/SC	,986	3	,777
	NG108 + OEC	,919	4	,530

Table 4.16- Shapiro-Wilk test for normality for all responses: number of neurons/ mm², neurite number/ neuron and neurite length/ neurite for the 5 days NG108 + OEC co-culture at atmospheric (A) and physiologic oxygen (B) data set.

(A)	co-culture	Shapiro-Wilk Statistic	df	Sig.
length	NG108	,921	3	,456
	NG108+F7/SC	,893	4	,399
	NG108+PA5	,965	3	,643
neurons	NG108	,900	3	,386
	NG108+F7/SC	,878	4	,330
	NG108+PA5	,912	3	,424
neurites	NG108	,841	3	,217
	NG108+F7/SC	,978	4	,887
	NG108+PA5	,897	3	,375

(B)	co-culture	Shapiro-Wilk Statistic	df	Sig.
length	NG108	,786	4	,080
	NG108+F7/SC	,903	4	,448
	NG108+PA5	,778	3	,063
neurons	NG108	,801	4	,105
	NG108+F7/SC	,995	4	,980
	NG108+PA5	,964	3	,637
neurites	NG108	,975	4	,872
	NG108+F7/SC	,908	4	,472
	NG108+PA5	,959	3	,611

(C)	co-culture	Shapiro-Wilk Statistic	df	Sig.
length	NG108	,998	3	,915
	NG108+F7/SC	,801	3	,118
	NG108+PA5	,988	3	,794
neurons	NG108	,848	3	,235
	NG108+F7/SC	,998	3	,923
	NG108+PA5	,840	3	,213
neurites	NG108	,964	3	,636
	NG108+F7/SC	,944	3	,542
	NG108+PA5	,988	3	,786

(D)	co-culture	Shapiro-Wilk Statistic	df	Sig.
length	NG108	,790	3	,091
	NG108+F7/S	,938	4	,644
	NG108+PA5	,963	3	,629
neurons	NG108	,978	3	,719
	NG108+F7/S	,864	4	,274
	NG108+PA5	,988	3	,791
neurites	NG108	,810	3	,140
	NG108+F7/S	,940	4	,652
	NG108+PA5	,993	3	,843

Table 4.17- Shapiro-Wilk test for normality for all responses: number of neurons/ mm², neurite number/ neuron and neurite length/ neurite for 3 (A and B) or 5 days (C and D) NG108 + PA5 co-culture at atmospheric (A and C) and physiologic oxygen (B and D) data set.

(A)	co-culture	Shapiro-Wilk Statistic	df	Sig.
length/ neurite	DRG	,996	3	,878
	DRG + F7/SC	,995	3	,862
	DRG + PA5	,953	3	,583
log10 (neurites/ neuron)	DRG	,840	3	,213
	DRG + F7/SC	,857	3	,259
	DRG + PA5	,997	3	,898

(B)	co-culture	Shapiro-Wilk Statistic	df	Sig.
neurites/ neuron	DRG	,910	3	,417
	DRG + F7/SC	,828	3	,183
	DRG + PA5	,964	3	,637
length/ neurite	DRG	,997	3	,890
	DRG + F7/SC	,942	3	,537
	DRG + PA5	,949	3	,567

(C)	co-culture	Shapiro-Wilk Statistic	df	Sig.
neurites/ neuron	DRG	,909	3	,414
	DRG + F7/SC	,797	3	,107
	DRG + PA5	,931	3	,493
double length/neurite	DRG	,852	3	,247
	DRG + F7/SC	,975	3	,694
	DRG + PA5	,893	3	,363

(D)	co-culture	Shapiro-Wilk Statistic	df	Sig.
neurites/ neuron	DRG	,923	3	,463
	DRG + F7/SC	,900	3	,386
	DRG + PA5	1,000	3	,962
length/ neurite	DRG	,996	3	,879
	DRG + F7/SC	,969	3	,663
	DRG + PA5	,766	3	,035

Tables 4.18- Shapiro-Wilk test for normality for all responses: neurite number/ neuron and neurite length/ neurite for 3 or 5 days co-culture DRG + PA5 co-culture at atmospheric or physiologic oxygen data set.

For the co-culture of DRG neurons on PA5 the 3 days co-culture at atmospheric oxygen the neurites per neuron data for DRG on F7/SC had a significant P value for alpha of 0.05 and was therefore non-normally distributed. As the samples were only n of 3 it was decided not to remove any data points but to transform the data instead. The neurite per neuron data was transformed to its decimal logarithm and the Shapiro-Wilk test performed again. All data sets had a p value higher than the alpha level of 0.05 and were therefore normally distributed.

For the 5 days co-culture at atmospheric oxygen the neurite length per neurite data for co-culture of DRG with PA5 had a significant P value for alpha of 0.05 and was therefore non-normally distributed. The neurite length per neurite data was transformed to its double and the Shapiro-Wilk test performed again. All data sets had a p value higher than the alpha level of 0.05 and were therefore normally distributed.

For the 5 days co-culture at physiologic oxygen the neurite length/ neurite for DRG culture on PA5 cells had a P value lower than the alpha level of 0.05. Several transformations of the variable neurite length/ neurite were

performed but none gave a P value higher than 0.035. Univariate normality does not guaranty multivariate normality although it is a good indicator (Tabachnick et al., 2001).

It was also verified if there was a linear relationship between each pair of dependent variables by plotting each pair on a scatter plot (figure 4.21-4.30). The R^2 is quite low on all the graphs meaning the dependent variables are not linearly correlated in this case which means the power of the test will be reduced (probability of the test correctly rejecting the null hypothesis).

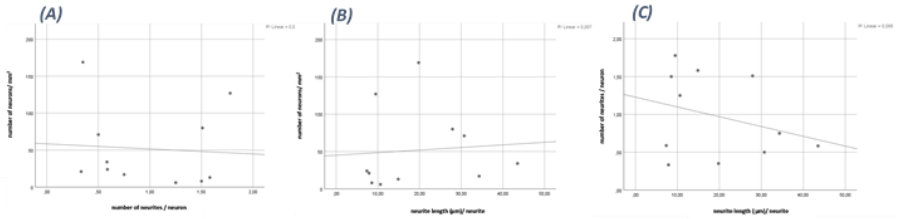

Figure 4.21- Scatter plots for pair of all responses number of neurons/ mm² (A), neurite number/ neuron (B) and neurite length/ neurite (C) for 3 days NG108 + OECs co-culture at atmospheric oxygen data set.

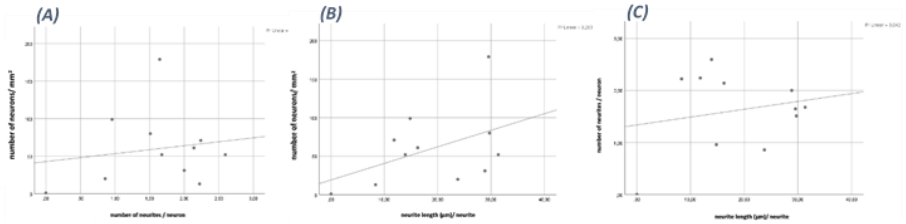

Figure 4.22- Scatter plots for pair of all responses number of neurons/ mm² (A), neurite number/ neuron (B) and neurite length/ neurite (C) for 3 days NG108 + OECs co-culture at physiologic oxygen data set.

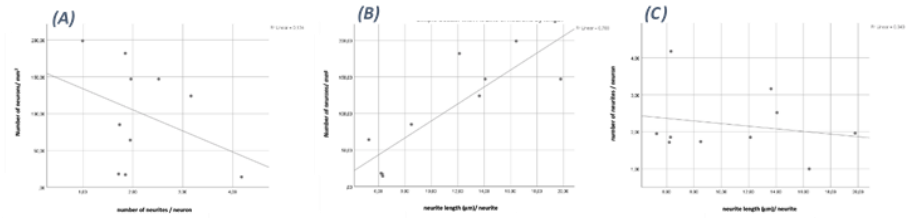

Figure 4.23- Scatter plots for pair of all responses number of neurons/ mm² (A), neurite number/ neuron (B) and neurite length/ neurite (C) for 5 days NG108 + OECs co-culture at atmospheric oxygen data set.

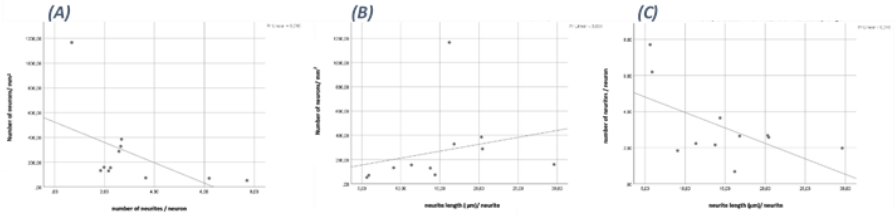

Figure 4.24- Scatter plots for pair of all responses number of neurons/ mm² (A), neurite number/ neuron (B) and neurite length/ neurite (C) for 5 days NG108 + OECs co-culture at physiologic oxygen data set.

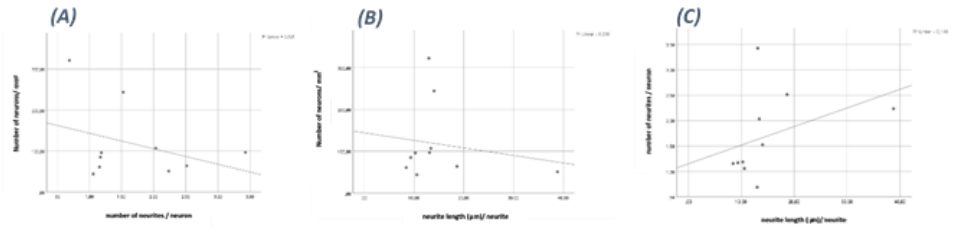

Figure 4.25- Scatter plots for pair of all responses number of neurons/ mm² (A), neurite number/ neuron (B) and neurite length/ neurite (C) for 3 days NG108 + PA5 co-culture at atmospheric oxygen data set.

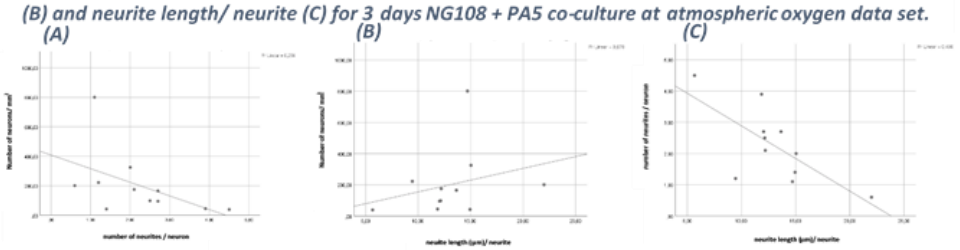

Figure 4.26- Scatter plots for pair of all responses number of neurons/ mm² (A), neurite number/ neuron (B) and neurite length/ neurite (C) for 3 days NG108 + PA5 co-culture at physiologic oxygen data set.

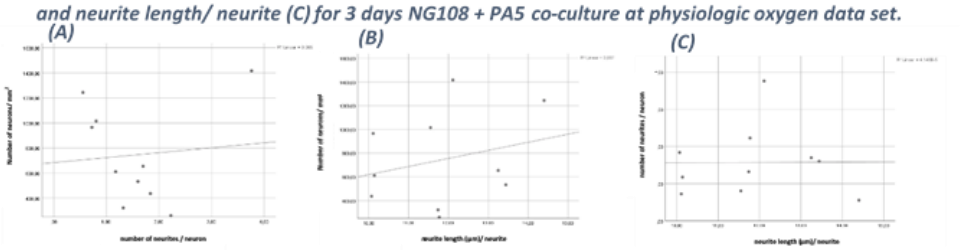

Figure 4.27- Scatter plots for pair of all responses number of neurons/ mm² (A), neurite number/ neuron (B) and neurite length/ neurite (C) for 5 days NG108 + PA5 co-culture at atmospheric oxygen data set.

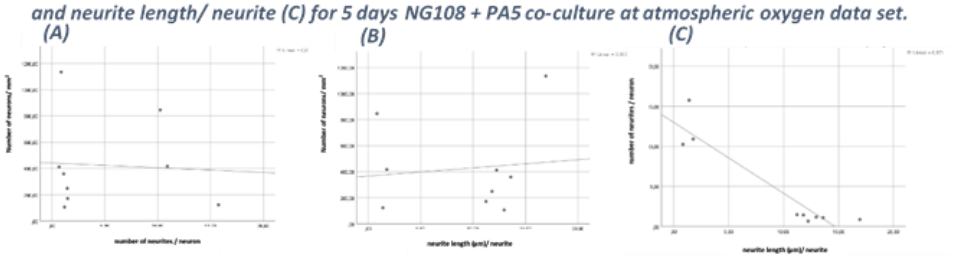

Figure 4.28- Scatter plots for pair of all responses number of neurons/ mm² (A), neurite number/ neuron (B) and neurite length/ neurite (C) for 5 days NG108 + PA5 co-culture at physiologic oxygen data set.

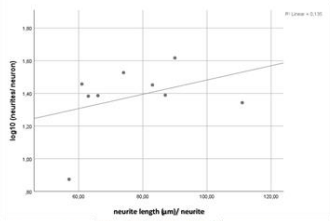

Figure 4.29- Scatter plots for pair of all responses neurite number/ neuron and neurite length/ neurite for 3 days DRG + PA5 co-culture at atmospheric oxygen data set.

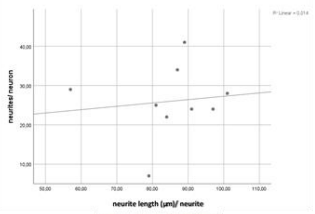

Figure 4. 30- Scatter plots for pair of all responses neurite number/ neuron and neurite length/ neurite for 3 days DRG + PA5 co-culture at physiologic oxygen data set.

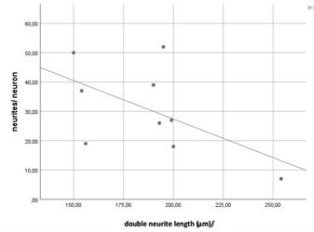

Figure 4.31- Scatter plots for pair of all responses neurite number/ neuron and neurite length/ neurite for 5 days DRG + PA5 co-culture at atmospheric oxygen data set.

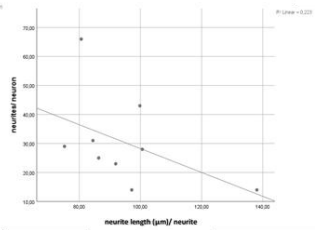

Figure 4.32- Scatter plots for pair of all responses neurite number/ neuron and neurite length/ neurite for 5 days DRG + PA5 co-culture at physiologic oxygen data set.

Lastly it was verified if the dependent variables were collinear by doing a regressions between all dependent variables for the whole data sets (tables 4.18-4.21). In this case all VIFs are well below 10 for all combinations of dependent variables which suggests that there is no multicollinearity.

(A)

Model		Collinearity Statistics	
		Tolerance	VIF
1	(Constant)		
	neurites	,999	1,001
	length	,999	1,001

a. Dependent Variable: neurons

(B)

Model		Collinearity Statistics	
		Tolerance	VIF
1	(Constant)		
	neurons	,944	1,059
	length	,944	1,059

a. Dependent Variable: neurites

(C)

Model		Collinearity Statistics	
		Tolerance	VIF
1	(Constant)		
	neurites	,992	1,008
	neurons	,992	1,008

a. Dependent Variable: length

Table 4.19- Regression statistics for the number of neurons/mm² (A), number of neurites per neuron (B) and neurite length per neurite (C) for NG108 + OEC co-culture experiment for 3 days.

(A)

Model		Collinearity Statistics	
		Tolerance	VIF
1	(Constant)		
	neurites	,876	1,142
	length	,876	1,142

a. Dependent Variable: neurons

(B)

Model		Collinearity Statistics	
		Tolerance	VIF
1	(Constant)		
	length	,856	1,168
	neurons	,856	1,168

a. Dependent Variable: neurites

(C)

Model		Collinearity Statistics	
		Tolerance	VIF
1	(Constant)		
	neurons	,875	1,142
	neurites	,875	1,142

a. Dependent Variable: length

Table 4.20- Regression statistics for the number of neurons/mm² (A), number of neurites per neuron (B) and neurite length per neurite (C) NG108 + OECs co-culture at atmospheric oxygen for 5 days.

(A)

Model		Collinearity Statistics	
		Tolerance	VIF
1	(Constant)		
	neurites	,740	1,352
	length	,740	1,352

a. Dependent Variable: neurons

(B)

Model		Collinearity Statistics	
		Tolerance	VIF
1	(Constant)		
	length	,993	1,007
	neurons	,993	1,007

a. Dependent Variable: neurites

(C)

Model		Collinearity Statistics	
		Tolerance	VIF
1	(Constant)		
	neurons	,998	1,002
	neurites	,998	1,002

a. Dependent Variable: length

Table 4.21- Regression statistics for the number of neurons/mm² (A), number of neurites per neuron (B) and neurite length per neurite (C) for 3 or 5 days NG108 + PA5 co-culture experiment at atmospheric or physiologic oxygen.

Model		Collinearity Statistics	
		Tolerance	VIF
1	(Constant)		
	double_length	1,000	1,000

a. Dependent Variable: log_neurites

Table 4.22- Regression statistics for the number of the decimal logarithm of neurites per neuron and the double of neurite length per neurite for 3 or 5 days co-culture DRG + PA5 co-culture at atmospheric and physiologic oxygen data set.

A MANOVA was performed on the complete data sets. The Box's M test for equality of covariance matrices across all the groups for the 3 and 5 day co-culture with rat OECs is not significant (P=0.203 and P=0.002, respectively) for a level of alpha of 0.001 (Tabachnick et al., 2001). For the co-culture of PA5 cells with NG108 neurons the Box's M test for equality of covariance matrices across all the groups is not significant (P=0.002) for a level of alpha of 0.001 (Tabachnick et al., 2001). For co-culture with DRG neurons the test is also not significant (P=0.086) for a level of alpha of 0.001.

The Levene's test for equality of variances was performed. For one of the response variables in each co-culture with rat OECs (table 4.22) the test is significant (neurite length per neurite for 3 day co-culture and neurite per neuron on 5 day co-culture) therefore the assumption that the variance of the error of the dependent variable is equal across groups is not met for that variable. The Levene's test is also significant for the number of neurites/ neuron in the PA5 co-culture with NG108 neurons (table 4.23) therefore the assumption that the variance of the error of the dependent variable is equal across groups is also not met. It is recommended that a more conservative alpha level is used in this case (Tabachnick et al., 2001), so a level of 0.025 will be used in those cases. In the DRG co-culture (table 4.24) the Levene's test for homogeneity of error variances showed no significance for any of the responses therefore the assumption that the variance of the error of the dependent variable is equal across groups is met.

(A)		Levene Statistic	df1	df2	Sig.
neurons	Based on Mean	7,372	5	16	,001
	Based on Median	2,539	5	16	,071
	Based on Median and with adjusted df	2,539	5	3,578	,210
	Based on trimmed mean	6,960	5	16	,001
neurites	Based on Mean	5,815	5	16	,003
	Based on Median	3,884	5	16	,017
	Based on Median and with adjusted df	3,884	5	6,982	,053
	Based on trimmed mean	5,578	5	16	,004
length	Based on Mean	10,188	5	16	,000
	Based on Median	8,000	5	16	,001
	Based on Median and with adjusted df	8,000	5	11,276	,002
	Based on trimmed mean	10,152	5	16	,000

(B)		Levene Statistic	df1	df2	Sig.
neurons	Based on Mean	4,535	5	15	,010
	Based on Median	1,335	5	15	,303
	Based on Median and with adjusted df	1,335	5	3,166	,426
	Based on trimmed mean	3,840	5	15	,019
neurites	Based on Mean	11,676	5	15	,000
	Based on Median	4,610	5	15	,010
	Based on Median and with adjusted df	4,610	5	7,741	,030
	Based on trimmed mean	11,167	5	15	,000
length	Based on Mean	2,110	5	15	,121
	Based on Median	1,490	5	15	,251
	Based on Median and with adjusted df	1,490	5	8,317	,290
	Based on trimmed mean	2,055	5	15	,128

Table 4.23-Levene's test for the number of neurons/ mm², number of neurites/ neuron and neurite length/ neurite for the 3 days (A) and 5 days (B) NG108 + OECs co-culture experiment at atmospheric and physiologic oxygen.

		Levene Statistic	df1	df2	Sig.
neurons	Based on Mean	5,151	11	28	,000
	Based on Median	,941	11	28	,518
	Based on Median and with adjusted df	,941	11	5,874	,562
	Based on trimmed mean	4,557	11	28	,001
neurites	Based on Mean	4,191	11	28	,001
	Based on Median	,911	11	28	,543
	Based on Median and with adjusted df	,911	11	5,678	,581
	Based on trimmed mean	3,719	11	28	,002
length	Based on Mean	6,975	11	28	,000
	Based on Median	3,270	11	28	,006
	Based on Median and with adjusted df	3,270	11	2,954	,182
	Based on trimmed mean	6,695	11	28	,000

Table 4.24 - Levene's test for the number of neurons/ mm², number of neurites/ neuron and neurite length/ neurite for 3 or 5 days NG108 + PA5 co-culture experiment at atmospheric or physiologic oxygen.

		Levene Statistic	df1	df2	Sig.
log_neurites	Based on Mean	2,005	11	24	,075
	Based on Median	,292	11	24	,981
	Based on Median and with adjusted df	,292	11	11,041	,974
	Based on trimmed mean	1,771	11	24	,117
double_length	Based on Mean	2,309	11	24	,042
	Based on Median	,822	11	24	,620
	Based on Median and with adjusted df	,822	11	9,482	,626
	Based on trimmed mean	2,185	11	24	,053

Table 4.25 -Levene's test for the decimal logarithm of the number of neurites/ neuron and double the neurite length/ neurite for 3 or 5 days co-culture DRG + PA5 co-culture at atmospheric or physiologic oxygen data set.

For the rat OECs co-culture for 3 days (table 4.25A) the multivariate test statistics Pillai's trace for the factor type of culture has P value lower than the level of alpha of 0.05 (P=0.009) showing a significant effect on the overall response with a big effect size (η^2=0.415) which means around 42% of the variation in all responses is attributable to the different cultures (Miles & Shevlin, 2001). The factor level of oxygen nor the interaction between the culture type and oxygen level had a significant effect on the overall response (P=0.216). For co-culture for 5 days (table 4.25B) the multivariate test statistics Pillai's trace for the factor type of culture has a lower P value than the level of alpha of 0.05 (P=0.021) showing a significant effect on the overall response with a big effect size (η^2=0.393) (Miles & Shevlin, 2001). The factor level of oxygen has also a significant effect on the overall response (P=0.029). The interaction between the two factors does not seem to have a significant effect on the overall response (P=0.607).

The multivariate test statistics Pillai's trace for PA5 co-culture on NG108 neurons (table 4.26) show that type of culture, oxygen level and duration have a P value is lower than the level of alpha of 0.05 (P<0.001, P<0.001 and P=0.018, respectively) showing a significant effect on the overall response with a big effect size (η^2=0.401, η^2=0.645 and η^2=0.317, respectively) (Miles & Shevlin, 2001). The power of the statistics is also quite high meaning there is a high chance of the test correctly rejecting the null hypothesis, although dependent on the P value which is quite lower in this case. The second and third degree interactions between the culture type,

duration and oxygen level had also a significant effect on the overall response (P=0.001 and P=P<0.001).

The multivariate test statistics Pillai's trace for co-culture with DRG neurons (table 4.27) show that all factors have a P value is lower than the level of alpha of 0.05 (P<0.001 for type and duration of culture and P<0,01 for level of oxygen) showing a significant effect on the overall response with a big effect size (η2=0.413, η2=0.624 and η2=0.375, respectively) (Miles & Shevlin, 2001). The power of the statistics is also quite high meaning there is a high chance of the test correctly rejecting the null hypothesis, although dependent on the P value which is quite low in this case. Looking at Pillai's Trace test statistic the interaction between the culture type and duration, culture type and oxygen level and duration and oxygen level all had a significant effect on the overall response (P<0.001, P<0.001 and P<0.001, respectively). The third degree interaction between type of culture, duration and oxygen level is also significant (P<0.001).

(A)

Effect		Value	F	Hypothesis df	Error df	Sig.	Partial Eta Squared	Noncent. Parameter	Observed Power[d]
co-culture	Pillai's Trace	,830	3,549	6,000	30,000	,009	,415	21,294	,899
	Wilks' Lambda	,296	3,913[b]	6,000	28,000	,006	,456	23,480	,924
	Hotelling's Trace	1,954	4,234	6,000	26,000	,004	,494	25,403	,941
	Roy's Largest Root	1,704	8,519[c]	3,000	15,000	,002	,630	25,558	,972
oxygen	Pillai's Trace	,265	1,685[b]	3,000	14,000	,216	,265	5,056	,346
	Wilks' Lambda	,735	1,685[b]	3,000	14,000	,216	,265	5,056	,346
	Hotelling's Trace	,361	1,685[b]	3,000	14,000	,216	,265	5,056	,346
	Roy's Largest Root	,361	1,685[b]	3,000	14,000	,216	,265	5,056	,346
co-culture * oxygen	Pillai's Trace	,359	1,095	6,000	30,000	,388	,180	6,567	,362
	Wilks' Lambda	,670	1,036[b]	6,000	28,000	,423	,182	6,216	,338
	Hotelling's Trace	,450	,975	6,000	26,000	,461	,184	5,852	,314
	Roy's Largest Root	,312	1,561[c]	3,000	15,000	,240	,238	4,682	,328

(B)

Effect		Value	F	Hypothesis df	Error df	Sig.	Partial Eta Squared	Noncent. Parameter	Observed Power[d]
co-culture	Pillai's Trace	,787	3,028	6,000	28,000	,021	,393	18,166	,832
	Wilks' Lambda	,355	2,935[b]	6,000	26,000	,025	,404	17,613	,811
	Hotelling's Trace	1,413	2,826	6,000	24,000	,032	,414	16,957	,784
	Roy's Largest Root	1,021	4,762[c]	3,000	14,000	,017	,505	14,287	,795
oxygen	Pillai's Trace	,487	4,120[b]	3,000	13,000	,029	,487	12,360	,719
	Wilks' Lambda	,513	4,120[b]	3,000	13,000	,029	,487	12,360	,719
	Hotelling's Trace	,951	4,120[b]	3,000	13,000	,029	,487	12,360	,719
	Roy's Largest Root	,951	4,120[b]	3,000	13,000	,029	,487	12,360	,719
co-culture * oxygen	Pillai's Trace	,280	,761	6,000	28,000	,607	,140	4,565	,250
	Wilks' Lambda	,736	,719[b]	6,000	26,000	,638	,142	4,317	,234
	Hotelling's Trace	,338	,676	6,000	24,000	,670	,145	4,056	,217
	Roy's Largest Root	,253	1,179[c]	3,000	14,000	,353	,202	3,537	,250

Table 4.26- Multivariate tests for 3 days (A) and 5 days (B) NG108 + OECs co-culture experiment at atmospheric and physiologic oxygen.

Effect		Value	F	Hypothesis df	Error df	Sig.	Partial Eta Squared	Noncent. Parameter	Observed Power[d]
co-culture	Pillai's Trace	,802	6,027	6,000	54,000	,000	,401	36,164	,996
	Wilks' Lambda	,306	7,000[b]	6,000	52,000	,000	,447	42,000	,999
	Hotelling's Trace	1,914	7,976	6,000	50,000	,000	,489	47,853	1,000
	Roy's Largest Root	1,707	15,363[c]	3,000	27,000	,000	,631	46,088	1,000
duration	Pillai's Trace	,645	15,734[b]	3,000	26,000	,000	,645	47,201	1,000
	Wilks' Lambda	,355	15,734[b]	3,000	26,000	,000	,645	47,201	1,000
	Hotelling's Trace	1,815	15,734[b]	3,000	26,000	,000	,645	47,201	1,000
	Roy's Largest Root	1,815	15,734[b]	3,000	26,000	,000	,645	47,201	1,000
oxygen	Pillai's Trace	,317	4,025[b]	3,000	26,000	,018	,317	12,074	,778
	Wilks' Lambda	,683	4,025[b]	3,000	26,000	,018	,317	12,074	,778
	Hotelling's Trace	,464	4,025[b]	3,000	26,000	,018	,317	12,074	,778
	Roy's Largest Root	,464	4,025[b]	3,000	26,000	,018	,317	12,074	,778
co-culture * duration	Pillai's Trace	,691	4,752	6,000	54,000	,001	,346	28,509	,981
	Wilks' Lambda	,339	6,219[b]	6,000	52,000	,000	,418	37,312	,997
	Hotelling's Trace	1,861	7,756	6,000	50,000	,000	,482	46,533	1,000
	Roy's Largest Root	1,812	16,312[c]	3,000	27,000	,000	,644	48,936	1,000
co-culture * oxygen	Pillai's Trace	,688	4,722	6,000	54,000	,001	,344	28,334	,981
	Wilks' Lambda	,319	6,688[b]	6,000	52,000	,000	,436	40,128	,998
	Hotelling's Trace	2,117	8,822	6,000	50,000	,000	,514	52,935	1,000
	Roy's Largest Root	2,107	18,965[c]	3,000	27,000	,000	,678	56,894	1,000
duration * oxygen	Pillai's Trace	,474	7,808[b]	3,000	26,000	,001	,474	23,424	,976
	Wilks' Lambda	,526	7,808[b]	3,000	26,000	,001	,474	23,424	,976
	Hotelling's Trace	,901	7,808[b]	3,000	26,000	,001	,474	23,424	,976
	Roy's Largest Root	,901	7,808[b]	3,000	26,000	,001	,474	23,424	,976
co-culture * duration * oxygen	Pillai's Trace	,702	4,868	6,000	54,000	,000	,351	29,207	,984
	Wilks' Lambda	,312	6,840[b]	6,000	52,000	,000	,441	41,042	,999
	Hotelling's Trace	2,155	8,981	6,000	50,000	,000	,519	53,887	1,000
	Roy's Largest Root	2,134	19,205[c]	3,000	27,000	,000	,681	57,615	1,000

Table 4.27- Multivariate tests for 3 or 5 days NG108 + PA5 co-culture experiment at atmospheric or physiologic oxygen.

Effect		Value	F	Hypothesis df	Error df	Sig.	Partial Eta Squared	Noncent. Parameter	Observed Power[d]
co-culture	Pillai's Trace	,439	3,374	4,000	48,000	,016	,219	13,496	,811
	Wilks' Lambda	,562	3,834[b]	4,000	46,000	,009	,250	15,335	,862
	Hotelling's Trace	,775	4,264	4,000	44,000	,005	,279	17,057	,898
	Roy's Largest Root	,772	9,265[c]	2,000	24,000	,001	,436	18,530	,960
duration	Pillai's Trace	,457	9,668[b]	2,000	23,000	,001	,457	19,337	,966
	Wilks' Lambda	,543	9,668[b]	2,000	23,000	,001	,457	19,337	,966
	Hotelling's Trace	,841	9,668[b]	2,000	23,000	,001	,457	19,337	,966
	Roy's Largest Root	,841	9,668[b]	2,000	23,000	,001	,457	19,337	,966
oxygen	Pillai's Trace	,116	1,516[b]	2,000	23,000	,241	,116	3,032	,289
	Wilks' Lambda	,884	1,516[b]	2,000	23,000	,241	,116	3,032	,289
	Hotelling's Trace	,132	1,516[b]	2,000	23,000	,241	,116	3,032	,289
	Roy's Largest Root	,132	1,516[b]	2,000	23,000	,241	,116	3,032	,289
co-culture * duration	Pillai's Trace	,111	,708	4,000	48,000	,590	,056	2,833	,213
	Wilks' Lambda	,890	,693[b]	4,000	46,000	,601	,057	2,770	,208
	Hotelling's Trace	,123	,676	4,000	44,000	,612	,058	2,702	,202
	Roy's Largest Root	,112	1,341[c]	2,000	24,000	,280	,101	2,682	,261
co-culture * oxygen	Pillai's Trace	,125	,798	4,000	48,000	,532	,062	3,193	,237
	Wilks' Lambda	,878	,770[b]	4,000	46,000	,550	,063	3,082	,228
	Hotelling's Trace	,135	,742	4,000	44,000	,568	,063	2,968	,220
	Roy's Largest Root	,099	1,190[c]	2,000	24,000	,322	,090	2,379	,235
duration * oxygen	Pillai's Trace	,082	1,021[b]	2,000	23,000	,376	,082	2,042	,206
	Wilks' Lambda	,918	1,021[b]	2,000	23,000	,376	,082	2,042	,206
	Hotelling's Trace	,089	1,021[b]	2,000	23,000	,376	,082	2,042	,206
	Roy's Largest Root	,089	1,021[b]	2,000	23,000	,376	,082	2,042	,206
co-culture * duration * oxygen	Pillai's Trace	,044	,271	4,000	48,000	,895	,022	1,082	,104
	Wilks' Lambda	,956	,261[b]	4,000	46,000	,902	,022	1,043	,102
	Hotelling's Trace	,046	,251	4,000	44,000	,908	,022	1,004	,100
	Roy's Largest Root	,039	,472[c]	2,000	24,000	,629	,038	,944	,118

Table 4.28- Multivariate tests for 3 or 5 days co-culture DRG + PA5 co-culture at atmospheric or physiologic oxygen.

Now that a significant effect of the type of culture was determined with the multivariate analysis it can be seen specifically in which responses it has a significant effect with the tests between subject's effects. For the 3 day co-culture of NG108 neurons with rat OECs the model seems to have an effect on all the responses (table 4.28A). The factor co-culture seems to have an effect on the number of neurons per mm^2 and neurite length per neuron (P=0.001 and P=0.023, respectively). The factor oxygen only has an effect on the number of neurite per neuron (P=0.036). The interaction between the factors type of co-culture and oxygen level had no effect on any of the responses. For the 5 day co-culture of NG108 neurons with rat OECs the model seems to have an effect on all the responses (table 4.28B). The factor co-culture seems to have an effect on the neurite length per neurite (P=0.005). The factor oxygen had no effect on any of the responses. The interaction between the factors type of co-culture and oxygen level had no effect on any of the responses.

For the co-culture of NG108 neurons with PA5 cells the model seems to have an effect on all the responses (table 4.29). The factor co-culture seems to have an effect on the number of neurite per neuron (P<0.001). The factor duration of co-culture had an effect on all responses neurons per mm^2, neurites per neuron and neurite length per neurite (P<0.001, P=0.003 and P=0.027, respectively). The factor oxygen level had an effect on neurons per mm^2 and neurites per neuron (P=0.043 and P=0.002, respectively). The second degree interaction between the factors type of co-culture and duration had an effect on the number of neurites per neuron and neurite

length per neurite (P0<0.001 and P=0.007), type of co-culture and oxygen level interaction had an influence on the number of neurites per neuron (P<0.001), duration and oxygen interaction had an influence on the number of neurites per neuron (P<0.001) and third degree interaction had an influence on the number of neurites per neuron (P<0.001) and neurite length per neurite (P=0.015).

The co-culture of DRG neurons with PA5 cells the co-culture type and duration of co-culture had an influence on the neurite length per neurite (P=0.010 and P=0.011, respectively).The oxygen level and none of the

(A)

Source	Dependent Variable	Type II Sum of Squares	df	Mean Square	F	Sig.	Partial Eta Squared	Noncent. Parameter	Observed Power[d]
Model	neurons	99927,583[a]	6	16654,597	11,648	,000	,814	69,887	1,000
	neurites	41,332[b]	6	6,889	16,057	,000	,858	96,341	1,000
	length	9234,336[c]	6	1539,056	15,562	,000	,854	93,372	1,000
co-culture	neurons	29160,820	2	14580,410	10,197	,001	,560	20,394	,964
	neurites	,059	2	,029	,069	,934	,008	,137	,059
	length	951,878	2	475,939	4,812	,023	,376	9,625	,714
oxygen	neurons	1286,560	1	1286,560	,900	,357	,053	,900	,145
	neurites	2,262	1	2,262	5,272	,036	,248	5,272	,578
	length	3,747	1	3,747	,038	,848	,002	,038	,054
co-culture * oxygen	neurons	1750,309	2	875,154	,612	,554	,071	1,224	,134
	neurites	1,882	2	,941	2,194	,144	,215	4,388	,382
	length	137,028	2	68,514	,693	,515	,080	1,386	,146
Error	neurons	22877,417	16	1429,839					
	neurites	6,864	16	,429					
	length	1582,370	16	98,898					
Total	neurons	122805,000	22						
	neurites	48,196	22						
	length	10816,706	22						

(B)

Source	Dependent Variable	Type II Sum of Squares	df	Mean Square	F	Sig.	Partial Eta Squared	Noncent. Parameter	Observed Power[d]
Model	neurons	1274933,00[a]	6	212488,833	4,790	,006	,657	28,738	,929
	neurites	170,356[b]	6	28,393	12,459	,000	,833	74,756	1,000
	length	3979,379[c]	6	663,230	28,004	,000	,918	168,023	1,000
co-culture	neurons	252560,715	2	126280,357	2,846	,090	,275	5,693	,474
	neurites	11,560	2	5,780	2,536	,113	,253	5,073	,429
	length	360,389	2	180,195	7,608	,005	,504	15,217	,892
oxygen	neurons	168737,205	1	168737,205	3,803	,070	,202	3,803	,446
	neurites	3,655	1	3,655	1,604	,225	,097	1,604	,220
	length	105,623	1	105,623	4,460	,052	,229	4,460	,506
co-culture * oxygen	neurons	138258,295	2	69129,147	1,558	,243	,172	3,116	,279
	neurites	3,570	2	1,785	,783	,475	,095	1,566	,159
	length	12,286	2	6,143	,259	,775	,033	,519	,084
Error	neurons	665462,000	15	44364,133					
	neurites	34,182	15	2,279					
	length	355,253	15	23,684					
Total	neurons	1940395,000	21						
	neurites	204,538	21						
	length	4334,633	21						

Table 4.29- Tests of between-subjects effects for 3 days (A) and 5 days (B) NG108 + OECs co-culture experiment at atmospheric and physiologic

second and third degree interactions had an influence on any of the responses.

Source	Dependent Variable	Type III Sum of Squares	df	Mean Square	F	Sig.	Partial Eta Squared	Noncent. Parameter	Observed Power[d]
Model	neurons	8323480,84[a]	12	693623,403	8,216	,000	,779	98,588	1,000
	neurites	576,012[b]	12	48,001	32,441	,000	,933	389,296	1,000
	length	6814,461[c]	12	567,872	24,306	,000	,912	291,667	1,000
co-culture	neurons	445839,874	2	222919,937	2,640	,089	,159	5,281	,482
	neurites	67,259	2	33,630	22,728	,000	,619	45,457	1,000
	length	41,005	2	20,503	,878	,427	,059	1,755	,186
duration	neurons	1790602,792	1	1790602,792	21,209	,000	,431	21,209	,993
	neurites	15,713	1	15,713	10,619	,003	,275	10,619	,882
	length	127,235	1	127,235	5,446	,027	,163	5,446	,615
oxygen	neurons	381071,428	1	381071,428	4,514	,043	,139	4,514	,536
	neurites	17,178	1	17,178	11,610	,002	,293	11,610	,908
	length	,351	1	,351	,015	,903	,001	,015	,052
co-culture * duration	neurons	56136,265	2	28068,133	,332	,720	,023	,665	,098
	neurites	56,552	2	28,276	19,110	,000	,577	38,220	1,000
	length	279,832	2	139,916	5,989	,007	,300	11,977	,844
co-culture * oxygen	neurons	29053,979	2	14526,990	,172	,843	,012	,344	,074
	neurites	74,166	2	37,083	25,062	,000	,642	50,125	1,000
	length	7,390	2	3,695	,158	,854	,011	,316	,072
duration * oxygen	neurons	122083,378	1	122083,378	1,446	,239	,049	1,446	,213
	neurites	35,810	1	35,810	24,202	,000	,464	24,202	,997
	length	53,211	1	53,211	2,278	,142	,075	2,278	,308
coculture * duration * oxygen	neurons	59614,844	2	29807,422	,353	,706	,025	,706	,101
	neurites	69,604	2	34,802	23,521	,000	,627	47,041	1,000
	length	228,151	2	114,075	4,883	,015	,259	9,765	,759
Error	neurons	2363947,247	28	84426,687					
	neurites	41,429	28	1,480					
	length	654,187	28	23,364					
Total	neurons	10687428,08	40						
	neurites	617,442	40						
	length	7468,649	40						

Table 4.30 - Tests of between-subjects effects for 3 or 5 days NG108 + PA5 co-culture experiment at atmospheric or physiologic oxygen.

Source	Dependent Variable	Type III Sum of Squares	df	Mean Square	F	Sig.	Partial Eta Squared	Noncent. Parameter	Observed Power[c]
Model	log_neurites	68,792[a]	12	5,733	93,064	,000	,979	1116,766	1,000
	double_length	1129388,93[b]	12	94115,744	111,064	,000	,982	1332,765	1,000
co-culture	log_neurites	,008	2	,004	,062	,940	,005	,124	,058
	double_length	9473,523	2	4736,761	5,590	,010	,318	11,179	,809
duration	log_neurites	,092	1	,092	1,494	,233	,059	1,494	,217
	double_length	6460,891	1	6460,891	7,624	,011	,241	7,624	,755
oxygen	log_neurites	,028	1	,028	,453	,507	,019	,453	,099
	double_length	731,504	1	731,504	,863	,362	,035	,863	,145
co-culture * duration	log_neurites	,019	2	,009	,154	,858	,013	,308	,071
	double_length	1289,114	2	644,557	,761	,478	,060	1,521	,164
co-culture * oxygen	log_neurites	,084	2	,042	,682	,515	,054	1,363	,151
	double_length	2015,779	2	1007,890	1,189	,322	,090	2,379	,235
duration * oxygen	log_neurites	,021	1	,021	,343	,563	,014	,343	,087
	double_length	453,136	1	453,136	,535	,472	,022	,535	,108
co-culture * duration * oxygen	log_neurites	,038	2	,019	,311	,736	,025	,621	,094
	double_length	760,321	2	380,160	,449	,644	,036	,897	,115
Error	log_neurites	1,478	24	,062					
	double_length	20337,667	24	847,403					
Total	log_neurites	70,270	36						
	double_length	1149726,596	36						

Table 4.31- Tests of between-subjects effects for 3 or 5 days co-culture DRG + PA5 co-culture at atmospheric or physiologic oxygen.

In the pairwise comparisons for oxygen level the Bonferroni adjustment for multiple comparisons was applied. There seems to be a significant difference between neurite number at atmospheric and physiologic oxygen for the alpha level of 0.05 for the 3 day co-culture. The neurite length was significantly different between atmospheric and physiologic oxygen for the 5 day co-culture. In the pairwise comparisons for duration of co-culture there is a significant difference between 3 and 5 days for all responses. For oxygen level there was a significant difference for number of neurons per mm2 and neurites per neuron. For PA5 co-culture with NG108 neurons the duration of co-culture had a significant difference between 3 and 5 days for all responses. For oxygen level there was a significant difference for number of neurons per mm^2 and neurites per neuron. For co-culture of DRG neurons with PA5 cells there was a significant difference in neurite length between culture for 3 and 5 days (P=0.011).

(A)

Dependent Variable	(I) oxygen	(J) oxygen	Mean Difference (I-J)	Std. Error	Sig.[b]	95% Confidence Interval for Difference[b] Lower Bound	Upper Bound
neurons	Atmospheric	Physiologic	-15,306	16,272	,361	-49,801	19,190
	Physiologic	Atmospheric	15,306	16,272	,361	-19,190	49,801
neurites	Atmospheric	Physiologic	-,607*	,282	,047	-1,205	-,010
	Physiologic	Atmospheric	,607*	,282	,047	,010	1,205
length	Atmospheric	Physiologic	-1,020	4,280	,815	-10,092	8,053
	Physiologic	Atmospheric	1,020	4,280	,815	-8,053	10,092

(B)

Dependent Variable	(I) oxygen	(J) oxygen	Mean Difference (I-J)	Std. Error	Sig.[b]	95% Confidence Interval for Difference[b] Lower Bound	Upper Bound
neurons	Atmospheric	Physiologic	-161,778	92,878	,102	-359,743	36,187
	Physiologic	Atmospheric	161,778	92,878	,102	-36,187	359,743
neurites	Atmospheric	Physiologic	-,865	,666	,213	-2,284	,554
	Physiologic	Atmospheric	,865	,666	,213	-,554	2,284
length	Atmospheric	Physiologic	-4,613*	2,146	,048	-9,187	-,039
	Physiologic	Atmospheric	4,613*	2,146	,048	,039	9,187

Tables 4.32- Pairwise comparisons with Bonferroni adjustment for 3 days (A) and 5 days (B) NG108 + OECs co-culture experiment between atmospheric and physiologic oxygen.

(A)

Dependent Variable	(I) duration	(J) duration	Mean Difference (I-J)	Std. Error	Sig.[b]	95% Confidence Interval for Difference[b] Lower Bound	Upper Bound
neurons	3 days	5 days	-427,055*	92,731	,000	-617,006	-237,105
	5 days	3 days	427,055*	92,731	,000	237,105	617,006
neurites	3 days	5 days	-1,265*	,388	,003	-2,060	-,470
	5 days	3 days	1,265*	,388	,003	,470	2,060
length	3 days	5 days	3,600*	1,543	,027	,440	6,760
	5 days	3 days	-3,600*	1,543	,027	-6,760	-,440

(B)

Dependent Variable	(I) oxygen	(J) oxygen	Mean Difference (I-J)	Std. Error	Sig.[b]	95% Confidence Interval for Difference[b] Lower Bound	Upper Bound
neurons	Atmospheric	Physiologic	-197,010*	92,731	,043	-386,960	-7,059
	Physiologic	Atmospheric	197,010*	92,731	,043	7,059	386,960
neurites	Atmospheric	Physiologic	1,323*	,388	,002	,528	2,118
	Physiologic	Atmospheric	-1,323*	,388	,002	-2,118	-,528
length	Atmospheric	Physiologic	-,189	1,543	,903	-3,349	2,971
	Physiologic	Atmospheric	,189	1,543	,903	-2,971	3,349

Tables 4.33- Pairwise comparisons with Bonferroni adjustment between 3 and 5 days (A) and at atmospheric or physiologic oxygen (B) for NG108 + PA5 co-culture experiment.

(A)

Dependent Variable	(I) duration	(J) duration	Mean Difference (I-J)	Std. Error	Sig.[b]	95% Confidence Interval for Difference[b] Lower Bound	Upper Bound
log_neurites	3 days	5 days	-,101	,083	,233	-,272	,070
	5 days	3 days	,101	,083	,233	-,070	,272
double_length	3 days	5 days	-26,793*	9,703	,011	-46,820	-6,766
	5 days	3 days	26,793*	9,703	,011	6,766	46,820

(B)

Dependent Variable	(I) oxygen	(J) oxygen	Mean Difference (I-J)	Std. Error	Sig.[a]	95% Confidence Interval for Difference[a] Lower Bound	Upper Bound
log_neurites	Atmospheric	Physiologic	,056	,083	,507	-,115	,226
	Physiologic	Atmospheric	-,056	,083	,507	-,226	,115
double_length	Atmospheric	Physiologic	9,015	9,703	,362	-11,011	29,042
	Physiologic	Atmospheric	-9,015	9,703	,362	-29,042	11,011

Tables 4.34- Pairwise comparisons with Bonferroni adjustment between 3 and 5 days (A) and at atmospheric or physiologic oxygen (B) for DRG + PA5 co-culture.

For the type of culture multiple comparisons the post-hoc comparison Tukey HSD (Honest Significance Difference) was used. For co-culture of rat OECs with NG108 neurons the multiple comparisons Tukey HSD post-hoc test suggest a significant difference in the number of neurons per mm^2 between the culture of NG108 neurons on PLL and on F7/SC (P=0.004) and between NG108 on F7/SC and NG108 on OECs (P=0.004) for the alpha level of 0.05. They also suggest a significant difference in neurite length between NG108 neurons on PLL and on F7/SC (P=0.025) for the alpha level of 0.025. For PA5 co-culture with NG108 the type of culture in multiple

comparisons with post-hoc comparison Tukey HSD (Honest Significance Difference) procedure assumes equal size of all compared groups, so a more conservative alpha level of 0.025 is assumed for the neurites/ neuron as the variance of the error is not homogenous (Tabachnick et al., 2001). There was a significant difference between the neurite length/ neurite for NG108 cells on PLL and NG108 on F7/SC ($P=0.005$) for an alpha level of 0.05 and a significant difference in the number of neurites per neuron between culture of NG108 on PLL and on PA5 ($P<0.001$) and between culture of NG108 on F7/SC and on PA5 ($P<0.001$). For co-culture of PA5 cells with DRG neurons the multiple comparisons with post-hoc test Tukey HSD (Honest Significance Difference) assumes equal size of all compared groups and in this case that assumption is met so the alpha level used will be 0.05. There was a significant difference in neurites/ neuron between NG108 on PA5 cells and NG108 cells on PLL or NG108 on F7/SC ($P<0.001$) for an alpha level of 0.05.

(A)

Dependent Variable	(I) co-culture	(J) co-culture	Mean Difference (I-J)	Std. Error	Sig.	95% Confidence Interval	
						Lower Bound	Upper Bound
neurons	NG108	NG108+F7/SC	-78,14*	20,212	,004	-130,30	-25,99
		NG108+OEC	-2,36	19,570	,992	-52,85	48,14
	NG108+F7/SC	NG108	78,14*	20,212	,004	25,99	130,30
		NG108+OEC	75,79*	19,570	,004	25,29	126,28
	NG108+OEC	NG108	2,36	19,570	,992	-48,14	52,85
		NG108+F7/SC	-75,79*	19,570	,004	-126,28	-25,29
neurites	NG108	NG108+F7/SC	,11	,350	,946	-,79	1,02
		NG108+OEC	,16	,339	,882	-,71	1,04
	NG108+F7/SC	NG108	-,11	,350	,946	-1,02	,79
		NG108+OEC	,05	,339	,988	-,82	,93
	NG108+OEC	NG108	-,16	,339	,882	-1,04	,71
		NG108+F7/SC	-,05	,339	,988	-,93	,82
length	NG108	NG108+F7/SC	-15,6395*	5,31569	,025	-29,3557	-1,9232
		NG108+OEC	-12,5178	5,14690	,077	-25,3985	1,1629
	NG108+F7/SC	NG108	15,6395*	5,31569	,025	1,9232	29,3557
		NG108+OEC	3,5217	5,14690	,776	-9,7590	16,8024
	NG108+OEC	NG108	12,5178	5,14690	,077	-1,1629	25,3985
		NG108+F7/SC	-3,5217	5,14690	,776	-16,8024	9,7590

(B)

Dependent Variable	(I) co-culture	(J) co-culture	Mean Difference (I-J)	Std. Error	Sig.	95% Confidence Interval	
						Lower Bound	Upper Bound
neurons	NG108	NG108+F7	-100,0000	117,18257	,677	-404,3782	204,3782
		NG108+OEC	-246,2500	109,01032	,093	-529,4011	36,9011
	NG108+F7	NG108	100,0000	117,18257	,677	-204,3782	404,3782
		NG108+OEC	-146,2500	113,75209	,424	-441,7177	149,2177
	NG108+OM	NG108	246,2500	109,01032	,093	-36,9011	529,4011
		NG108+F7	146,2500	113,75209	,424	-149,2177	441,7177
neurites	NG108	NG108+F7	1,2396	,83985	,330	-,9419	3,4211
		NG108+OEC	1,8026	,78128	,096	-,2268	3,8319
	NG108+F7	NG108	-1,2396	,83985	,330	-3,4211	,9419
		NG108+OEC	,5630	,81526	,773	-1,5547	2,6806
	NG108+OM	NG108	-1,8026	,78128	,096	-3,8319	,2268
		NG108+F7	-,5630	,81526	,773	-2,6806	1,5547
length	NG108	NG108+F7	-10,1768*	2,70751	,005	-17,2095	-3,1442
		NG108+OEC	-5,5899	2,51869	,100	-12,1321	,9524
	NG108+F7	NG108	10,1768*	2,70751	,005	3,1442	17,2095
		NG108+OEC	4,5870	2,62825	,221	-2,2398	11,4138
	NG108+OM	NG108	5,5899	2,51869	,100	-,9524	12,1321
		NG108+F7	-4,5870	2,62825	,221	-11,4138	2,2398

Table 4.35- Multiple comparisons Tukey HSD post-hoc test for 3 days (A) and 5 days (B) NG108 + OECs co-culture experiment at atmospheric and physiologic oxygen.

Dependent Variable	(I) co-culture	(J) co-culture	Mean Difference (I-J)	Std. Error	Sig.	95% Confidence Interval	
						Lower Bound	Upper Bound
neurons	NG108	NG108+F7/SC	-246,9463	110,10362	,081	-519,3812	25,4887
		NG108+PA5	-78,4094	116,31818	,780	-366,2213	209,4025
	NG108+F7/SC	NG108	246,9463	110,10362	,081	-25,4887	519,3812
		NG108+PA5	168,5368	112,53445	,307	-109,9128	446,9865
	NG108+PA5	NG108	78,4094	116,31818	,780	-209,4025	366,2213
		NG108+F7/SC	-168,5368	112,53445	,307	-446,9865	109,9128
neurites	NG108	NG108+F7/SC	,0879	,46093	,980	-1,0526	1,2284
		NG108+PA5	-2,7541*	,48695	,000	-3,9590	-1,5492
	NG108+F7/SC	NG108	-,0879	,46093	,980	-1,2284	1,0526
		NG108+PA5	-2,8420*	,47111	,000	-4,0077	-1,6763
	NG108+PA5	NG108	2,7541*	,48695	,000	1,5492	3,9590
		NG108+F7/SC	2,8420*	,47111	,000	1,6763	4,0077
length	NG108	NG108+F7/SC	-1,7760	1,83161	,602	-6,3081	2,7560
		NG108+PA5	,4499	1,93499	,971	-4,3379	5,2378
	NG108+F7/SC	NG108	1,7760	1,83161	,602	-2,7560	6,3081
		NG108+PA5	2,2259	1,87205	,469	-2,4062	6,8581
	NG108+PA5	NG108	-,4499	1,93499	,971	-5,2378	4,3379
		NG108+F7/SC	-2,2259	1,87205	,469	-6,8581	2,4062

Table 4.36- Multiple comparisons Tukey HSD post-hoc test for 3 or 5 days NG108 + PA5 co-culture experiment at atmospheric or physiologic oxygen.

Dependent Variable	(I) co-culture	(J) co-culture	Mean Difference (I-J)	Std. Error	Sig.	95% Confidence Interval	
						Lower Bound	Upper Bound
log_neurites	DRG	DRG + F7/SC	,0057	,10132	,998	-,2473	,2588
		DRG + PA5	-,0276	,10132	,960	-,2807	,2254
	DRG + F7/SC	DRG	-,0057	,10132	,998	-,2588	,2473
		DRG + PA5	-,0333	,10132	,942	-,2864	,2197
	DRG + PA5	DRG	,0276	,10132	,960	-,2254	,2807
		DRG + F7/SC	,0333	,10132	,942	-,2197	,2864
double_length	DRG	DRG + F7/SC	-28,6847	11,88418	,060	-58,3629	,9935
		DRG + PA5	-38,1558*	11,88418	,010	-67,8340	-8,4776
	DRG + F7/SC	DRG	28,6847	11,88418	,060	-,9935	58,3629
		DRG + PA5	-9,4712	11,88418	,708	-39,1494	20,2070
	DRG + PA5	DRG	38,1558*	11,88418	,010	8,4776	67,8340
		DRG + F7/SC	9,4712	11,88418	,708	-20,2070	39,1494

Table 4.37- Multiple comparisons Tukey HSD post-hoc test for 3 days or 5 days DRG + PA5 co-culture at atmospheric or physiologic oxygen.

4.1.3 *In vitro* 3D functional assays

Contraction studies

For the whole data set an exploratory analysis of descriptive statistics on SPSS was done for each group (combination of factors).

To rule out univariate outliers the data was represented in a boxplot.

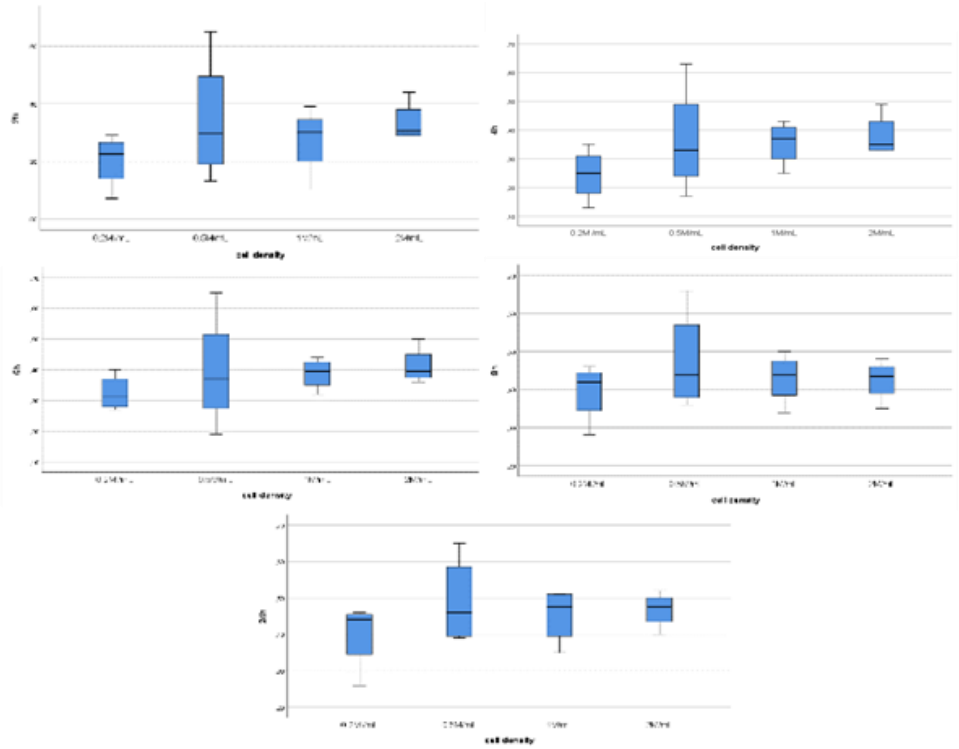

Figure 8.36 - Boxplots for gel contraction after 2 (A), 4 (B), 6 (C), 8 (D) and 24h (E) and cell density 0.2, 0.5, 1 and 2 million cells/ mL.

The group 0.2M/mL cell density after 24h of contraction had an uneven spread of values so an outlier was removed. Both 2M/mL cell density at 2h and 4h are quite uneven too but interestingly the Shapiro-Wilk normality tests are above the alpha level of 0.05 (0.051 and 0.086, respectively) although with low significance values. Nonetheless ANOVA is quite robust for non-normality so no outliers were removed (A. P. Field, 2009).

A Shapiro-Wilk to test for normality (Shapiro & Wilk, 1965) was performed. All the data sets for each group had non-significant P values for alpha of 0.05 and were therefore normally distributed.

		Shapiro-Wilk		
	cell density	Statistic	df	Sig.
2h	0.2M /mL	,980	3	,726
	0.5M/mL	,935	4	,624
	1M/mL	,881	4	,344
	2M/mL	,763	4	,051
4h	0.2M /mL	,964	3	,637
	0.5M/mL	,934	4	,621
	1M/mL	,949	4	,712
	2M/mL	,791	4	,086
6h	0.2M /mL	,997	3	,900
	0.5M/mL	,941	4	,658
	1M/mL	,971	4	,850
	2M/mL	,865	4	,279
8h	0.2M /mL	,987	3	,780
	0.5M/mL	,907	4	,468
	1M/mL	,958	4	,765
	2M/mL	,931	4	,598
24h	0.2M /mL	,964	3	,637
	0.5M/mL	,885	4	,359
	1M/mL	,856	4	,246
	2M/mL	,947	4	,697

Table 4.38- Shapiro-Wilk test for normality for gel contraction after 2, 4, 6, 8 and 24h of contraction and cell densities of 0.2, 0.5, 1 and 2 million cells/ mL.

A two way-ANOVA was performed on the complete data set. The Levene's test was performed and the P value was lower than 0.05 therefore the assumption of equal variance was met.

Looking at previous similar experiments measuring collagen gel contraction related to cell alignment (O'Rourke et al., 2015) the exact mean values and standard deviations are not stated for each condition to be able to compute the effect size for contraction with time and cell density.

		Levene Statistic	df1	df2	Sig.
contraction	Based on Mean	1,133	19	60	,344
	Based on Median	,784	19	60	,716
	Based on Median and with adjusted df	,784	19	28,728	,706
	Based on trimmed mean	1,066	19	60	,407

Table 4.39 -Levene's test for the gel contraction

Using the group variance for each group sample ${s_1}^2$, the pooled standard deviation s the effect size Cohen's *d* can be determined for each comparison. Using the tables in Jack Cohen, 1988 the sample size can be estimated.

Using the lowest explained variance partial eta squared, η^2, 0.030, calculated with the tests between subject effects for each response gives an f^2 of 0.030 which is a small effect and for an ANOVA with 2 groups at 0.05 alpha level and statistical power of 0.8 requires a sample size of at least 393 (Jacob Cohen, 1992b).

In this experiment changes in contraction with time and cell density are subtle, especially between consecutive cell densities and contraction times. Therefore a much bigger sample size would be needed to detect such small effects.

Source	Type II Sum of Squares	df	Mean Square	F	Sig.	Partial Eta Squared	Noncent. Parameter	Observed Power[b]
Model	11,844[a]	20	,592	48,355	,000	,942	967,094	1,000
cell density	,122	3	,041	3,320	,026	,142	9,959	,729
time of contraction	,291	4	,073	5,947	,000	,284	23,790	,977
cell density * time of contraction	,023	12	,002	,154	,999	,030	1,854	,098
Error	,735	60	,012					
Total	12,579	80						

Table 4.40 - Tests of between-subjects effects for gel contraction.

The tests between subjects effects show the observed power and variance explained by the model (η^2= 0.942, stat power=1.000), the factor cell density (η^2= 0.142, stat power=0.729), the factor time of contraction (η^2= 0.284, stat power=0.729) and the second degree interaction between cell density and time of contraction (η^2= 0.030, stat power=0.098).

The multiple comparisons with the post-hoc comparison Tukey HSD (Honest Significance Difference) were performed between cell densities and times of contraction. There seems to be a significant difference in gel contraction between 0.2 and 0.5 million cell per mL (P=0.029). There seems to be also a significant difference in gel contraction between 2h and 8h (P=0.005), 2h and 24h (P=0.001) and 4h and 24h (P=0.033).

(I) cell density	(J) cell density	Mean Difference (I-J)	Std. Error	Sig.	95% Confidence Interval	
					Lower Bound	Upper Bound
0,2M /mL	0,5M/mL	-,1000*	,03500	,029	-,1925	-,0075
	1M/mL	-,0660	,03500	,245	-,1585	,0265
	2M/mL	-,0905	,03500	,057	-,1830	,0020
0,5M/mL	0,2M /mL	,1000*	,03500	,029	,0075	,1925
	1M/mL	,0340	,03500	,768	-,0585	,1265
	2M/mL	,0095	,03500	,993	-,0830	,1020
1M/mL	0,2M /mL	,0660	,03500	,245	-,0265	,1585
	0,5M/mL	-,0340	,03500	,768	-,1265	,0585
	2M/mL	-,0245	,03500	,896	-,1170	,0680
2M/mL	0,2M /mL	,0905	,03500	,057	-,0020	,1830
	0,5M/mL	-,0095	,03500	,993	-,1020	,0830
	1M/mL	,0245	,03500	,896	-,0680	,1170

Table 4.4 ...*0.2, 0.5, 1*

(I) time (h)	(J) time (h)	Mean Difference (I-J)	Std. Error	Sig.	95% Confidence Interval	
					Lower Bound	Upper Bound
2,00	4,00	-,0481	,03913	,734	-,1582	,0619
	6,00	-,0919	,03913	,144	-,2019	,0182
	8,00	-,1431*	,03913	,005	-,2532	-,0331
	24,00	-,1644*	,03913	,001	-,2744	-,0543
4,00	2,00	,0481	,03913	,734	-,0619	,1582
	6,00	-,0438	,03913	,796	-,1538	,0663
	8,00	-,0950	,03913	,122	-,2050	,0150
	24,00	-,1163*	,03913	,033	-,2263	-,0062
6,00	2,00	,0919	,03913	,144	-,0182	,2019
	4,00	,0438	,03913	,796	-,0663	,1538
	8,00	-,0512	,03913	,686	-,1613	,0588
	24,00	-,0725	,03913	,354	-,1825	,0375
8,00	2,00	,1431*	,03913	,005	,0331	,2532
	4,00	,0950	,03913	,122	-,0150	,2050
	6,00	,0512	,03913	,686	-,0588	,1613
	24,00	-,0213	,03913	,982	-,1313	,0888
24,00	2,00	,1644*	,03913	,001	,0543	,2744
	4,00	,1163*	,03913	,033	,0062	,2263
	6,00	,0725	,03913	,354	-,0375	,1825
	8,00	,0213	,03913	,982	-,0888	,1313

Table 4.42 - Multiple comparisons Tukey HSD post-hoc test between 2, 4, 6, 8 and 24h of contraction for gel contraction

4.1.4 Definitions

Shapiro Wilk test

The null-hypothesis of this test is that the population is normally distributed. Therefore if the p-value is less than the chosen alpha level (in this case 0.05), the null hypothesis is rejected and there is evidence that the data tested are not normally distributed. Alternatively, if the p-value is superior to the chosen alpha level, then the null hypothesis that the data came from a normally distributed population cannot be rejected (Shapiro & Wilk, 1965).

Box's M

Box's M test tends to be very strict thus the level of significance is typically 0.001. This test has however very little power (Fallis, 2013) for small sample sizes (which is the case, n=4) meaning it has an decreased likelihood of correctly rejecting the null hypothesis, which in this case is that the covariance matrices are equal. This means that the covariance matrices are not necessarily equal.

Levene's test

The Levene's test for homogeneity of error variances tests the assumption that the variance of the error of the dependent variable is equal across groups. The value based on the median with adjusted degrees of freedom was used because it gives a more robust statistical test while retaining statistical power (M. B. Brown & Forsythe, 1974) and adjusts the degrees of freedom to account for the unequal variance between samples which can be due to unequal sample size (Spellman & Whiting, 2013).

Multivariate analysis

The multivariate test statistics assess whether there are statistically significant differences across the levels of the independent variables for a linear combination of dependent variables.

Effect size

The effect size is represented by eta squared (η^2) which measures the proportion of the total variance of the dependent variable explained by the independent variables. The partial eta squared is the same measure but partitioned for each independent variables and interactions (J. M. Hoenig & Heisey, 2011).

Observed power

The observed power (stat power) is the probability that the test correctly rejects the null hypothesis (H_0) when a specific alternative hypothesis (H_1) is true. In other words it is the likelihood that a study will detect an effect when there is an effect there to be detected. The statistical power ranges from 0 to 1, and as statistical power increases, the probability of making a type II error decreases meaning concluding that there is no effect when in fact there is one (Ellis, 2010). Nonetheless the use of post-hoc statistical power is controversial to say the least. The analysis of "observed power" conducted after a study has been completed uses the obtained sample size and effect size to determine what the power was in the study, assuming the effect size in the sample is equal to the effect size in the population. It was observed that post-hoc "observed power" is dependent on the p-value (Hoenig & Heisey, 2011): the lower the p-value the higher the

stat power. It is widely accepted the utility of prospect power analysis where an adequate sample size is determined for an adequate statistical power, usually 0.8 and expected effect size. In practice the population values are not known and must be estimated from previous similar experiments or the actual experiment sample values.

Tests between subjects' effects

In a MANOVA or ANOVA the tables with the Tests between subjects' effects determine how the dependent variables differ for each of the independent variables (https://statistics.laerd.com/spss-tutorials/one-way-manova-using-spss-statistics-2.php, 08/10/2018). In this case the model stands for the overall factors studied as a source of variation. That is why in cases where only one factor was studied the tests between subjects' effects values are the same as for the factor studied.

Bonferroni Correction

When testing a statistical hypothesis the null hypothesis is rejected if the likelihood of the observed data under the null hypotheses is low. In multivariate analysis, there is a higher chance of an exceptional event occurring therefore, the likelihood rejecting a null hypothesis when it is correct (i.e., making a Type I error) increases (Mittelhammer, Judge, & Miller, 2000). The Bonferroni correction compensates for that increase by testing each individual hypothesis at a significance level of alpha divided by the number of hypothesis (R. G. Miller, 1981).

Tukey's HSD post-hoc test

Tukey's test determines which groups in a sample differ. It uses the "Honest Significant Difference," a number that represents the distance between groups, to compare every mean with every other mean (Brillinger, 1984). It performs all pairwise comparisons and provides the simplest way to control probability of type I error occurs when a set (family) of tests is performed and is considered as the most preferable method when all pairwise comparisons are performed (Kim, 2015). As Tukey's HSD procedure assumes equal size of all compared groups, a modified Tukey-Kramer method can be applied for comparisons of unequal-sized groups. In this case SPSS does not have Tukey-Kramer method available so a more conservative alpha level is assumed for the neurite length as the variance of the error is not homogenous.

Effect size estimation for NT-3 addition timing and Arac exposure experiments

Looking at previous similar experiments measuring p75NTR, S100β, α-SMA and Thy1.1 positive cell number it can be found the typical effect size, difference between conditions divided by the pooled variance (Jack Cohen, 1988; A. P. Field, 2009), however the none could be found in literature that had the exact mean values and standard deviations.

The Mead's resource equation (Hubrecht, Kirkwood, & Universities Federation for Animal Welfare, 2010) can be used to estimate the number of laboratory animals to use in an experiment. The equation is E= N - B- T,

where E is the degrees of freedom of the error component and it should be between 10 and 20, N is the number of individuals or units in the study minus 1, B is the is the blocking component, representing environmental effects allowed for in the design, minus 1 and T is the number of groups in the experiment minus 1. Calculating the degrees of freedom for the error for this experiment it goes: 23 (3 rats x 4 experimental repeats x 2 conditions - 1) – 0 (no blocking component because there is no stratification) – 1 (2 conditions - 1) equals 22 which is higher than 20. According to this equation one rat per experimental repeat with 3 or 4 repeats (E< 20 = N – 1 (=) N<19, 1 rat x 4 repeats x 2 groups -1 or 1 rat x 3 repeats x 2 groups-1) would have been enough. The availability of OECs within a mucosal sample was very low so one rat might not have been enough to yield any useful amount of OECs, so we use 3 rats per experimental repeat.

Considering the standard statistical power of 0.8 and the effect size (the expected difference between the means of the target values between the experimental group and the control group, divided by the pooled standard deviation) within the sample (including outliers) the necessary sample size can also be computed for each individual comparisons between groups.

According to Jack Cohen, 1988, the effect size Cohen's d can be defined as $d = \frac{x_1 - x_2}{s}$ where $s = \sqrt{\frac{(n_1-1){s_1}^2 + (n_2-1){s_2}^2}{n_1+n_2-2}}$ and the variance of each of the groups is defined as ${s_1}^2 = \frac{1}{n_1-1}\sum_{i=1}^{n_1}(x_{1,i} - x_1)^2$ where x is the mean value of the response for that group. Calculating the group variance

for each group sample $s_1{}^2$ and the pooled standard deviation s the effect size d for yield and proportion of each marker can be determined in this experiment. Using the tables in Kenny, 1987 the sample size can be estimated.

For the NT-3 addition experiment it can be seen that according to the sample the effect size on p75NTR, Thy1.1 and S100β yield is small (Jack Cohen, 1988; Sawilowsky, 2009) which leads to the need for a much higher sample size in order to detect the effect for a set statistical power. For α-SMA yield the effect size seems to be very big which lead to a negative sample size. In practice it means that a lower statistical power with a big enough sample size would still be able to detect that effect.

For proportion it is observed that the effect size is quite small (Jack Cohen, 1988; Sawilowsky, 2009) which leads to a big sample size to detect it for the set statistical power of 0.8.

(A)

yield		p75NTR	Thy1.1	S100β	α-SMA
effect size d		-0,28	-0.002	0,08	1,13
sample size		308	127	697	-16
pooled SD		117	94	99	104
group variance	day 1	201	16166	2407	4386
	day 6	40503	2076	25808	25808

(B)

purity		p75NTR	Thy1.1	S100β	α-SMA
effect size d		0,3	0,4	0,4	0,0
sample size		244	180	227	613
pooled SD		0,1	0,3	0,3	0,4
group variance	day 1	0,0	0,0	0,2	0,3
	day 6	0,0	0,2	0,1	0,0

Tables 8.10- Power analysis for yield (A) and purity (B) for NT-3 addition experiment after 1 or 6 days Cohen's d effect size.

According to the samples for the yield in the addition of AraC experiment the effect size is smaller for Thy1.1 comparing to the remaining markers which leads to the need for a much bigger sample size in order to detect an effect for a set statistical power for Thy1.1.

For proportion it is observed that the effect size is quite small (Jack Cohen, 1988; Sawilowsky, 2009) except for α-SMA which leads to a bigger sample size to detect the effects for the set statistical power of 0.8. Again there is a negative sample size for α-SMA which means in practice that a lower statistical power with a big enough sample size would still be able to detect that effect for a set alpha level and vice versa.

Nonetheless Cohen's d measure of effect size is highly influenced by extreme values (in skewed and heavy tailed distributions) in the sample by altering the difference between means in the numerator and the variance in the denominator.

Other option is to use the variance explained partial eta squared, η^2, calculated with the tests between subject effects for each response and calculate f^2 other measure for effect sized used for F-test in ANOVA (Steiger, 2004). Since the lowest the partial eta squared the bigger the sample size, to determine the minimum sample size for this experiment one only need to calculate f^2 for the lowest partial eta squared and that will give the biggest sample size needed from all the responses. For the NT-3 addition experiment the lowest partial eta squared is 0.521 which gives a large effect size f^2 of 1.09 leading to a sample size of at least 26 for an ANOVA with two groups at 0.05 alpha level and statistical power of 0.8. For the AraC addition

experiment the lowest partial eta squared is 0.509 which gives a f^2 of 1.03 again leading to at least a sample size of 26 using the same table (Jacob Cohen, 1992b).

Effect size estimation

Rat OECs co-culture with NG108

The Mead's resource equation (Hubrecht et al., 2010) can be used to estimate the number of laboratory animals to use in an experiment. Calculating the degrees of freedom for the error for this experiment it goes: 71 (3 rats x 4 experimental repeats x 3 culture types x 2 oxygen levels - 1) – 0 (no blocking component because there is no stratification) – 5 (3 culture types x 2 oxygen levels - 1) equals 66 which is higher than 20. According to this equation 1 rat per experimental repeat with 3 or 4 repeats (E< 20 = N – 5 (=) N<25, 1 rat x 4 repeats x 6 groups -1 or 1 rat x 3 repeats x 6 groups) would have been enough. As mentioned before, the availability of OECs within a mucosal sample was very low so one rat might not have been enough to yield any useful amount of OECs, so we use 3 rats per experimental repeat.

Looking at previous similar experiments using neurons and OECs it can be found the typical effect size, difference between conditions divided by the pooled variance (Jack Cohen, 1988; A. P. Field, 2009). Using the neurite length values from Kafitz & Greer, 1999 it gives a Cohen d of 2.47 which is a very large effect. This results in a negative sample size which means in practice that a lower statistical power with a big enough sample

size would still be able to detect that effect for a set alpha level or vice-versa. Values for the number of neurons or neurites and their exact variance were not found in literature, therefore no estimations can be made regarding their effect size.

Using the group variance for each group sample ${s_1}^2$, the pooled standard deviation s the effect size Cohen's *d* can be determined for each comparison in each response (number of neurons per mm^2, number of neurites per neuron and neurite length per neurite). Using the tables in Jacob Cohen, 1992a the sample size can be estimated. Due to the great variation for this co-culture with NG108, especially in neuron number per mm^2 the effect sizes are huge but not necessarily due to the effect rat OEC.

Using the lowest explained variance partial eta squared, η^2, 0.008, calculated with the tests between subject effects for each response gives an f^2 of 0.008 which is a small effect and for an ANOVA with 2 groups at 0.05 alpha level and statistical power of 0.8 requires a sample size of more than 393 (Jacob Cohen, 1992a).

Both effect size measurements hint that NG108 neurons for this assay have a too high variance to detect the tested factors' effects in all responses.

PA5 cells co-culture with NG108

Using the group variance for each group sample ${s_1}^2$, the pooled standard deviation s the effect size Cohen's *d* can be determined for each comparison in each response (number of neurons per mm^2, number of

neurites per neuron and neurite length per neurite). Using the tables in Jack Cohen, 1988 the sample size can be estimated. Due to the great variation for this co-culture with NG108, especially in neuron number per mm^2 the effect sizes are huge, which does not necessarily translate into an actual effect of a factor.

Using the lowest explained variance partial eta squared, η^2, 0.011, calculated with the tests between subject effects for each response gives an f^2 of 0.011 which is a small effect and for an ANOVA with 3 groups at 0.05 alpha level and statistical power of 0.8 requires a sample size of more than 322 (Jacob Cohen, 1992a).

The effect size measurement seems to suggest that more experimental repeats would be necessary to detect all effects of the studied factors.

PA5 co-culture with rat DRG neurons

Using the group variance for each group sample ${s_1}^2$, the pooled standard deviation s the effect size Cohen's *d* can be determined for each comparison in each response (number of neurons per mm^2, number of neurites per neuron and neurite length per neurite). Using the tables in Jack Cohen, 1988 the sample size can be estimated. Probably due to the great variation for this co-culture with primary rat DRG neurons, the calculated effect sizes are huge, around 20, which does not necessarily translate into an actual effect of a factor.

Using the lowest explained variance partial eta squared, η^2, 0.013, calculated with the tests between subject effects for each response gives an f^2 of 0.013 which is a small effect and for an ANOVA with 3 groups at 0.05 alpha level and statistical power of 0.8 requires a sample size of more than 322 (Jacob Cohen, 1992a).

The effect size measurement seems to suggest that more experimental repeats would be necessary to detect all effects of the studied factors.

Contraction studies with PA5 cells

Using the group variance for each group sample ${s_1}^2$, the pooled standard deviation s the effect size Cohen's *d* can be determined for each comparison in the contraction proportion response. Using the tables in Jack Cohen, 1988 the sample size can be estimated. As mentioned before the differences in contraction are minimal between cell densities so effect sizes are small (0.05-0.2) (Sawilowsky, 2009).

Using the lowest explained variance partial eta squared, η^2, 0.142, calculated with the tests between subject effects for proportion of contraction gives an f^2 of 0.166 which is considered a medium effect and for an ANOVA with 2 groups at 0.05 alpha level and statistical power of 0.8 requires a sample size of at least 64 (Jacob Cohen, 1992a).

The effect size measurement seems to suggest that more experimental repeats would be necessary to detect all effects of the studied factors.

5. References

Acheson, A., Barker, P. A., Alderson, R. F., Miller, F. D., & Murphy, R. A. (1991). Detection of brain-derived neurotrophic factor-like activity in fibroblasts and Schwann cells: Inhibition by antibodies to NGF. *Neuron*, *7*(2), 265–275. https://doi.org/10.1016/0896-6273(91)90265-2

Ahuja, C. S., Martin, A. R., & Fehlings, M. (2016). Recent advances in managing a spinal cord injury secondary to trauma. *F1000Research*, *5*, 1017. https://doi.org/10.12688/f1000research.7586.1

Airaksinen, M. S., & Saarma, M. (2002). The GDNF family: Signalling, biological functions and therapeutic value. *Nature Reviews Neuroscience*, *3*(5), 383–394. https://doi.org/10.1038/nrn812

Alexander, C. L., Fitzgerald, U. F., & Barnett, S. C. (2002). Identification of growth factors that promote long-term proliferation of olfactory ensheathing cells and modulate their antigenic phenotype. *Glia*, *37*(4), 349–364. https://doi.org/10.1002/glia.10044

Allt, G. (1975). The node of Ranvier in experimental allergic neuritis: An electron microscope study. *Journal of Neurocytology*, *4*(1), 63–76. https://doi.org/10.1007/BF01099096

Anderson, K. D., Guest, J. D., Dietrich, W. D., Bunge, M. B., Curiel, R., Dididze, M., … Levi, A. D. (2017). Safety of Autologous Human Schwann Cell Transplantation in Subacute Thoracic Spinal Cord Injury. *Journal of Neurotrauma*, neu.2016.4895.

https://doi.org/10.1089/neu.2016.4895

Andrews, M. R., & Stelzner, D. J. (2007). Evaluation of Olfactory Ensheathing and Schwann Cells after Implantation into a Dorsal Injury of Adult Rat Spinal Cord. *Journal of Neurotrauma*, *24*(11), 1773–1792. https://doi.org/10.1089/neu.2007.0353

Andrews, P. W., Damjanov, I., Simon, D., Banting, G. S., Carlin, C., Dracopoli, N. C., & Føgh, J. (1984). Pluripotent embryonal carcinoma clones derived from the human teratocarcinoma cell line Tera-2. Differentiation in vivo and in vitro. *Laboratory Investigation; a Journal of Technical Methods and Pathology*, *50*(2), 147–162. https://doi.org/6694356

Assinck, P., Duncan, G. J., Hilton, B. J., Plemel, J. R., & Tetzlaff, W. (2017). Cell transplantation therapy for spinal cord injury. *Nature Neuroscience*, *20*(05), 637–647. https://doi.org/10.1038/nn.4541

Au, E., & Roskams, a. J. (2003). Olfactory ensheathing cells of the lamina propria in vivo and in vitro. *Glia*, *41*(April 2002), 224–236. https://doi.org/10.1002/glia.10160

Au, W. W., Treloar, H. B., & Greer, C. A. (2002). Sublaminar organization of the mouse olfactory bulb nerve layer. *Journal of Comparative Neurology*, *446*(1), 68–80. https://doi.org/10.1002/cne.10182

Averill, S., Michael, G. J., Shortland, P. J., Leavesley, R. C., King, V. R., Bradbury, E. J., … Priestley, J. V. (2004). NGF and GDNF ameliorate the increase in ATF3 expression which occurs in dorsal root ganglion cells

in response to peripheral nerve injury. *The European Journal of Neuroscience*, *19*(6), 1437–1445. https://doi.org/10.1111/j.1460-9568.2004.03241.x

Babiarz, J., Kane-Goldsmith, N., Basak, S., Liu, K., Young, W., & Grumet, M. (2011). Juvenile and adult olfactory ensheathing cells bundle and myelinate dorsal root ganglion axons in culture. *Experimental Neurology*, *229*(1), 72–79. https://doi.org/10.1016/j.expneurol.2010.08.028

Baichwal, R. R., Bigbee, J. W., & DeVries, G. H. (1988). Macrophage-mediated myelin-related mitogenic factor for cultured Schwann cells. *Proceedings of the National Academy of Sciences of the United States of America*, *85*(5), 1701–1705. https://doi.org/10.1073/pnas.85.5.1701

Balentine, J. D. (1988). Spinal cord trauma: in search of the meaning of granular axoplasm and vesicular myelin. *Journal of Neuropathology and Experimental Neurology*, *47*(2), 77–92. Retrieved from http://www.ncbi.nlm.nih.gov/pubmed/3276818

Bamber, N. I., Li, H., Lu, X., Oudega, M., Aebischer, P., & Xu, X. M. (2001). Neurotrophins BDNF and NT-3 promote axonal re-entry into the distal host spinal cord through Schwann cell-seeded mini-channels. *European Journal of Neuroscience*, *13*(2), 257–268. https://doi.org/10.1046/j.1460-9568.2001.01387.x

Barakat, D. J., Gaglani, S. M., Neravetla, S. R., Sanchez, A. R., Andrade, C.

M., Pressman, Y., … Pearse, D. D. (2005). Survival, integration, and axon growth support of glia transplanted into the chronically contused spinal cord. In *Cell Transplantation* (Vol. 14, pp. 225–240). https://doi.org/10.3727/000000005783983106

Barber, P. C., & Dahl, D. (1987). Glial fibrillary acidic protein (GFAP)-like immunoreactivity in normal and transected rat olfactory nerve. *Experimental Brain Research*, *65*(3), 681–685. https://doi.org/10.1007/BF00235993

Barber, P. C., & Lindsay, R. M. (1982). Schwann cells of the olfactory nerves contain glial fibrillary acidic protein and resemble astrocytes. *Neuroscience*, *7*, 3077–3090. https://doi.org/10.1016/0306-4522(82)90231-7

Bareyre, F. M., Kerschensteiner, M., Raineteau, O., Mettenleiter, T. C., Weinmann, O., & Schwab, M. E. (2004). The injured spinal cord spontaneously forms a new intraspinal circuit in adult rats. *Nature Neuroscience*, *7*(3), 269–277. https://doi.org/10.1038/nn1195

Barnett, S. C. C., Alexander, C. L., Iwashita, Y., Gilson, J. M., Crowther, J., Clark, L., … Franklin, R. J. M. (2000). Identification of a human olfactory ensheathing cell that can effect transplant-mediated remyelination of demyelinated CNS axons. *Brain*, *123*(8), 1581–1588. https://doi.org/10.1093/brain/123.8.1581

Barnett, S. C., Hutchins, A.-M., & Noble, M. (1993). Purification of Olfactory Nerve Ensheathing Cells from the Olfactory Bulb. *Developmental*

Biology. https://doi.org/10.1006/dbio.1993.1033

Barnett, S. C., & Riddell, J. S. (2007, March 1). Olfactory ensheathing cell transplantation as a strategy for spinal cord repair - What can it achieve? *Nature Clinical Practice Neurology*. Nature Publishing Group. https://doi.org/10.1038/ncpneuro0447

Barnett, S. C., & Roskams, A. J. (2008). Olfactory ensheathing cells: isolation and culture from the neonatal olfactory bulb. *Methods in Molecular Biology (Clifton, N.J.)*, *438*, 85–94. https://doi.org/10.1007/978-1-59745-133-8_8

Barnett, S. C. S. C., & Chang, L. (2004). Olfactory ensheathing cells and CNS repair: Going solo or in need of a friend? *Trends in Neurosciences*, *27*(1), 54–60. https://doi.org/10.1016/j.tins.2003.10.011

Barraud, P., Seferiadis, A. A., Tyson, L. D., Zwart, M. F., Szabo-rogers, H. L., Ruhrberg, C., … Baker, C. V. H. (2010). Neural crest origin of olfactory ensheathing glia. https://doi.org/10.1073/pnas.1012248107/-/DCSupplemental.www.pnas.org/cgi/doi/10.1073/pnas.1012248107

Bartkowska, K., Turlejski, K., & Djavadian, R. L. (2010). Neurotrophins and their receptors in early development of the mammalian nervous system. *Acta Neurobiologiae Experimentalis*, *70*(4), 454–467. https://doi.org/7049 [pii]

Bauer, S., Kerr, B. J., & Patterson, P. H. (2007). The neuropoietic cytokine family in development, plasticity, disease and injury. *Nature Reviews. Neuroscience*, *8*(3), 221–232. https://doi.org/10.1038/nrn2054

Bettinger, C. J., Langer, R., & Borenstein, J. T. (2009, July 13). Engineering substrate topography at the Micro- and nanoscale to control cell function. *Angewandte Chemie - International Edition*. https://doi.org/10.1002/anie.200805179

Bhattacharyya, A., Frank, E., Ratner, N., & Brackenbury, R. (1991). P0 is an early marker of the Schwann cell lineage in chickens. *Neuron*, *7*, 831–844. https://doi.org/10.1016/0896-6273(91)90285-8

Bianco, J. I., Perry, C., Harkin, D. G., Mackay-Sim, A., & Féron, F. (2004). Neurotrophin 3 promotes purification and proliferation of olfactory ensheathing cells from human nose. *Glia*, *45*(2), 111–123. https://doi.org/10.1002/glia.10298

Blakemore, W. F. (1975). Remyelination by Schwann cells of axons demyelinated by intraspinal injection of 6-aminonicotinamide in the rat. *Journal of Neurocytology*, *4*(6), 745–757. https://doi.org/10.1007/BF01181634

Blakemore, W. F., & Crang, A. J. (1985). The use of cultured autologous Schwann cells to remyelinate areas of persistent demyelination in the central nervous system. *Journal of the Neurological Sciences*, *70*(2), 207–223. https://doi.org/10.1016/0022-510X(85)90088-7

Blanes, T. (1898). Sobre algunos puntos dudosos del la estructura del bulbo olfactorio. *Rev. Trim. Micrograf.*, *3*.

Blesch, A., Fischer, I., & Tuszynski, M. H. (2012). Gene therapy, neurotrophic factors and spinal cord regeneration. *Handbook of*

Clinical Neurology, *109*, 563–574. https://doi.org/10.1016/B978-0-444-52137-8.00035-8

Blesch, A., & Tuszynski, M. H. (2009, January 1). Spinal cord injury: plasticity, regeneration and the challenge of translational drug development. *Trends in Neurosciences*. Elsevier. https://doi.org/10.1016/j.tins.2008.09.008

Blight, A. R., & Young, W. (1989). Central axons in injured cat spinal cord recover electrophysiological function following remyelination by Schwann cells. *Journal of the Neurological Sciences*, *91*(1–2), 15–34. https://doi.org/10.1016/0022-510X(89)90073-7

Bomze, H. M., Bulsara, K. R., Iskandar, B. J., Caroni, P., & Pate Skene, J. H. (2001). Spinal axon regeneration evoked by replacing two growth cone proteins in adult neurons. *Nature Neuroscience*, *4*(1), 38–43. https://doi.org/10.1038/82881

Boruch, A. V, Conners, J. J., Pipitone, M., Deadwyler, G., Storer, P. D., & Devries, G. H. (2001). Neurotrophic and Migratory Properties of an Olfactory Ensheathing Cell Line. *Glia*, *229*(April 2000), 225–229.

Bovolenta, P., Fernaud-Espinosa, I., Mendez-Otero, R., & Nieto-Sampedro, M. (1997). Neurite outgrowth inhibitor of gliotic brain tissue. Mode of action and cellular localization, studied with specific monoclonal antibodies. *European Journal of Neuroscience*, *9*(5), 977–989. https://doi.org/10.1111/j.1460-9568.1997.tb01448.x

Bovolenta, P., Wandosell, F., & Nieto-Sampedro, M. (1992). CNS glial scar

tissue: a source of molecules which inhibit central neurite outgrowth. *Progress in Brain Research*, *94*(C), 367–379. https://doi.org/10.1016/S0079-6123(08)61765-3

Bovolenta, P., Wandosell, F., & Nieto-Sampedro, M. (1993). Characterization of a Neurite Outgrowth Inhibitor Expressed After CNS Injury. *European Journal of Neuroscience*, *5*(5), 454–465. https://doi.org/10.1111/j.1460-9568.1993.tb00512.x

Boyd, J. G., Doucette, R., & Kawaja, M. D. (2005). Defining the role of olfactory ensheathing cells in facilitating axon remyelination following damage to the spinal cord. *The FASEB Journal : Official Publication of the Federation of American Societies for Experimental Biology*, *19*(7), 694–703. https://doi.org/10.1096/fj.04-2833rev

Boyd, J. G., & Gordon, T. (2003). Neurotrophic factors and their receptors in axonal regeneration and functional recovery after peripheral nerve injury. *Molecular Neurobiology*, *27*(3), 277–324. https://doi.org/10.1385/MN:27:3:277

Boyd, J., & Gordon, T. (2003). Glial cell line-derived neurotrophic factor and brain-derived neurotrophic factor sustain the axonal regeneration of chronically axotomized motoneurons in vivo. *Experimental Neurology*, *183*(2), 610–619. https://doi.org/10.1016/S0014-4886(03)00183-3

Bozkurt, A., Deumens, R., Beckmann, C., Olde Damink, L., Schügner, F., Heschel, I., … Pallua, N. (2009). In vitro cell alignment obtained with a Schwann cell enriched microstructured nerve guide with longitudinal

guidance channels. *Biomaterials*, *30*(2), 169–179. https://doi.org/10.1016/j.biomaterials.2008.09.017

Bresnahan, J. C. (1978). An electron-microscopic analysis of axonal alterations following blunt contusion of the spinal cord of the rhesus monkey (Macaca mulatta). *Journal of the Neurological Sciences*, *37*(1–2), 59–82. https://doi.org/10.1016/0022-510X(78)90228-9

Brillinger, D. R. (1984). *The Collected Works of John W. Tukey*. Wadsworth.

Brockes, J. P., Fields, K. L., & Raff, M. C. (1979). Studies on cultured rat Schwann cells. I. Establishment of purified populations from cultures of peripheral nerve. *Brain Research*, *165*(1), 105–118. https://doi.org/10.1016/0006-8993(79)90048-9

Brockes, J. P., & Raff, M. C. (1979). Studies on cultured rat Schwann cells. II. Comparison with a rat Schwann cell line. *In Vitro*, *15*(10), 772–778.

Brown, M. B., & Forsythe, A. B. (1974). Robust Tests for the Equality of Variances. *Journal of the American Statistical Association*, (69), 364–367.

Brown, R. A., Wiseman, M., Chuo, C. B., Cheema, U., & Nazhat, S. N. (2005). Ultrarapid engineering of biomimetic materials and tissues: Fabrication of nano- and microstructures by plastic compression. *Advanced Functional Materials*, *15*(11), 1762–1770. https://doi.org/10.1002/adfm.200500042

Bunge, M. B. (2008). Novel combination strategies to repair the injured

mammalian spinal cord. *Journal of Spinal Cord Medicine*, *31*(3), 262–269. https://doi.org/10.1080/10790268.2008.11760720

Burke, K. E., Naughton, G., & Cassai, N. (1985). A histological, immunological, and electron microscopic study of bovine collagen implants in the human. *Annals of Plastic Surgery*, *14*(6), 515–522.

Busch, S. A., & Silver, J. (2007, February). The role of extracellular matrix in CNS regeneration. *Current Opinion in Neurobiology*. https://doi.org/10.1016/j.conb.2006.09.004

Cajal, S. R. y. (1991). Cajal's Degeneration and Regeneration of the Nervous System.

Cao, L., Su, Z., Zhou, Q., Lv, B., Liu, X., Jiao, L., … He, C. (2006). Glial cell line-derived neurotrophic factor promotes olfactory ensheathing cells migration. *Glia*, *54*(6), 536–544. https://doi.org/10.1002/glia.20403

Card, A. L., & Pfeiffer, S. E. (1990). Two Proliferative Stages of the Oligodendrocyte Lineage (A2B5+04- and 04+GalC-) under Different Mito&nic Control. *Neuron, 5*, 615–625.

Carri, N. G., Perris, R., Johansson, S., & Ebendal, T. (1988). Differential outgrowth of retinal neurites on purified extracellular matrix molecules. *Journal of Neuroscience Research*, *19*(4), 428–439. https://doi.org/10.1002/jnr.490190407

Chan, K. K., Wong, C. K. Y., Lui, V. C. H., Tam, P. K. H., & Sham, M. H. (2003). Analysis ofSOX10 mutations identified in Waardenburg-Hirschsprung

patients: Differential effects on target gene regulation. *Journal of Cellular Biochemistry*, *90*(3), 573–585. https://doi.org/10.1002/jcb.10656

Chau, C. H., Shum, D. K., Li, H., Pei, J., Lui, Y. Y., Wirthlin, L., … Xu, X. M. (2004). Chondroitinase ABC enhances axonal regrowth through Schwann cell-seeded guidance channels after spinal cord injury. *The FASEB Journal : Official Publication of the Federation of American Societies for Experimental Biology*, *18*(1), 194–196. https://doi.org/10.1096/fj.03-0196fje

Chehrehasa, F., Windus, L. C. E., Ekberg, J. A. K., Scott, S. E., Amaya, D., Mackay-Sim, A., & St John, J. A. (2010). Olfactory glia enhance neonatal axon regeneration. *Molecular and Cellular Neuroscience*, *45*(3), 277–288. https://doi.org/10.1016/j.mcn.2010.07.002

Cheng, E. T., Utley, D. S., Ho, P. R., Tarn, D. M., Coan, G. M., Verity, A. N., … Terris, D. J. (1998). Functional recovery of transected nerves treated with systemic BDNF and CNTF. *Microsurgery*, *18*(1), 35–41.

Cheng, H., Cao, Y., & Olson, L. (1996). Spinal Cord Repair in Adult Paraplegic Rats: Partial Restoration of Hind Limb Function. *Science*. American Association for the Advancement of Science. https://doi.org/10.2307/2890521

Cheng, L., Hu, W., Qiu, B., Zhao, J., Yu, Y., Guan, W., … Pei, G. (2014). Generation of neural progenitor cells by chemical cocktails and hypoxia. *Cell Research*, *24*(6), 665–679.

https://doi.org/10.1038/cr.2014.32

Chhabra, H. S., Lima, C., Sachdeva, S., Mittal, A., Nigam, V., Chaturvedi, D., … Khan, T. a H. (2009). Autologous mucosal transplant in chronic spinal cord injury: an Indian Pilot Study. *Spinal Cord*, *47*(12), 887–895. https://doi.org/10.1038/sc.2009.54

Cho, H., Shin, J., Shin, C. Y., Lee, S.-Y. Y., & Oh, U. (2002). Mechanosensitive ion channels in cultured sensory neurons of neonatal rats. *The Journal of Neuroscience*, *22*(4), 1238–1247. https://doi.org/22/4/1238 [pii]

Choi, D., Li, D., Law, S., Powell, M., & Raisman, G. (2008). A prospective observational study of the yield of olfactory ensheathing cells cultured from biopsies of septal nasal mucosa. *Neurosurgery*, *62*, 1140. https://doi.org/10.1227/01.NEU.0000313571.44795.49

Chuah l., M., Tennent, R., & Jacobs, I. (1995). Response of olfactory Schwann cells to intranasal zinc sulfate irrigation. *Journal of Neuroscience Research*, *42*(4), 470–478. https://doi.org/10.1002/jnr.490420405

Chuah, M. . I., & Teague, R. (1999). Basic fibroblast growth factor in the primary olfactory pathway: mitogenic effect on ensheathing cells. *Neuroscience*, *88*(4), 1043–1050. https://doi.org/10.1016/S0306-4522(98)00277-2

Chuah, M. I., & Au, C. (1991). Olfactory Schwann cells are derived from precursor cells in the olfactory epithelium. *Journal of Neuroscience Research*, *29*(2), 172–180. https://doi.org/10.1002/jnr.490290206

Chuah, M. I., & Au, C. (1993). Cultures of ensheathing cells from neonatal rat olfactory bulbs. *Brain Research*, *601*(1–2), 213–220. https://doi.org/10.1016/0006-8993(93)91713-3

Chuah, M. I., & Au, C. (1994). Olfactory cell cultures on ensheathing cell monolayers. *Chemical Senses*, *19*(1), 25–34.

Chuah, M. I., Choi-Lundberg, D., Weston, S., Vincent, A. J., Chung, R. S., Vickers, J. C., & West, A. K. (2004). Olfactory ensheathing cells promote collateral axonal branching in the injured adult rat spinal cord. *Experimental Neurology*, *185*(1), 15–25. https://doi.org/10.1016/J.EXPNEUROL.2003.09.008

Chuah, M. I., David, S., & Blaschuk, O. (1991). Differentiation and survival of rat olfactory epithelial neurons in dissociated cell culture. *Developmental Brain Research*, *60*(2), 123–132. https://doi.org/10.1016/0165-3806(91)90040-P

Chuah M.I. (2011). Anti-bacterial properties of Olfactory Ensheathing Cells. *Glia*, *59*(S1), S8–S37. https://doi.org/10.1002/glia.21208

Chung, R. S., Woodhouse, A., Fung, S., Dickson, T. C., West, A. K., Vickers, J. C., & Chuah, M. I. (2004). Olfactory ensheathing cells promote neurite sprouting of injured axons in vitro by direct cellular contact and secretion of soluble factors. *Cellular and Molecular Life Sciences*, *61*(10), 1238–1245. https://doi.org/10.1007/s00018-004-4026-y

Cohen, J. (1988). *Statistical Power Analysis for the Behavioral Sciences, Second Edition*.

Cohen, J. (1992a). *A Power Primer*. *Association July* (Vol. 112). Retrieved from http://www.personal.kent.edu/~marmey/quant2spring04/Cohen (1992) - PB.pdf

Cohen, J. (1992b). Statistical Power Analysis. *Current Directions in Psychological Science*, *1*(3), 98–101. https://doi.org/10.1111/1467-8721.ep10768783

Collazos-Castro, J. E., Muñetón-Gómez, V. C., & Nieto-Sampedro, M. (2005). Olfactory glia transplantation into cervical spinal cord contusion injuries. *Journal of Neurosurgery: Spine*, *3*(4), 308–317. https://doi.org/10.3171/spi.2005.3.4.0308

Couly, G. F., & Le Douarin, N. M. (1985). Mapping of the early neural primordium in quail-chick chimeras. I. Developmental relationships between placodes, facial ectoderm, and prosencephalon. *Developmental Biology*, *110*(2), 422–439. https://doi.org/10.1016/0012-1606(85)90101-0

Crandall, J. E., Dibble, C., Butler, D., Pays, L., Ahmad, N., Kostek, C., … Schwarting, G. A. (2000). Patterning of olfactory sensory connections is mediated by extracellular matrix proteins in the nerve layer of the olfactory bulb. *Journal of Neurobiology*, *45*(4), 195–206. https://doi.org/10.1002/1097-4695(200012)45:4<195::AID-NEU1>3.0.CO;2-Y

Cregg, J. M., DePaul, M. A., Filous, A. R., Lang, B. T., Tran, A., & Silver, J.

(2014, March 1). Functional regeneration beyond the glial scar. *Experimental Neurology*. Academic Press. https://doi.org/10.1016/j.expneurol.2013.12.024

Cui, X. P., Xing, Y., Chen, J. M., Dong, S. W., Ying, D. J., & Yew, D. T. (2011). Wnt/beta-catenin is involved in the proliferation of hippocampal neural stem cells induced by hypoxia. *Irish Journal of Medical Science*, *180*(2), 387–393. https://doi.org/10.1007/s11845-010-0566-3

Cuschieri, A., & Bannister, L. H. (1975). The development of the olfactory mucosa in the mouse: light microscopy. *Journal of Anatomy*, *119*(Pt 2), 277–286.

Daniel Pearse, D., Eduardo Marcillo, A., Oudega, M., Paul Lynch, M., McGhee Wood, P., & Bartlett Bunge, M. (2004). Transplantation of Schwann Cells and Olfactory Ensheathing Glia after Spinal Cord Injury: Does Pretreatment with Methylprednisolone and Interleukin-10 Enhance Recovery? *Journal of Neurotrauma*, *21*(9), 1223–1239. https://doi.org/10.1089/neu.2004.21.1223

David, S., & Lacroix, S. (2003). Molecular approaches to spinal cord repair. *Annual Review of Neuroscience*, *26*(1), 411–440. https://doi.org/10.1146/annurev.neuro.26.043002.094946

Davies, S. J., Goucher, D. R., Doller, C., & Silver, J. (1999). Robust regeneration of adult sensory axons in degenerating white matter of the adult rat spinal cord. *The Journal of Neuroscience : The Official Journal of the Society for Neuroscience*, *19*(14), 5810–5822.

De Lorenzo, A. J. (1957). Electron microscopic observations of the olfactory mucosa and olfactory nerve. *Biophys. Biochem. Cytol.*, *3*(6), 839–850.

Dechant, G., & Barde, Y. A. (2002, November 1). The neurotrophin receptor p75NTR: Novel functions and implications for diseases of the nervous system. *Nature Neuroscience*. https://doi.org/10.1038/nn1102-1131

Deister, C., & Schmidt, C. E. (2006). Optimizing neurotrophic factor combinations for neurite outgrowth. *Journal of Neural Engineering*, *3*(2), 172–179. https://doi.org/10.1088/1741-2560/3/2/011

DeLucia, T. A., Conners, J. J., Brown, T. J., Cronin, C. M., Khan, T., & Jones, K. J. Use of a cell line to investigate olfactory ensheathing cell-enhanced axonal regeneration, 271 Anatomical Record - Part B New Anatomist § (2003). https://doi.org/10.1002/ar.b.10014

Deng, C., Gorrie, C., Hayward, I., Elston, B., Venn, M., Mackay-Sim, A., & Waite, P. (2006). Survival and migration of human and rat olfactory ensheathing cells in intact and injured spinal cord. *Journal of Neuroscience Research*, *83*(7), 1201–1212. https://doi.org/10.1002/jnr.20817

Deng, L.-X., Deng, P., Ruan, Y., Xu, Z. C., Liu, N.-K., Wen, X., … Xu, X.-M. (2013). A Novel Growth-Promoting Pathway Formed by GDNF-Overexpressing Schwann Cells Promotes Propriospinal Axonal Regeneration, Synapse Formation, and Partial Recovery of Function after Spinal Cord Injury. *Journal of Neuroscience*, *33*(13), 5655–5667. https://doi.org/10.1523/JNEUROSCI.2973-12.2013

Deng, L. X., Hu, J., Liu, N., Wang, X., Smith, G. M., Wen, X., & Xu, X. M. (2011). GDNF modifies reactive astrogliosis allowing robust axonal regeneration through Schwann cell-seeded guidance channels after spinal cord injury. *Experimental Neurology*, *229*(2), 238–250. https://doi.org/10.1016/j.expneurol.2011.02.001

Denis-Donini, S., & Estenoz, M. (1988). Interneurons versus efferent neurons: heterogeneity in their neurite outgrowth response to glia from several brain regions. *Developmental Biology*, *130*, 237–249. https://doi.org/10.1016/0012-1606(88)90430-7

Deshpande, D. M., Kim, Y.-S., Martinez, T., Carmen, J., Dike, S., Shats, I., … Kerr, D. A. (2006). Recovery from paralysis in adult rats using embryonic stem cells. *Annals of Neurology*, *60*(1), 32–44. https://doi.org/10.1002/ana.20901

Deumens, R., Koopmans, G. C. C., Den Bakker, C. G. J., Maquet, V., Blacher, S., Honig, W. M. M., … Joosten, E. A. J. (2004). Alignment of glial cells stimulates directional neurite growth of CNS neurons in vitro. *Neuroscience*, *125*(3), 591–604. https://doi.org/10.1016/j.neuroscience.2004.02.010

Deumens, R., Koopmans, G. C., Lemmens, M., Möllers, S., Honig, W. M., Steinbusch, H. W., … Joosten, E. A. (2006). Neurite outgrowth promoting effects of enriched and mixed OEC/ONF cultures. *Neuroscience Letters*, *397*(1–2), 20–24. https://doi.org/10.1016/j.neulet.2005.11.063

Devon, R., & Doucette, R. (1992). Olfactory ensheathing cells myelinate dorsal root ganglion neurites. *Brain Research*, *589*(1), 175–179. https://doi.org/10.1016/0006-8993(92)91182-E

Devon, R., & Doucette, R. (1995). Olfactory ensheathing cells do not requirel-ascorbic acid in vitro to assemble a basal lamina or to myelinate dorsal root ganglion neurites. *Brain Research*, *688*(1–2), 223–229. https://doi.org/10.1016/0006-8993(95)00562-5

Ditunno, J. F., Young, W., Donovan, W. H., & Creasey, G. (1994). The international standards booklet for neurological and functional classification of spinal cord injury. American Spinal Injury Association. *Paraplegia*, *32*(2), 70–80. https://doi.org/10.1038/sc.1994.13

Docherty, R. J., & Brown, D. A. (1991). *Cellular Neurobiology: A Practical Approach*.

Donato, R. (1986). S-100 proteins. *Cell Calcium*, *7*, 123–145. https://doi.org/10.1016/0143-4160(86)90017-5

Dou, C. L., & Levine, J. M. (1994). Inhibition of neurite growth by the NG2 chondroitin sulfate proteoglycan. *The Journal of Neuroscience : The Official Journal of the Society for Neuroscience*, *14*(12), 7616–7628.

Doucette, J. R. (1984). The glial cells in the nerve fiber layer of the rat olfactory bulb. *Anat Rec*, *210*, 385–391. https://doi.org/10.1002/ar.1092100214

Doucette, J. R., Kiernan, J. A., & Flumerfelt, B. A. (1983). The re-innervation

of olfactory glomeruli following transection of primary olfactory axons in the central or peripheral nervous system. *Journal of Anatomy*, *137 (Pt 1)*(Pt 1), 1–19.

Doucette, R. (1989). Development of the nerve fiber layer in the olfactory bulb of mouse embryos. *The Journal of Comparative Neurology*, *285*(4), 514–527. https://doi.org/10.1002/cne.902850407

Doucette, R. (1990). Glial influences on axonal growth in the primary olfactory system. *Glia*, *3*(6), 433–449. https://doi.org/10.1002/glia.440030602

Doucette, R. (1991). PNS-CNS transitional zone of the first cranial nerve. *The Journal of Comparative Neurology*, *312*(3), 451–466. https://doi.org/10.1002/cne.903120311

Doucette, R. (1993). Glial progenitor cells of the nerve fiber layer of the olfactory bulb: effect of astrocyte growth media. *Journal of Neuroscience Research*, *35*(3), 274–287. https://doi.org/10.1002/jnr.490350307

Doucette, R. (1995). Olfactory ensheathing cells: Potential for glial cell transplantation into areas of CNS injury. *Histology and Histopathology*.

East, E., de Oliveira, D. B., Golding, J. P., & Phillips, J. B. (2010). Alignment of Astrocytes Increases Neuronal Growth in Three-Dimensional Collagen Gels and Is Maintained Following Plastic Compression to Form a Spinal Cord Repair Conduit. *Tissue Engineering Part A*, *16*(10), 3173–3184. https://doi.org/10.1089/ten.tea.2010.0017

Ebel, C., Brandes, G., Radtke, C., Rohn, K., & Wewetzer, K. (2013). Clonal in vitro analysis of neurotrophin receptor p75-immunofluorescent cells reveals phenotypic plasticity of primary rat olfactory ensheathing cells. *Neurochemical Research*, *38*(5), 1078–1087. https://doi.org/10.1007/s11064-013-1023-2

Ekberg, J. A. K., Amaya, D., Mackay-Sim, A., & St John, J. a. (2012). The migration of olfactory ensheathing cells during development and regeneration. *Neurosignals*, *20*, 147–158. https://doi.org/10.1159/000330895

Ekberg, J. A. K., & St John, J. A. (2014). Crucial roles for olfactory ensheathing cells and olfactory mucosal cells in the repair of damaged neural tracts. *Anatomical Record (Hoboken, N.J. : 2007)*, *297*(1), 121–128. https://doi.org/10.1002/ar.22803

Ellis, P. D. (2010). *The essential guide to effect sizes: Statistical power, meta-analysis, and the interpretation of research results*. *Journal of Chemical Information and Modeling* (Vol. 53). Cambridge University Press. https://doi.org/10.1017/CBO9781107415324.004

Erceg, S., Ronaghi, M., Oria, M., García Roselló, M., Aragó, M. A. P., Lopez, M. G., … Stojkovic, M. (2010). Transplanted Oligodendrocytes and Motoneuron Progenitors Generated from Human Embryonic Stem Cells Promote Locomotor Recovery After Spinal Cord Transection. *STEM CELLS*, *28*(9), 1541–1549. https://doi.org/10.1002/stem.489

Erecińska, M., & Silver, I. A. (2001). Tissue oxygen tension and brain

sensitivity to hypoxia. In *Respiration Physiology* (Vol. 128, pp. 263–276). https://doi.org/10.1016/S0034-5687(01)00306-1

Fallis, A. . (2013). *Explaining Psychological Statistics*. *Journal of Chemical Information and Modeling* (Vol. 53). John Wiley. https://doi.org/10.1017/CBO9781107415324.004

Fawcett, J. W., & Asher, R. a. (1999). The glial scar and central nervous system repair. *Brain Research Bulletin*, *49*(6), 377–391. https://doi.org/10.1016/S0361-9230(99)00072-6

Feigin, I., & Ogata, J. (1971). Schwann cells and peripheral myelin within human central nervous tissues: the mesenchymal character of Schwann cells. *Journal of Neuropathology and Experimental Neurology*, *30*(4), 603–612.

Felling, R. J. (2006). Neural Stem/Progenitor Cells Participate in the Regenerative Response to Perinatal Hypoxia/Ischemia. *Journal of Neuroscience*, *26*(16), 4359–4369. https://doi.org/10.1523/JNEUROSCI.1898-05.2006

Féron, F., MacKay-Sim, A., Andrieu, J. L., Matthaei, K. I., Holley, A., & Sicard, G. (1999). Stress induces neurogenesis in non-neuronal cell cultures of adult olfactory epithelium. *Neuroscience*, *88*(2), 571–583. https://doi.org/10.1016/S0306-4522(98)00233-4

Féron, F., Perry, C., Cochrane, J., Licina, P., Nowitzke, A., Urquhart, S., … Mackay-Sim, A. (2005). Autologous olfactory ensheathing cell transplantation in human spinal cord injury. *Brain*, *128*(12), 2951–

2960. https://doi.org/10.1093/brain/awh657

Fidler, P. S., Schuette, K., Asher, R. A., Dobbertin, A., Thornton, S. R., Calle-Patino, Y., … Fawcett, J. W. (1999). Comparing astrocytic cell lines that are inhibitory or permissive for axon growth: the major axon-inhibitory proteoglycan is NG2. *The Journal of Neuroscience : The Official Journal of the Society for Neuroscience*, *19*(20), 8778–8788.

Field, A. P. (2009). *Discovering statistics using SPSS (and sex and drugs and rock & roll)*. *Discovering Statistics Using SPSS (and sex and drugs and rock "n" roll)*. SAGE Publications. https://doi.org/10.1234/12345678

Field, P., Li, Y., & Raisman, G. (2003). Ensheathment of the olfactory nerves in the adult rat. *Journal of Neurocytology*, *32*(3), 317–324. https://doi.org/10.1023/B:NEUR.0000010089.37032.48

Filbin, M. T. (2003). Myelin-associated inhibitors of axonal regeneration in the adult mammalian CNS. *Nature Reviews Neuroscience*, *4*(9), 703–713. https://doi.org/10.1038/nrn1195

Flora, G., Joseph, G., Patel, S., Singh, A., Bleicher, D., Barakat, D. J., … Pearse, D. D. (2013). Combining neurotrophin-transduced Schwann cells and rolipram to promote functional recovery from subacute spinal cord injury. *Cell Transplantation*, *22*(12), 2203–2217. https://doi.org/10.3727/096368912X658872

Fouad, K. (2005). Combining Schwann Cell Bridges and Olfactory-Ensheathing Glia Grafts with Chondroitinase Promotes Locomotor Recovery after Complete Transection of the Spinal Cord. *Journal of*

Neuroscience, *25*(5), 1169–1178. https://doi.org/10.1523/JNEUROSCI.3562-04.2005

Fournier, A. E., Gould, G. C., Liu, B. P., & Strittmatter, S. M. (2002). Truncated soluble Nogo receptor binds Nogo-66 and blocks inhibition of axon growth by myelin. *The Journal of Neuroscience*, *22*(20), 8876–8883. https://doi.org/10.1523/jneurosci.1103-06.2006

Fracek, S. P., Guo, L., & Schafer, R. (1994). Morphological characteristics of cultured olfactory bulb cells. *Experimental Brain Research. Experimentelle Hirnforschung. Expérimentation Cérébrale*, *100*(3), 421–436.

Franceschini, I. A., & Barnett, S. C. (1996). Low-affinity NGF-receptor and E-N-CAM expression define two types of olfactory nerve ensheathing cells that share a common lineage. *Developmental Biology*, *173*, 327–343. https://doi.org/10.1006/dbio.1996.0027

Franklin, R. J. M. (2003). Remyelination by transplanted olfactory ensheathing cells. *Anatomical Record. Part B, New Anatomist*, *271*(1), 71–76. https://doi.org/10.1002/ar.b.10013

Franklin, R. J. M., Gilson, J. M., & Blakemore, W. F. (1997). Local recruitment of remyelinating cells in the repair of demyelination in the central nervous system. *Journal of Neuroscience Research*, *50*(2), 337–344. https://doi.org/10.1002/(SICI)1097-4547(19971015)50:2<337::AID-JNR21>3.0.CO;2-3

Franklin, R. J. M., Gilson, J. M., Franceschini, I. A., & Barnett, S. C. (1996).

Schwann cell-like myelination following transplantation of an olfactory bulb-ensheathing cell line into areas of demyelination in the adult CNS. *Glia*, *17*(3), 217–224. https://doi.org/10.1002/(SICI)1098-1136(199607)17:3<217::AID-GLIA4>3.0.CO;2-Y

Franssen, E. H. P., De Bree, F. M., Essing, A. H. W., Ramón-Cueto, A., & Verhaagen, J. (2008). Comparative gene expression profiling of olfactory ensheathing glia and Schwann cells indicates distinct tissue repair characteristics of olfactory ensheathing glia. *Glia*, *56*, 1285–1298. https://doi.org/10.1002/glia.20697

Franssen, E. H. P., de Bree, F. M., & Verhaagen, J. (2007, November 1). Olfactory ensheathing glia: Their contribution to primary olfactory nervous system regeneration and their regenerative potential following transplantation into the injured spinal cord. *Brain Research Reviews*. Elsevier. https://doi.org/10.1016/j.brainresrev.2007.07.013

Franssen, E. H. P., Roet, K. C. D., de Bree, F. M., & Verhaagen, J. (2009). Olfactory ensheathing glia and Schwann cells exhibit a distinct interaction behavior with meningeal cells. *Journal of Neuroscience Research*, *87*(7), 1556–1564. https://doi.org/10.1002/jnr.21979

Franzen, R., Martin, D., Daloze, A., Moonen, G., & Schoenen, J. (1999). Grafts of meningeal fibroblasts in adult rat spinal cord lesion promote axonal regrowth. *NeuroReport*, *10*(7), 1551–1556. https://doi.org/10.1097/00001756-199905140-00029

French, A., Macedo, M., Poulsen, J., Waterson, T., Yu, A., Tabachnick, B. G.,

& Fidell, L. S. (2011). Multivariate Analysis of Variance (MANOVA). In *International Encyclopedia of Statistical Science* (pp. 902–904). Berlin, Heidelberg: Springer Berlin Heidelberg. https://doi.org/10.1007/978-3-642-04898-2_394

Froud, S. J. (1999). The development, benefits and disadvantages of serum-free media. *Developments in Biological Standardization*, *99*, 157–166. Retrieved from http://www.ncbi.nlm.nih.gov/pubmed/10404887

Fudge, N. J., & Mearow, K. M. (2013). Extracellular matrix-associated gene expression in adult sensory neuron populations cultured on a laminin substrate. *BMC Neuroscience*, *14*(1), 15. https://doi.org/10.1186/1471-2202-14-15

García-Alías, G., López-Vales, R., Forés, J., Navarro, X., & Verdú, E. (2004). Acute Transplantation of Olfactory Ensheathing Cells or Schwann Cells Promotes Recovery after Spinal Cord Injury in the Rat. *Journal of Neuroscience Research*, *75*(5), 632–641. https://doi.org/10.1002/jnr.20029

García-Escudero, V., Gargini, R., Gallego-Hernández, M. T., García-Gómez, A., Martín-Bermejo, M. J., Simón, D., … Lim, F. (2011). A neuroregenerative human ensheathing glia cell line with conditional rapid growth. *Cell Transplantation*, *20*(2), 153–166. https://doi.org/10.3727/096368910X522108

Gasser, H. S. (1956). Olfactory nerve fibres. *J. Gen. Physiol.*, *39*.

Genetos, D. C., Cheung, W. K., Decaris, M. L., & Leach, J. K. (2010). Oxygen

tension modulates neurite outgrowth in PC12 cells through a mechanism involving HIF and VEGF. *Journal of Molecular Neuroscience : MN*, *40*(3), 360–366. https://doi.org/10.1007/s12031-009-9326-0

Geoffroy, C. G., & Zheng, B. (2014, August). Myelin-associated inhibitors in axonal growth after CNS injury. *Current Opinion in Neurobiology*. NIH Public Access. https://doi.org/10.1016/j.conb.2014.02.012

Georgiou, M., Bunting, S. C. J., Davies, H. a., Loughlin, A. J., Golding, J. P., & Phillips, J. B. (2013). Engineered neural tissue for peripheral nerve repair. *Biomaterials*, *34*(30), 7335–7343. https://doi.org/10.1016/j.biomaterials.2013.06.025

Georgiou, M., dos Reis, J. N., Wood, R., Esteban, P. P., Roberton, V., Mason, C., … Wall, I. (2018). Bioprocessing strategies to enhance the challenging isolation of neuro-regenerative cells from olfactory mucosa. *Scientific Reports*, *8*(1), 14440. https://doi.org/10.1038/s41598-018-32748-w

Georgiou, M., Golding, J. P., Loughlin, A. J., Kingham, P. J., & Phillips, J. B. (2015). Engineered neural tissue with aligned, differentiated adipose-derived stem cells promotes peripheral nerve regeneration across a critical sized defect in rat sciatic nerve. *Biomaterials*, *37*, 242–251. https://doi.org/10.1016/j.biomaterials.2014.10.009

Gerberich, B. G., & Bhatia, S. K. (2013, January). Tissue scaffold surface patterning for clinical applications. *Biotechnology Journal*.

https://doi.org/10.1002/biot.201200131

Gerzanich, V., Woo, S. K., Vennekens, R., Tsymbalyuk, O., Ivanova, S., Ivanov, A., … Simard, J. M. (2009). De novo expression of Trpm4 initiates secondary hemorrhage in spinal cord injury. *Nature Medicine*, *15*(2), 185–191. https://doi.org/10.1038/nm.1899

Gilmore, S. A., & Duncan, D. (1968). On the presence of peripheral???like nervous and connective tissue within irradiated spinal cord. *The Anatomical Record*, *160*(4), 675–689. https://doi.org/10.1002/ar.1091600403

Goldberg, J. L., Klassen, M. P., Hua, Y., & Barres, B. A. (2002). Amacrine-signaled loss of intrinsic axon growth ability by retinal ganglion cells. *Science*, *296*(5574), 1860–1864. https://doi.org/10.1126/science.1068428

Golden, K. L., Pearse, D. D., Blits, B., Garg, M. S., Oudega, M., Wood, P. M., & Bunge, M. B. (2007). Transduced Schwann cells promote axon growth and myelination after spinal cord injury. *Experimental Neurology*, *207*(2), 203–217. https://doi.org/10.1016/j.expneurol.2007.06.023

Golgi, C. (1875). Sulla fina anatomia del bulbi olfactorii. *Ti Rivista Sperimentale Di Freniatria 1.*, 403–425.

Gomez, R. M. (2009). *The use of olfactory ensheathing glia cells and synthetic proteins for functional recovery in a model of spinal cord section in vivo*.

Gómez, R. M., Sánchez, M. Y., Portela-Lomba, M., Ghotme, K., Barreto, G. E., Sierra, J., & Moreno-Flores, M. T. (2018). Cell therapy for spinal cord injury with olfactory ensheathing glia cells (OECs). *Glia*, *66*(7), 1267–1301. https://doi.org/10.1002/glia.23282

Gong, Q., Liu, W. L., Srodon, M., Foster, T. D., & Shipley, M. T. (1996). Olfactory epithelial organotypic slice cultures: A useful tool for investigating olfactory neural development. *International Journal of Developmental Neuroscience*, *14*(7–8), 841–852. https://doi.org/10.1016/S0736-5748(96)00056-1

Goodman, M. N., Silver, J., & Jacobberger, J. W. (1993). Establishment and neurite outgrowth properties of neonatal and adult rat olfactory bulb glial cell lines. *Brain Research*, *619*(1–2), 199–213. https://doi.org/10.1016/0006-8993(93)91613-W

Goodman, M. N., Silver, J., Jacobberger, J. W., Goodman, M. N., Silver, J., & Jacobberger, J. W. (1993). Establishment and neurite outgrowth properties of neonatal and adult rat olfactory bulb glial cell lines. *Brain Research*, *619*(1–2), 199–213. https://doi.org/10.1016/0006-8993(93)91613-W

Granger, N., Blamires, H., Franklin, R. J. M., & Jeffery, N. D. (2012). Autologous olfactory mucosal cell transplants in clinical spinal cord injury: a randomized double-blinded trial in a canine translational model. *Brain*, *135*(11), 3227–3237. https://doi.org/10.1093/brain/aws268

Graziadei, P. P. C., & Graziadei, G. A. M. (1979). Neurogenesis and neuron regeneration in the olfactory system of mammals. I. Morphological aspects of differentiation and structural organization of the olfactory sensory neurons. *Journal of Neurocytology*, *8*(1), 1–18. https://doi.org/10.1007/BF01206454

Greene, L. A., & Tischler, A. S. (1976). Establishment of a noradrenergic clonal line of rat adrenal pheochromocytoma cells which respond to nerve growth factor. *Proceedings of the National Academy of Sciences of the United States of America*, *73*(7), 2424–2428. Retrieved from http://www.ncbi.nlm.nih.gov/pubmed/1065897

Griffiths, I. R., Burns, N., & Crawford, A. R. (1978). Early vascular changes in the spinal grey matter following impact injury. *Acta Neuropathologica*, *41*(1), 33–39. https://doi.org/10.1007/BF00689554

Grill, R. J., Blesch, A., & Tuszynski, M. H. (1997). Robust growth of chronically injured spinal cord axons induced by grafts of genetically modified NGF-secreting cells. *Experimental Neurology*, *148*(2), 444–452. https://doi.org/10.1006/exnr.1997.6704

Grill, R., Murai, K., Blesch, A., Gage, F. H., & Tuszynski, M. H. (1997). Cellular delivery of neurotrophin-3 promotes corticospinal axonal growth and partial functional recovery after spinal cord injury. *The Journal of Neuroscience : The Official Journal of the Society for Neuroscience*, *17*(14), 5560–5572. https://doi.org/10.1523/JNEUROSCI.17-14-05560.1997

Gstraunthaler, G. (2003). Alternatives to the use of fetal bovine serum: serum-free cell culture. *ALTEX : Alternativen Zu Tierexperimenten*, *20*(4), 275–281.

Gudiño-Cabrera, G., & Nieto-Sampedro, M. (2000). Schwann-like macroglia in adult rat brain. *GLIA*, *30*(1), 49–63. https://doi.org/10.1002/(SICI)1098-1136(200003)30:1<49::AID-GLIA6>3.0.CO;2-M

Guérout, N., Derambure, C., Drouot, L., Bon-Mardion, N., Duclos, C., Boyer, O., & Marie, J.-P. P. (2010). Comparative gene expression profiling of olfactory ensheathing cells from olfactory bulb and olfactory mucosa. *Glia*, *58*(May), 1570–1580. https://doi.org/10.1002/glia.21030

Hannila, S. S., & Filbin, M. T. (2008). The role of cyclic AMP signaling in promoting axonal regeneration after spinal cord injury. *Experimental Neurology*, *209*(2), 321–332. Retrieved from https://www.sciencedirect.com/science/article/pii/S0014488607002646?via%3Dihub

Hapner, S. J., Boeshore, K. L., Large, T. H., & Lefcort, F. (1998). Neural differentiation promoted by truncated trkC receptors in collaboration with p75(NTR). *Developmental Biology*, *201*, 90–100. https://doi.org/10.1006/dbio.1998.8970

Harding, J., Graziadei, P. P. C., Monti Graziadei, G. A., Margolis, F. L., Graziadei, G. A. M., & Margolis, F. L. (1977). Denervation in the primary olfactory pathway of mice. IV. Biochemical and morphological

evidence for neuronal replacement following nerve section. *Brain Research*, *132*(1), 11–28. https://doi.org/10.1016/0006-8993(77)90703-X

Hardy, R., & Reynolds, R. (1991). Proliferation and differentiation potential of rat forebrain oligodendroglial progenitors both in vitro and in vivo. *Development*, (111), 1061–1080.

Harris, J. A., West, A. K., & Chuah, M. I. (2009). Olfactory ensheathing cells: Nitric oxide production and innate immunity. *GLIA*, *57*, 1848–1857. https://doi.org/10.1002/glia.20899

Hartnick, C. J., Staecker, H., Malgrange, B., Lefebvre, P. P., Liu, W., Moonen, G., & Van de Water, T. R. (1996). Neurotrophic effects of BDNF and CNTF, alone and in combination, on postnatal day 5 rat acoustic ganglion neurons. *Journal of Neurobiology*, *30*(2), 246–254. https://doi.org/10.1002/(SICI)1097-4695(199606)30:2<246::AID-NEU6>3.0.CO;2-5

Hayat, S., Thomas, A., Afshar, F., Sonigra, R., & Wigley, C. B. (2003). Manipulation of Olfactory Ensheathing Cell Signaling Mechanisms: Effects on Their Support for Neurite Regrowth from Adult CNS Neurons in Coculture. *GLIA*, *44*(3), 232–241. https://doi.org/10.1002/glia.10299

He, B. R., Xie, S. T., Wu, M. M., Hao, D. J., & Yang, H. (2014). Phagocytic removal of neuronal debris by olfactory ensheathing cells enhances neuronal survival and neurite outgrowth via p38MAPK activity.

Molecular Neurobiology, *49*(3), 1501–1512. https://doi.org/10.1007/s12035-013-8588-2

He, X. L., Bazan, J. F., McDermott, G., Park, J. B., Wang, K., Tessier-Lavigne, M., … Garcia, K. C. (2003). Structure of the Nogo receptor ectodomain: A recognition module implicated in myelin inhibition. *Neuron*, *38*(2), 177–185. https://doi.org/10.1016/S0896-6273(03)00232-0

He, Z., & Koprivica, V. (2004). The nogo signaling pathway for regeneration block. *Annual Review of Neuroscience*, *27*(1), 341–368. https://doi.org/10.1146/annurev.neuro.27.070203.144340

Heathman, T. R., Nienow, A. W., McCall, M. J., Coopman, K., Kara, B., & Hewitt, C. J. (2015). The translation of cell-based therapies: clinical landscape and manufacturing challenges. *Regenerative Medicine*, *10*(1), 49–64. https://doi.org/10.2217/rme.14.73

Hendriks, W. T. J., Ruitenberg, M. J., Blits, B., Boer, G. J., & Verhaagen, J. (2004). Viral vector-mediated gene transfer of neurotrophins to promote regeneration of the injured spinal cord. In *Progress in Brain Research* (Vol. 146, pp. 451–476). Elsevier. https://doi.org/10.1016/S0079-6123(03)46029-9

Heumann, R., Lindholm, D., Bandtlow, C., Meyer, M., Radeke, M. J., Misko, T. P., … Thoenen, H. (1987). Differential regulation of mRNA encoding nerve growth factor and its receptor in rat sciatic nerve during development, degeneration, and regeneration: role of macrophages. *Proceedings of the National Academy of Sciences of the United States*

of America, *84*(23), 8735–8739. https://doi.org/10.1073/pnas.84.23.8735

Higginson, J. R., & Barnett, S. C. (2011). The culture of olfactory ensheathing cells (OECs)--a distinct glial cell type. *Experimental Neurology*, *229*(1), 2–9. https://doi.org/10.1016/j.expneurol.2010.08.020

Higginson, J. R., Thompson, S. M., Santos-Silva, A., Guimond, S. E., Turnbull, J. E., & Barnett, S. C. (2012). Differential Sulfation Remodelling of Heparan Sulfate by Extracellular 6-O-Sulfatases Regulates Fibroblast Growth Factor-Induced Boundary Formation by Glial Cells: Implications for Glial Cell Transplantation. *Journal of Neuroscience*, *32*(45), 15902–15912. https://doi.org/10.1523/JNEUROSCI.6340-11.2012

Hill, C. E., Guller, Y., Raffa, S. J., Hurtado, A., & Bunge, M. B. (2010). A Calpain Inhibitor Enhances the Survival of Schwann Cells In Vitro and after Transplantation into the Injured Spinal Cord. *Journal of Neurotrauma*, *27*(9), 1685–1695. https://doi.org/10.1089/neu.2010.1272

Hill, C. E., Hurtado, A., Blits, B., Bahr, B. A., Wood, P. M., Bartlett Bunge, M., & Oudega, M. (2007). Early necrosis and apoptosis of Schwann cells transplanted into the injured rat spinal cord. *European Journal of Neuroscience*, *26*(6), 1433–1445. https://doi.org/10.1111/j.1460-9568.2007.05771.x

Hirano, A., Zimmerman, H. M., & Levine, S. (1969). Electron microscopic observations of peripheral myelin in a central nervous system lesion. *Acta Neuropathologica*, *12*(4), 348–365. https://doi.org/10.1007/BF00809131

Hoenig, J., & Heisey, D. (2001). The abuse of power: The pervasive falacy of power calculations for data analysis. *Am Stat*, *55*(1), 19–24. https://doi.org/10.1198/000313001300339897

Hoenig, J. M., & Heisey, D. M. (2011). Eta squared and partial eta squared as measures of effect size in educational research. *Educational Research Review*, *6*(2), 135–147. https://doi.org/10.1016/J.EDUREV.2010.12.001

Hollis, E. R., & Tuszynski, M. H. (2011, October 9). Neurotrophins: Potential Therapeutic Tools for the Treatment of Spinal Cord Injury. *Neurotherapeutics*. https://doi.org/10.1007/s13311-011-0074-9

Hompson, D. E. M. T., & Uettner, H. E. M. B. (2006). Neurite Outgrowth Is Directed by Schwann Cell Alignment in the Absence of Other Guidance Cues. *Annals of Biomedical Engineering*, *34*(1), 161–168. https://doi.org/10.1007/s10439-005-9013-4

Honoré, A., Le Corre, S., Derambure, C., Normand, R., Duclos, C., Boyer, O., … Guérout, N. (2012). Isolation, characterization, and genetic profiling of subpopulations of olfactory ensheathing cells from the olfactory bulb. *Glia*, *60*(3), 404–413. https://doi.org/10.1002/glia.22274

Horner, P. J., & Gage, F. H. (2000). Regenerating the damaged central nervous system. *Nature*, *407*(6807), 963–970. https://doi.org/10.1038/35039559

Huang, Z., Wang, Y., Cao, L., Su, Z., Zhu, Y., Chen, Y., … He, C. (2008). Migratory properties of cultured olfactory ensheathing cells by single-cell migration assay. *Cell Research*, *18*(4), 479–490. https://doi.org/10.1038/cr.2008.38

Hubrecht, R., Kirkwood, J. K., & Universities Federation for Animal Welfare. (2010). The UFAW handbook on the care and management of laboratory and other research animals. *UFAW*. Wiley-Blackwell. https://doi.org/10.1002/9781444318777

Ibrahim, A. G., Kirkwood, P. A., Raisman, G., & Li, Y. (2009). Restoration of hand function in a rat model of repair of brachial plexus injury. *Brain*, *132*(5), 1268–1276. https://doi.org/10.1093/brain/awp030

Imaizumi, T., Lankford, K. L., Burton, W. V., Fodor, W. L., & Kocsis, J. D. (2000). Xenotransplantation of transgenic pig olfactory ensheathing cells promotes axonal regeneration in rat spinal cord. *Nature Biotechnology*, *18*(9), 949–953. https://doi.org/10.1038/79432

Imaizumi, T., Lankford, K. L., & Kocsis, J. D. (2000). Transplantation of olfactory ensheathing cells or Schwann cells restores rapid and secure conduction across the transected spinal cord. *Brain Research*, *854*(1–2), 70–78. https://doi.org/10.1016/S0006-8993(99)02285-4

Imaizumi, T., Lankford, K. L., Waxman, S. G., Greer, C. A., & Kocsis, J. D.

(1998). Transplanted olfactory ensheathing cells remyelinate and enhance axonal conduction in the demyelinated dorsal columns of the rat spinal cord. *The Journal of Neuroscience : The Official Journal of the Society for Neuroscience*, *18*(16), 6176–6185. https://doi.org/10.1523/JNEUROSCI.18-16-06176.1998

Ito, D., Fujita, N., Ibanez, C., Sasaki, N., Franklin, R. J. M., & Jeffery, N. D. (2007). Serum-Free Medium Provides a Clinically Relevant Method to Increase Olfactory Ensheathing Cell Numbers in Olfactory Mucosa Cell Culture. *Cell Transplantation*, *16*(10), 1021–1027. https://doi.org/10.3727/000000007783472345

Jahed, A. L. I., Rowland, J. W., Donald, T. M. C., Boyd, J. G., Doucette, R., Kawaja, M. D., … Kawaja, M. D. (2007). Olfactory ensheathing cells express smooth muscle alpha-actin in vitro and in vivo. *The Journal of Comparative Neurology*, *503*(2), 209–223. https://doi.org/10.1002/cne.21385

James, G., Witten, D., Hastie, T., & Tibshirani, R. (2013). An Introduction to Statistical Learning. *Springer Texts in Statistics*.

Jani, H. R., & Raisman, G. (2004). Ensheathing cell cultures from the olfactory bulb and mucosa. *Glia*, *47*(2), 130–137. https://doi.org/10.1002/glia.20038

Jessen, K. R., & Mirsky, R. (1984). Nonmyelin-forming Schwann cells coexpress surface proteins and intermediate filaments not found in myelin-forming cells: a study of Ran-2, A5E3 antigen and glial fibrillary

acidic protein. *Journal of Neurocytology*, *13*, 923–934. https://doi.org/10.1007/BF01148594

Jessen, K. R., & Mirsky, R. (1991). Schwann cell precursors and their development. *Glia*, *4*, 185–194.

Jessen, K. R., & Mirsky, R. (2005, September). The origin and development of glial cells in peripheral nerves. *Nature Reviews Neuroscience*. https://doi.org/10.1038/nrn1746

Jessen, K. R., Morgan, L., Stewart, H. J. S., & Mirsky, R. (1990). Three markers of adult non-myelin-forming Schwann cells , 217c (Ran-1), A5E3 and GFAP : development and regulation by neuron-Schwann cell interactions. *Development*, *103*, 91–103.

Jochems, C. E. A., Van der Valk, J. B. F., Stafleu, F. R., & Baumans, V. (2002). The use of fetal bovine serum: Ethical or scientific problem? *ATLA Alternatives to Laboratory Animals*, *30*(2), 219–227.

Jones, D. M., Tucker, B. A., Rahimtula, M., & Mearow, K. M. (2003). The synergistic effects of NGF and IGF-1 on neurite growth in adult sensory neurons: convergence on the PI 3-kinase signaling pathway. *Journal of Neurochemistry*, *86*(5), 1116–1128. Retrieved from http://www.ncbi.nlm.nih.gov/pubmed/12911620

Jones, L. L., Margolis, R. U., & Tuszynski, M. H. (2003). The chondroitin sulfate proteoglycans neurocan, brevican, phosphacan, and versican are differentially regulated following spinal cord injury. *Experimental Neurology*, *182*(2), 399–411. https://doi.org/10.1016/S0014-

4886(03)00087-6

Jones, L. L., Oudega, M., Bunge, M. B., & Tuszynski, M. H. (2001, May 1). Neurotrophic factors, cellular bridges and gene therapy for spinal cord injury. *Journal of Physiology*. Wiley/Blackwell (10.1111). https://doi.org/10.1111/j.1469-7793.2001.0083b.x

Jones, L. L., Sajed, D., & Tuszynski, M. H. (2003). Axonal regeneration through regions of chondroitin sulfate proteoglycan deposition after spinal cord injury: a balance of permissiveness and inhibition. *The Journal of Neuroscience : The Official Journal of the Society for Neuroscience*, *23*(28), 9276–9288. https://doi.org/23/28/9276 [pii]

Jones, L. L., Yamaguchi, Y., Stallcup, W. B., & Tuszynski, M. H. (2002). NG2 Is a Major Chondroitin Sulfate Proteoglycan Produced after Spinal Cord Injury and Is Expressed by Macrophages and Oligodendrocyte Progenitors. *The Journal of Neuroscience*, *22*(7), 2792–2803. https://doi.org/20026258

Joosten, E. A. J., & Gribnau, A. A. M. (1989). Astrocytes and guidance of outgrowing corticospinal tract axons in the rat. An immunocytochemical study using anti-vimentin and anti-glial fibrillary acidic protein. *Neuroscience*, *31*(2), 439–452. https://doi.org/10.1016/0306-4522(89)90386-2

Kafitz, K. W. K. W., & Greer, C. a. (1999). Olfactory Ensheathing Cells Promote Neurite Extension From Embryonic Embryonic Olfactory Receptor Cells In Vitro. *Glia*, *110*(July 1998), 99–110.

https://doi.org/10.1002/(SICI)1098-1136(19990115)25:23.0.CO;2-V

Kalbermatten, D. F., Erba, P., Mahay, D., Wiberg, M., Pierer, G., & Terenghi, G. (2008). Schwann Cell Strip for Peripheral Nerve Repair. *Journal of Hand Surgery (European Volume)*, *33*(5), 587–594. https://doi.org/10.1177/1753193408090755

Kanno, H., Pearse, D. D., Ozawa, H., Itoi, E., & Bunge, M. B. (2015, January 1). Schwann cell transplantation for spinal cord injury repair: Its significant therapeutic potential and prospectus. *Reviews in the Neurosciences*. De Gruyter. https://doi.org/10.1515/revneuro-2014-0068

Kanno, H., Pressman, Y., Moody, A., Berg, R., Muir, E. M., Rogers, J. H., … Bunge, M. B. (2014). Combination of Engineered Schwann Cell Grafts to Secrete Neurotrophin and Chondroitinase Promotes Axonal Regeneration and Locomotion after Spinal Cord Injury. *Journal of Neuroscience*, *34*(5), 1838–1855. https://doi.org/10.1523/JNEUROSCI.2661-13.2014

Katoh, H., Shibata, S., Fukuda, K., Sato, M., Satoh, E., Nagoshi, N., … Okano, H. (2011). The dual origin of the peripheral olfactory system: placode and neural crest. *Molecular Brain*, *4*(1), 34. https://doi.org/10.1186/1756-6606-4-34

Kawaja, M. D., Boyd, J. G., Smithson, L. J., Jahed, A., & Doucette, R. (2009). Technical strategies to isolate olfactory ensheathing cells for intraspinal implantation. *Journal of Neurotrauma*, *26*(2), 155–177.

https://doi.org/10.1089/neu.2008.0709

Kelamangalath, L., & Smith, G. M. (2013). Neurotrophin treatment to promote regeneration after traumatic CNS injury. *Frontiers in Biology*, *8*(5), 486–495. https://doi.org/10.1007/s11515-013-1269-8

Kemshead, J. T., Ritter, M. A., Cotmore, S. F., & Greaves, M. F. (1982). Human Thy-1: expression on the cell surface of neuronal and glial cells. *Brain Research*, *236*(2), 451–461.

Kenny, D. A. (1987). *Statistics for the social and behavioral sciences*. Little, Brown. Retrieved from https://www.amazon.com/Statistics-social-behavioral-sciences-David/dp/0316489158

Khankan, R. R., Wanner, I. B., & Phelps, P. E. (2015a). Olfactory ensheathing cell–neurite alignment enhances neurite outgrowth in scar-like cultures. *Experimental Neurology*, *269*, 93–101. https://doi.org/10.1016/j.expneurol.2015.03.025

Khankan, R. R., Wanner, I. B., & Phelps, P. E. (2015b). Olfactory ensheathing cell–neurite alignment enhances neurite outgrowth in scar-like cultures. *Experimental Neurology*, *269*, 93–101. https://doi.org/10.1016/j.expneurol.2015.03.025

Kim, H.-Y. (2015). Statistical notes for clinical researchers: post-hoc multiple comparisons. *Restorative Dentistry & Endodontics*, *40*(2), 172–176. https://doi.org/10.5395/rde.2015.40.2.172

Kirke Rogers, W., & Todd, M. (2016). Acute spinal cord injury. *Best Practice*

and Research: Clinical Anaesthesiology, *30*(1), 27–39. https://doi.org/10.1016/j.bpa.2015.11.003

Klingman, A. M., & Armstrong, R. C. (1986). Histologic Response to Intradermal Zyderm and Zyplast (Glutaraldehyde Cross-Linked) Collagen in Humans. *The Journal of Dermatologic Surgery and Oncology*, *12*(4), 351–357. https://doi.org/10.1111/j.1524-4725.1986.tb01920.x

Knoferle, J., Koch, J. C., Ostendorf, T., Michel, U., Planchamp, V., Vutova, P., … Lingor, P. (2010). Mechanisms of acute axonal degeneration in the optic nerve in vivo. *Proceedings of the National Academy of Sciences*, *107*(13), 6064–6069. https://doi.org/10.1073/pnas.0909794107

Knuth, D. E., & E., D. (1973). *The art of computer programming*. Addison-Wesley Pub. Co. Retrieved from https://dl.acm.org/citation.cfm?id=270146

Kraus, D., Boyle, V., Leibig, N., Stark, G. B., & Penna, V. (2015). The Neuro-spheroid-A novel 3D in vitro model for peripheral nerve regeneration. *Journal of Neuroscience Methods*, *246*, 97–105. https://doi.org/10.1016/j.jneumeth.2015.03.004

Kueh, J. L.-L., Raisman, G., Li, Y., Stevens, R., & Li, D. (2011). Comparison of bulbar and mucosal olfactory ensheathing cells using FACS and simultaneous antigenic bivariate cell cycle analysis. *Glia*, *59*(11), 1658–1671. https://doi.org/10.1002/glia.21213

Kutner, M. H., Nachtsheim, C., & Neter, J. (2004). *Applied linear regression models.* McGraw-Hill/Irwin.

Labrador, R. O., Butí, M., & Navarro, X. (1995). Peripheral nerve repair: role of agarose matrix density on functional recovery. *Neuroreport*, *6*, 2022–2026. https://doi.org/10.1097/00001756-199510010-00017

Lakatos, A., Barnett, S. C., & Franklin, R. J. M. (2003). Olfactory ensheathing cells induce less host astrocyte response and chondroitin sulphate proteoglycan expression than Schwann cells following transplantation into adult CNS white matter. *Experimental Neurology*, *184*(1), 237–246. https://doi.org/10.1016/S0014-4886(03)00270-X

Lakatos, A., Franklin, R. J. M., & Barnett, S. C. S. C. (2000). Olfactory ensheathing cells and Schwann cells differ in their in vitro interactions with astrocytes. *GLIA*, *32*(3), 214–225. https://doi.org/10.1002/1098-1136(200012)32:3<214::AID-GLIA20>3.0.CO;2-7

Lamond, R., & Barnett, S. C. (2013). Schwann Cells But Not Olfactory Ensheathing Cells Inhibit CNS Myelination via the Secretion of Connective Tissue Growth Factor. *Journal of Neuroscience*, *33*(47), 18686–18697. https://doi.org/10.1523/JNEUROSCI.3233-13.2013

Lankford, K. L., Brown, R. J., Sasaki, M., & Kocsis, J. D. (2014). Olfactory ensheathing cells, but not schwann cells, proliferate and migrate extensively within moderately X-Irradiated juvenile rat brain. *GLIA*, *62*(1), 52–63. https://doi.org/10.1002/glia.22583

Lankford, K. L., Sasaki, M., Radtke, C., & Kocsis, J. D. (2008). Olfactory

ensheathing cells exhibit unique migratory, phagocytic, and myelinating properties in the x-irradiated spinal cord not shared by schwann cells. *Glia*, *56*(15), 1664–1678. https://doi.org/10.1002/glia.20718

Laroni, A., Novi, G., De Rosbo, N. K., & Uccelli, A. (2013, December 12). Towards clinical application of mesenchymal stem cells for treatment of neurological diseases of the central nervous system. *Journal of Neuroimmune Pharmacology*. Springer US. https://doi.org/10.1007/s11481-013-9456-6

Laywell, E. D., Kukekov, V. G., & Steindler, D. A. (1999). Multipotent neurospheres can be derived from forebrain subependymal zone and spinal cord of adult mice after protracted postmortem intervals. *Experimental Neurology*, *156*(2), 430–433. https://doi.org/10.1006/exnr.1999.7029

Leader, M., Collins, M., Patel, J., & Henry, K. (1987). Vimentin: an evaluation of its role as a tumour marker. *Histopathology*, *11*, 63–72.

Leaver, S. G., Harvey, A. R., & Plant, G. W. (2006). Adult olfactory ensheathing glia promote the long-distance growth of adult retinal ganglion cell neurites in vitro. *Glia*, *53*(5), 467–476. https://doi.org/10.1002/glia.20311

Lee, I. H., Bulte, J. W. M., Schweinhardt, P., Douglas, T., Trifunovski, A., Hofstetter, C., … Spenger, C. (2004). In vivo magnetic resonance tracking of olfactory ensheathing glia grafted into the rat spinal cord.

Experimental Neurology, *187*(2), 509–516. https://doi.org/10.1016/j.expneurol.2004.02.007

Leng, Z., He, X., Li, H., Wang, D., & Cao, K. (2013). Olfactory ensheathing cell transplantation for spinal cord injury: An 18-year bibliometric analysis based on the Web of Science. *Neural Regeneration Research*, *8*(14), 1286–1296. https://doi.org/10.3969/j.issn.1673-5374.2013.14.005

Leung, J. Y. K., Chapman, J. A., Harris, J. A., Hale, D., Chung, R. S., West, A. K., & Chuah, M. I. (2008). Olfactory ensheathing cells are attracted to, and can endocytose, bacteria. *Cellular and Molecular Life Sciences*, *65*, 2732–2739. https://doi.org/10.1007/s00018-008-8184-1

Levine, C., & Marcillo, A. (2008). Regarding several points of doubt of the structure of the olfactory bulb: as described by T. Blanes. *Anatomical Record (Hoboken, N.J. : 2007)*, *291*(7), 751–762. https://doi.org/10.1002/ar.20680

Lewin, S. L., Utley, D. S., Cheng, E. T., Verity, A. N., & Terris, D. J. (1997). Simultaneous Treatment With BDNF and CNTF After Peripheral Nerve Transection and Repair Enhances Rate of Functional Recovery Compared With BDNF Treatment Alone. *The Laryngoscope*, *107*(7), 992–999. https://doi.org/10.1097/00005537-199707000-00029

Li, B. C., Li, Y., Chen, L. F., Chang, J. Y., & Duan, Z. X. (2011). Olfactory ensheathing cells can reduce the tissue loss but not the cavity formation in contused spinal cord of rats. *Journal of the Neurological*

Sciences, *303*(1–2), 67–74. https://doi.org/10.1016/j.jns.2011.01.013

Li, Y., Field, P. M., & Raisman, G. (1997). Repair of adult rat corticospinal tract by transplants of olfactory ensheathing cells. *Science (New York, N.Y.)*, *277*(5334), 2000–2002. https://doi.org/10.1126/science.277.5334.2000

Li, Y., Field, P. M., & Raisman, G. (1998). Regeneration of adult rat corticospinal axons induced by transplanted olfactory ensheathing cells. *JOURNAL OF NEUROSCIENCE*, *18*(24), 10514–10524. https://doi.org/10.1523/JNEUROSCI.18-24-10514.1998

Li, Y., Li, D., & Raisman, G. (2005). Interaction of olfactory ensheathing cells with astrocytes may be the key to repair of tract injuries in the spinal cord: The "pathway hypothesis." *Journal of Neurocytology*, *34*(3–5), 343–351. https://doi.org/10.1007/s11068-005-8361-1

Li, Y., Li, D., & Raisman, G. (2007). Transplanted Schwann cells, not olfactory ensheathing cells, myelinate optic nerve fibres. *Glia*, *55*(3), 312–316. https://doi.org/10.1002/glia.20458

Li, Y., Sauve, Y., Li, D., Lund, R. D., & Raisman, G. (2003). Transplanted olfactory ensheathing cells promote regeneration of cut adult rat optic nerve axons. *J Neurosci*, *23*(21), 7783–7788.

Lietz, M., Dreesmann, L., Hoss, M., Oberhoffner, S., & Schlosshauer, B. (2006). Neuro tissue engineering of glial nerve guides and the impact of different cell types. *Biomaterials*, *27*(8), 1425–1436. https://doi.org/10.1016/j.biomaterials.2005.08.007

Lim, J. Y., & Donahue, H. J. (2007). Cell sensing and response to micro- and nanostructured surfaces produced by chemical and topographic patterning. *Tissue Engineering*, *13*(8), 1879–1891. https://doi.org/10.1089/ten.2006.0154

Lima, C., Escada, P., Pratas-Vital, J., Branco, C., Arcangeli, C. A., Lazzeri, G., … Peduzzi, J. D. (2010). Olfactory Mucosal Autografts and Rehabilitation for Chronic Traumatic Spinal Cord Injury. *Neurorehabilitation and Neural Repair*, *24*(1), 10–22. https://doi.org/10.1177/1545968309347685

Lima, C., Pratas-Vital, J., Escada, P., Hasse-Ferreira, A., Capucho, C., & Peduzzi, J. D. (2006). Olfactory mucosa autografts in human spinal cord injury: a pilot clinical study. *The Journal of Spinal Cord Medicine*, *29*(3), 191-203; discussion 204-6.

Lindsay, S. L., & Barnett, S. C. (2017). Are nestin-positive mesenchymal stromal cells a better source of cells for CNS repair? *Neurochemistry International*, *106*, 101–107. https://doi.org/10.1016/j.neuint.2016.08.001

Lindsay, S. L., Riddell, J. S., & Barnett, S. C. (2010, January 15). Olfactory mucosa for transplant-mediated repair: A complex tissue for a complex injury? *GLIA*. Wiley-Blackwell. https://doi.org/10.1002/glia.20917

Lindsay, S. L., Toft, A., Griffin, J., M. M. Emraja, A., Barnett, S. C., & Riddell, J. S. (2017). Human olfactory mesenchymal stromal cell transplants

promote remyelination and earlier improvement in gait co-ordination after spinal cord injury. *GLIA*, *65*(4), 639–656. https://doi.org/10.1002/glia.23117

Lipson, A. C., Widenfalk, J., Lindqvist, E., Ebendal, T., & Olson, L. (2003). Neurotrophic properties of olfactory ensheathing glia. *Experimental Neurology*, *180*(2), 167–171. https://doi.org/10.1016/S0014-4486(02)00058-4

Littlewood, T. D., Hancock, D. C., Danielian, P. S., Parker, M. G., & Evan, G. I. (1995). A modified oestrogen receptor ligand-binding domain as an improved switch for the regulation of heterologous proteins. *Nucleic Acids Research*, *23*(10), 1686–1690. https://doi.org/10.1093/nar/23.10.1686

Liu, Y., Teng, X., Yang, X., Song, Q., Lu, R., Xiong, J., … Liang, S. (2010). Shotgun proteomics and network analysis between plasma membrane and extracellular matrix proteins from rat olfactory ensheathing cells. *Cell Transplantation*, *19*(2), 133–146. https://doi.org/10.3727/096368910X492607

Liu, Z., Jin, Y.-Q., Chen, L., Wang, Y., Yang, X., Cheng, J., … Shen, Z. (2015). Specific Marker Expression and Cell State of Schwann Cells during Culture In Vitro. *PLOS ONE*, *10*(4), e0123278. https://doi.org/10.1371/journal.pone.0123278

López-Vales, R., Forés, J., Navarro, X., & Verdú, E. (2007). Chronic transplantation of olfactory ensheathing cells promotes partial

recovery after complete spinal cord transection in the rat. *GLIA*, *55*(3), 303–311. https://doi.org/10.1002/glia.20457

López-Vales, R., Forés, J., Verdú, E., & Navarro, X. (2006). Acute and delayed transplantation of olfactory ensheathing cells promote partial recovery after complete transection of the spinal cord. *Neurobiology of Disease*, *21*(1), 57–68. https://doi.org/10.1016/j.nbd.2005.06.011

López-Vales, R., García-Alías, G., Forés, J., Navarro, X., & Verdú, E. (2004). Increased Expression of Cyclo-Oxygenase 2 and Vascular Endothelial Growth Factor in Lesioned Spinal Cord by Transplanted Olfactory Ensheathing Cells. *Journal of Neurotrauma*, *21*(8), 1031–1043. https://doi.org/10.1089/0897715041651105

Losey, P., & Anthony, D. (2014). Impact of vasculature damage to the outcome of spinal cord injury: a new collagenase-induced model may give new insights into the mechanisms involved. *Neural Regeneration Research*, *9*(20), 1783. https://doi.org/10.4103/1673-5374.143422

Losey, P., Young, C., Krimholtz, E., Bordet, R., & Anthony, D. C. (2014). The role of hemorrhage following spinal-cord injury. *Brain Research*, *1569*, 9–18. https://doi.org/10.1016/J.BRAINRES.2014.04.033

Lozano, A. M., Schmidt, M., & Roach, A. (1995). A convenient in vitro assay for the inhibition of neurite outgrowth by adult mammalian CNS myelin using immortalized neuronal cells. *Journal of Neuroscience Methods*, *63*(1–2), 23–28. https://doi.org/10.1016/0165-0270(95)00081-X

Lu, J., & Ashwell, K. (2002). Olfactory ensheathing cells: their potential use for repairing the injured spinal cord. *Spine*, *27*(8), 887–892. https://doi.org/10.1097/00007632-200204150-00021

Lu, J., Féron, F., Ho, S. M., Mackay-Sim, A., & Waite, P. M. E. (2001). Transplantation of nasal olfactory tissue promotes partial recovery in paraplegic adult rats. *Brain Research*, *889*(1–2), 344–357. https://doi.org/10.1016/S0006-8993(00)03235-2

Lu, J., Féron, F., Mackay-Sim, A., Waite, P. M. E., Feron, F., Mackay-Sim, A., & Waite, P. M. E. (2002). Olfactory ensheathing cells promote locomotor recovery after delayed transplantation into transected spinal cord. *Brain*, *125*(Pt 1), 14–21. https://doi.org/10.1093/brain/awf014

Lu, P., Wang, Y., Graham, L., McHale, K., Gao, M., Wu, D., … Tuszynski, M. H. (2012). Long-Distance Growth and Connectivity of Neural Stem Cells after Severe Spinal Cord Injury. *Cell*, *150*(6), 1264–1273.

Lu, P., Yang, H., Culbertson, M., Graham, L., Roskams, A. J., & Tuszynski, M. H. (2006). Olfactory Ensheathing Cells Do Not Exhibit Unique Migratory or Axonal Growth-Promoting Properties after Spinal Cord Injury. *Journal of Neuroscience*, *26*(43), 11120–11130. https://doi.org/10.1523/JNEUROSCI.3264-06.2006

Lukovic, D., Valdés-Sanchez, L., Sanchez-Vera, I., Moreno-Manzano, V., Stojkovic, M., Bhattacharya, S. S., & Erceg, S. (2014). Brief report: Astrogliosis promotes functional recovery of completely transected

spinal cord following transplantation of hESC-derived oligodendrocyte and motoneuron progenitors. *Stem Cells*, *32*(2), 594–599. https://doi.org/10.1002/stem.1562

Mackay-Sim, A., Feron, F., Cochrane, J., Bassingthwaighte, L., Bayliss, C., Davies, W., … Geraghty, T. (2008). Autologous olfactory ensheathing cell transplantation in human paraplegia: a 3-year clinical trial. *Brain*, *131*(9), 2376–2386. https://doi.org/10.1093/brain/awn173

Maisonpierre, P. C., Belluscio, L., Squinto, S., Ip, N. Y., Furth, M. E., Lindsay, R. M., & Yancopoulos, G. D. (1990). Neurotrophin-3: a neurotrophic factor related to NGF and BDNF. *Science (New York, N.Y.)*, *247*(4949 Pt 1), 1446–1451.

Martens, W., Sanen, K., Georgiou, M., Struys, T., Bronckaers, A., Ameloot, M., … Lambrichts, I. (2014). Human dental pulp stem cells can differentiate into Schwann cells and promote and guide neurite outgrowth in an aligned tissue-engineered collagen construct in vitro. *The FASEB Journal*, *28*(4), 1634–1643. https://doi.org/10.1096/fj.13-243980

Mathur, M., Xiang, J. S., & Smolke, C. D. (2017). Mammalian synthetic biology for studying the cell. *Journal of Cell Biology*, *216*(1), 73–82. https://doi.org/10.1083/jcb.201611002

Mayeur, A., Duclos, C., Honoré, A., Gauberti, M., Drouot, L., do Rego, J.-C., … Guérout, N. (2013). Potential of olfactory ensheathing cells from different sources for spinal cord repair. *PloS One*, *8*(4), e62860.

https://doi.org/10.1371/journal.pone.0062860

McCallister, W. V, Tang, P., Smith, J., & Trumble, T. E. (2001). Axonal regeneration stimulated by the combination of nerve growth factor and ciliary neurotrophic factor in an end-to-side model. *The Journal of Hand Surgery*, *26*(3), 478–488. https://doi.org/10.1053/jhsu.2001.24148

McDonald, J. W., & Sadowsky, C. (2002). Spinal-cord injury. *The Lancet*, *359*(9304), 417–425. https://doi.org/10.1016/S0140-6736(02)07603-1

McKeon, R. J., Höke, A., & Silver, J. (1995). Injury-induced proteoglycans inhibit the potential for laminin-mediated axon growth on astrocytic scars. *Experimental Neurology*, *136*(1), 32–43. https://doi.org/10.1006/exnr.1995.1081

McKeon, R. J., Schreiber, R. C., Rudge, J. S., & Silver, J. (1991). Reduction of Neurite Outgrowth in a Model of Glial Scarring Following CNS Injury Is Correlated With the Expression of Inhibitory Molecules on Reactive Astrocytes. *Journal of Neuroscience*, *11*(11), 3398–3411. https://doi.org/10.1523/JNEUROSCI.11-11-03398.1991

Meyer, M., Matsuoka, I., Wetmore, C., Olson, L., & Thoenen, H. (1992). Enhanced synthesis of brain-derived neurotrophic factor in the lesioned peripheral nerve: Different mechanisms are responsible for the regulation of BDNF and NGF mRNA. *Journal of Cell Biology*, *119*(1), 45–54. https://doi.org/10.1083/jcb.119.1.45

Michalczyk, K., & Ziman, M. (2005). Nestin structure and predicted function

in cellular cytoskeletal organisation. *Histology and Histopathology*.

Miles, J., & Shevlin, M. (2001). *Applying regression & correlation : a guide for students and researchers*. Sage Publications.

Miller, R. G. (1981). *Simultaneous Statistical Inference*. New York, NY: Springer New York. https://doi.org/10.1007/978-1-4613-8122-8

Miller, R. H., Ffrench-constant, C., & Raff, M. C. (1989). The macroglial cells of the rat optic nerve. *Annu. Rev. Neurosci.*, 517–534.

Miller, R. H., Williams, B. P., Cohen, J., & Raff, M. C. (1984). A4: An antigenic marker of neural tube-derived cells. . . *J. Neurocytol.*, *13*, 329– 338.

Mirsky, R., Winter, J., Abney, E. A., Pruss, R., Gavrilovie, J., & Raff C., M. (1980). Myelin-specific proteins and glycolipids in rat Schwann cells and oligodendrocytes in culture. *J. Cell. Biol.*, *84*, 483– 494.

Mittelhammer, R., Judge, G. G., & Miller, D. (2000). *Econometric foundations*. Cambridge University Press. Retrieved from https://www.cambridge.org/gb/academic/subjects/economics/economic-development-and-growth/econometric-foundations?format=WW&isbn=9780521623940

Miyazono, M., Nowell, P. C., Finan, J. L., Lee, V. M. Y., & Trojanowski, J. Q. (1996). Long-term integration and neuronal differentiation of human embryonal carcinoma cells (NTera-2) transplanted into the caudoputamen of nude mice. *Journal of Comparative Neurology*, *376*(4), 603–613. https://doi.org/10.1002/(SICI)1096-

9861(19961223)376:4<603::AID-CNE8>3.0.CO;2-5

Mocchetti, I., & Wrathall, J. R. (2009). Neurotrophic Factors in Central Nervous System Trauma. *Journal of Neurotrauma*, *12*(5), 853–870. https://doi.org/10.1089/neu.1995.12.853

Moradi, F., Bahktiari, M., Joghataei, M. T., Nobakht, M., Soleimani, M., Hasanzadeh, G., … Maleki, F. (2012). BD PuraMatrix peptide hydrogel as a culture system for human fetal Schwann cells in spinal cord regeneration. *Journal of Neuroscience Research*, *90*(12), 2335–2348. https://doi.org/10.1002/jnr.23120

Moreno-Flores, M. T., & Avila, J. (2006). The quest to repair the damaged spinal cord. *Recent Patents on CNS Drug Discovery*, *1*(1), 55–63. https://doi.org/10.2174/157488906775245264

Moreno-Flores, M. T., & Avila, J. (2010). *The quest to repair the damaged spinal cord* (Frontiers). U.A.E: Ben-tham books.

Moreno-Flores, M. T., Bradbury, E. J., Martín-Bermejo, M. J., Agudo, M., Lim, F., Pastrana, É., … Wandosell, F. (2006). A clonal cell line from immortalized olfactory ensheathing glia promotes functional recovery in the injured spinal cord. *Molecular Therapy*, *13*(3), 598–608. https://doi.org/10.1016/j.ymthe.2005.11.014

Moreno-Flores, M. T., Díaz-Nido, J., Wandosell, F., & Avila, J. (2002). Olfactory ensheathing glia: Drivers of axonal regeneration in the central nervous system? *Journal of Biomedicine and Biotechnology*. Hindawi. https://doi.org/10.1155/S1110724302000372

Moreno-Manzano, V., Rodríguez-Jiménez, F. J., García-Roselló, M., Laínez, S., Erceg, S., Calvo, M. T., … Stojkovic, M. (2009). Activated Spinal Cord Ependymal Stem Cells Rescue Neurological Function. *Stem Cells*, *27*(3), 733–743. https://doi.org/10.1002/stem.24

Morrison, S. J., White, P. M., Zock, C., & Anderson, D. J. (1999). Prospective Identification, Isolation by Flow Cytometry, and In Vivo Self-Renewal of Multipotent Mammalian Neural Crest Stem Cells. *Cell*, *96*(5), 737–749. https://doi.org/10.1016/S0092-8674(00)80583-8

Muir, D., Engvall, E., Varon, S., & Manthorpe, M. (1989). Schwannoma cell-derived inhibitor of the neurite-promoting activity of laminin. *Journal of Cell Biology*, *109*(5), 2353–2362. https://doi.org/10.1083/jcb.109.5.2353

Nakamura, Y., Muguruma, Y., Yahata, T., Miyatake, H., Sakai, D., Mochida, J., … Ando, K. (2006). Expression of CD90 on keratinocyte stem/progenitor cells. *British Journal of Dermatology*, *154*(6), 1062–1070. https://doi.org/10.1111/j.1365-2133.2006.07209.x

Nazareth, L., Lineburg, K. E., Chuah, M. I., Velasquez, J. T., Chehrehasa, F., John, J. A. S., … Information, G. (2014). Olfactory ensheathing cells are the main phagocytic cells that remove axon debris during early development of the olfactory system. *The Journal of Comparative Neurology Research in Systems Neuroscience*, 45. https://doi.org/10.1002/cne.

Neuberger, T. J., & De Vries, G. H. (1993). Distribution of fibroblast growth

factor in cultured dorsal root ganglion neurons and Schwann cells. II. Redistribution after neural injury. *Journal of Neurocytology*, *22*(6), 449–460. https://doi.org/10.1007/BF01181565

Niederöst, B. P., Zimmermann, D. R., Schwab, M. E., & Bandtlow, C. E. (1999). Bovine CNS myelin contains neurite growth-inhibitory activity associated with chondroitin sulfate proteoglycans. *The Journal of Neuroscience : The Official Journal of the Society for Neuroscience*, *19*(20), 8979–8989. https://doi.org/20026637

Nirmalanandhan, V. S., Levy, M. S., Huth, A. J., & Butler, D. L. (2006). Effects of Cell Seeding Density and Collagen Concentration on Contraction Kinetics of Mesenchymal Stem Cell–Seeded Collagen Constructs. *Tissue Engineering*, *12*(7), 1865–1872. https://doi.org/10.1089/ten.2006.12.1865

Nocentini, S., Reginensi, D., Garcia, S., Carulla, P., Moreno-Flores, M. T., Wandosell, F., … del Río, J. A. (2011). Olfactory ensheathing cells exhibit unique migratory, phagocytic, and myelinating properties in the x-irradiated spinal cord not shared by schwann cells. *Cellular and Molecular Life Sciences*, *69*(10), 1689–1703. https://doi.org/10.1007/s00018-011-0893-1

Nocentini, S., Reginensi, D., Garcia, S., Carulla, P., Moreno-Flores, M. T., Wandosell, F., … del Río, J. A. (2012). Myelin-associated proteins block the migration of olfactory ensheathing cells: an in vitro study using single-cell tracking and traction force microscopy. *Cellular and*

Molecular Life Sciences, *69*(10), 1689–1703. https://doi.org/10.1007/s00018-011-0893-1

Novikova, L. N., Brohlin, M., Kingham, P. J., Novikov, L. N., & Wiberg, M. (2011). Neuroprotective and growth-promoting effects of bone marrow stromal cells after cervical spinal cord injury in adult rats. *Cytotherapy*, *13*(7), 873–887. https://doi.org/10.3109/14653249.2011.574116

Novikova, L. N., Lobov, S., Wiberg, M., & Novikov, L. N. (2011). Efficacy of olfactory ensheathing cells to support regeneration after spinal cord injury is influenced by method of culture preparation. *Experimental Neurology*, *229*(1), 132–142. https://doi.org/10.1016/j.expneurol.2010.09.021

O'Neill, P., Lindsay, S. L., Pantiru, A., Guimond, S. E., Fagoe, N., Verhaagen, J., … Barnett, S. C. (2017). Sulfatase-mediated manipulation of the astrocyte-Schwann cell interface. *GLIA*, *65*(1), 19–33. https://doi.org/10.1002/glia.23047

O'Rourke, C., Drake, R. a., Cameron, G. W., Jane Loughlin, A., & Phillips, J. B. (2015). Optimising contraction and alignment of cellular collagen hydrogels to achieve reliable and consistent engineered anisotropic tissue. *Journal of Biomaterials Applications*, *0*(0), 1–9. https://doi.org/10.1177/0885328215597818

O'Toole, D. A., West, A. K., & Chuah, M. I. (2007). Effect of olfactory ensheathing cells on reactive astrocytes in vitro. *Cellular and*

Molecular Life Sciences, *64*(10), 1303–1309. https://doi.org/10.1007/s00018-007-7106-y

O'Toole, D. A., West, A. K., Chuah, M. I., O'Toole, D. A., West, A. K., Chuah, M. I., … Chuah, M. I. (2007). Effect of olfactory ensheathing cells on reactive astrocytes in vitro. *Cellular and Molecular Life Sciences*, *64*(10), 1303–1309. https://doi.org/10.1007/s00018-007-7106-y

Offenhäuser, N., Böhm-Matthaei, R., Tsoulfas, P., Parada, L., & Meyer, M. (1995). Developmental Regulation of Full-length trkC in the Rat Sciatic Nerve. *European Journal of Neuroscience*, *7*(5), 917–925. https://doi.org/10.1111/j.1460-9568.1995.tb01079.x

Okano, H. (2002). Stem cell biology of the central nervous system. *Journal of Neuroscience Research*, *69*(6), 698–707. https://doi.org/10.1002/jnr.10343

Oudega, M., & Xu, X.-M. (2006). Schwann Cell Transplantation for Repair of the Adult Spinal Cord. *Journal of Neurotrauma*, *23*(3–4), 453–467. https://doi.org/10.1089/neu.2006.23.453

Oudega, M., Xu, X. M., Guenard, V., Kleitman, N., Bunge, M. B., Gu  nard, V., … Bunge, M. B. (1997). A combination of insulin-like growth factor-I and platelet-derived growth factor enhances myelination but diminishes axonal regeneration into Schwann cell grafts in the adult rat spinal cord. *Glia*, *19*(3), 247–258. https://doi.org/10.1002/(SICI)1098-1136(199703)19:3<247::AID-GLIA7>3.0.CO;2-W

Panni, P., Ferguson, I. A., Beacham, I., Mackay-Sim, A., Ekberg, J. A. K., & St John, J. A. (2013). Phagocytosis of bacteria by olfactory ensheathing cells and Schwann cells. *Neuroscience Letters*, *539*, 65–70. https://doi.org/10.1016/j.neulet.2013.01.052

Paquet-Durand, F., & Bicker, G. (2007). Human model neurons in studies of brain cell damage and neural repair. *Current Molecular Medicine*, *7*(6), 541–554. https://doi.org/10.2174/156652407781695747

Park, H., Cannizzaro, C., Vunjak-Novakovic, G., Langer, R., Vacanti, C. A., & Farokhzad, O. C. (2007). Nanofabrication and Microfabrication of Functional Materials for Tissue Engineering. *Tissue Engineering*, *13*(8), 1867–1877. https://doi.org/10.1089/ten.2006.0198

Pastrana, E., Moreno-Flores, M. T., Gurzov, E. N., Avila, J., Wandosell, F., & Diaz-Nido, J. (2006). Genes associated with adult axon regeneration promoted by olfactory ensheathing cells: a new role for matrix metalloproteinase 2. *The Journal of Neuroscience : The Official Journal of the Society for Neuroscience*, *26*(20), 5347–5359. https://doi.org/10.1523/JNEUROSCI.1111-06.2006

Patel, V., Joseph, G., Patel, A., Patel, S., Bustin, D., Mawson, D., … Pearse, D. D. (2010). Suspension Matrices for Improved Schwann-Cell Survival after Implantation into the Injured Rat Spinal Cord. *Journal of Neurotrauma*, *27*(5), 789–801. https://doi.org/10.1089/neu.2008.0809

Pateman, C. J., Harding, A. J., Glen, A., Taylor, C. S., Christmas, C. R.,

Robinson, P. P., … Haycock, J. W. (2015). Nerve guides manufactured from photocurable polymers to aid peripheral nerve repair. *Biomaterials*, *49*, 77–89. https://doi.org/10.1016/j.biomaterials.2015.01.055

Pearse, D. D., Pereira, F. C., Marcillo, A. E., Bates, M. L., Berrocal, Y. A., Filbin, M. T., & Bunge, M. B. (2004). cAMP and Schwann cells promote axonal growth and functional recovery after spinal cord injury. *Nature Medicine*, *10*(6), 610–616. https://doi.org/10.1038/nm1056

Pearse, D. D., Sanchez, A. R., Pereira, F. C., Andrade, C. M., Puzis, R., Pressman, Y., … Bunge, M. B. (2007). Transplantation of Schwann cells and/or olfactory ensheathing glia into the contused spinal cord: Survival, migration, axon association, and functional recovery. *GLIA*, *55*(9), 976–1000. https://doi.org/10.1002/glia.20490

Peled, A., Grabovsky, V., Habler, L., Sandbank, J., Arenzana-Seisdedos, F., Petit, I., … Alon, R. (1999). The chemokine SDF-1 stimulates integrin-mediated arrest of CD34+ cells on vascular endothelium under shear flow. *Journal of Clinical Investigation*, *104*(9), 1199–1211. https://doi.org/10.1172/JCI7615

Pellitteri, R., Catania, M. V., Bonaccorso, C. M., Ranno, E., Albani, P. D., & Zaccheo, D. (2014). Viability of Olfactory Ensheathing Cells After Hypoxia and Serum Deprivation : Implication for Therapeutic Transplantation. *Journal of Neuroscience Research*, *1766*, 1757–1766. https://doi.org/10.1002/jnr.23442

Pellitteri, R., Cova, L., Zaccheo, D., Silani, V., & Bossolasco, P. (2016). Phenotypic Modulation and Neuroprotective Effects of Olfactory Ensheathing Cells: a Promising Tool for Cell Therapy. *Stem Cell Reviews and Reports*, *12*(2), 224–234. https://doi.org/10.1007/s12015-015-9635-3

Pellitteri, R., Russo, A., Stanzani, S., & Zaccheo, D. (2015). Olfactory ensheathing cells protect cortical neuron cultures exposed to hypoxia. *CNS & Neurological Disorders Drug Targets*, *14*(1), 68–76.

Pellitteri, R., Spatuzza, M., Russo, A., Zaccheo, D., & Stanzani, S. (2009). Olfactory ensheathing cells represent an optimal substrate for hippocampal neurons: an in vitro study. *International Journal of Developmental Neuroscience*, *27*(5), 453–458. https://doi.org/10.1016/j.ijdevneu.2009.05.001

Pellitteri, R., Spatuzza, M., Stanzani, S., & Zaccheo, D. (2010). Biomarkers expression in rat olfactory ensheathing cells. *Frontiers in Bioscience (Scholar Edition)*, *2*, 289–298.

Pérez-Bouza, A., Wigley, C. B., Nacimiento, W., Noth, J., & Brook, G. A. (1998). Spontaneous orientation of transplanted olfactory glia influences axonal regeneration. *NeuroReport*, *9*(13), 2971–2975. https://doi.org/10.1097/00001756-199809140-00010

Phillips, J. B. (2014). Monitoring neuron and astrocyte interactions with a 3D cell culture system. *Methods in Molecular Biology (Clifton, N.J.)*, *1162*, 113–124. https://doi.org/10.1007/978-1-4939-0777-9_9

Phillips, J. B., & Brown, R. (2011). Micro-structured materials and mechanical cues in 3D collagen gels. *Methods in Molecular Biology*, *695*, 183–196. https://doi.org/10.1007/978-1-60761-984-0

Pixley, S. K. (1992). The olfactory nerve contains two populations of glia, identified both in vitro and in vivo. *Glia*, *5*, 269–284.

Pixley, S. K. (1996). Characterization of olfactory receptor neurons and other cell types in dissociated rat olfactory cell cultures. *International Journal of Developmental Neuroscience*, *14*(7), 823–839. https://doi.org/10.1016/S0736-5748(96)00057-3

Plant, G. W., Christensen, C. L., Oudega, M., & Bunge, M. B. (2003). Delayed Transplantation of Olfactory Ensheathing Glia Promotes Sparing/Regeneration of Supraspinal Axons in the Contused Adult Rat Spinal Cord. *Journal of Neurotrauma*, *20*(1), 1–16. https://doi.org/10.1089/08977150360517146

Plant, G. W., Currier, P. F., Cuervo, E. P., Bates, M. L., Pressman, Y., Bunge, M. B., & Wood, P. M. (2002). Purified Adult Ensheathing Glia Fail to Myelinate Axons under Culture Conditions that Enable Schwann Cells to Form Myelin. *The Journal of Neuroscience*, *22*(14), 6083–6091. https://doi.org/20026627

Plemel, J. R., Keough, M. B., Duncan, G. J., Sparling, J. S., Yong, V. W., Stys, P. K., & Tetzlaff, W. (2014, June). Remyelination after spinal cord injury: Is it a target for repair? *Progress in Neurobiology*. https://doi.org/10.1016/j.pneurobio.2014.02.006

Plunet, W., Kwon, B. K., & Tetzlaff, W. (2002). Promoting axonal regeneration in the central nervous system by enhancing the cell body response to axotomy. *Journal of Neuroscience Research*, *68*(1), 1–6. https://doi.org/10.1002/jnr.10176

Podrygajlo, G., Tegenge, M. A., Gierse, A., Paquet-Durand, F., Tan, S., Bicker, G., & Stern, M. (2009). Cellular phenotypes of human model neurons (NT2) after differentiation in aggregate culture. *Cell and Tissue Research*, *336*(3), 439–452. https://doi.org/10.1007/s00441-009-0783-0

Pollock, K., Stroemer, P., Patel, S., Stevanato, L., Hope, A., Miljan, E., … Sinden, J. D. (2006). A conditionally immortal clonal stem cell line from human cortical neuroepithelium for the treatment of ischemic stroke. *Experimental Neurology*, *199*(1), 143–155. https://doi.org/10.1016/j.expneurol.2005.12.011

Popot, J. L., Dinh, D. P., & Dautigny, A. (1991). Major myelin proteolipid: The 4-α-helix topology. *The Journal of Membrane Biology*, *120*(3), 233–246. https://doi.org/10.1007/BF01868534

Purves, D., & Williams, S. M. (Stephen M. (2001). *Neuroscience*. Sinauer Associates.

Rabchevsky, A. G., & Streit, W. J. (1997). Grafting of cultured microglial cells into the lesioned spinal cord of adult rats enhances neurite outgrowth. *Journal of Neuroscience Research*, *47*(1), 34–48. https://doi.org/10.1002/(SICI)1097-4547(19970101)47:1<34::AID-

JNR4>3.0.CO;2-G

Raff, M. C., & Miller, R. H. (1983). A glial progenitor cell that develops in vitro into an astrocyte or an oligodendrocyte depending on culture medium. *Nature*, *303*, 390 –396.

Raine, C. S. (1976). On the occurrence of Schwann cells within the normal central nervous system. *Journal of Neurocytology*, *5*(3), 371–380.

Raisman, G. (1985). Specialized neuroglial arrangement may explain the capacity of vomeronasal axons to reinnervate central neurons. *Neuroscience*, *14*(1), 237–254. https://doi.org/10.1016/0306-4522(85)90176-9

Raisman, G. (2001). Olfactory ensheathing cells — another miracle cure for spinal cord injury? *Nature Reviews Neuroscience*, *2*(5), 369–375. https://doi.org/10.1038/35072576

Raisman, G., & Li, Y. (2007). Repair of neural pathways by olfactory ensheathing cells. *Nature Reviews Neuroscience*, *8*(4), 312–319. https://doi.org/10.1038/nrn2099

Ramer, L. M., Au, E., Richter, M., Liu, J., Tetzlaff, W., & Roskams, A. J. (2004). Peripheral Olfactory Ensheathing Cells Reduce Scar and Cavity Formation and Promote Regeneration after Spinal Cord Injury. *Journal of Comparative Neurology*, *473*(1), 1–15. https://doi.org/10.1002/cne.20049

Ramón-Cueto, A., & Avila, J. (1998). Olfactory ensheathing glia : Properties

and function. *Brain Research Bulletin*, *46*(3), 175–187.

Ramón-Cueto, A., Cordero, M. I., Santos-Benito, F. F., & Avila, J. (2000). Functional recovery of paraplegic rats and motor axon regeneration in their spinal cords by olfactory ensheathing glia. *Neuron*, *25*, 425–435. https://doi.org/10.1016/S0896-6273(00)80905-8

Ramón-Cueto, A., & Nieto-Sampedro, M. (1992). Glial cells from adult rat olfactory bulb: immunocytochemical properties of pure cultures of ensheathing cells. *Neuroscience*, *47*, 213–220. https://doi.org/10.1016/0306-4522(92)90134-N

Ramón-Cueto, A., & Nieto-Sampedro, M. (1994). Regeneration into the spinal cord of transected dorsal root axons is promoted by ensheathing glia transplants. *Experimental Neurology*, *127*, 232–244. https://doi.org/10.1006/exnr.1994.1099

Ramón-Cueto, A., Pérez, J., & Nieto-Sampedro, M. (1993). In vitro enfolding of olfactory neurites by p75 NGF receptor positive ensheathing cells from adult rat olfactory bulb. *The European Journal of Neuroscience*, *5*(9), 1172–1180. https://doi.org/10.1111/j.1460-9568.1993.tb00971.x

Ramón-Cueto, A., Plant, G. W., Avila, J., & Bunge, M. B. (1998). Long-distance axonal regeneration in the transected adult rat spinal cord is promoted by olfactory ensheathing glia transplants. *The Journal of Neuroscience : The Official Journal of the Society for Neuroscience*, *18*, 3803–3815.

Ramón-Cueto, A., & Valverde, F. (1995). Olfactory Bulb Ensheathing Glia : A

Unique Cell Type With Axonal Growth-Promoting Properties. *Glia*, *173*.

Redden, R. A., & Doolin, E. J. (2003). Collagen crosslinking and cell density have distinct effects on fibroblast-mediated contraction of collagen gels. *Skin Research and Technology : Official Journal of International Society for Bioengineering and the Skin (ISBS) [and] International Society for Digital Imaging of Skin (ISDIS) [and] International Society for Skin Imaging (ISSI)*, *9*(3), 290–293. Retrieved from http://www.ncbi.nlm.nih.gov/pubmed/12877693

Reginensi, D., Carulla, P., Nocentini, S., Seira, O., Serra-Picamal, X., Torres-Espín, A., … Del Río, J. A. (2015). Increased migration of olfactory ensheathing cells secreting the Nogo receptor ectodomain over inhibitory substrates and lesioned spinal cord. *Cellular and Molecular Life Sciences*, *72*(14), 2719–2737. https://doi.org/10.1007/s00018-015-1869-3

Reier, P. J. (1994, July 1). The Neurobiology of Central Nervous System Trauma. *Neurology*. Wolters Kluwer Health, Inc. on behalf of the American Academy of Neurology. https://doi.org/10.1212/WNL.47.1.314-b

Richter, M., Fletcher, P. A., Liu, J., Tetzlaff, W., & Roskams, a J. (2005). Lamina propria and olfactory bulb ensheathing cells exhibit differential integration and migration and promote differential axon sprouting in the lesioned spinal cord. *The Journal of Neuroscience :*

The Official Journal of the Society for Neuroscience, *25*(46), 10700–10711. https://doi.org/10.1523/JNEUROSCI.3632-05.2005

Richter, M., & Roskams, A. J. (2008). Olfactory ensheathing cell transplantation following spinal cord injury: Hype or hope? *Experimental Neurology*, *209*(2), 353–367. https://doi.org/10.1016/j.expneurol.2007.06.011

Richter, M., Westendorf, K., & Roskams, A. J. (2008). Culturing olfactory ensheathing cells from the mouse olfactory epithelium. *Methods in Molecular Biology (Clifton, N.J.)*, *438*, 95–102. https://doi.org/10.1007/978-1-59745-133-8_9

Rizek, P. N., & Kawaja, M. D. (2006). Cultures of rat olfactory ensheathing cells are contaminated with Schwann cells. *Neuroreport*, *17*(5), 459–462. https://doi.org/10.1097/01.wnr.0000209000.32857.1b

Roberts, T. T., Leonard, G. R., & Cepela, D. J. (2017). Classifications In Brief: American Spinal Injury Association (ASIA) Impairment Scale. *Clinical Orthopaedics and Related Research®*, *475*(5), 1499–1504. https://doi.org/10.1007/s11999-016-5133-4

Roche, P., Alekseeva, T., Widaa, A., Ryan, A., Matsiko, A., Walsh, M., … O'Brien, F. J. (2017). Olfactory Derived Stem Cells Delivered in a Biphasic Conduit Promote Peripheral Nerve Repair In Vivo. *Stem Cells Translational Medicine*, *6*(10), 1894–1904. https://doi.org/10.1002/sctm.16-0420

Roloff, F., Ziege, S., Baumgärtner, W., Wewetzer, K., & Bicker, G. (2013).

Schwann cell-free adult canine olfactory ensheathing cell preparations from olfactory bulb and mucosa display differential migratory and neurite growth-promoting properties in vitro. *BMC Neuroscience*, *14*, 141. https://doi.org/10.1186/1471-2202-14-141

Rønn, L. C., Hartz, B. P., & Bock, E. (1998). The neural cell adhesion molecule (NCAM) in development and plasticity of the nervous system. *Experimental Gerontology*, *33*, 853–864.

Rowland, J. W., Hawryluk, G. W. J., Kwon, B., & Fehlings, M. G. (2008). Current status of acute spinal cord injury pathophysiology and emerging therapies: promise on the horizon. *Neurosurgical Focus*, *25*(5), E2. https://doi.org/10.3171/FOC.2008.25.11.E2

Ruitenberg, M. J., Levison, D. B., Lee, S. V., Verhaagen, J., Harvey, A. R., & Plant, G. W. (2005). NT-3 expression from engineered olfactory ensheathing glia promotes spinal sparing and regeneration. *Brain*, *128*(4), 839–853. https://doi.org/10.1093/brain/awh424

Ruitenberg, M. J., Plant, G. W., Hamers, F. P. T., Wortel, J., Blits, B., Dijkhuizen, P. A., … Verhaagen, J. (2003). Ex vivo adenoviral vector-mediated neurotrophin gene transfer to olfactory ensheathing glia: effects on rubrospinal tract regeneration, lesion size, and functional recovery after implantation in the injured rat spinal cord. *The Journal of Neuroscience : The Official Journal of the Society for Neuroscience*, *23*(18), 7045–7058. https://doi.org/23/18/7045 [pii]

Ruitenberg, M. J., Vukovic, J., Sarich, J., Busfield, S. J., & Plant, G. W. (2006).

Olfactory Ensheathing Cells : Characteristics , Genetic SOURCE OF OLFACTORY. *JOURNAL OF NEUROTRAUMA*, *23*(3), 468–478.

Salzer, J. L., & Bunge, R. P. (1980). Studies of schwann cell proliferation : I. An analysis in tissue culture of proliferation during development, wallerian degeneration, and direct injury. *Journal of Cell Biology*, *84*(3), 739–752. https://doi.org/10.1083/jcb.84.3.739

Salzer, J. L., Lovejoy, L., Linder, M. C., & Rosen, C. (1998). Ran-2, a glial lineage marker, is a GPI-anchored form of ceruloplasmin. *Journal of Neuroscience Research*, *54*, 147–157. https://doi.org/10.1002/(SICI)1097-4547(19981015)54:2<147::AID-JNR3>3.0.CO;2-E

Sandvig, A., Berry, M., Barrett, L. B., Butt, A., & Logan, A. (2004, May). Myelin-, reactive glia-, and scar-derived CNS axon growth inhibitors: Expression, receptor signaling, and correlation with axon regeneration. *GLIA*. Wiley-Blackwell. https://doi.org/10.1002/glia.10315

Santos-Silva, A., Fairless, R., Frame, M. C., Montague, P., Smith, G. M., Toft, A., … Barnett, S. C. (2007). FGF/Heparin Differentially Regulates Schwann Cell and Olfactory Ensheathing Cell Interactions with Astrocytes: A Role in Astrocytosis. *Journal of Neuroscience*, *27*(27), 7154–7167. https://doi.org/10.1523/JNEUROSCI.1184-07.2007

Sasaki, M., Black, J. A., Lankford, K. L., Tokuno, H. A., Waxman, S. G., & Kocsis, J. D. (2006). Molecular reconstruction of nodes of Ranvier after

remyelination by transplanted olfactory ensheathing cells in the demyelinated spinal cord. *The Journal of Neuroscience : The Official Journal of the Society for Neuroscience*, *26*(6), 1803–1812. https://doi.org/10.1523/JNEUROSCI.3611-05.2006

Sawilowsky, S. S. (2009). New Effect Size Rules of Thumb. *Journal of Modern Applied Statistical Methods*, *8*(2), 597–599. https://doi.org/10.22237/jmasm/1257035100

Saxe, D. F., Takahashi., N., Hood, L., & Simon, M. I. (1985). Localization of the human myelin basic protein gene (MBP) to region 18q22→qter by in situ hybridization. *Cytogenetic and Genome Research*, *39*(4), 246–249. https://doi.org/10.1159/000132152

Schaal, S. M., Kitay, B. M., Cho, K. S., Lo, T. P., Barakat, D. J., Marcillo, A. E., … Pearse, D. D. (2007). Schwann cell transplantation improves reticulospinal axon growth and forelimb strength after severe cervical spinal cord contusion. In *Cell Transplantation* (Vol. 16, pp. 207–228). https://doi.org/10.3727/000000007783464768

Schwanzel-Fukuda, M., & Pfaff, D. W. (1989). Origin of luteinizing hormone-releasing hormone neurons. *Nature*, *338*(6211), 161–164. https://doi.org/10.1038/338161a0 [doi]

Seeds, I. W., Gilman, A. G., Amano, T., & Nirenberg L, M. W. (1970). Regulation of Axon Formation by Clonal Lines of a Neural Tumor. *Proceedings of the XaLimmZ Acadm~ of Sciences*, *66*(1), 16–17.

Seijffers, R., & Benowitz, L. (2008). Intrinsic determinants of axon

regeneration. In *CNS Regeneration* (pp. 1–39). Elsevier. https://doi.org/10.1016/B978-012373994-0.50003-8

Sethi, R., Sethi, R., Redmond, A., & Lavik, E. (2014). Olfactory Ensheathing Cells Promote Differentiation of Neural Stem Cells and Robust Neurite Extension. *Stem Cell Reviews*. https://doi.org/10.1007/s12015-014-9539-7

Shapiro, S. S., & Wilk, M. B. (1965). An Analysis of Variance Test for Normality. *Biometrika*, *52*(3), 591–596. https://doi.org/10.1093/biomet/52.3-4.591

Sharma, H. S., & Hari Shanker Sharma. (2007). *Neurotrophic factors in combination: a possible new therapeutic strategy to influence pathophysiology of spinal cord injury and repair mechanisms. Current pharmaceutical design* (Vol. 13). https://doi.org/10.2174/138161207780858410

Shepherd, G. M., Greer, C. a, Mazzarello, P., & Sassoè-Pognetto, M. (2011). The first images of nerve cells: Golgi on the olfactory bulb 1875. *Brain Research Reviews*, *66*(1–2), 92–105. https://doi.org/10.1016/j.brainresrev.2010.09.009

Shy, M. E. (2006). Peripheral neuropathies caused by mutations in the myelin protein zero. In *Journal of the Neurological Sciences* (Vol. 242, pp. 55–66). https://doi.org/10.1016/j.jns.2005.11.015

Sieber-Blum, M. (1998). *Neurotrophins and the Neural Crest*. CRC Press.

Silver, J., & Miller, J. H. (2004). Regeneration beyond the glial scar. *Nature Reviews Neuroscience*, *5*(2), 146–156. https://doi.org/10.1038/nrn1326

Simpson, P. B., Bacha, J. I., Palfreyman, E. L., Woollacott, A. J., McKernan, R. M., & Kerby, J. (2001). Retinoic acid evoked-differentiation of neuroblastoma cells predominates over growth factor stimulation: an automated image capture and quantitation approach to neuritogenesis. *Analytical Biochemistry*, *298*(2), 163–169. https://doi.org/10.1006/abio.2001.5346

Siriphorn, A., Chompoopong, S., & Floyd, C. L. (2010). 17β-Estradiol protects Schwann cells against H2O2-induced cytotoxicity and increases transplanted Schwann cell survival in a cervical hemicontusion spinal cord injury model. *Journal of Neurochemistry*, *115*(4), 864–872. https://doi.org/10.1111/j.1471-4159.2010.06770.x

Smith-Thomas, L. C., Fok-Seang, J., Stevens, J., Du, J. S., Muir, E., Faissner, A., … Fawcett, J. W. (1994). An inhibitor of neurite outgrowth produced by astrocytes. *Journal of Cell Science*, *107 (Pt 6*, 1687–1695.

Smith, D. S., Skene, J. H., Lichtman, J., Sanes, J., & Milner, R. (1997). A transcription-dependent switch controls competence of adult neurons for distinct modes of axon growth. *The Journal of Neuroscience : The Official Journal of the Society for Neuroscience*, *17*(2), 646–658. https://doi.org/10.1523/jneurosci.0612-07.2007

Snow, D. M., Lemmon, V., Carrino, D. A., Caplan, A. I., & Silver, J. (1990).

Sulfated proteoglycans in astroglial barriers inhibit neurite outgrowth in vitro. *Experimental Neurology*, *109*(1), 111–130. https://doi.org/10.1016/S0014-4886(05)80013-5

Sonigra, R. J., Brighton, P. C., Jacoby, J., Hall, S., & Wigley, C. B. (1999). Adult rat olfactory nerve ensheathing cells are effective promoters of adult central nervous system neurite outgrowth in coculture. *GLIA*, *25*(3), 256–269. https://doi.org/10.1002/(SICI)1098-1136(19990201)25:3<256::AID-GLIA6>3.0.CO;2-Y

Sonigra, R. J., Kandiah, S. S., & Wigley, C. B. (1996). Spontaneous immortalisation of ensheathing cells from adult rat olfactory nerve. *Glia*, *16*, 247–256. https://doi.org/10.1002/(SICI)1098-1136(199603)16:3<247::AID-GLIA7>3.0.CO;2-Z

Sorensen, A., Moffat, K., Thomson, C., & Barnett, S. C. (2008). Astrocytes, but not olfactory ensheathing cells or Schwann cells, promote myelination of CNS axons in vitro. *Glia*, *56*(7), 750–763. https://doi.org/10.1002/glia.20650

Sowa, Y., Kishida, T., Tomita, K., Yamamoto, K., Numajiri, T., & Mazda, O. (2017). Direct conversion of human fibroblasts into schwann cells that facilitate regeneration of injured peripheral nerve in vivo. *Stem Cells Translational Medicine*, *6*(4), 1207–1216. https://doi.org/10.1002/sctm.16-0122

Spellman, F. R., & Whiting, N. E. (2013). *Handbook of mathematics and statistics for the environment*.

Spitzbarth, I., Bock, P., Haist, V., Stein, V. M., Tipold, A., Wewetzer, K., … Beineke, A. (2011). Prominent Microglial Activation in the Early Proinflammatory Immune Response in Naturally Occurring Canine Spinal Cord Injury. *Journal of Neuropathology & Experimental Neurology*, *70*(8), 703–714. https://doi.org/10.1097/NEN.0b013e3182270f8e

Springer, J. E., Mu, X., Bergmann, L. W., & Trojanowski, J. Q. (1994). Expression of GDNF mRNA in Rat and Human Nervous Tissue. *Experimental Neurology*, *127*(2), 167–170. https://doi.org/10.1006/exnr.1994.1091

Steiger, J. H. (2004). Beyond the F test: Effect size confidence intervals and tests of close fit in the analysis of variance and contrast analysis. *Psychological Methods*, *9*(2), 164–182. https://doi.org/10.1037/1082-989X.9.2.164

Stemple, D. L., & Anderson, D. J. (1992). Isolation of a stem cell for neurons and glia from the mammalian neural crest. *Cell*, *71*(6), 973–985. https://doi.org/10.1016/0092-8674(92)90393-Q

Stephens, M. A. (1974). EDF statistics for goodness of fit and some comparisons. *Journal of the American Statistical Association*, *69*(347), 730–737. https://doi.org/10.1080/01621459.1974.10480196

Stoop, R., & Poo, M. M. (1996). Synaptic modulation by neurotrophic factors: differential and synergistic effects of brain-derived neurotrophic factor and ciliary neurotrophic factor. *The Journal of*

Neuroscience : The Official Journal of the Society for Neuroscience, *16*(10), 3256–3264.

Su, Z., Cao, L., Zhu, Y., Liu, X., Huang, Z., Huang, A., & He, C. (2007). Nogo enhances the adhesion of olfactory ensheathing cells and inhibits their migration. *Journal of Cell Science*, *120*(Pt 11), 1877–1887. https://doi.org/10.1242/jcs.03448

Su, Z., Chen, J., Qiu, Y., Yuan, Y., Zhu, F., Zhu, Y., … He, C. (2013). Olfactory ensheathing cells: the primary innate immunocytes in the olfactory pathway to engulf apoptotic olfactory nerve debris. *Glia*, *61*(4), 490–503. https://doi.org/10.1002/glia.22450

Su, Z., & He, C. (2010). Olfactory ensheathing cells: biology in neural development and regeneration. *Prog Neurobiol*, *92*, 517–532. https://doi.org/10.1016/j.pneurobio.2010.08.008

Su, Z., Yuan, Y., Chen, J., Cao, L., Zhu, Y., Gao, L., … He, C. (2009). Reactive astrocytes in glial scar attract olfactory ensheathing cells migration by secreted TNF-alpha in spinal cord Lesion Of Rat. *PLoS ONE*, *4*(12). https://doi.org/10.1371/journal.pone.0008141

Sun, M., & Downes, S. (2007). Solvent-cast PCL films support the regeneration of NG108-15 nerve cells (p. 64230E). https://doi.org/10.1117/12.779219

Suzuki, Y., Schafer, J., & Farbman, A. I. (1995). Phagocytic cells in the rat olfactory epithelium after bulbectomy. *Experimental Neurology*, *136*(2), 225–233. https://doi.org/10.1006/exnr.1995.1099

Suzuki, Y., Takeda, M., & Farbman, A. I. (1996). Supporting cells as phagocytes in the olfactory epithelium after bulbectomy. *Journal of Comparative Neurology*, *376*(4), 509–517. https://doi.org/10.1002/(SICI)1096-9861(19961223)376:4<509::AID-CNE1>3.0.CO;2-5

Szigeti, V., & Miller, R. H. (1993). A cell surface antigen expressed by astrocytes and their precursors. *Glia*, *8*, 20–32. https://doi.org/10.1002/glia.440080104 ET - 1993/05/01

Tabachnick, B. G., Fidell, L. S., & Osterlind, S. J. (2001). *Using multivariate statistics*. Pearson Education. https://doi.org/10.1037/022267

Tabakow, P., Jarmundowicz, W., Czapiga, B., Fortuna, W., Miedzybrodzki, R., Czyz, M., … Raisman, G. (2013). Transplantation of autologous olfactory ensheathing cells in complete human spinal cord injury. *Cell Transplantation*, *22*(9), 1591–1612. https://doi.org/10.3727/096368913X663532

Tabakow, P., Raisman, G., Fortuna, W., Czyz, M., Huber, J., Li, D., … Jarmundowicz, W. (2014). Functional regeneration of supraspinal connections in a patient with transected spinal cord following transplantation of bulbar olfactory ensheathing cells with peripheral nerve bridging. *Cell Transplantation*, *23*(12), 1–70. https://doi.org/10.3727/096368914X685131

Takami, T., Oudega, M., Bates, M. L., Wood, P. M., Kleitman, N., & Bunge, M. B. (2002). Schwann cell but not olfactory ensheathing glia

transplants improve hindlimb locomotor performance in the moderately contused adult rat thoracic spinal cord. *The Journal of Neuroscience : The Official Journal of the Society for Neuroscience*, *22*(15), 6670–6681. https://doi.org/20026636

Taoka, Y., Okajima, K., Uchiba, M., Murakami, K., Kushimoto, S., Johno, M., … Takatsuki, K. (1997). Role of neutrophils in spinal cord injury in the rat. *Neuroscience*, *79*(4), 1177–1182. Retrieved from http://www.ncbi.nlm.nih.gov/pubmed/9219976

Tator, C. H. (1998, April 1). Biology of neurological recovery and functional restoration after spinal cord injury. *Neurosurgery*. Oxford University Press. https://doi.org/10.1097/00006123-199804000-00007

Tator, C. H., & Fehlings, M. G. (1991). Review of the secondary injury theory of acute spinal cord trauma with emphasis on vascular mechanisms. *Journal of Neurosurgery*, *75*(1), 15–26. https://doi.org/10.3171/jns.1991.75.1.0015

Tator, C. H., & Koyanagi, I. (1997). Vascular mechanisms in the pathophysiology of human spinal cord injury. *Journal of Neurosurgery*, *86*(3), 483–492. https://doi.org/10.3171/jns.1997.86.3.0483

Tegenge, M. A., Roloff, F., & Bicker, G. (2011). Rapid differentiation of human embryonal carcinoma stem cells (NT2) into neurons for neurite outgrowth analysis. *Cellular and Molecular Neurobiology*, *31*(4), 635–643. https://doi.org/10.1007/s10571-011-9659-4

Tisay, K. T., & Key, B. (1999). The extracellular matrix modulates olfactory

neurite outgrowth on ensheathing cells. *The Journal of Neuroscience : The Official Journal of the Society for Neuroscience*, *19*(22), 9890–9899.

Toft, A., Scott, D. T., Barnett, S. C., & Riddell, J. S. (2007). Electrophysiological evidence that olfactory cell transplants improve function after spinal cord injury. *Brain*, *130*(4), 970–984. https://doi.org/10.1093/brain/awm040

Toft, A., Tome, M., Barnett, S. C., & Riddell, J. S. (2013). A comparative study of glial and non-neural cell properties for transplant-mediated repair of the injured spinal cord. *GLIA*, *61*(4), 513–528. https://doi.org/10.1002/glia.22452

Tomasek, J. J., Gabbiani, G., Hinz, B., Chaponnier, C., & Brown, R. a. (2002). Myofibroblasts and mechano-regulation of connective tissue remodelling. *Nature Reviews. Molecular Cell Biology*, *3*(5), 349–363. https://doi.org/10.1038/nrm809

Tse, C., Whiteley, R., Yu, T., Stringer, J., MacNeil, S., Haycock, J. W., & Smith, P. J. (2016). Inkjet printing Schwann cells and neuronal analogue NG108-15 cells. *Biofabrication*, *8*(1), 015017. https://doi.org/10.1088/1758-5090/8/1/015017

Tuszynski, M. H., Murai, K., Blesch, A., Grill, R., & Miller, I. (1997). FUNCTIONAL CHARACTERIZATION OF NGF-SECRETING CELL GRAFTS TO THE ACUTELY INJURED SPINAL CORD. *Cell Transplantation*, *6*(3), 361–368. https://doi.org/10.1016/S0963-6897(97)00021-3

Tuszynski, M. H., Weidner, N., McCormack, M., Miller, I., Powell, H., & Conner, J. (1998). Grafts of genetically modified Schwann cells to the spinal cord: survival, axon growth, and myelination. *Cell Transplantation*, *7*(2), 187–196. Retrieved from http://www.ncbi.nlm.nih.gov/pubmed/9588600

Valverde, F., & Lopez-Mascaraque, L. (1991). Neuroglial arrangements in the olfactory glomeruli of the hedgehog. *The Journal of Comparative Neurology*, *307*(4), 658–674. https://doi.org/10.1002/cne.903070411

Valverde, F., Santacana, M., & Heredia, M. (1992). Formation of an olfactory glomerulus: Morphological aspects of development and organization. *Neuroscience*, *49*(2), 255–275. https://doi.org/10.1016/0306-4522(92)90094-I

Van Den Pol, A. N., & Santarelli, J. G. (2003). Olfactory ensheathing cells: Time lapse imaging of cellular interactions, axonal support, rapid morphologic shifts, and mitosis. *Journal of Comparative Neurology*, *458*(2), 175–194. https://doi.org/10.1002/cne.10577

Varon, S. S., Conner, J. M., & Kuang, R. Z. (1995). Neurotrophic factors: repair and regeneration in the central nervous system. *Restorative Neurology and Neuroscience*, *8*(1), 85–94. https://doi.org/10.3233/RNN-1995-81221

Vickland, H., Westrum, L. E., Kott, J. N., Patterson, S. L., & Bothwell, M. A. (1991). Nerve growth factor receptor expression in the young and adult rat olfactory system. *Brain Research*, *565*(2), 269–279.

https://doi.org/10.1016/0006-8993(91)91659-O

Vincent, A. J., Taylor, J. M., Choi-Lundberg, D. L., West, A. K., & Chuah, M. I. (2005). Genetic expression profile of olfactory ensheathing cells is distinct from that of Schwann cells and astrocytes. *Glia*, *51*(August 2004), 132–147. https://doi.org/10.1002/glia.20195

Vincent, A. J., West, A. K., & Chuah, M. I. (2003). Morphological plasticity of olfactory ensheathing cells is regulated by cAMP and endothelin-1. *GLIA*, *41*(4), 393–403. https://doi.org/10.1002/glia.10171

Vincent, A. J., West, A. K., & Chuah, M. inn. (2005). Morphological and functional plasticity of olfactory ensheathing cells, *80*, 65–80.

Vukovic, J., Marmorstein, L. Y., McLaughlin, P. J., Sasaki, T., Plant, G. W., Harvey, A. R., & Ruitenberg, M. J. (2009). Lack of fibulin-3 alters regenerative tissue responses in the primary olfactory pathway. *Matrix Biology*, *28*(7), 406–415. https://doi.org/10.1016/j.matbio.2009.06.001

Wang, H., Liu, C., & Ma, X. (2012). Alginic acid sodium hydrogel co-transplantation with Schwann cells for rat spinal cord repair. *Archives of Medical Science : AMS*, *8*(3), 563–568. https://doi.org/10.5114/aoms.2012.29412

Wang, Y., Teng, H.-L., Gao, Y., Zhang, F., Ding, Y.-Q., & Huang, Z.-H. (2016). Brain-derived Neurotrophic Factor Promotes the Migration of Olfactory Ensheathing Cells Through TRPC Channels. *Glia*, *64*(12), 2154–2165. https://doi.org/10.1002/glia.23049

Weinstein, D. E., & Wu, R. (2001). Isolation and Purification of Primary Schwann Cells. In *Current Protocols in Neuroscience*. Hoboken, NJ, USA: John Wiley & Sons, Inc. https://doi.org/10.1002/0471142301.ns0317s08

Wewetzer, K., Grothe, C., & Claus, P. (2001). In vitro expression and regulation of ciliary neurotrophic factor and its α receptor subunit in neonatal rat olfactory ensheathing cells. *Neuroscience Letters*, *306*(3), 165–168. https://doi.org/10.1016/S0304-3940(01)01891-2

Wewetzer, K., Kern, N., Ebel, C., Radtke, C., & Brandes, G. (2005). Phagocytosis of O4+ axonal fragments in vitro by p75- neonatal rat olfactory ensheathing cells. *GLIA*, *49*, 577–587. https://doi.org/10.1002/glia.20149

Windus, L. C. E., Claxton, C., Allen, C., Key, B., & St John, J. A. (2007). Motile Membrane Protrusions Regulate Cell–Cell Adhesion and Migration of Olfactory Ensheathing Glia. *Glia*, *55*(August), 1708–1719. https://doi.org/10.1002/glia

Woerly, S., Plant, G. W., & Harvey, A. R. (1996). Cultured rat neuronal and glial cells entrapped within hydrogel polymer matrices: a potential tool for neural tissue replacement. *Neuroscience Letters*, *205*(3), 197–201. https://doi.org/10.1016/0304-3940(96)12349-1

Woodhall, E., West, A. K., & Chuah, M. I. (2001). Cultured olfactory ensheathing cells express nerve growth factor, brain-derived neurotrophic factor, glia cell line-derived neurotrophic factor and their

receptors. *Molecular Brain Research*, *88*(1–2), 203–213. https://doi.org/10.1016/S0169-328X(01)00044-4

Wray, S., Grant, P., & Gainer, H. (1989). Evidence that cells expressing luteinizing hormone-releasing hormone mRNA in the mouse are derived from progenitor cells in the olfactory placode (prenatal development/in situ hybridization/histochenustry/immunocytochemistry/[3H]thymidine autoradiography). *Neurobiology*, *86*, 8132–8136. https://doi.org/10.1073/pnas.86.20.8132

Xie, Y., Zhang, J., Lin, Y., Gaeta, X., Meng, X., Wisidagama, D. R. R., … Lowry, W. E. (2014). Defining the role of oxygen tension in human neural progenitor fate. *Stem Cell Reports*, *3*(5), 743–757. https://doi.org/10.1016/j.stemcr.2014.09.021

Xu, X. M., Chen, A., Guénard, V., Kleitman, N., & Bunge, M. B. (1997). Bridging Schwann cell transplants promote axonal regeneration from both the rostral and caudal stumps of transected adult rat spinal cord. *J Neurocytol*, *26*(1), 1–16. https://doi.org/10.1023/A:1018557923309

Xu, X. M., Guénard, V., Kleitman, N., & Bunge, M. B. (1995). Axonal regeneration into Schwann cell-seeded guidance channels grafted into transected adult rat spinal cord. *Journal of Comparative Neurology*, *351*(1), 145–160. https://doi.org/10.1002/cne.903510113

Yamamoto, M., Raisman, G., Li, D., & Li, Y. (2009). Transplanted olfactory mucosal cells restore paw reaching function without regeneration of

severed corticospinal tract fibres across the lesion. *Brain Research*, *1303*, 26–31. https://doi.org/10.1016/j.brainres.2009.09.073

Yan, H., Lu, D., & Rivkees, S. A. (2003). Lysophosphatidic acid regulates the proliferation and migration of olfactory ensheathing cells in vitro. *Glia*, *44*(1), 26–36. https://doi.org/10.1002/glia.10265

Yan, Q., & Johnson, E. M. (1988). An immunohistochemical study of the nerve growth factor receptor in developing rats. *The Journal of Neuroscience*, *8*(9), 3481–3498. https://doi.org/2845023

Yang, H., He, B.-R., & Hao, D.-J. (2014). Biological Roles of Olfactory Ensheathing Cells in Facilitating Neural Regeneration: A Systematic Review. *Molecular Neurobiology*. https://doi.org/10.1007/s12035-014-8664-2

Yiu, G., & He, Z. (2006). Glial inhibition of CNS axon regeneration. *Nature Reviews. Neuroscience*, *7*(8), 617–627. https://doi.org/10.1038/nrn1956

Yu, W. R., & Fehlings, M. G. (2011). Fas/FasL-mediated apoptosis and inflammation are key features of acute human spinal cord injury: implications for translational, clinical application. *Acta Neuropathologica*, *122*(6), 747–761. https://doi.org/10.1007/s00401-011-0882-3

Zhang, J. F., Zhao, F. S., Wu, G., Kong, Q. F., Sun, B., Cao, J., … Li, H. L. (2011). Therapeutic effect of co-transplantation of neuregulin 1-transfected-Schwann cells and bone marrow stromal cells on spinal

cord hemisection syndrome. *Neuroscience Letters*, *497*(2), 128–133. https://doi.org/10.1016/j.neulet.2011.04.045

Zhang, P., Liu, Y., Li, J., Kang, Q., Tian, Y., Chen, X., … Song, T. (2006). Cell proliferation in ependymal/subventricular zone and nNOS expression following focal cerebral ischemia in adult rats. *Neurol Res*, *28*(1), 91–96. https://doi.org/10.1179/016164106X91942

Zhao, Y., Wang, B., Gao, Y., Zhao, Y., Xiao, Z., Zhao, W., … Dai, J. (2007). Olfactory ensheathing cell apoptosis induced by hypoxia and serum deprivation. *Neuroscience Letters*, *421*(3), 197–202. https://doi.org/10.1016/j.neulet.2007.04.028

Zheng, Z., Liu, G., Chen, Y., & Wei, S. (2013). Olfactory ensheathing cell transplantation improves sympathetic skin responses in chronic spinal cord injury. *Neural Regeneration Research*, *8*(30), 2849–2855. https://doi.org/10.3969/j.issn.1673-5374.2013.30.007

Zhu, Y., Cao, L., Su, Z., Mu, L., Yuan, Y., Gao, L., … He, C. (2010). Olfactory ensheathing cells: Attractant of neural progenitor migration to olfactory bulb. *GLIA*, *58*(6), 716–729. https://doi.org/10.1002/glia.20957

Ziege, S., Wewetzer, K., Schöne, K., & Baumgärtner, W. (2013). Special neurite growth-promoting capacity and growth factor responsiveness of nasal mucosa-derived olfactory ensheathing cells unraveled by Schwann cell depletion. *Exp. Neurol.*

Zurita, M., J, V., Bonilla, C., Santos M., De Haro, J., Oya, S., & Aguayao, C.

(2008). Functional Recovery of Chronic Paraplegic Pigs After Autologous Transplantation of Bone Marrow Stromal Cells. *Transplantation*, *86*(6), 845–853. https://doi.org/10.1097/tp.0b013e318186198f

Zurita, M., & Vaquero, J. (2006). Bone marrow stromal cells can achieve cure of chronic paraplegic rats: Functional and morphological outcome one year after transplantation. *Neuroscience Letters*, *402*(1–2), 51–56. https://doi.org/10.1016/J.NEULET.2006.03.069

www.nlm.nih.gov/cgi/mesh/2011/MB_cgi?mode=&term=Growth+Factors

htttp://www.who.int

https://www.nscisc.uab.edu

http://www.ninds.nih.gov/disorders/sci/detail_sci.htm#268123233

https://www.sigmaaldrich.com/catalog/product/sigma/cb_93031204?lang=en&region=GB

https://www.sigmaaldrich.com/catalog/product/sigma/cb_88112302?lang=en&region=GB&gclid=CjwKCAjwkcblBRB_EiwAFmfyy9ZIVSrOBElcPdd1N5TWqJGwoINbe1jq2nXRW9ZlSmh07LufblZchRoCRAQQAvD_BwE